Carbon Dioxide Sequestration by Mineral Carbonation

Wouter J. J. Huijgen

CARBON DIOXIDE SEQUESTRATION
BY MINERAL CARBONATION

PROEFSCHRIFT

Ter verkrijging van de graad van doctor
op gezag van de rector magnificus
van Wageningen Universiteit,
prof. dr. M.J. Kropff,
in het openbaar te verdedigen
op vrijdag 12 januari 2007
des namiddags te vier uur in de Aula.

CONTENTS

SUMMARY

SUMMARY

The increasing atmospheric carbon dioxide (CO_2) concentration, mainly caused by fossil fuel combustion, has lead to concerns about global warming. A possible technology that can contribute to the reduction of carbon dioxide emissions is CO_2 sequestration by mineral carbonation. The basic concept behind mineral CO_2 sequestration is the mimicking of natural weathering processes in which calcium or magnesium containing minerals react with gaseous CO_2 and form solid calcium or magnesium carbonates:

$$(Ca,Mg)SiO_3 \text{ (s)} + CO_2 \text{ (g)} \rightarrow (Ca,Mg)CO_3 \text{ (s)} + SiO_2 \text{ (s)}$$
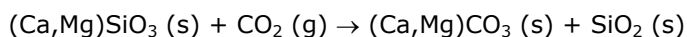
Potential advantages of mineral CO_2 sequestration compared to, e.g., geological CO_2 storage include (1) the permanent and inherently safe sequestration of CO_2, due to the thermodynamic stability of the carbonate product formed and (2) the vast potential sequestration capacity, because of the widespread and abundant occurrence of suitable feedstock. In addition, carbonation is an exothermic process, which potentially limits the overall energy consumption and costs of CO_2 emission reduction. However, weathering processes are slow, with timescales at natural conditions of thousands to millions of years. For industrial implementation, a reduction of the reaction time to the order of minutes has to be achieved by developing alternative process routes.

The **aim** of this thesis is an investigation of the technical, energetic, and economic feasibility of CO_2 sequestration by mineral carbonation.

In **Chapter 1** the literature published on CO_2 sequestration by mineral carbonation is reviewed. Among the potentially suitable mineral feedstock for mineral CO_2 sequestration, Ca-silicates, more particularly wollastonite ($CaSiO_3$), a mineral ore, and steel slag, an industrial alkaline solid residue, are selected for further research. Alkaline Ca-rich residues seem particularly promising, since these materials are inexpensive and available near large industrial point sources of CO_2. In addition, residues tend to react relatively rapidly with CO_2 due to their (geo)chemical instability.

Various process routes have been proposed for mineral carbonation, which often include a pre-treatment of the solid feedstock (e.g., size reduction and/or thermal activation). The only available pre-treatment option that has proven to be energetically and potentially economically feasible is conventional grinding.

Two main types of process routes can be distinguished: (1) direct routes in which carbonation takes place in a single step process, either in a gas-solid or a gas-liquid-solid process, and (2) indirect routes in which the Ca is first extracted from the silicate matrix and subsequently carbonated in a separate process step. The aqueous route in which Ca-silicates are directly carbonated in an aqueous suspension at elevated temperature and CO_2 pressure is selected as the most promising process route for further investigation. The following key issues for further research are identified: the reaction rates and mechanisms of mineral carbonation as well as its energy consumption and sequestration costs. Another important aspect of mineral carbonation is the destination of the carbonated products.

In **Chapter 2** the mechanisms of aqueous steel slag carbonation are studied experimentally. Process variables, such as particle size, temperature, and carbon dioxide pressure are systematically varied and their influence on the carbonation rate is investigated. The maximum carbonation degree reached is 74% of the Ca content in 30 minutes at 19 bar CO_2 pressure, 100 °C, and a particle size of <38 μm. The two most important factors determining the reaction rate are particle size (<2 mm to <38 μm) and reaction temperature (25-225 °C). The carbonation reaction is found to occur in two steps: (1) leaching of calcium from the steel slag particles into the solution and (2) precipitation of calcite on the surface of these particles. The first step and, more in particular, the diffusion of calcium through the solid matrix towards the surface, appears to be the rate-determining reaction step. The Ca-diffusion is found to be hindered by the formation of a $CaCO_3$-coating and a Ca-depleted silicate zone during the carbonation process.

In **Chapter 3** the mechanisms of aqueous steel slag carbonation are further investigated, together with the environmental properties of the (carbonated) steel slag. Steel slag samples are carbonated to a varying extent and leaching experiments and geochemical modelling are used to identify solubility-controlling processes of both major and minor elements that are present in the slag. Carbonation is shown to reduce the leaching of alkaline earth metals (except Mg) by conversion of Ca-phases, such as portlandite, ettringite, and Ca-(Fe)-silicates into calcite, possibly containing traces of Ba and Sr. The leaching of vanadium increases substantially upon carbonation, probably due to the dissolution of a Ca-vanadate. The increased reactive surface area of Al- and Fe-(hydr)oxides after carbonation tends to reduce the leaching of sorption-controlled trace elements. Sorption on Mn-(hydr)oxides is found to be also required to adequately model the leaching of divalent cations, but is not influenced by carbonation. Consideration of these three distinct reactive surfaces and possible (surface) precipitation reactions resulted in adequate modelling

predictions of oxyanion and trace metal leaching from (carbonated) steel slag. Hence, these surfaces exert a major influence on the environmental properties of both fresh and carbonated steel slag.

In **Chapter 4**, the mechanisms of aqueous wollastonite carbonation as a possible carbon dioxide sequestration process are investigated experimentally by systematic variation of the reaction temperature, CO_2 pressure, particle size, reaction time, liquid-to-solid ratio, and agitation power. The carbonation reaction is observed to occur via the aqueous phase in two steps: (1) Ca leaching from the $CaSiO_3$ matrix and (2) $CaCO_3$ nucleation and growth. Leaching is hindered by a Ca-depleted silicate rim resulting from incongruent Ca-dissolution. Two temperature regimes are identified in the overall carbonation process. At temperatures below an optimum reaction temperature, the overall reaction rate is probably limited by the leaching rate of Ca. At higher temperatures, nucleation and growth of calcium carbonate is probably limiting the carbonation rate, due to a reduced (bi)carbonate activity. The mechanisms for the aqueous carbonation of wollastonite are shown to be similar to those of steel slag (Chapter 2) and of the Mg-silicate olivine. The carbonation of wollastonite proceeds rapidly relative to Mg-silicates, with a maximum conversion of 70% in 15 min at 200 °C, 20 bar CO_2 partial pressure, and a particle size of <38 μm.

The obtained insight in the reaction mechanisms in **Chapter 2** - **4** is used as the (experimental) basis for the energetic and economic assessment of CO_2 sequestration by mineral carbonation in **Chapters 5** & **6**.

The energy consumption of a mineral carbonation plant causes extra CO_2 emssions and, thereby, reduces the net amount of CO_2 sequestered by the process. **Chapter 5** studies the energetic CO_2 sequestration efficiency (i.e., the fraction of CO_2 that is sequestered effectively) of the aqueous mineral carbonation in dependence of various process variables using either wollastonite or steel slag as feedstock. A flowsheet of a mineral carbonation plant is designed and the process is simulated to determine the properties of streams as well as the power and heat consumption of the process equipment. For wollastonite, the maximum energetic efficiency within the ranges of process conditions studied is 75% at 200 °C, 20 bar CO_2, and a particle size of <38 μm. The main energy-consuming process steps are the grinding of the feedstock and the compression of the CO_2 feed. At these conditions, a significantly lower efficiency is determined for steel slag (69%), mainly due to the lower Ca content of the feedstock. The CO_2 sequestration efficiency might be improved substantially for both types of feedstock by e.g. reducing the amount of process water applied and further grinding of the feedstock.

In **Chapter 6** a cost evaluation of CO_2 sequestration by aqueous mineral carbonation is presented, using either wollastonite or steel slag as feedstock. On the basis of a basic design of the major process equipment, the total investment costs are estimated with the help of publicly available literature and a factorial cost estimation method. Subsequently, the sequestration costs are determined on the basis of the depreciation of investments and variable and fixed operating costs. Estimated costs are 102 and 77 €/ton CO_2 net avoided for wollastonite and steel slag, respectively. For wollastonite, major costs are associated with the feedstock and the electricity consumption for grinding and compression (54 and 26 €/ton CO_2 avoided, respectively). The sequestration costs for steel slag are significantly lower due to the absence of costs for the feedstock. A sensitivity analysis shows that additional influential parameters in the sequestration costs include the liquid-to-solid ratio in the carbonation reactor and the possible value of the carbonated product.

In the **Epilogue** the main conclusions of this thesis are summarised and recommendations for further research are given.

This thesis shows that CO_2 sequestration by carbonation of Ca-silicates is possible at technically feasible process conditions. Altough the energy consumption of current mineral carbonation processes is substantial, the identified possibilities to reduce the energy demands of the process suggest that mineral carbonation may become energetically feasible after further technology development. Finally, the costs of CO_2 sequestration by mineral ore carbonation processes are relatively high compared to other CO_2 storage technologies and (current) CO_2 market prices. (Niche) applications of mineral carbonation based on the use of a solid residue as feedstock and/or the production of a carbonation product with positive value, hold significantly better prospects for an economically feasible process.

Overall, mineral CO_2 sequestration is (still) a longer-term option compared to other 'carbon capture & storage'-technologies and probably has limited potential in the short term. However, the possibilities identified for further process improvement, the permanent and inherently safe character of the CO_2 sequestration, and the large sequestration potential warrant further research on mineral CO_2 sequestration. This research should primarily focus on cost reduction, which is a prerequisite for mineral CO_2 sequestration to become part of a broad portfolio of employable CO_2 mitigation options.

SAMENVATTING

SAMENVATTING

De stijging van de concentratie koolstofdioxide (CO_2) in de atmosfeer, voornamelijk veroorzaakt door het gebruik van fossiele brandstoffen, heeft geleid tot zorgen omtrent het mogelijk optreden van klimaatverandering ten gevolge van een versterkt broeikaseffect. Een mogelijke technologie die kan bijdragen aan de reductie van de CO_2 emissies is minerale CO_2 vastlegging. Minerale CO_2 vastlegging is gebaseerd op het industrieel nabootsen van natuurlijke verweringsprocessen waarin calcium of magnesium bevattende mineralen reageren met gasvormig CO_2, waarna calcium of magnesium carbonaten gevormd worden:

$$(Ca,Mg)SiO_3 \text{ (s)} + CO_2 \text{ (g)} \rightarrow (Ca,Mg)CO_3 \text{ (s)} + SiO_2 \text{ (s)}$$
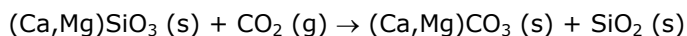
Minerale CO_2 vastlegging kent een aantal voordelen ten opzichte van b.v. geologische CO_2 opslag. Ten eerste is het CO_2 vastleggingspotentieel zeer groot aangezien geschikte grondstoffen wijdverspreid aanwezig zijn. Daarnaast wordt de CO_2 op een permanente en inherent veilige wijze vastgelegd ten gevolge van de thermodynamische stabiliteit van het gevormde carbonaat. Tot slot is carbonatatie een exotherm proces, hetgeen kan leiden tot een verlaging van het energieverbruik en kosten van CO_2 vastlegging. Verweringsprocessen zijn echter langzaam; een typische tijdschaal onder natuurlijke condities bedraagt duizenden tot miljoenen jaren. Voor industriële implementatie dient een reductie van de reactietijd tot een ordegrootte van minuten behaald te worden door het ontwikkelen van alternatieve procesroutes.

De **doelstelling** van dit proefschrift is het onderzoeken van de technische, energetische en economische haalbaarheid van reductie van CO_2 emissie door middel van carbonatatie van mineralen.

In **Hoofdstuk 1** wordt een overzicht gegeven van de literatuur die gepubliceerd is op het gebied van minerale CO_2 vastlegging. Van de mogelijk geschikte grondstoffen voor minerale CO_2 vastlegging worden Ca-silicaten en meer in het bijzonder, de delfstof wollastoniet ($CaSiO_3$) en de alkalische industriële reststof staalslak, geselecteerd voor verder onderzoek. Alkalische reststoffen die veel calcium bevatten lijken een veelbelovende grondstof aangezien deze materialen goedkoop zijn en beschikbaar zijn nabij grote puntbronnen aan CO_2. Bovendien reageren reststoffen over het algemeen relatief snel met CO_2 vanwege hun (geo)chemische instabiliteit.

Diverse mogelijke procesroutes voor minerale CO_2 vastlegging zijn gepubliceerd, meestal inclusief voorbehandeling van de vaste grondstof, b.v. deeltjesgrootte verkleining of thermische behandeling. De enige voorbehandeling die energetisch en potentieel economisch haalbaar lijkt, is conventioneel malen. De procesroutes kunnen in twee categorieën worden verdeeld: (1) directe routes waarin de carbonatatie in één enkele stap plaatsvindt, hetzij in een gas-vast, hetzij in een gas-vast-vloeistof proces, en (2) indirecte routes waarin calcium of magnesium eerst wordt geëxtraheerd uit de silicaatmatrix met behulp van bijvoorbeeld een zuur en vervolgens wordt gecarbonateerd in een tweede processtap. Als meest veelbelovende procesroute voor nader onderzoek wordt geselecteerd: de directe carbonatatie van calciumsilicaten in een waterige suspensie bij verhoogde CO_2 druk en temperatuur. Als hoofdaandachtspunten voor onderzoek zijn geïdentificeerd: de reactiesnelheden en -mechanismen van het carbonatatie proces, het bijbehorend energieverbruik en de CO_2 vastleggingskosten. Een ander belangrijk aandachtspunt is de eindbestemming van de gecarbonateerde producten.

In **Hoofdstuk 2** worden de mechanismen van staalslak carbonatatie in waterige suspensie experimenteel onderzocht bij verhoogde CO_2 spanning en temperatuur. Procesvariabelen zoals deeltjesgrootte, temperatuur en CO_2 druk worden systematisch gevarieerd, waarbij hun invloed op de carbonatatie snelheid wordt onderzocht. De maximaal bereikte carbonatatiegraad is 74% van het calciumgehalte binnen 30 minuten bij 19 bar CO_2 druk, 100 °C en een deeltjesgrootte van <38 µm. De twee meest belangrijke factoren die de reactiesnelheid bepalen blijken de deeltjesgrootte (<2 mm tot <38 µm) en de reactietemperatuur (25-225 °C). De carbonatatiereactie verloopt in twee stappen: (1) uitloging van calcium vanuit de staalslakdeeltjes naar de oplossing en (2) precipitatie van calciet op het oppervlak van deze deeltjes. De eerste stap en meer in het bijzonder de diffusie van calcium door de vaste matrix richting het oppervlak lijkt de snelheidsbepalende stap te zijn. Deze calciumdiffusie blijkt gehinderd te worden door de vorming van een laag calciumcarbonaat aan de buitenzijde van de staalslakdeeltjes, alsmede door een silicaatrijke zone die tijdens het proces verarmd raakt aan calcium.

In **Hoofdstuk 3** worden de carbonatatiemechanismen van staalslak in waterige suspensie nader bestudeerd samen met de milieuhygiënische eigenschappen van (gecarbonateerde) staalslak. Hiertoe worden staalslakmonsters gecarbonateerd en worden uitloogexperimenten en geochemische modellering toegepast om oplosbaarheidcontrolerende processen voor specifieke elementen te identificeren. Carbonatatie blijkt de uitloging van aardalkalimetalen, met uitzondering van magnesium, te reduceren door omzetting van calcium fasen zoals portlandiet, ettringiet en Ca-(Fe)-silicaten naar een calciet fase die

mogelijk sporen van barium en strontium bevat. De uitloging van vanadium neemt sterk toe door carbonatatie, waarschijnlijk ten gevolge van het oplossen van een calciumvanadaat fase. Het toegenomen reactief oppervlak van aluminium- en ijzer(hydr)oxyden na carbonatatie vermindert de uitloging van spoorelementen waarvan de concentraties in oplossing door sorptie worden bepaald. Sorptie aan Mn-(hydr)oxyden blijkt een aanvullend proces dat nodig is voor het modelmatig beschrijven van de uitloging van tweewaardige kationen, maar wordt niet beïnvloed door carbonatatie. Beschouwing van deze drie verschillende reactieve oppervlakken en (oppervlakte)precipitatie reacties heeft geresulteerd in een goede modelmatige beschrijving van de uitloging van oxyanionen en spoormetalen uit (gecarbonateerde) staalslak. Deze reactieve oppervlakken blijken dan ook een belangrijke invloed uit te oefenen op de milieuhygiënische eigenschappen van zowel verse als gecarbonateerde staalslak.

In **Hoofdstuk 4** worden de reactiemechanismen van het carbonateren van wollastoniet in waterige suspensie, als mogelijk vastleggingsproces voor koolstofdioxide, experimenteel onderzocht door middel van het systematisch variëren van reactietemperatuur, CO_2 druk, deeltjesgrootte, reactietijd, vloeistof-vaste stof verhouding en roervermogen. De carbonatatiereactie blijkt in twee stappen te verlopen via de waterige oplossing: (1) uitloging van calcium uit de wollastoniet matrix en (2) nucleatie en groei van calciet. De uitloging wordt gehinderd door een silicaatlaag rondom het wollastonietdeeltje. Deze laag wordt gevormd door het incongruent oplossen van calcium tijdens het carbonatatieproces. Twee temperatuurregimes blijken te kunnen worden geïdentificeerd. Bij temperaturen onder een optimale reactietemperatuur wordt de totale reactiesnelheid waarschijnlijk gelimiteerd door de snelheid van calciumuitloging. Bij hogere temperaturen limiteren nucleatie en groei van calciumcarbonaat waarschijnlijk de carbonatatie snelheid vanwege een verminderde (bi)carbonaat activiteit. De carbonatatie mechanismen van wollastoniet blijken vergelijkbaar te zijn met die van staalslak (Hoofdstuk 2) en het Mg-silicaat olivijn. De carbonatatie van wollastoniet verloopt echter relatief snel vergeleken met Mg-silicaten. De maximale omzettingsgraad is 70% binnen 15 minuten bij 200 °C, 20 bar CO_2 druk en een deeltjesgrootte <38 µm.

Het in **Hoofdstukken 2** - **4** verkregen inzicht in de reactiemechanismen vormt de basis voor de energetische en economische analyses van minerale CO_2 vastlegging in **Hoofdstukken 5** & **6**.

Het energieverbruik van een minerale CO_2 vastleggingsfabriek veroorzaakt extra CO_2 emissies en vermindert hiermee de netto hoeveelheid CO_2 die wordt vastgelegd in het proces. In **Hoofdstuk 5** wordt de energetische CO_2 vastleggingsefficiëntie (d.w.z., de fractie van CO_2 die effectief wordt vastgelegd)

van minerale CO_2 vastlegging onderzocht voor zowel wollastoniet als staalslak. Een stroomschema van een minerale CO_2 vastleggingsfabriek wordt ontworpen en het proces wordt gesimuleerd om de eigenschappen van stromen te bepalen, alsmede het elektriciet- en warmteverbruik van de procesapparatuur. De maximale energetische efficiëntie bij de bestudeerde procescondities is in geval van wollastoniet 75% bij 200 °C, 20 bar CO_2 en een deeltjesgrootte <38 µm. De belangrijkste energieverbruikende processtappen zijn het malen van de grondstof en het comprimeren van de CO_2 voeding. Bij deze procescondities wordt een significant lagere energetische efficiëntie gevonden voor staalslak (69%), voornamelijk vanwege het lagere calciumgehalte van deze grondstof. Het netto CO_2 vastleggingsrendement zou substantieel kunnen worden verbeterd voor beide grondstoffen door b.v. de hoeveelheid proceswater die wordt gebruikt te reduceren en de grondstof fijner te malen.

Hoofdstuk 6 richt zich op de kostenevaluatie van CO_2 vastlegging door middel van carbonatatie van wollastoniet of staalslak. Op basis van een ontwerp op hoofdlijnen van de belangrijkste procesapparatuur en gegevens die beschikbaar zijn in de openbare literatuur, worden de investeringskosten geraamd. Vervolgens worden de CO_2 vastleggingskosten berekend op basis van de afschrijvingskosten van de investering en de vaste en variabele bedrijfskosten. Geraamde kosten bedragen 102 en 77 €/ton vermeden CO_2 voor respectievelijk wollastoniet en staalslak. In geval van wollastoniet zijn de grootste kostenposten de grondstof en het elektriciteitsverbruik voor malen en comprimeren (respectievelijk, 54 en 26 €/ton vermeden CO_2). De vastleggingskosten zijn in het geval van staalslak significant lager vanwege de afwezigheid van kosten voor de grondstof. Een gevoeligheidsanalyse laat zien dat hiernaast de vloeistof-vaste stof verhouding in de carbonatatie reactor en de eventuele waarde van het gecarbonateerde product een grote invloed op de vastleggingskosten hebben.

In de **Epiloog** worden de belangrijkste conclusies van dit proefschrift samengevat en worden aanbevelingen gedaan voor verder onderzoek.

Dit proefschrift laat zien dat CO_2 vastlegging door carbonatatie van Ca-silicaten mogelijk is bij procescondities die technisch haalbaar lijken te zijn. Hoewel de energieconsumptie van huidige minerale CO_2 vastleggingsprocessen groot is, laten de geïdentificeerde mogelijkheden om de energetische efficiëntie te verbeteren zien dat minerale CO_2 vastlegging energetisch haalbaar kan worden na verdere technologieontwikkeling. Tot slot lijken de kosten van CO_2 vastlegging door carbonatatie van delfstoffen relatief hoog ten opzichte van zowel andere CO_2 opslagtechnologieën als (huidige) CO_2 marktprijzen. (Niche) toepassingen van minerale CO_2 vastlegging met een industriële reststof als

grondstof en/of een nuttig toepasbaar carbonatatie product met een substantiële waarde lijken een duidelijk beter perspectief te hebben op economische haalbaarheid.

Al met al is minerale CO_2 vastlegging (nog steeds) een langere termijn optie vergeleken met andere 'CO_2 afvangst & opslag'-technologieën en heeft deze optie relatief weinig potentieel op de korte termijn. Echter de mogelijkheden die geïdentificeerd zijn voor verdere procesontwikkeling, het permanente en inherent veilige karakter van de CO_2 opslag en de potentieel zeer grote vastleggingscapaciteit rechtvaardigen verder onderzoek naar minerale CO_2 vastlegging. Dit onderzoek dient zich primair te richten op kostenreductie, hetgeen noodzakelijk is om minerale CO_2 vastlegging onderdeel te laten worden van een breed portfolio aan inzetbare CO_2 reductie- en opslag-technologieën.

INTRODUCTION AND OUTLINE
OF THESIS
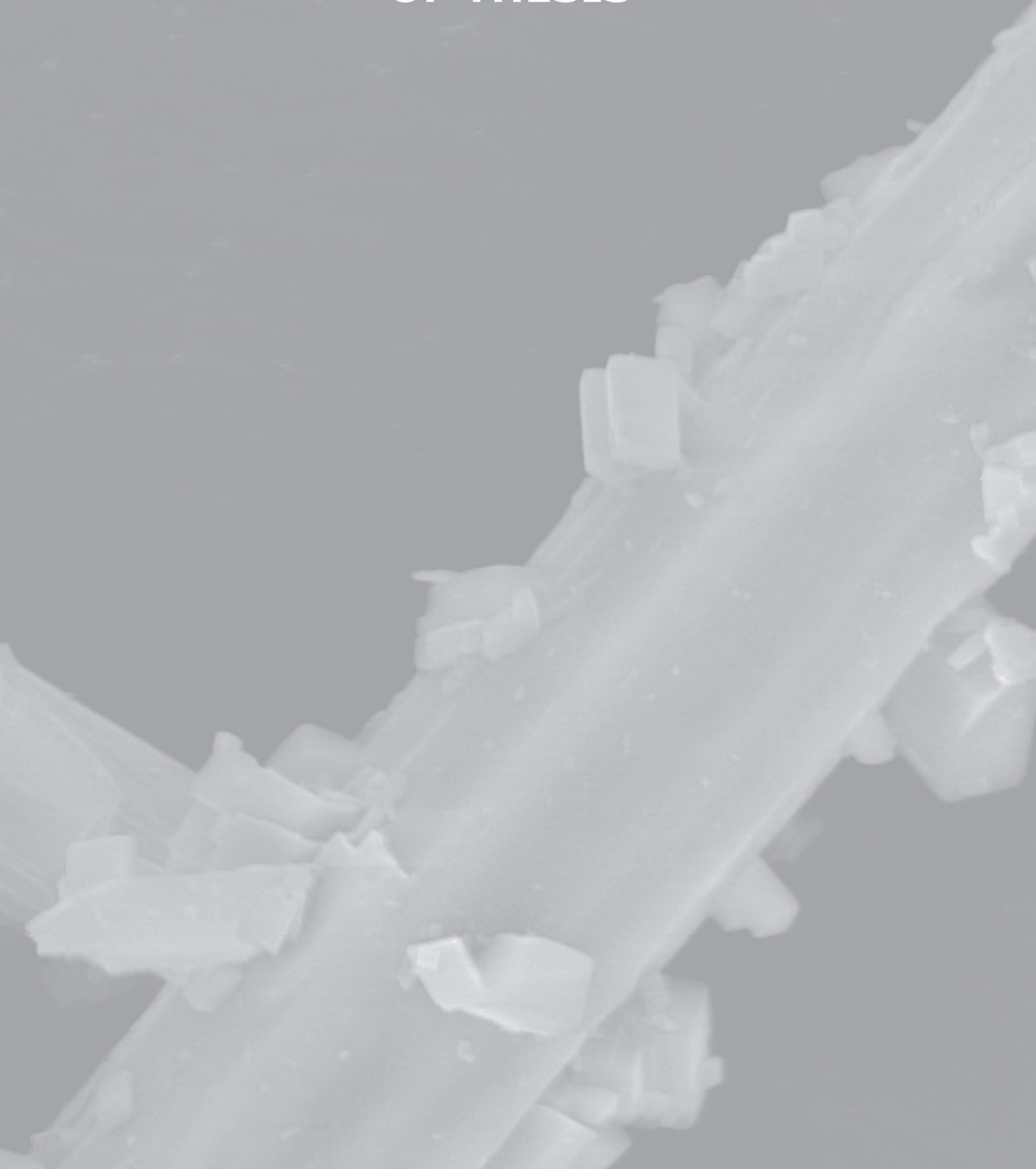
INTRODUCTION AND OUTLINE OF THESIS

Background

Today, there seems to be considerable scientific evidence that human activities may cause climate change due to the enhanced greenhouse effect (IPCC, 2001). The consequences of possible climate change include e.g. melting of polar ice caps and glaciers, a sea level rise, mainly due to thermal expansion of the ocean water, and increased extreme weather events (IPCC, 2001). Carbon dioxide (CO_2) is by far the largest contributor to the assumed enhanced greenhouse effect among the various greenhouse gases, such as CO_2, CH_4, N_2O, and halocarbons. The CO_2 emissions due to human activities are mainly caused by the use of fossil fuels for energy supply (IPCC, 2005). The global annual emission of CO_2 was about 23.5 Gt CO_2/yr in 2000 (IPCC, 2005). The concentration of CO_2 in the atmosphere has increased progressively since the beginning of the Industrial Age by about 30% from 280 (1750) to 367 ppm (1999) (IPCC, 2001).

In order to prevent a major climate change, the atmospheric CO_2 concentration should be stabilised by either increasing the (biological) CO_2 up-take from the atmosphere or reducing the CO_2 emissions. Three major approaches for reduction of CO_2 emissions can be distinguished: (1) reduction of the energy consumption based on fossil fuels, (2) energy generation by non-fossil sources such as solar, wind, biomass, and nuclear energy, and (3) carbon capture and storage (CCS). In CCS-technologies, CO_2 is separated from the flue gas of a stationary CO_2 source, such as a fossil fuel based power plant, and subsequently stored for long-term isolation from the atmosphere (IPCC, 2005).

Carbon Capture and Storage

Fossil fuels are still the main energy source and will probably continue to be so for the coming decades. First, the available reserves of oil, gas, and particularly coal are still large enough to provide energy to the world for the coming decades. In addition, renewable fuels will probably remain relatively expensive in the near future and energy saving will probably not have an impact large enough to substantially reduce the amount of CO_2 emitted into the atmosphere. Therefore, carbon capture and storage technologies are investigated to reduce CO_2 emissions in the relatively short term and to enable a transition to a sustainable future based on non-fossil energy sources. The aim of CCS is to

store the carbon dioxide released by the use of fossil fuels in order to prevent its emission into the atmosphere. CCS-technologies generally consist of three steps: capture, transportation, and storage.

Capture. Carbon dioxide in flue gases resulting from fossil fuel combustion is generally diluted due to the use of air for oxidation. Therefore, CO_2 separation from the flue gas is often required to avoid the storage of a large amount of N_2. A commercially available technology for CO_2 separation is absorption with monoethanolamine (MEA) followed by stripping with steam. This absorption technology in its current state is energy-intensive and costly (IPCC, 2005). To reduce the energy consumption, alternative technologies such as adsorption, membranes, and cryogenic separation are being developed (IEA Coal Research, 1999; IPCC, 2005). In addition, processes based on carbonation / calcination cycles are investigated to capture CO_2 (Abanades, 2002).

Transportation. CO_2 transportation from its source toward the storage site can be either performed by pipeline or by ships. Transportation of CO_2 on a large scale seems technically and economically feasible (IPCC, 2005).

Storage. Various possibilities have been investigated for CO_2 storage: geologic storage in depleted oil and gas fields, aquifers or coal bed seams, ocean storage, and mineral carbonation (Figure 0.1) (IPCC, 2005).
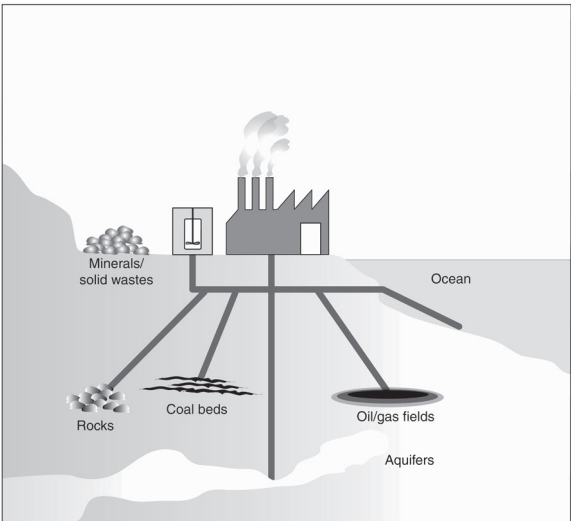
Figure 0.1: *CO_2 storage options (IEA GHG, 2001).*

Table 0.1 shows the estimated CO_2 storage capacity of various CCS-technologies.

Table 0.1: *Estimated CO_2 storage capacity of CCS-options.*

Option	Estimated global capacity [GtC][a]
Mineral carbonation	Very large [b]
Ocean storage	>1000 [c]
Geological storage	
Aquifers	275 - 2750 [d]
Depleted oil and gas fields	180 - 250 [d]
Unminable coals seams	1 - 55 [d]

[a] For comparison, yearly global CO_2 emission: 6 GtC/yr (IPCC, 2005). Proven economic coal reserves worldwide: >1000 Gt (Lackner, 2002). [b] No exact number can be given, but a vast potential for carbon sequestration in solid carbonated form can be expected (Dunsmore, 1992; IPCC, 2005). [c] Kohlmann (2001). Without adding alkalinity, the maximum capacity in oceans is limited to about 300-600 GtC (Lackner, 2002). [d] IPCC (2005). Aquifers numbers are uncertain.

Ocean storage has two major disadvantages: its potential environmental impact (i.e., change of ocean chemistry, pH decrease) and the temporary character of the storage (although CO_2 can be isolated from the atmosphere for centuries, eventually it will partially return to the atmosphere) (IPCC, 2005). Geological storage would require infinite continuous monitoring of the large amounts of concentrated CO_2 present, both because of possible slow leakage of CO_2 into the atmosphere as well as accidental rapid release of CO_2, which may cause health risks due to asphyxiation. An alternative CCS-technology that can potentially store large amounts of carbon dioxide in a safe, permanent, and environmentally benign manner is mineral carbonation.

Mineral Carbonation

CO_2 sequestration by mineral carbonation (often briefly called mineral CO_2 sequestration or CO_2 mineralization) is based on industrial imitation of natural weathering processes. In weathering processes, eroded rock surfaces come into contact with rainwater saturated with dissolved atmospheric CO_2. Subsequently, alkali and alkaline earth elements (e.g., Na, K, Ca, and Mg) dissolve into the water and, eventually, carbonate minerals may form. Over geological timescales, weathering processes have reduced the high atmospheric CO_2 concentrations present in the early-days of the earth to the levels of today and have thereby enabled live. Today, about 80% of all carbon in the world is present in the form of carbonate rocks (Dunsmore, 1992). If these weathering or carbonation processes could be enhanced and industrially applied, they could be used to bind gaseous carbon dioxide into a solid carbonate (a process also

called 'sequestration') and thus prevent the emission of CO_2 into the atmosphere.

The most straightforward carbonation reactions for, e.g., Ca or Mg-minerals are:

$$CaO\ (s) + CO_2\ (g) \rightarrow CaCO_3\ (s)\ (\Delta H_r = -179\ kJ/mol) \qquad (eq\ 0.1)$$
$$MgO\ (s) + CO_2\ (g) \rightarrow MgCO_3\ (s)\ (\Delta H_r = -118\ kJ/mol) \qquad (eq\ 0.2)$$
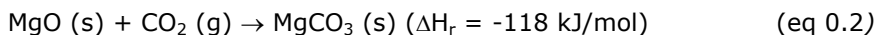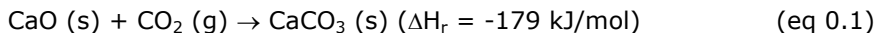
Since carbonate is the lowest energy-state of carbon, these carbonation reactions are exothermic (Lackner et al., 1995)[1]. However, pure magnesium and calcium (hydr)oxides are rare in nature and Mg and Ca occur typically as calcium and magnesium silicates. Thus, the general reaction involved in mineral CO_2 sequestration is:

$$(Ca/Mg)_xSi_yO_{x+2y+z}H_{2z}\ (s) + x\ CO_2\ (g) \rightarrow$$
$$x\ (Ca/Mg)CO_3\ (s) + y\ SiO_2\ (s) + z\ H_2O\ (l/g) \qquad (eq\ 0.3)$$
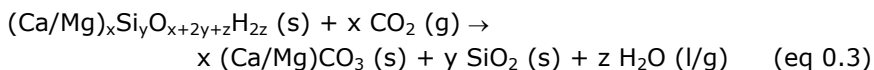
These reactions are still exothermic, but to a smaller extent than the carbonation of pure oxides. For example (Kojima et al., 1997):

$$CaSiO_3\ (s)\ (wollastonite) + CO_2\ (g) \rightarrow CaCO_3\ (s) + SiO_2\ (s)$$
$$(\Delta H_r = -87\ kJ/mol) \qquad (eq\ 0.4)$$
$$Mg_2SiO_4\ (s)\ (olivine) + 2\ CO_2\ (g) \rightarrow 2\ MgCO_3\ (s) + SiO_2\ (s)$$
$$(\Delta H_r = -90\ kJ/mol) \qquad (eq\ 0.5)$$
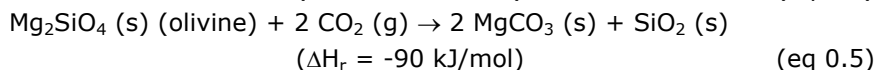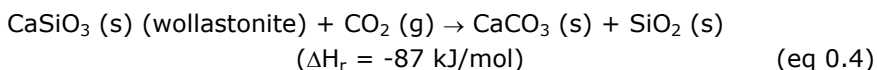
In addition to the use of natural mineral ores as feedstock for mineral CO_2 sequestration, also industrial residues such as slags and combustion ashes might be used (see §1.2.2). Figure 0.2 shows a schematic drawing of a mineral CO_2 sequestration process on the basis of both ore and residue carbonation. The carbonated product may be either used for mine reclamation, beneficially reused or disposed (land-filled).

---

[1] For comparison: C (s) + O_2 (g) $\rightarrow$ CO_2 (g) (ΔH_r = -394 kJ/mol) (Lackner et al., 1995).
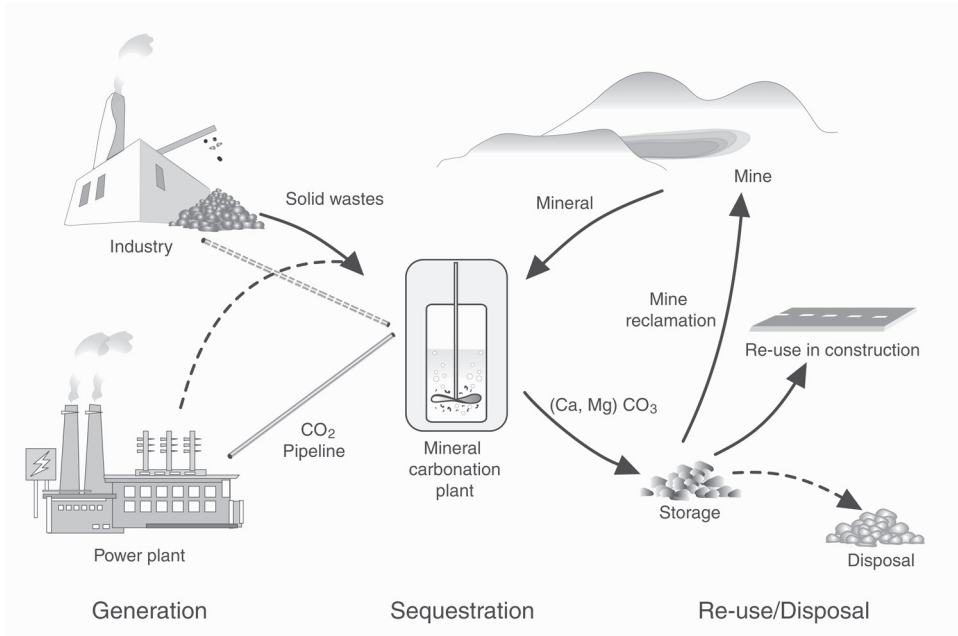
Figure 0.2: *Schematic drawing of a mineral CO$_2$ sequestration process.*

Compared to other carbon dioxide storage routes, mineral CO$_2$ sequestration has a number of advantages:

- Mineral carbonation is a chemical sequestration route of which the formed products are thermodynamically stable and environmentally benign. The formed mineral carbonates are end-products of geologic processes and are known to be stable over geological time periods. Therefore, the storage of CO$_2$ is permanent and inherently safe.
- The carbonation reaction is exothermic. The reaction energy may potentially be applied usefully.
- The potential CO$_2$ sequestration capacity of mineral carbonation is very large. Sufficient minerals can potentially be mined worldwide to sequester all future CO$_2$ emitted from fossil fuel combustion (Lackner et al., 1995).

Mineral carbonation is a relatively new CO$_2$ mitigation option. The idea was originally proposed in 1990 (Seifritz, 1990) and the first study on this concept was published in 1995 (Lackner et al., 1995). At the start of this PhD research in 2002, a relatively limited number of studies had been published on this technology and the technology was still in its infancy. It had become clear that a critical issue in the development of a CO$_2$ mineralization process was the enhancement of the carbonation reaction. Important research questions included the chemical and technical feasibility of enhancing mineral carbonation

processes, in order to make them suitable for industrial implementation. In addition, the energetic performance and costs of CO_2 sequestration by mineral carbonation were unclear. Finally, the re-use possibilities of carbonated materials resulting from mineral CO_2 sequestration had barely been studied.

Purpose and Content of this Thesis

The **aim** of this thesis is an:

> *Investigation of the Technical, Energetic, and Economic Feasibility of CO_2 Sequestration by Mineral Carbonation.*

More in particular, the first part of this thesis focuses on the reaction mechanisms of mineral carbonation processes. In this part, special attention is paid to the use of industrial solid residues as feedstock for mineral CO_2 sequestration and to the effect of carbonation on the leaching properties of these residues. In the second part of this thesis, the energetic performance and costs of CO_2 emission reduction by mineral carbonation are evaluated.

This thesis focuses solely on CO_2 sequestration by ex-situ (on the surface) mineral carbonation. Other approaches for CO_2 sequestration on the basis of carbonation, such as subsurface (in-situ) carbonation of rocks are left out of consideration (see also e.g. Lackner, 2002). Moreover, this study is limited to processes that use a solid feedstock as the source of alkalinity (e.g., Ca/Mg-silicates); potential alkaline liquid raw materials are ignored. Finally, only the sequestration step will be discussed; capture and transportation of CO_2 are outside the scope of this thesis.

The **outline** of this thesis is as follows:

Chapter 1 reviews the literature published on mineral carbonation. First, suitable solid raw materials are selected for further investigation. Second, an overview is given of various process routes proposed for mineral carbonation. These routes are reviewed and a process route is selected for further research. Meanwhile, the key issues to be addressed in further research on mineral carbonation are defined.
Chapters 2 and **3** focus on the use of industrial solid residues as feedstock for mineral CO_2 sequestration. **Chapter 2** studies the aqueous carbonation of steel slag. The influence of process conditions on the carbonation rate is investigated and the reaction mechanisms and rate-determining reaction steps are

determined. **Chapter 3** discusses the effect of carbonation on the leaching properties of steel slag. The consequences for the resulting environmental quality with respect to re-use possibilities are assessed and additional information on the carbonation mechanisms of particularly trace elements is obtained.

Chapter 4 deals with CO_2 sequestration by carbonation of the mineral ore wollastonite. In an experimental study, the reaction mechanisms of aqueous wollastonite carbonation are studied. A comparison between various possible feedstock for aqueous mineral carbonation is presented.

Chapters 5 and **6** present a system study of an aqueous mineral carbonation process. In these chapters the energetic and economic bottlenecks as well as possibilities for process improvement are identified. In **Chapter 5**, the energetic efficiency of mineral CO_2 sequestration using both wollastonite and steel slag as feedstock is studied and possibilities for further optimisation are evaluated. For these purposes, a mineral CO_2 sequestration plant is designed and simulated in order to determine the mass flows and energy consumption. **Chapter 6** presents a cost evaluation of CO_2 sequestration by mineral carbonation. The investment costs of a mineral carbonation plant are estimated and costs for CO_2 emission reduction by Ca-silicate carbonation are determined.

Finally, in the **Epilogue** the final conclusions on the feasibility of CO_2 sequestration by mineral carbonation are drawn and recommendations for further research are given.

CHAPTER 1

CARBON DIOXIDE SEQUESTRATION BY MINERAL CARBONATION: LITERATURE REVIEW

This chapter reviews literature on mineral CO_2 sequestration published before January 2005 and is a summary of ECN reports ECN-C--03-016 and ECN-C--05-022.

Huijgen, W.J.J. & Comans, R.N.J. (2003) *Carbon dioxide sequestration by mineral carbonation: Literature review*, ECN-C--03-016, Energy Research Centre of The Netherlands, Petten, The Netherlands.

International Energy Agency Greenhouse Gas program (IEA-GHG) (2005) *Carbon dioxide storage by mineral carbonation*, report PH05/11, Cheltenham, United Kingdom. Prepared by Huijgen, W.J.J. & Comans, R.N.J. (2005), Energy Research Centre of The Netherlands, Petten, The Netherlands.
(also published as: *Carbon dioxide sequestration by mineral carbonation: Literature review update 2003-2004*, ECN-C--05-022).

CARBON DIOXIDE SEQUESTRATION BY MINERAL CARBONATION: LITERATURE REVIEW

Wouter J.J. Huijgen[1] *& Rob N.J. Comans*[1,2]

In this chapter, a mineral carbonation process and a solid feedstock are selected for further research, by reviewing literature on mineral CO_2 sequestration. Among the elements that can potentially be carbonated, Ca and Mg hold best prospects due to their abundant occurrence and the stability of the carbonates formed. Two types of feedstock that contain these elements in a substantial amount are mineral ores (Ca/Mg-silicates) and industrial residues. From these two categories, wollastonite ($CaSiO_3$) and steel slag are selected for further research. A large number of process routes for mineral CO_2 sequestration has been developed including possible pre-treatment of the solid feedstock. Two main types of process routes can be distinguished: direct routes in which the mineral is carbonated in a single step and indirect routes in which the reactive components are first extracted from the mineral matrix and then carbonated in a separate step. Pre-treatment of the solid feedstock by e.g. size reduction has been reported to result in a major improvement of the carbonation rate. The most promising route available appears to be the direct aqueous carbonation route (i.e., carbonation of a Mg/Ca-silicate in an aqueous solution at elevated temperature and CO_2 pressure). Key issues for further research are the reaction rates and mechanisms and the energy consumption and costs of mineral CO_2 sequestration. Other important aspects of mineral carbonation are the transport of the materials involved and the destination of the products.

---

[1] Energy Research Centre of The Netherlands.
[2] Wageningen University.

1.1   Introduction

Ex-situ mineral carbonation is a process to sequester CO_2 on the basis of the imitation of natural weathering processes (see Introduction). Mineral CO_2 sequestration is a relatively new research area. The possibility to apply mineral carbonation for CO_2 emission reduction was first put forward by Seifritz (1990). The first studies on this concept were performed at Los Alamos National Laboratory (LANL) from 1995 (Lackner et al., 1995). Since 1995, mineral CO_2 sequestration has been studied with increasing interest worldwide, which is reflected by the large increase in literature published on this subject in the last few years.

A few earlier review studies on mineral carbonation processes have been published. In his review on 'carbonate chemistry for sequestering fossil carbon' Lackner discussed a few possible process routes aiming at the storage of CO_2 as a stable carbonate (Lackner, 2002), but, unfortunately, these routes were not compared. Haywood et al. compared six mineral carbon sequestration routes and concluded that all routes were environmentally unacceptable (Haywood et al., 2001). Newall et al. came to the same conclusions on the basis of both environmental and cost analyses of various mineral sequestration technologies (IEA GHG, 2000). However, in recent years research on mineral carbonation has made significant progress and some new alternative process routes for mineral carbonation have emerged (particularly, the 'direct aqueous carbonation route', §1.3.2). Therefore, a new review of mineral carbonation research is warranted.

By reviewing the literature on mineral CO_2 sequestration, this chapter aims at:
- (1) Selection of a solid feedstock for further mineral carbonation research (section 1.2).
- (2) Selection of the mineral carbonation process route that holds best prospects for this research (sections 1.3 and 1.4).
- (3) Discussion of other issues to be addressed in further research on mineral carbonation (section 1.5).

This chapter gives a short review of the literature published on mineral CO_2 sequestration. For a more extensive overview of this literature, we here refer to the ECN reports that form the basis of this chapter (ECN-C--03-016 & ECN-C--05-022).

1.2   Selection Solid Feedstock

The selection of solid feedstock suitable for mineral CO_2 sequestration is performed in two steps: first, suitable elements that can potentially be carbonated are selected and, second, minerals that contain these elements.

1.2.1   Selection Element

Both alkali (e.g., Na, K) and alkaline earth (e.g., Ca, Mg) metals as well as a number of other metals (e.g., Mn, Fe, Co, Ni, Cu, and Zn) can potentially be carbonated. However, most of the latter elements are either too rare or too valuable to be suitable as feedstock for mineral carbonation. Iron is available in a substantial amount, but carbonating of this metal implies consuming valuable iron ore. In addition, alkali metals are unsuitable, since alkali (bi)carbonates are too soluble for long-term CO_2 sequestration (i.e., upon dissolution CO_2 will return to the atmosphere). Of the alkaline earth metals, calcium and magnesium are by far the most common in nature. Magnesium and calcium comprise ~2.0 and 2.1 mol% of the earth's crust, respectively (Goff & Lackner, 1998). Therefore, calcium and magnesium are selected as the most suitable elements to be carbonated for CO_2 sequestration purposes.

1.2.2   Selection Mineral

Two types of feedstock for mineral CO_2 sequestration that may contain a significant amount of Ca/Mg can be distinguished: mineral ores (primary minerals) and industrial residues (secondary materials).

Calcium and Magnesium Ores. Not all calcium and magnesium minerals provide the alkalinity required for the reaction with acid CO_2. Alkalinity is typically derived from (hydr)oxides or silicates, which can be shown by their dissolution reactions, e.g.:

$$CaO \text{ (s) (lime)} + H_2O \text{ (l)} \rightarrow Ca^{2+} \text{ (aq)} + 2\ OH^- \text{ (aq)} \qquad \text{(eq 1.1)}$$
$$Mg_2SiO_4 \text{ (s) (olivine)} + 2\ H_2O \text{ (l)} \rightarrow$$
$$2\ Mg^{2+} \text{ (aq)} + SiO_2 \text{ (s)} + 4\ OH^- \text{ (aq)} \qquad \text{(eq 1.2)}$$
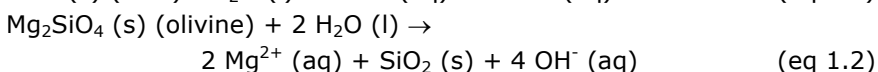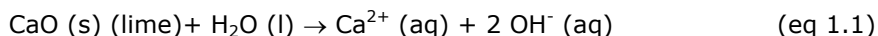
Other (weaker) sources of alkalinity are carbonates, which can be illustrated by the dissolution of calcite and the subsequent second dissociation step of carbonic acid.

$$CaCO_3 \text{ (s)} \rightarrow Ca^{2+} \text{ (aq)} + CO_3^{2-} \text{ (aq)} \qquad \text{(eq 1.3)}$$
$$CO_3^{2-} \text{ (aq)} + H_2O \text{ (l)} \leftrightarrow HCO_3^{-} \text{ (aq)} + OH^{-} \text{ (aq)} \qquad \text{(eq 1.4)}$$
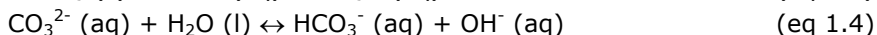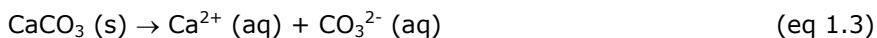
Although, in principle, it is easier to convert carbonates into bicarbonates than to form carbonates from silicates (Lackner, 2002), carbonates are not suitable to be used as feedstock for ex-situ mineral carbonation. Controlled storage is namely only possible for carbonates, because bicarbonates are fairly soluble in water, while (Ca and Mg) carbonates have a much lower solubility. Thus, part of the sequestered carbon dioxide might be released, when bicarbonates come into contact with rainwater.

Therefore, mineral carbonation processes preferably end at the carbonate stage. The most simple carbonation reactions for calcium and magnesium minerals are:

$$CaO \text{ (s)} + CO_2 \text{ (g)} \rightarrow CaCO_3 \text{ (s)} \ (\Delta H_r = -179 \text{ kJ/mol}) \qquad \text{(eq 1.5)}$$
$$MgO \text{ (s)} + CO_2 \text{ (g)} \rightarrow MgCO_3 \text{ (s)} \ (\Delta H_r = -118 \text{ kJ/mol}) \qquad \text{(eq 1.6)}$$
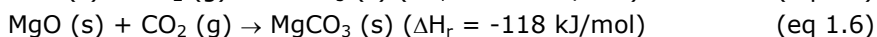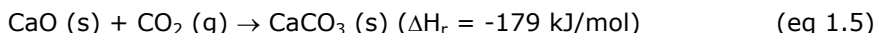
These carbonation reactions are exothermic, since carbonate is the lowest energy-state of carbon (Lackner et al., 1995). However, calcium and magnesium rarely occur as binary oxides in nature. They are typically found in silicate minerals. These minerals are also capable of being carbonated because carbonic acid is a stronger acid than silicic acid (H_4SiO_4). Thus, silica present in the mineral is exchanged with carbonate and the mineral is carbonated. Therefore, the principal reaction involved in mineral CO_2 sequestration is:

$$(Ca,Mg)_xSi_yO_{x+2y+z}H_{2z} \text{ (s)} + x \ CO_2 \text{ (g)} \rightarrow$$
$$x \ (Ca,Mg)CO_3 \text{ (s)} + y \ SiO_2 \text{ (s)} + z \ H_2O \text{ (l/g)} \qquad \text{(eq 1.7)}$$
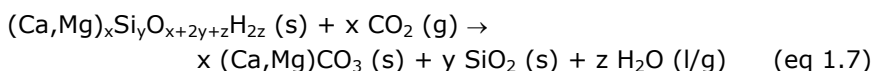
These reactions are still exothermic, but to a lesser extent than the carbonation of pure oxides. For example (Lackner et al., 1995):

$$CaSiO_3 \text{ (s)} + CO_2 \text{ (g)} \rightarrow CaCO_3 \text{ (s)} + SiO_2 \text{ (s)}$$
$$(\Delta H_r = -87 \text{ kJ/mol}) \qquad \text{(eq 1.8)}$$
$$Mg_2SiO_4 \text{ (s)} + 2 \ CO_2 \text{ (g)} \rightarrow 2 \ MgCO_3 \text{ (s)} + SiO_2 \text{ (s)}$$
$$(\Delta H_r = -90 \text{ kJ/mol}) \qquad \text{(eq 1.9)}$$
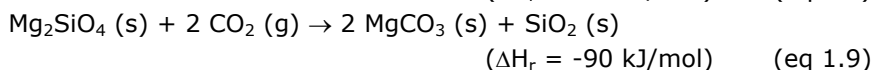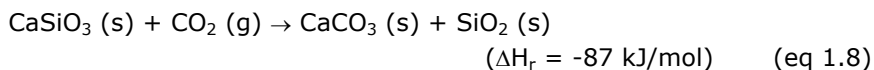
These Ca/Mg-silicate minerals can be obtained from e.g. igneous rocks, which are particularly suitable for CO_2 fixation because they are essentially free of carbonates. The main candidate magnesium-rich ultramafic rocks are dunites, peridotites, and serpentinites. The first two can be mined for olivine, a solid solution of forsterite (Mg_2SiO_4) and fayalite (Fe_2SiO_4). Ore grade olivine may also contain alteration products, such as serpentine ($Mg_3Si_2O_5(OH)_4$) and talc

$(Mg_3Si_4O_{10}(OH)_2)$. Serpentine mined from serpentinite rock can take the form of antigorite, lizardite, and chrysotile. The main calcium-containing candidate ore is wollastonite ($CaSiO_3$). Basalt, which is also rich in calcium, is ubiquitous, but it is difficult to extract the reactive components from this mineral matrix (Lackner, 2002). As an example, the composition of some candidate rocks and minerals and their specific CO_2 sequestration capacity are given in Table 1.1.

Table 1.1: *Composition of some selected rocks and pure minerals and their potential carbon dioxide sequestration capacity.*

Rock Mineral	MgO [wt%]	CaO [wt%]	R_{CO2} [kg/kg] [a]
Serpentinite [b]	~40	~0	~2.3
Serpentine, Mg₃Si₂O₅(OH)₄	48.6		1.9
Dunite [b]	49.5	0.3	1.8
Olivine, Mg₂SiO₄	57.3		1.6
Wollastonite [c]	0.8	43.7	2.9
Wollastonite, CaSiO₃		48.3	2.6
Talc [c]	34.7	0.0	2.6
Talc, Mg₃Si₄O₁₀(OH)₂	31.9		2.9
Basalt [b]	6.2	9.4	7.1

[a] R_{CO2} = mass ratio of rock to CO_2 required for CO_2 sequestration. [b] (Lackner, 2002).
[c] (Wu et al., 2001).

Los Alamos National Laboratory has investigated the suitability, amounts, and occurrence of ultramafic rocks (i.e., Ca/Mg-silicates), mainly within the USA, for mineral CO_2 sequestration (Goff & Lackner, 1998; Goff et al., 2002). Particularly serpentine is found in large deposits worldwide. Large reservoirs are known, for example, on both the East and West Coast of North America and in Scandinavia. Studies have been performed at individual peridotite / serpentinite bodies. Two selected reservoirs in the United States are Twin Sisters, Washington, and Wilbur Springs, California, which are individually capable of sequestering the globally emitted carbon dioxide for 2 and 5 years, respectively (Goff & Lackner, 1998). In recent years, an extensive source and sink mapping has been made for the USA (O'Connor et al., 2005) and a first start has been published for British Colombia, Canada (Voormeij et al., 2004). However, for the rest of the world only limited or no information is available. A major gap in mineral CO_2 sequestration research appears to be a worldwide evaluation of the amount and occurrence of silicate ores that can (cost-)effectively be excavated for mineral CO_2 sequestration.

Among the Ca/Mg-silicates, Mg-silicates have the advantage of being available worldwide in large amounts and in relatively high purity compared to

Ca-silicates. In addition, Mg has a lower molar weight (24.31 vs. 40.08 g/mol) and thus the amount of oxide required to bind carbon dioxide from burning one ton of carbon favours magnesium oxide at 3.3 ton compared to 4.7 ton for calcium oxide. Of the main Mg-silicates, serpentine has the disadvantage of requiring an (energy-consuming) pre-treatment step to become sufficiently reactive for carbonation (section 1.3.1). Therefore, olivine seems to be the most suitable Mg-silicate mineral.

The advantage of Ca-silicates is that they tend to be more reactive towards carbonation than Mg-silicates. However, wollastonite resources are relatively small (Lackner, 2002). If a significant fraction of the future emissions of carbon dioxide would be sequestered using the mineral route, the use of Mg-silicates seems to be the only option. However, on a smaller scale the use of wollastonite as feedstock appears to be interesting, since it can facilitate the realisation of a first industrial process. Since the key issue in mineral carbonation research is enhancement of the carbonation rate, we have chosen to use Ca-silicates, and more in particular wollastonite, for further investigation (see also Chapter 4).

Residues. An alternative feedstock for mineral carbonation is solid industrial residues, of which some examples are given in Table 1.2. In general, the selected materials are by-products of (combustion) processes at high temperatures or construction residues.

Table 1.2: *Examples of solid residues potentially suitable for mineral carbonation.*

Residue group	Example
Ash	MSWI bottom ash [a]
Slag	Coal slag
	Steel slag
	Blast furnace slag
Fly ash	Coal fly ash
	MSWI fly ash
APC residue [b]	MSWI APC residue
Construction and demolition waste	Cement
	Concrete
Other	Mine tailings

[a] Municipal solid waste incinerator. [b] Air pollution control.

Solid industrial residues are generally alkaline, inorganic, and rich in Ca (and possibly Mg) and can therefore be applied as an additional feedstock for mineral CO_2 sequestration. Residues tend to have a number of advantages compared to ores, e.g., their availability in industrial areas, low costs, and possibly higher reactivity due to their (geo)chemical instability. Since in alkaline solid wastes

calcium minerals are the prominent alkaline compounds, it can be expected that the carbonation of wastes is a faster process than that of predominantly magnesium-containing minerals. In addition, owing to its relatively open structure, the reactive surface area of, for example, municipal solid waste incinerator bottom ash is probably larger than that of primary minerals. The availability of suitable industrial residues is limited compared to ores. Solid residues seem particularly suitable for niche applications, such as at steel plants and municipal solid waste incinerators, where both the residue and carbon dioxide are present.

Because of the large number and variety of industrial residues, a selection of potentially suitable residues for mineral carbon dioxide sequestration has been made for the Dutch context on the basis of the following requirements (Huijgen & Comans, 2005) (for more details, we refer to the original report):
- The residue is solid.
- The residue is of inorganic nature.
- The residue is alkaline (pH>8).
- The residue contains non-carbonated calcium minerals in an available form (i.e., for reaction with CO_2).
- The residue is generated (or otherwise available) in The Netherlands.
- The residue has a high potential CO_2 sequestration capacity per unit of mass.
  A high specific CO_2 sequestration capacity reduces the amount of material that has to be processed to sequester a certain amount of carbon dioxide.
- The residue represents a high potential *total* CO_2 sequestration capacity in The Netherlands.
  A high total CO_2 sequestration capacity enables a larger contribution to the reduction of CO_2 emissions. In addition, given the variable composition of residues, the optimal process conditions for the various residues do probably also differ. For reasons of 'economy of scale', it is preferable to develop carbon sequestration routes for residues that are available in sufficiently large amounts.

On the basis of these requirements, steel slag was selected for the first studies on mineral carbonation because of its high potential carbon dioxide sequestration capacity (Chapters 2 & 3). Later on, MSWI bottom ash and construction and demolition waste may be used because of the large amount in which these materials are generated within The Netherlands.

1.3   Process Routes Mineral Carbonation

Many different process routes for mineral CO_2 sequestration have been described in the literature. Some of them include a pre-treatment of the solid feedstock. The pre-treatment options are discussed first (section 1.3.1), followed by a description of the mineral carbonation routes. Two main types of routes are distinguished:

1. Direct routes in which the mineral is carbonated in a single process step (section 1.3.2.).
2. Indirect routes in which the reactive components (i.e., Ca or Mg) are first extracted from the mineral matrix and then carbonated in a separate step (section 1.3.3).

Process routes for other feedstock than Ca/Mg-silicate ores are discussed in section 1.3.4. Finally, in section 1.5 process routes are compared with each other and a selection of a process route is made.

1.3.1   Pre-treatment Feedstock

Various options for pre-treatment of the solid feedstock, aimed at an increase of the carbonation rate, have been investigated. Size reduction, heat activation, surface activation techniques, and magnetic separation are individually described below, followed by other pre-treatment options.

Size Reduction. In order to increase the reaction rate, the minerals can be ground since the reaction rate typically increases with the surface area. Among many others, O'Connor et al. examined the influence of particle size on the conversion (O'Connor et al., 2000 & 2005). These authors found that a reduction from 106-150 µm to <37 µm increased the conversion in their experiments from 10 to 90% (O'Connor et al., 2000). However, grinding consumes energy and, thereby, causes extra CO_2 emissions. For example, Kojima and co-workers estimated that an extra 18.7 kg CO_2 has to be sequestered to crush 1 ton of wollastonite ore from 0.2 m to 75 µm in their process (Kojima et al., 1997) (1 ton wollastonite ore can potentially sequester 278 kg CO_2 (Wu et al., 2001)).

In addition to conventional grinding, other types of grinding have been investigated. High-energy attrition grinding can be used to induce imperfections into the crystal lattice (Gerdemann et al., 2002; O'Connor et al., 2002a), which results in a higher conversion than size reduction to the same diameter using conventional grinding (during attrition grinding, the sample is stirred in a chamber filled with small stainless steel balls). Attrition grinding, however, is

energy intensive and difficult to conduct on a large scale (Gerdemann et al., 2002).

The grinding step and the carbonation reaction can be integrated in a so-called mechanochemical process (Nelson, 2004). Thus, the carbonation reaction potentially proceeds rapidly because fresh surface area is continuously created during the carbonation process. In addition, process costs are potentially lower due to a simplification of the process design. Research performed on this approach, however, has not succeeded in significant carbonation of various silicate minerals so far (Nelson, 2004).

Heat Activation. Serpentine ($Mg_3Si_2O_5(OH)_4$) contains up to 13wt% chemically bound water. Thermal activation was studied to activate serpentine for carbonation. By heating the serpentine to typically 600-650 °C, the hydroxyl groups are removed and an open structure is created (O'Connor et al., 2000). For example, the specific surface area of antigorite was reported to increase from 8.5 to 18.7 m^2/g by heat treatment (NETL, 2001). Thus, a significant improvement of the carbonation rate has been obtained. However, heat-treatment is energy intensive (i.e., ~200-300 kWh/ton serpentine) resulting in a process that sequesters negative amounts of CO_2 (O'Connor et al., 2001a & 2004). At the moment, there seems to be general consensus that heat activation is infeasible from an energetic point-of-view and this pre-treatment option should therefore not be applied (O'Connor et al., 2005).

Surface Activation Techniques. In so-called surface activation techniques the specific surface area of a mineral is increased by treatment with acids, steam (NETL, 2001) or supercritical water (O'Connor et al., 2000). Also combinations of steam treatment and chemical activation by acids (e.g., sulphuric or nitric acid) have been investigated (e.g., Maroto-Valer et al., 2002b & 2004a). Thus, the specific surface area of serpentine was increased from 8 to 330 m^2/g resulting in an increase of the reactivity (Maroto-Valer et al., 2002a). In addition to increased sequestration costs, a possible drawback of chemical activation is a reduction of the Mg-content of the feedstock due to leaching (Maroto-Valer et al., 2001).

Magnetic Separation. If Fe is present in an ore such as olivine, the oxidation of iron may slow down the carbonation of serpentine due to the formation of a layer of hematite on the mineral surface (Fauth et al., 2000). Execution of the process in a non-oxidising atmosphere complicates the process and increases the costs significantly. Magnetic separation of the iron compounds prior to the carbonation process could help to resolve this complication (NETL, 2001).

Furthermore, a potentially marketable iron ore by-product may be formed (O'Connor et al., 2001a).

Other Pre-treatment Options. Many other pre-treatment options have been investigated, but did not result in a higher reactivity, such as ultrasonic pre-treatment of olivine (O'Connor et al., 2001a) and chemical pre-treatment steps combined with size reduction. Among the latter, wet grinding in a caustic solution (1M NaOH, 1M NaCl) was found to be most effective, but still insufficient to achieve a reasonable reaction rate (O'Connor et al., 2001a).

Conclusion. The only available pre-treatment option that has proven to be energetically and potentially economically feasible is conventional grinding (O'Connor et al., 2005). In particular, thermal treatment is very energy-consuming and should, if possible, be avoided. The feasibility of chemical activation methods is unclear and needs further investigation. In any case, the benefits of all pre-treatment options should be balanced by their extra costs and energy consumption.

1.3.2   Direct Carbonation Mg/Ca-Ores

Direct carbonation of a mineral in a single process step can be reached in two major ways: through a direct dry gas-solid reaction or in an aqueous solution. These routes are discussed below.

Direct Gas-Solid Carbonation

Ca/Mg-Silicates. The most straightforward approach for mineral carbonation is direct gas-solid carbonation of Ca/Mg-silicates:

$$Ca/Mg\text{-silicate (s)} + CO_2 \text{ (g)} \rightarrow (Ca/Mg)CO_3 \text{ (s)} + SiO_2 \text{ (s)} \qquad \text{(eq 1.10)}$$

Or, for example in the case of olivine:

$$Mg_2SiO_4 \text{ (s)} + 2\ CO_2 \text{ (g)} \rightarrow 2\ MgCO_3 \text{ (s)} + SiO_2 \text{ (s)} \qquad \text{(eq 1.11)}$$
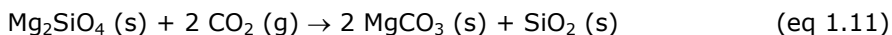
Direct gas-solid carbonation was studied in the beginning of mineral carbonation research (Lackner et al., 1995 & 1997). Major advantages of this process route over three-phase carbonation processes are its simple process design and a better ability to apply the reaction heat generated by the carbonation reaction. The carbonation of Ca/Mg-silicates, however, proceeds very slowly at room temperature and pressure (Lackner et al., 1995 & 1997). An increase of the

temperature and CO_2 pressure, possibly to supercritical conditions (Zevenhoven & Kohlmann, 2002), is required to obtain reasonable reaction rates (e.g., for serpentinite, 30% conversion was reported at T = 300 °C and p_{CO2} = 340 bar (Lackner et al., 1997)). However, the possible increase of the temperature is thermodynamically restricted because the chemical equilibrium favours gaseous CO_2 over solid-bound CO_2 at high temperatures due to entropy effects. The maximum temperature at which the carbonation occurs spontaneously depends on the CO_2 pressure and the type of mineral (Table 1.3).

Table 1.3: *Maximum allowable reaction temperature at corresponding pressure for a number of minerals (Lackner et al., 1995).*

Mineral	T_{max} [°C]	p_{CO2} [bar]
Calcium oxide (CaO)	888	1
	1397	200
Magnesium oxide (MgO)	407	1
	657	200
Calcium hydroxide (Ca(OH)$_2$)	888 (T_{deh}= 518) [a]	1
Magnesium hydroxide (Mg(OH)$_2$)	407 (T_{deh}= 265)	1
Wollastonite (CaSiO$_3$)	281	1
Forsterite (olivine) (Mg$_2$SiO$_4$)	242	1
Chrysotile (serpentine) (Mg$_3$Si$_2$O$_5$(OH)$_4$)	407 (T_{deh}= 535)	1

[a] T_{deh} is the temperature above which the mineral dehydrates.

The direct gas-solid mineral carbonation process has been studied extensively (e.g., Chizmeshya et al., 2002; Koljonen et al., 2004; Teir et al., 2004; Zevenhoven & Kavaliauskaite, 2004). Recently, an exergy analysis of direct dry carbonation of Mg-silicates has showed that this process can result in a net overall exothermic heat effect (Zevenhoven & Kavaliauskaite, 2004). However, the authors' conclusion that the rate of direct mineral carbonation is the most urgent problem to be resolved can only be underlined. Activation of the feedstock by heat treatment can significantly improve the carbonation rate, but is very energy-consuming (Zevenhoven & Kohlmann, 2002; Zevenhoven & Teir, 2004) (see also §1.3.1). In recent years, research at most institutes has moved away from direct gas-solid carbonation to other approaches and it can be concluded that the direct carbonation of Ca/Mg-silicates probably does not hold prospects to become an industrially viable process.

Ca/Mg-(Hydr)Oxides. Direct dry carbonation of Mg(OH)$_2$ has been studied in detail at Los Alamos National Laboratory (Butt et al., 1996 & 1998) and Arizona State University (McKelvy et al., 2001; Bearat et al., 2002; Sharma et al., 2004). The overall reaction consists of two steps:

$$Mg(OH)_2 \text{ (s)} \rightarrow MgO \text{ (s)} + H_2O \text{ (g) (dehydroxylation)} \qquad \text{(eq 1.12)}$$
$$MgO \text{ (s)} + CO_2 \text{ (g)} \rightarrow MgCO_3 \text{ (s) (carbonation)} \qquad \text{(eq 1.13)}$$
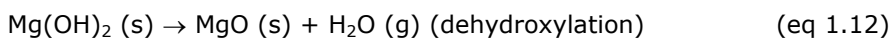
The first step is an equilibrium reaction and can also proceed backwards:

$$MgO \text{ (s)} + H_2O \text{ (g)} \rightarrow Mg(OH)_2 \text{ (s) (rehydroxylation)} \qquad \text{(eq 1.14)}$$
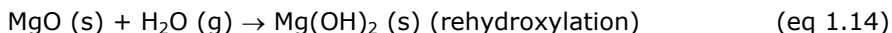
Research has focused on the dehydroxylation/rehydroxylation reactions of magnesium hydroxide, because control of these reactions can speed up the carbonation process further (Butt et al., 1996). The net activation energy of the combined carbonation and dehydroxylation reaction is 304 kJ/mol. The optimum temperature determined was 375 °C. At this temperature the reaction proceeds rapidly and the carbonated product is favoured thermodynamically (Butt et al., 1996). During the reactions a thin layer of the carbonate product is formed, which acts as a diffusion barrier to both the outward diffusion of H_2O and the inward diffusion of CO_2. Thus both dehydroxylation and carbonation are hindered resulting in a reduction of the reaction speed (Butt et al., 1998).

Direct gas-solid carbonation of Ca/Mg-(hydr)oxides proceeds much faster than for Ca/Mg-silicates and can be fast enough for an industrial process, although a high temperature and CO_2 pressure are required in case of $Mg(OH)_2$ (e.g., 100% conversion of $Mg(OH)_2$ was reported at 500 °C and 340 bar CO_2 within 2h (Lackner et al., 1997)). Thus, direct gas-solid carbonation of Ca/Mg-(hydr)-oxides can be considered as a feasible process step. However, since Ca/Mg-(hydr)oxides do not occur in a significant amount in nature (section 1.2), these would have to be produced from Ca/Mg-silicates. The conversion of Ca/Mg-silicates into hydroxides (i.e., indirect carbonation) is discussed further in section 1.3.3.

Direct Aqueous Carbonation

As can be learned from natural weathering processes, the presence of water significantly enhances the reaction rate of carbonation processes. A process developed on the basis of this principle is the direct aqueous carbonation route (O'Connor et al., 2000), in which a Ca/Mg-silicate is carbonated in an aqueous suspension.

The aqueous carbonation process consists of three steps, which take place simultaneously in a single reactor. First, carbon dioxide dissolves into the water phase and dissociates to bicarbonate and H^+, resulting in a mildly acidic environment with HCO_3^- as the dominant carbonate species:

$$CO_2 \text{ (g)} + H_2O \text{ (l)} \rightarrow H_2CO_3 \text{ (aq)} \rightarrow H^+ \text{ (aq)} + HCO_3^- \text{ (aq)} \qquad \text{(eq 1.15)}$$
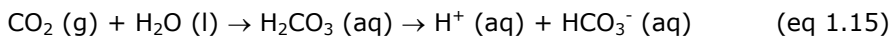
Secondly, Ca/Mg leaches from the mineral matrix, facilitated by the protons present:

$$Ca/Mg\text{-silicate (s)} + 2\ H^+ \text{ (aq)} \rightarrow$$
$$(Ca/Mg)^{2+} \text{ (aq)} + SiO_2 \text{ (s)} + H_2O \text{ (l)} \qquad \text{(eq 1.16)}$$
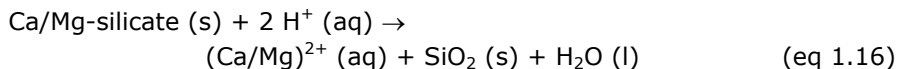
Finally, magnesium or calcium carbonate precipitates:

$$(Ca/Mg)^{2+} \text{ (aq)} + HCO_3^- \text{ (aq)} \rightarrow (Ca/Mg)CO_3 \text{ (s)} + H^+ \text{ (aq)} \qquad \text{(eq 1.17)}$$

A large amount of work has been done on this process route in the period 2000-2004 by a number of research institutes around the world (e.g., Carey et al., 2003; McKelvy et al., 2003; Schulze et al., 2004; O'Connor et al., 2005). A first step taken to maximise the reaction rate of the aqueous carbonation process are studies on the influence of process conditions such as particle size, temperature, and CO_2 pressure. In case of aqueous carbonation, the enhancement of reaction rates upon a temperature increase is counteracted by a solubility decrease of carbon dioxide in the water phase. These effects result in an optimum temperature, e.g., 185 °C (p_{CO2} = 152 bar) and 155 °C (p_{CO2} = 116 bar) for olivine and heat-treated serpentine, respectively (Gerdemann et al., 2002; O'Connor et al., 2005). Examples of conversions published are 91% in 24 h (olivine) (O'Connor et al., 2001b), 34% in 24 h (serpentine) (O'Connor et al., 2001b), and 82% in 1 h (wollastonite) (O'Connor et al., 2005) (80% of feedstock ground to <38 µm). Since wollastonite reacts faster than Mg-silicates, a lower CO_2 pressure (typically, 10-40 bar instead of 100-175 bar) was found to be required to obtain a substantial conversion (O'Connor et al., 2005).

For further increase of the carbonation rate, the reaction mechanisms of direct aqueous carbonation and the corresponding rate-limiting reaction step have been investigated. Research using different feedstock, i.e., olivine (O'Connor et al., 2002b; Chizmeshya et al., 2003 & 2004) and serpentine (O'Connor et al., 2002b; Schulze et al., 2004), has shown that aqueous carbonation of Mg-silicates occurs in two steps rather than single step solid-state conversion, i.e., (1) dissolution of Mg and (2) precipitation of Mg-carbonate. At typical process conditions, the rate-determining reaction step is the leaching of Mg from Mg-silicates. However, at specific process conditions (e.g., high temperature and/or low CO_2 pressure), the carbonation may become limited by inhibition of growth or suppression of nucleation of the carbonate (Carey et al., 2003).

The dissolution rate differs among the various minerals. Olivine, for example, dissolves faster than lizardite (NETL, 2001). Another important factor is the possible formation of a silica-enriched layer on the dissolving particles, which reduces the leaching rate (e.g., Wu et al., 2001). This layer is formed by incongruent dissolution (NETL, 2001), during which calcium and magnesium dissolve into the solution, while other parts of the matrix (e.g., Si) remain in the solid form. The structure, composition and dissolution mechanisms of the SiO_2-rim hindering further carbonation have been studied (Chizmeshya et al., 2004).

The mechanisms of aqueous mineral carbonation indicate that an increase of the dissolution and carbonation rates could be accomplished by, for example, an increase of the specific surface area, removal of the SiO_2-layer and lowering the $(Ca,Mg)^{2+}$-activity in solution. Published options are pre-treatment of the silicate ore (see §1.3.1), the application of additives (salts, complexing agents, acids or bases), and non-chemical removal of the developed SiO_2-layer.

Salt additives that have been used in carbonation studies include NaCl, $NaHCO_3$, and $(Na/K)NO_3$ (Geerlings et al., 2002; O'Connor et al., 2005). These salts reduce the Ca/Mg-activity in solution by an increase of the ionic strength of the solution and, thereby, enhance the release of Ca^{2+}/Mg^{2+}-ions from the Ca/Mg-mineral. In addition to their effect on the ionic strength, some additives form complexes with dissolved Ca or Mg, e.g. Cl^- (Fauth et al., 2001):

$$Mg^{2+} (aq) + n\ Cl^- (aq) \rightarrow MgCl_n^{2-n} (aq) \qquad\qquad (eq\ 1.18)$$
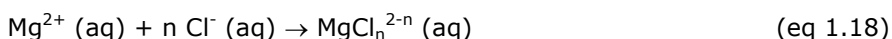
Addition of sodium bicarbonate was reported to buffer the pH of the solution at pH 7.7 to 8.0 (O'Connor et al., 2001a). At these pH-values, the sequence of reactions changes. For example, for olivine:

    1. $Mg_2SiO_4 (s) + 2\ HCO_3^- (aq) \rightarrow$

$$2\ MgCO_3 (s) + SiO_2 (s) + 2\ OH^- (aq)\ (eq\ 1.19)$$

    2. $OH^- (aq) + CO_2 (g) \rightarrow HCO_3^- (aq)$ $(eq\ 1.20)$
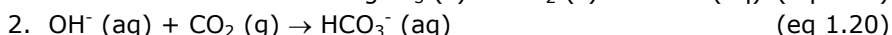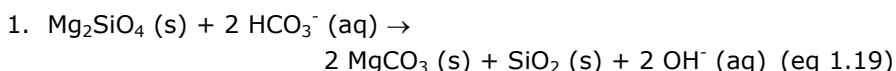
(the reaction of the hydroxyl ion with gaseous carbon dioxide regenerates the bicarbonate ion).

In the case of olivine (forsterite) and heat-treated serpentine (antigorite), application of a 1M NaCl and 0.64M $NaHCO_3$ salt solution was found to result in a substantial increase of the carbonation rate; from 91 and 34% conversion in 24h to 81 and 92% in 1h, respectively (test conditions: 80% <38 µm, T = 185 °C, p_{CO2} = 115 - 150 atm) (O'Connor et al., 2001b & 2005).

Acids and complexing agents can also be used to increase the reaction rate. Possible acid additives include HCl (Park et al., 2003b), acetic acid (Park et al., 2003b), and citric acid (Lackner, 2002). A combination of orthophosphoric acid, oxalic acid, and EDTA has been reported to increase the dissolution of serpentine significantly (Park et al., 2003b). In that case, the dissolution step of the alkaline earth metal no longer controls the overall reaction rate, but the dissolution of CO_2 was reported to become rate-limiting (Park et al., 2003a). It is important to realise that acids and complexing agents, while enhancing the dissolution step, may complicate the carbonation step by lowering the pH too much or by forming complexes too strong for carbonate precipitation to occur. Therefore, a careful optimisation of process conditions is needed.

A detailed energetic and economic assessment of the aqueous carbonation route resulted in best-case costs of 45 €/ton CO_2 sequestered for olivine[1], 53 €/ton for wollastonite, and 65 €/ton for serpentine (O'Connor et al., 2005). Sequestration costs rise to e.g. 65 €/ton CO_2 avoided for olivine if the extra energy consumption of the mineral carbonation process is taken into account (O'Connor et al., 2005). The energy consumption and costs of the direct aqueous mineral carbonation route will be discussed in more detail in §1.5.

1.3.3 Indirect Carbonation Mg/Ca-Ores

As stated above, carbonation proceeds much faster for Ca/Mg-(hydr)oxides than for silicates. Many process schemes have been proposed and studied on the basis of extraction of the reactive compound (i.e., Ca or Mg), conversion to a (hydr)oxide and subsequent carbonation. These process schemes are discussed below.

HCl Extraction Route

Lackner proposed to use hydrochloric acid to extract Ca or Mg from a silicate matrix (Lackner et al., 1995; Butt et al., 1998). As an example, the process steps using serpentine as feedstock are given. First, magnesium is extracted from the mineral using HCl (T = 100 °C, t ~ 1 h).

$$Mg_3Si_2O_5(OH)_4 \ (s) + 6 \ HCl \ (l) \rightarrow$$
$$3 \ MgCl_2 \ (aq) + 2 \ SiO_2 \ (s) + 5 \ H_2O \ (l) \quad (eq \ 1.21)$$
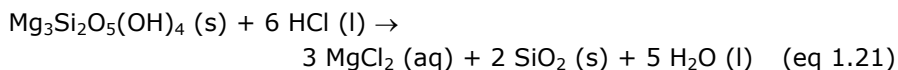
After boiling off the water and excess HCl, the formed solid $MgCl_2 \cdot 6H_2O$ decomposes upon heating to about 150 °C. Thus, the HCl is regenerated:

---

[1] All costs in this chapter are given in the euro currency (with rate 1 € = 1.2 $).

$$MgCl_2 \cdot 6H_2O \text{ (s)} \rightarrow Mg(OH)Cl \text{ (s)} + HCl \text{ (g)} + 5 \text{ } H_2O \text{ (g)} \quad \text{(eq 1.22)}$$

Subsequently, the MgCl(OH) reforms to magnesium hydroxide when water is reintroduced.

$$2 \text{ } Mg(OH)Cl \text{ (s)} \rightarrow Mg(OH)_2 \text{ (s)} + MgCl_2 \text{ (aq)} \quad \text{(eq 1.23)}$$
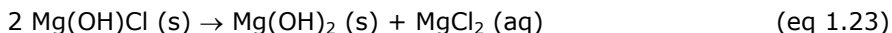
Finally, the $Mg(OH)_2$ is separated and carbonated:

$$Mg(OH)_2 \text{ (s)} + CO_2 \text{ (g)} \rightarrow MgCO_3 \text{ (s)} + H_2O \text{ (g)} \quad \text{(eq 1.24)}$$
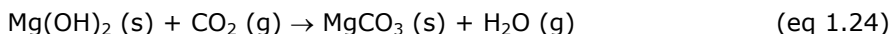
In order to successfully recover the HCl, the formation of soluble chlorides has to be avoided. Since e.g. alkali metal chlorides are soluble, alkali metals should be absent in the feedstock. Since solid wastes in general contain significant amounts of alkali metals, this route seems not to be useful for alkaline solid waste carbonation. The loss of hydrochloric acid would be too large.

The thermodynamics of the process have been studied in detail by Wendt et al. (1998b). The energy consumption of the third step of the process in which $Mg(OH)_2$ is formed is considerable (see Figure 1.1). Changing the extraction medium might lower energy consumption (dashed line).
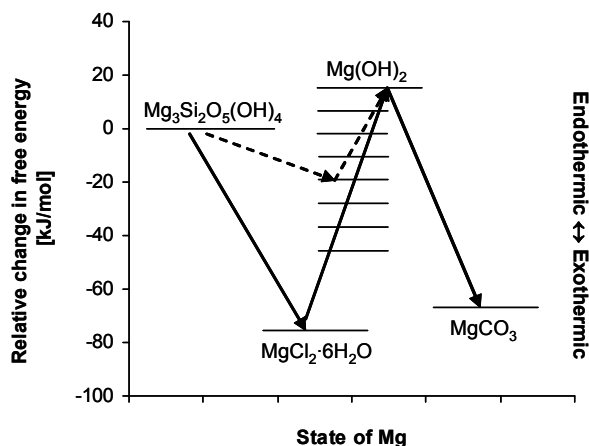
Figure 1.1: *Free energy at main stages in the HCl extraction route (based on Butt et al., 1998).*

Major drawbacks of the HCl extraction route are the costs associated with the use of HCl (i.e., both make-up and the need for corrosion resistant materials) and the energy consumption caused by the H_2O evaporation step. It was demonstrated that the energy consumption of the dehydration and crystallisation steps in the process exceed the energy generated by the power

plant producing the carbon dioxide by a factor of 4 (IEA GHG, 2000). The sequestration costs calculated are very high at >175 €/ton CO_2 (IEA GHG, 2000). Overall, the HCl extraction route can be considered to be energetically and economically infeasible.

Molten Salt Process

A first approach towards lowering the energy consumption caused by the H_2O evaporation step in the HCl extraction route is the use of a molten salt ($MgCl_2 \cdot 3.5H_2O$) as an alternative extraction agent, which is recycled within the process (Wendt et al., 1998b; IEA GHG, 2000) (i.e., indirect molten salt process). Using serpentine again as example, serpentine is first dissolved in the molten salt (T = ±200 °C):

$$Mg_3Si_2O_5(OH)_4 \text{ (s)} + 3\ MgCl_2 \cdot 3.5H_2O \text{ (l)} \rightarrow$$
$$6\ Mg(OH)Cl \text{ (s)} + 2\ SiO_2 \text{ (s)} + 2.5\ H_2O \text{ (l)} \qquad \text{(eq 1.25)}$$
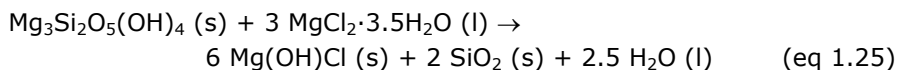
Subsequently, $Mg(OH)_2$ precipitates upon dilution:

$$2\ Mg(OH)Cl \text{ (s)} \rightarrow MgCl_2 \text{ (aq)} + Mg(OH)_2 \text{ (s)} \qquad \text{(eq 1.26)}$$
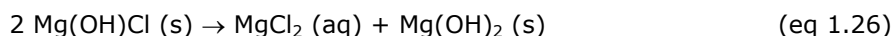
The magnesium hydroxide is separated and carbonated:

$$Mg(OH)_2 \text{ (s)} + CO_2 \text{ (g)} \rightarrow MgCO_3 \text{ (s)} + H_2O \text{ (g)} \qquad \text{(eq 1.27)}$$
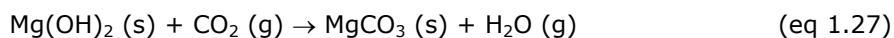
Finally, the $MgCl_2$ solution is partially dehydrated (T up to 250 °C) in order to recover the solvent $MgCl_2 \cdot 3.5H_2O$ (l).

An important drawback of this route is the corrosive nature of the solvent, which imposes constructional and operational constraints. Furthermore, in spite of recycling, some molten salt will be lost during the process and make-up $MgCl_2 \cdot 3.5H_2O$ will be required. On the basis of a detailed assessment, Newall et al. concluded that a commercial supply of $MgCl_2$ of this scale is probably unrealistic and, if at all possible, unaffordable (IEA GHG, 2000). The net CO_2 savings are (still) limited by the presence of an energy consuming partial dehydration and evaporation stage (30 MW for a 100 MW power plant (IEA GHG, 2000)). The high costs associated with the use of corrosive chemicals, the make-up HCl or $MgCl_2$ required, and the energy consumption make this process route economically unattractive.

Reactions 1.25-1.27 might also be integrated into a process in which carbonation takes place directly in the melt (i.e., direct molten salt process)

(Wendt et al., 1998a; IEA GHG, 2000). The overall reaction becomes:

$$Mg_3Si_2O_5(OH)_4 \ (s) + 3 \ CO_2 \ (g) \xrightarrow{\ MgCl_2 \cdot 3.5H_2O \ (l)\ }$$
$$3 \ MgCO_3 \ (s) + 2 \ SiO_2 \ (s) + 2 \ H_2O \ (l) \quad \text{(eq 1.28)}$$
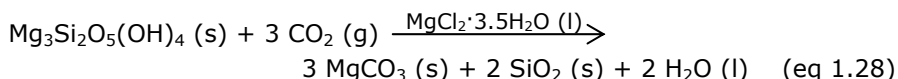
The estimated costs for this direct molten salt process are 52 €/ton CO_2 assuming on-site production of make-up $MgCl_2$ (IEA GHG, 2000). As in case of the indirect molten salt process, the direct process would imply the import of large quantities of either $MgCl_2$ or HCl (in case of on-site $MgCl_2$ production). The energy consumption associated with the production of these chemicals is not included in the costs mentioned above. If this consumption would be included, the net sequestration costs would increase considerably (IEA GHG, 2000).

Acetic Acid Route

A second approach towards the reduction of energy consumption of indirect carbonation routes is the use of other acids or extractants than HCl or salts. Possible extraction agents are weak acids, NH_4Cl, and EDTA (Goldberg & Walters, 2002). Kakizawa et al. selected acetic acid to extract calcium ions from wollastonite (Kakizawa et al., 2001). The possible route suggested by these authors consists of two steps. First, wollastonite is treated with acetic acid:

$$CaSiO_3 \ (s) + 2 \ CH_3COOH \ (l) \rightarrow$$
$$Ca^{2+} \ (aq) + 2 \ CH_3COO^- \ (aq) + H_2O \ (l) + SiO_2 \ (s) \quad \text{(eq 1.29)}$$
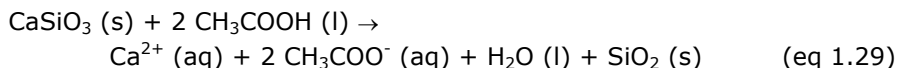
Subsequently, the calcium is carbonated in a combined step with the recovering of the acetic acid:

$$Ca^{2+} \ (aq) + 2 \ CH_3COO^- \ (aq) + CO_2 \ (g) + H_2O \ (l) \rightarrow$$
$$CaCO_3 \ (s)\downarrow + 2 \ CH_3COOH \ (l) \quad \text{(eq 1.30)}$$
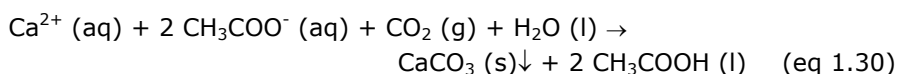
For the crystallization step within the acetic acid extraction route, a 20% conversion within 1h was obtained at 60 °C and 30 bar CO_2 during preliminary experiments with wollastonite (Kakizawa et al., 2001). An energy consumption of 20 MW for a 100 MW power plant has been reported (Kakizawa et al., 2001). Sequestration costs of about 45 €/ton CO_2 avoided were estimated on the basis of the estimated energy costs (Kakizawa et al., 2001). Unfortunately, this estimate does not include other variable and investment costs. The application of a non-corrosive acid to enhance the carbonation rate makes this approach a potentially attractive process route. However, it is unclear if the 'acetic acid route' can resolve the problems associated with indirect process routes (i.e., cost-effective and energetically feasible recycling of the acid/extraction agent).

Other Acids-Based Processes[1]

Maroto-Valer et al. proposed another process on the basis of the application of acids to enhance the dissolution of Ca/Mg from its matrix (Maroto-Valer et al., 2004b). This process consists of two steps, e.g. serpentine with sulphuric acid:

$$Mg_3Si_2O_5(OH)_4 + 3\ H_2SO_4 \rightarrow$$
$$3\ MgSO_4 + 5\ H_2O + 2\ SiO_2 \qquad\text{(eq 1.31)}$$
$$MgSO_4 + H_2O + CO_2 \rightarrow MgCO_3 + H_2SO_4 \qquad\text{(eq 1.32)}$$
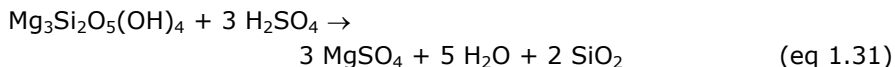
This route can be extended with an extra step in order to form $Mg(OH)_2$ to be carbonated in a separate gas-solid reaction (Maroto-Valer et al., 2004b). After reaction 1.31:

$$MgSO_4 + 2\ NaOH \rightarrow Mg(OH)_2 + Na_2SO_4 \qquad\text{(eq 1.33)}$$
$$Mg(OH)_2 + CO_2 \rightarrow MgCO_3 + H_2O \qquad\text{(eq 1.34)}$$
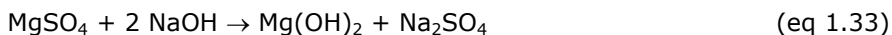
Another possibility proposed is the addition of both $Ca(NO_3)_2$ and $Ca(OH)_2$ in the following scheme. After reaction 1.31:

$$MgSO_4 + Ca(NO_3)_2 + 2\ H_2O \rightarrow CaSO_4 \cdot 2H_2O + Mg(NO_3)_2 \qquad\text{(eq 1.35)}$$
$$Mg(NO_3)_2 + Ca(OH)_2 \rightarrow Mg(OH)_2 + Ca(NO_3)_2 \qquad\text{(eq 1.36)}$$
$$Mg(OH)_2 + CaSO_4 \cdot 2H_2O + 2\ CO_2 \rightarrow$$
$$MgCO_3 + CaCO_3 + H_2SO_4 + H_2O \qquad\text{(eq 1.37)}$$
overall:
$$Mg_3Si_2O_5(OH)_4 + Ca(OH)_2 + 4\ CO_2 \rightarrow$$
$$3\ MgCO_3 + CaCO_3 + 2\ SiO_2 + 3\ H_2O \qquad\text{(eq 1.38)}$$
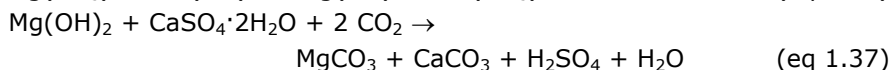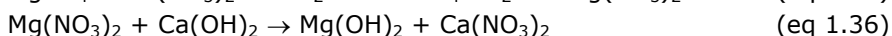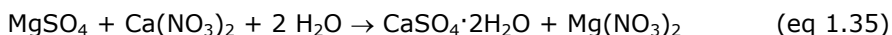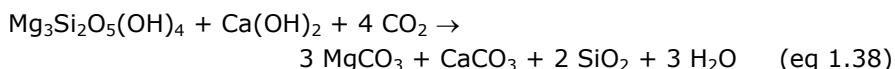
$Ca(OH)_2$ is consumed in the process alternative and its source on any large scale, without causing large additional CO_2 emissions by production of this base, remains unclear from the literature published. Also in alternative 1, NaOH is converted into Na_2SO_4 and thereby consumed. Any application of chemicals without recycling should be avoided for both cost and environmental reasons given the large scale of any industrial mineral CO_2 sequestration plant. Therefore, both alternative routes proposed seem to be unfeasible.

It is unclear if the use of sulphuric acid instead of HCl could lead to a reduction of the drawbacks of the HCl extraction route. No technological and cost

---

[1] Formulation of the reactions is adopted from the original reference, in which phases of the reactants and products are not specified.

evaluation of such a process has been made. Until then, the conclusions for the HCl extraction route are assumed to also apply to the H_2SO_4-based alternative.

NaOH-Based Process[1]

Blencoe et al. (Oak Ridge National Laboratory) have developed a new approach on the basis of plagioclase carbonation (Blencoe et al., 2003), which in their opinion is the most suitable feedstock for mineral CO_2 sequestration being an abundant Ca/Mg-source which is relatively evenly distributed among the globe (Blencoe et al., 2004). In principle, their approach can also be applied to other Ca/Mg-silicates. NaOH is used to enhance the extraction of calcium from its three-dimensional structure in which it is kept by silicon and aluminium atoms. A three-stage process was proposed (indicative process conditions: T = 200 °C, p < 15 atm, t = 1 h - 3 days):

$$3\ CaAl_2Si_2O_8\ (s)\ (anorthite) + 8\ NaOH\ (aq) \rightarrow$$
$$3\ Ca(OH)_2\downarrow + Na_8(AlSiO_4)_6(OH)_2\downarrow \qquad (eq\ 1.39)$$
$$2\ NaOH\ (aq) + CO_2\ (g) \rightarrow Na_2CO_3\ (aq) + H_2O\ (l) \qquad (eq\ 1.40)$$
$$2\ Na_2CO_3\ (aq) + Ca(OH)_2\ (s) + Na_8(AlSiO_4)_6(OH)_2\ (s) + 2\ H_2O\ (l) \rightarrow$$
$$4\ NaOH\ (aq) + CaCO_3\downarrow + Na_8(AlSiO_4)_6CO_3 \cdot 2H_2O\downarrow \quad (eq\ 1.41)$$
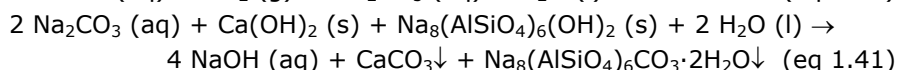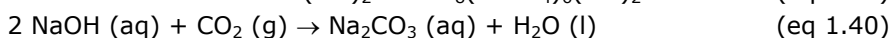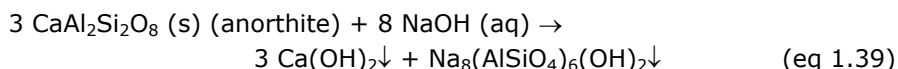
An analysis of the overall net reaction of reactions 1.41-1.43 results in:
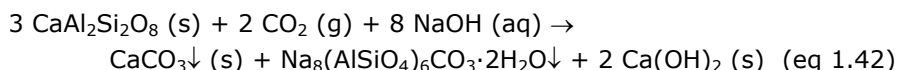
$$3\ CaAl_2Si_2O_8\ (s) + 2\ CO_2\ (g) + 8\ NaOH\ (aq) \rightarrow$$
$$CaCO_3\downarrow (s) + Na_8(AlSiO_4)_6CO_3 \cdot 2H_2O\downarrow + 2\ Ca(OH)_2\ (s) \quad (eq\ 1.42)$$
(assuming the NaOH generated in eq 1.44 is used for eq 1.42 or 1.43)

In addition, if all precipitated portlandite is carbonated, the overall reaction becomes:

$$3\ CaAl_2Si_2O_8\ (s) + 4\ CO_2\ (g) + 8\ NaOH\ (aq) \rightarrow$$
$$3\ CaCO_3\downarrow (s) + Na_8(AlSiO_4)_6CO_3 \cdot 2H_2O\downarrow + 2\ H_2O\ (l) \qquad (eq\ 1.43)$$
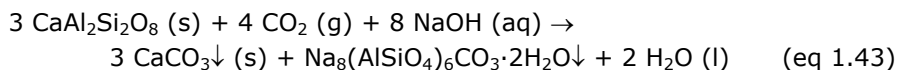
Three major drawbacks of this route can be distinguished: (1) reaction times reported are still (too) long for industrial application, (2) the feedstock was milled to <10 μm for the experiments reported, which causes a significantly higher grinding energy consumption compared to the <38 μm typically applied in aqueous carbonation, and (3) large quantities of NaOH will be required. Since there are no indications how these drawbacks could be overcome simultaneously, the process as proposed seems unattractive.

---

[1] Formulation of the reactions and phase notation are adopted from the original reference.

Two-Step Aqueous Route

The addition of acids and complexing agents in a single step aqueous carbonation process causes the need to balance the process conditions between the optima for the dissolution and for the precipitation step (§1.3.2). Therefore, it might be advantageous to perform the aqueous carbonation route in two separate steps.

Park & Fan proposed a process based on the aqueous carbonation route extended with a so-called pH swing process and in-situ physical activation of the feedstock minerals (Park & Fan, 2004). The pH swing process consists of a first step at low pH to dissolve Mg from serpentine and a second step at high pH to form carbonates. The in-situ physical activation was proposed to remove the rate-limiting SiO_2-rim during the Mg-dissolution step. Various forms of in-situ activation were tested on serpentine particles with a SiO_2-rim including internal grinding with inert balls and ultrasonic and acoustic treatment (Park & Fan, 2004).

The overall proposed process starts with a dissolution step in which serpentine is dissolved with the help of an acid, while being fluidised with internal grinding media (Park & Fan, 2004):

$$Mg_3Si_2O_5(OH)_4 \text{ (s)} + 6 \text{ H}^+ \text{ (aq)} \xrightarrow{T=70°C, \, d<38\mu m}$$
$$3 \text{ Mg}^{2+} \text{ (aq)} + 2 \text{ SiO}_2 \text{ (s)} + 5 \text{ H}_2\text{O (l)} \quad \text{(eq 1.44)}$$
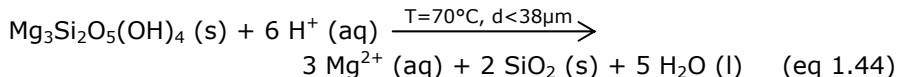
Two types of acidic solvents were tested: (a) a mixture of 1 vol% orthophosphoric acid, 0.9 wt% of oxalic acid, and 0.1 wt% EDTA that was identified as the most effective solvent out of a set of solvents for enhancing the mineral dissolution (Park et al., 2003b) and (b) 1.4M ammonium bisulfate. After dissolution, the Mg- and Fe-rich solution was filtered to remove the SiO_2-rich precipitate and cooled to ambient temperature. Subsequently, NH_4OH was added to increase the pH to about 8.6 in order to remove Fe from the solution by precipitation of iron oxide. Finally, gaseous CO_2 was bubbled through the remaining Mg-rich solution until the solution was saturated with CO_2 and, subsequently, additional NH_4OH was added to stimulate precipitation of $MgCO_3$ by increasing the pH to about 9.5. The overall conversion reported was about 65% and 42% for solvent (a) and (b), respectively.

The process conditions required to obtain a significant carbonation conversion in the above process (70 °C and 1 atm) are significantly milder than those typical for direct aqueous carbonation of Mg-silicates (185 °C and 150 atm, §1.3.2). As for all indirect process routes, heat integration between the two reaction steps is

essential for the further development of this process. Furthermore, since different chemicals are used in the process, a detailed study of the costs and environmental impact of the proposed process is recommended. At the moment, this process route seems unattractive for further development.

1.3.4   Carbonation Processes Industrial Residues

The process routes for carbonation of Mg/Ca-ores can in principle also be applied for the carbonation of industrial residues. Indirect carbonation routes, however, are less attractive for residues because of the diversity of elements present. First of all, the recovery of the solvent is probably poor due to the heterogeneous composition of alkaline solid wastes and corresponding side-reactions. Secondly, the environmental quality of the produced materials would very likely be less than those produced by the direct route. By extracting main constituents such as calcium and magnesium, the solid matrix that can retain contaminants is largely destroyed, which in turn would lead to enhanced leaching of heavy metals. Although the latter does in principle also apply to primary Mg/Ca-ores, it is particularly disadvantageous for residues with enhanced levels of trace elements.

Table 1.4: *Selected studies on carbonation of residues including process conditions*

Residue	Details carbonation process	T [°C]	p_{CO2} [bar]	d [mm]
Blast furnace slag		25	3	NA [a]
Cement-immobilised slag	Supercritical CO_2	50	250	
Coal fly ash	Aqueous route [b]	185	115	NA
Coal fly ash	20% moisture	25	2.8	<0.25
Deinking ash		25	3	NA
FBC coal ash	Aqueous route [b]	155	75	NA
FGD coal ash	Aqueous route [b]	185	115	NA
MSWI ash		25	3	NA
MSWI bottom ash [c]	Water content: moisture.	20	60 (l)	<10
		40	150 (sc)	
		50	250 (sc)	
OPC cement		25	3	NA
Portland cement pastes [d]	W/c: 0.6	59	97	NA
Pulverised fuel ash	Water:solid 0.1 – 0.2	25	3	NA
Spent oil shale	20% mositure	25	2.8	<0.25
Stainless steel slag		25	3	NA
Waste Dravo-Lime	Aqueous route [b]	185	115	NA

[a] Not available. [b] Additives used: 0.5M Na_2CO_3 / 0.5M $NaHCO_3$ / 1.0M NaCl.

Table 1.4 gives an overview of selected studies on the carbonation of industrial residues. These studies generally focus on direct residue carbonation in the presence of water. This process can either be conducted at low temperature and pressure (typically, long reaction times and low conversions) or at elevated temperature and pressure (i.e., the aqueous process route). The latter type of process is more relevant for the purpose of this thesis.

Other proposed process routes include carbonation of waste concrete via the acetic acid route (Fujii et al., 2001), carbonation of waste cement in a two-step aqueous pressure-swing process (i.e., extraction at high p_{CO2} and subsequent precipitation at low p_{CO2}) (Iizuka et al., 2004), and carbonation of waste concrete and steel and blast furnace slags in a two-step process based on aqueous extraction of Ca (Stolaroff et al., 2004).

In §1.2.2, it was suggested that solid residues can be expected to carbonate rapidly relative to ores. Experimental data verifying this assumption are limited, but, for example, coal fly ash was carbonated for 80% using the aqueous route with a $Na_2CO_3/NaHCO_3/NaCl$-solution. Under the same process conditions, the conversion of olivine was 70% and that of serpentine only 12% (NETL, 2001) (see also Chapter 4).

applied and carbonation degree obtained.

Time [h]	CO₂ uptake [g/kg]	(Ca)-conversion [%]	Reference
24	3	9	(Johnson, 2000)
0.25	14.8		(Ginneken van et al., 2002)
0.5		84	(NETL, 2001)
120	16.7 - 61.6		(Reddy et al., 1994)
24	170	17	(Johnson, 2000)
1	159	51	(Fauth et al., 2002)
1	191	72	(Fauth et al., 2002)
24	60 – 140	39 – 50	(Johnson, 2000)
1	15		(Devoldere et al., 2000)
1	20		
1	20		
24	22	22	(Johnson, 2000)
24	162		(Short et al., 2000)
24	15	57	(Johnson, 2000)
120	17.6 - 35.2		(Reddy et al., 1994)
24	210	21	(Johnson, 2000)
0.5		10	(NETL, 2001)

[c] Magnetic separation ferrous fraction. [d] Dry samples showed no conversion.

1.4   Selection Process Route

On the basis of the overview given in §1.3, a process route is selected for further mineral carbonation research, first for mineral ores and second for industrial residues.

Mineral Ores. Some general differences appear when comparing the direct and indirect process routes. A major advantage of the direct routes is their straightforward design. In addition, the costs and energy consumption associated with (incomplete) recycling of solvents are avoided. The reaction rate, however, is generally lower and the CO_2 pressure required for carbonation is generally higher than in the indirect process routes. On the basis of these considerations, a direct carbonation route was selected for further research.

Within the group of direct processes, the two main types of process routes are the direct gas-solid and the aqueous carbonation route. The major advantage of the aqueous carbonation route is its carbonation rate, which seems (potentially) sufficient for industrial implementation. The gas-solid carbonation reaction proceeds too slowly at thermodynamically allowed temperatures. A disadvantage of the aqueous carbonation route is that the heat of the reaction is less suitable for practical purposes. In the dry process, the heat of reaction is available at higher temperatures and can therefore be applied more easily. A possible additional disadvantage of the aqueous route with modified solution chemistry is the need for additional chemicals. Finally, the products may have to be de-watered and perhaps even dried, depending on their final destination.

Overall, the most promising route at this moment seems to be the direct aqueous carbonation. Therefore, this process route was selected for further research.

Alkaline Solid Residues. The conclusions drawn above on the various process routes for ore carbonation are, in principle, also valid for alkaline solid residues. However, direct carbonation routes seem even more preferable in the case of residues (§1.3.4). Since residues tend to react relatively rapidly, direct gas-solid carbonation with (moisturised) CO_2 might be an interesting option for this type of raw materials. However, since the aim of this thesis is CO_2 *sequestration*, rather than carbonation per se, aqueous carbonation at elevated temperature and pressure seems a better alternative to obtain sufficient carbonation within reasonable reaction times.

1.5 Other Aspects Mineral CO$_2$ Sequestration

1.5.1 Process Lay-Out

Because the development of mineral CO$_2$ sequestration is still in a lab-scale phase, only a limited number of process studies have been published. Most postulated processes are end-of-pipe technologies in which the CO$_2$ is captured first from a flue gas and subsequently reacted with alkaline minerals.

In designing a mineral carbonation process, a major aspect to be taken into account is the large amount of materials that has to be processed within a mineral carbonation process. Both the amount of minerals needed as feedstock for mineral CO$_2$ sequestration and the amount of produced (by)-products are very large. Dahlin and co-workers give a good example of the scale of operation (Dahlin et al., 2000). A single 500 MW power plant generates about 10,000 ton CO$_2$/day. To sequester this amount of CO$_2$ via the mineral route would require approximately 23,000 ton/day of magnesium silicate ore. Thus, the scale of the feedstock mining is very large, in case of a coal-fired power plant, even larger than that of the coal used. The large amount of feedstock involved implies that transportation is an important factor. In order to avoid the transport of large quantities of rock, transportation of the carbon dioxide by pipeline or ships is preferable. Therefore, the sequestration facilities should be placed near the mining locations, which imposes geographical constraints on the mineral sequestration option.

Since a large part of the costs of mineral CO$_2$ sequestration is due to the extra energy consumption caused (see below), it could be worthwhile to develop integrated concepts such as a mineral carbonation plant integrated with a power plant. Studies have been performed on hydrogen production on the basis of integrated coal gasification and mineral CO$_2$ sequestration (e.g., Yegulalp et al., 2001). Unfortunately, conditions required for both processes probably differ too much to integrate these into a single unit (Tang et al., 2002).

Another integration possibility proposed is the combination of CO$_2$ capture with carbonation (Wesker & Geerlings, 2004). Thus, the significant costs and energy consumption associated with current CO$_2$ separation techniques might be lowered, e.g. by utilizing the reaction heat of the carbonation process. Carbon dioxide is dissolved in a water phase and the carbonate ion reacts with (Ca,Mg)$^{2+}$ (from different sources) to form carbonates (Bond et al., 2001; Dziedzic et al., 2004). However, the possible accompanying need for large-scale transport of solid feedstock seems unattractive for both energetic and economic reasons.

Finally, the application of industrial solid residues as feedstock for mineral CO_2 sequestration offers another integration possibility since carbon dioxide and the solid feedstock are produced at the same location and transportation is no longer required.

All studies on integrated concepts are in a first design phase and no detailed technical and economical assessment of such an approach has been made yet.

Performing mineral CO_2 sequestration on any significant scale causes the need for continuous reactors. The necessary long residence time complicates the selection of an appropriate reactor for an industrial process. For the aqueous carbonation route, the most straightforward reactor type is a continuous-flow leach-type autoclave and exists of a multi-chamber layout of a stirred tank reactor. Other options proposed include a high temperature and pressure fluidised bed (Park et al., 2002) and a continuous pipeline reactor, which consists of a bent sequence of static mixers and 'empty' pipe reactors (Penner et al., 2004). Studies on the latter have started with a prototype continuous flow-loop reactor to determine the (mechanical) behaviour of such a reactor and formulate design specifications for a pilot-scale pipeline reactor. Remarkably, a higher conversion for coarse particles has been obtained in the continuous reactor than in an autoclave system (Penner et al., 2004). Probably, the intensified mixing causes high-energy particle-particle interactions, which remove the SiO_2-layer and enhance the reaction rate (Gerdemann et al., 2004).

1.5.2   Energy Consumption and Costs

Mineral CO_2 sequestration can be expected to be in general more expensive than other CO_2 storage possibilities, because of the additional equipment and the more complicated nature of the process needed. The (extra) costs have to be weighed against factors such as the technical feasibility, environmental benefits, and public acceptance. Potentially, costs might be limited by using the exothermic nature of the reactions. Furthermore, mining for mineral carbonation may create valuable by-products, such as chromium, nickel, and manganese (Goff & Lackner, 1998). Finally, re-use of the resulting products could improve the economic returns of the process. For the total sequestration costs, also the costs of CO_2 capture and transportation have to be taken into account[1], which applies to all CO_2 storage options.

---

[1] For example, cost ranges for CO_2 capture based on absorption / desorption of 37-74, 13-37, and 29 - 51 €/ton CO_2 have been reported for a Natural Gas Combined Cycle (NGCC), an Integrated Gasification Combined Cycle (IGCC), and a Pulverised Coal Power Cycle (PC), respectively (IPCC, 2005).

Of the aqueous carbonation route, a detailed energy and economic evaluation has been made (O'Connor et al., 2005). This evaluation is based on a conventional continuous-flow autoclave reactor. The total energy consumption including grinding and heating was reported to be larger than the heat generated by the exothermic reaction. A 27% energy penalty was found for a power plant of which 75% is due to grinding of the feedstock. The sequestration costs were calculated for seven regions in the USA where both large ultramafic bodies and a large amount of CO_2 are present. The best-case costs were 45 €/ton CO_2 sequestered for olivine, 53 €/ton for wollastonite, and 65 €/ton for serpentine. Sequestration costs rise to 65 €/ton CO_2 avoided for olivine if the extra energy consumption of the mineral carbonation process is taken into account.

1.5.3   Other Environmental Issues

Potential negative environmental effects of mineral CO_2 sequestration include: (1) the environmental impact of large-scale mining of ores, (2) the extra emission of non-CO_2 pollutants due to the increased energy consumption, (3) the destination of the carbonated products, and (4) the possible make-up of solvents or extractants used.

1. Potential feedstock minerals are already produced as by-products at existing mines and as residue at industrial facilities. However, a massive increase in mining activities would be required to facilitate large-scale mineral CO_2 sequestration. These activities would have consequences for landscapes and ecosystems (Goff & Lackner, 1998). In addition, the transportation of the large amount of feedstock would have a negative environmental impact.

2. In addition to the energy consumption of the CO_2 capture step[1], mineral CO_2 sequestration causes extra energy consumption. Assuming that the required energy is provided by fossil fuels, mineral sequestration would enhance the use of fossil fuels. Thus, the emission of non-CO_2 pollutants, such as NO_x, SO_x, and fine dust, might be increased and the depletion rate of the fossil fuel reserves will increase (e.g., the energy penalty of 27% reported for the aqueous mineral carbonation route (§1.3.2) would implicate a 1.37 times larger fossil fuel consumption).

---

[1] For example, based on current technology, capture energy requirements of 11 - 22, 14 - 25, and 14 - 25 % increase of input/kWh power output of the power plant have been reported for a Natural Gas Combined Cycle (NGCC), an Integrated Gasification Combined Cycle (IGCC), and a Pulverised Coal Power Cycle (PC), respectively (IPCC, 2005).

3. The destination of the (carbonated) products is an issue that has not been given much attention in the literature so far. The amount of products resulting from mineral CO_2 sequestration on any significant scale is large and, therefore, studies on re-use possibilities and the environmental impact of carbonated products are required. In addition, an environmentally acceptable and cost-effective application of the products can potentially increase public acceptance and lower sequestration costs. It is important to note that large-scale mineral CO_2 sequestration could produce such large quantities of products that any possible application market would be over-saturated. However, it might well turn out that mineral CO_2 sequestration can only be (economically) feasible if the product can be usefully applied, which may put limits on the scale of application. Potential re-use of the carbonated product includes applications as construction material and cement filler.

If the carbonated product cannot be re-used, carbonated ores can potentially be returned to the mines in order to restore the landscape. However, since the volume of the products resulting from carbonation is larger than that of the reactants, part of the material cannot be used for mine reclamation, but has to be land-filled or re-used otherwise (e.g., molar volumes of CaO and calcite are 16.8 and 36.9 cm^3/mol, respectively, and molar volumes of wollastonite and quartz + calcite are 34.3 and 22.7 + 36.9 = 59.6 cm^3/mol, respectively (Lide, 2002)). The impact of such storage would be limited on a global scale, but could have severe consequences on a local scale because of environmental or land-use constraints.

4. The environmental consequences of the use of chemicals such as acids in the indirect carbonation routes have to be examined. Although the acid is recycled in the process, some acid may be lost and end up in, e.g., the (by-)products. This loss of acid may cause environmental concerns and extra acid has to be produced with additional energy demands. Therefore, process routes using a large amount of acid or extraction agent seem less attractive.

Besides the potential negative environmental effects, mineral CO_2 sequestration may also have positive environmental side effects in addition to the CO_2 emission reduction. (1) In case residues are used as feedstock, residue properties relevant for their utilisation in construction might potentially improve due to carbonation. First, carbonation is known to reduce the leaching of contaminants from solid wastes (e.g., Meima et al., 2002) (see Chapter 3 for more information). Second, carbonation can improve the constructive properties of materials. The application of slags in concrete, asphalt aggregate, and filling materials is often hindered by the high water absorption and expansion properties due to the hydration of Ca/Mg-oxides. Carbonation can reduce these

problems by conversion of the oxides into carbonates (Stolaroff et al., 2004). (2) CO_2 sequestration by mineral carbonation might be used to simultaneously reduce the SO_2 emissions. The reaction between SO_2 (g) and Ca from Ca-silicates would lead to the formation of gypsum ($CaSO_4$), similarly to the principle behind current desulphurisation technologies.

1.6   Conclusions

In this chapter, the literature on mineral carbonation published before January 2005 has been reviewed in order to (1) select a solid feedstock for further mineral carbonation research, (2) select a mineral carbonation process route, and (3) identify other issues to be addressed in further research on mineral carbonation.

The key challenge for further development of mineral carbonation as a CO_2 sequestration technology was found to be the enhancement of the carbonation rate (Introduction). The following main preconditions in realising this enhancement were identified: the energy consumption, environmental impact, and costs of the sequestration process. Both feedstock and process route were selected with this research aim and these preconditions in mind.

Potential starting materials include (1) primary Ca- and Mg-minerals such as olivine, serpentine, and wollastonite and (2) Ca-rich alkaline industrial residues. Ca-silicates (i.e., wollastonite and residues) seem to be the most attractive raw materials, since these minerals react rapidly relative to Mg-silicates. Among the various industrial residues that are produced and potentially suitable for mineral carbonation, steel slag was selected for the first studies on mineral carbonation because of its high potential CO_2 sequestration capacity.

For both ores and residues, the direct aqueous route was identified as the most promising mineral carbonation route for further research. (Potential) advantages compared to other process routes include its relatively easy process design (i.e., the dissolution and carbonation reactions are combined in a single unit operation), its lack of extraction agents, and its process rates, which seem (potentially) sufficient for industrial implementation. Thus, the aqueous carbonation route holds prospects for lower sequestration costs compared to other mineral carbonation processes. A potential drawback of the aqueous route is the difficulty to apply the reaction heat usefully due to the lower reaction temperature and the dilution of the reactants. In addition, (salt) additives might be required to enhance the carbonation reaction sufficiently.

In this thesis, studies on the aqueous carbonation of both steel slag (Chapters 2 & 3) and wollastonite (Chapter 4) will be presented. Moreover, Chapter 3 deals with the environmental properties of carbonated steel slag. Finally, in Chapters 5 & 6, the energy consumption and costs of aqueous Ca-silicate carbonation will be assessed.

CHAPTER 2

MINERAL CO$_2$ SEQUESTRATION BY STEEL SLAG CARBONATION
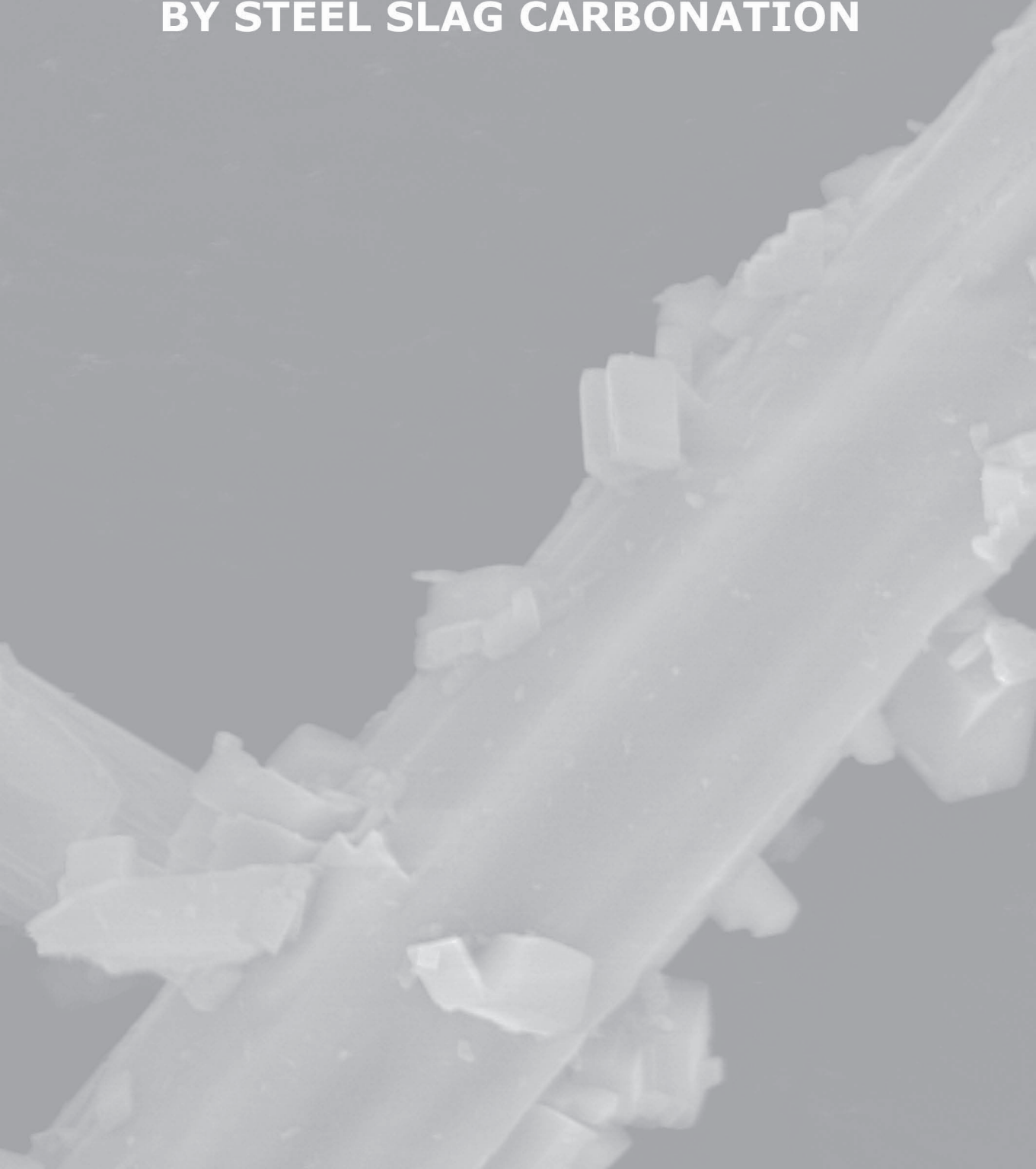
Published in similar form as:

Huijgen, W.J.J., Witkamp, G.J. & Comans, R.N.J. (2005) *Mineral CO$_2$ sequestration by steel slag carbonation*, Environmental Science and Technology 39(*24*), 9676-9682.

Reproduced with permission. Copyright 2005 American Chemical Society.

MINERAL CO$_2$ SEQUESTRATION BY STEEL SLAG CARBONATION

Wouter J.J. Huijgen[1], Geert-Jan Witkamp[2] & Rob N.J. Comans[1,3]

Mineral CO$_2$ sequestration, i.e., carbonation of alkaline silicate Ca/Mg minerals, analogous to natural weathering processes, is a possible technology for the reduction of carbon dioxide emissions to the atmosphere. In this paper, alkaline Ca-rich industrial residues are presented as a possible feedstock for mineral CO$_2$ sequestration. These materials are cheap, available near large point sources of CO$_2$, and tend to react relatively rapidly with CO$_2$ due to their chemical instability. Ground steel slag was carbonated in aqueous suspensions to study its reaction mechanisms. Process variables, such as particle size, temperature, carbon dioxide pressure, and reaction time, were systematically varied, and their influence on the carbonation rate was investigated. The maximum carbonation degree reached was 74% of the Ca content in 30 min at 19 bar CO$_2$ pressure, 100 °C, and a particle size of <38 μm. The two most important factors determining the reaction rate are particle size (<2 mm to <38 μm) and reaction temperature (25-225 °C). The carbonation reaction was found to occur in two steps: (1) leaching of calcium from the steel slag particles into the solution; (2) precipitation of calcite on the surface of these particles. The first step and, more in particular, the diffusion of calcium through the solid matrix toward the surface appeared to be the rate-determining reaction step. The Ca diffusion was found to be hindered by the formation of a CaCO$_3$-coating and a Ca-depleted silicate zone during the carbonation process. Research on further enhancement of the reaction rate, which would contribute to the development of a cost-effective CO$_2$ sequestration process, should focus particularly on this mechanism.

---

[1] Energy Research Centre of The Netherlands.
[2] Delft University of Technology.
[3] Wageningen University.

2.1   Introduction

The increasing atmospheric CO$_2$ concentration, mainly caused by fossil fuel combustion, has led to concerns about global warming. A possible technology that can contribute to the reduction of carbon dioxide emissions is CO$_2$ sequestration by mineral carbonation, as originally proposed by Seifritz (1990) and first studied in more detail by Lackner et al. (1995). The basic concept behind mineral CO$_2$ sequestration is to mimic natural weathering processes in which calcium- or magnesium-containing minerals are converted into calcium or magnesium carbonates:

$$(Ca,Mg)SiO_3 \text{ (s)} + CO_2 \text{ (g)} \rightarrow (Ca,Mg)CO_3 \text{ (s)} + SiO_2 \text{ (s)} \qquad \text{(eq 2.1)}$$
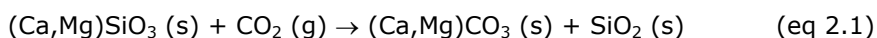
Compared to other CO$_2$ storage options, such as storage in empty gas fields, oceans, and aquifers, mineral CO$_2$ sequestration has some potential advantages. First, mineral sequestration is a chemical sequestration route of which the products are thermodynamically stable. Therefore, the storage of CO$_2$ is permanent and inherently safe. In addition, the energy consumption and costs of carbon sequestration may be limited by the exothermic nature of the carbonation reaction. A disadvantage of mineral CO$_2$ sequestration is that large amounts of Ca/Mg minerals are required to sequester a significant fraction of the CO$_2$ emitted from fossil fuel combustion, although sufficient suitable ores are available on a global scale (Lackner et al., 1995).

Natural weathering proceeds too slowly to effectively mitigate global warming. Therefore, mineral sequestration research aims at accelerating the reaction to obtain a viable industrial process. For this purpose, many process routes have been developed for mineral CO$_2$ sequestration (e.g. IEA GHG, 2000; Lackner, 2002) of which the aqueous carbonation route (O'Connor et al., 2005) was selected for experiments on the basis of technological and economical considerations, which are outlined in more detail in Chapter 1. In a simplified form, the aqueous carbonation of a calcium silicate can be written as:

$$CO_2 \text{ (g)} + H_2O \text{ (l)} \rightarrow 2\, H^+ \text{ (aq)} + CO_3^{2-} \text{ (aq)} \qquad \text{(eq 2.2)}$$
$$CaSiO_3 \text{ (s)} + 2\, H^+ \text{ (aq)} \rightarrow Ca^{2+} \text{ (aq)} + SiO_2 \text{ (s)} + H_2O \text{ (l)} \qquad \text{(eq 2.3)}$$
$$Ca^{2+} \text{ (aq)} + CO_3^{2-} \text{ (aq)} \rightarrow CaCO_3\downarrow \text{ (s)} \qquad \text{(eq 2.4)}$$
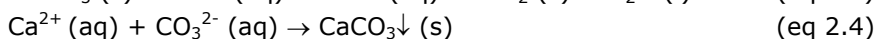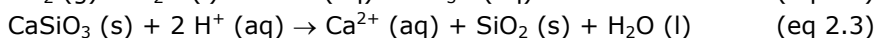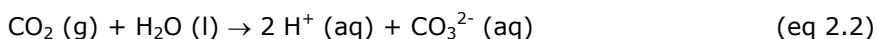
Research on the aqueous carbonation route has focused mainly on Mg silicates so far. Typical process conditions reported to obtain a sufficient reaction rate include either an energy-consuming pre-treatment step or high CO$_2$ pressures (typically >100 bar) (Chapter 1).

A possible feedstock for mineral CO_2 sequestration, which has not attained much attention so far, is industrial solid waste, such as combustion residues, slags, and fly ashes. These materials are generally alkaline and rich in calcium. Major advantages compared to ores are their low costs and widespread availability in industrial areas, i.e., near large point sources of CO_2. No mining is needed and consumption of raw materials is avoided. Moreover, these residues tend to be more reactive for carbonation than primary minerals due to their chemical instability and thus their use might enable a reduction of the energy consumption and costs of mineral CO_2 sequestration (Meima et al., 2002). In addition to advantages from a CO_2 sequestration perspective, research has shown that carbonation of alkaline solid residues can lead to an improvement of their environmental quality (e.g. Reddy et al., 1994; Meima et al., 2002). Although their total CO_2 sequestration capacity is limited compared to primary minerals, the use of alkaline solid residues could facilitate the realization of the first cost-effective mineral CO_2 sequestration plants. In addition, this alternative route could be of interest at sites where both large quantities of CO_2 and suitable solid residues are produced, such as steel production facilities and municipal waste incineration plants. Various alkaline solid waste streams can be used as feedstock for mineral CO_2 sequestration. Steel slag was selected for the experiments presented in this paper because of its high specific sequestration capacity.

Research on the carbonation of industrial residues published so far has focused mainly on improvement of their environmental quality (e.g. Reddy et al., 1991 & 1994; Tawfic et al., 1995; Ecke, 2003) and their mechanical properties with regard to utilization in construction (e.g. Isoo et al., 2000; Johnson et al., 2003). Some of these earlier studies have suggested that the carbonation of alkaline residues may also contribute to the minimization of atmospheric CO_2 emissions (Reddy et al., 1991; Tawfic et al., 1995). However, very limited research has been published in this area for the specific purposes of carbon sequestration (e.g. Johnson, 2000; Fauth et al., 2002). This paper presents a first systematic study of the reaction mechanisms of CO_2 sequestration by carbonation of an alkaline solid residue. The rate-determining reaction steps are identified, and routes for further process optimisation are indicated.

2.2 Experimental Section

2.2.1 Materials Processing

Linz Donawitz steel slag (size class 0-20 mm) was dried at 60 °C in an oven and stored in containers under a nitrogen atmosphere. Representative samples were taken from the steel slag and ground until all material passed predetermined sieve sizes (d, <38 μm to <2 mm). Homogeneous sub-samples of the prepared batches were taken for the carbonation experiments with a sample splitter.

Carbonation experiments were performed in a 450 mL AISI316 autoclave reactor (Limbo 350, Büchi Glas Uster). A suspension of steel slag and Nanopure-demineralised water, at a desired liquid-to-solid ratio (L/S, 2-20 kg/kg), was stirred at a specific stirring rate (n, 100-2000 rpm) using a Rushton turbine. The reactor was closed and heated to the reaction temperature (T, 25-225 °C) and maintained at that temperature during the reaction time (t, 2-30 min). When the temperature had reached the set point, CO_2 was added directly into the solution using a gas booster (Haskel AG75) until a specific CO_2 pressure was established (p_{CO2}, 1-30 bar). During the reaction time, the CO_2 pressure was kept constant within ±0.2 bar of its set point by replenishment of the consumed CO_2. A hollow stirring axis was used to enhance mass transfer of CO_2 by transporting the gas through the axis from the gas phase into the solution by the underpressure caused by the stirrer. When the reaction time had elapsed, the addition of CO_2 was stopped and the autoclave was cooled to 40 °C, depressurised, and opened. The suspension was immediately filtered quantitatively over a 0.2 μm membrane filter, and the solid was dried overnight at 50 °C in an oven. Finally, the product was analysed to determine the conversion of the reaction.

The heating and cooling times were approximately 11 and 8 min, respectively, for a set of typical conditions used (T = 100 °C, n = 1000 rpm, L/S = 10 kg/kg). During the experiment, the temperature of the reactor and the heating jacket and the total pressure inside the reactor were recorded with a data acquisition unit (Agilent 34970A). The partial CO_2 pressure was calculated from the total pressure and the water vapour and air pressure corresponding with the temperature inside the reactor.

At one carbonation experiment, the chemical composition was measured of the aqueous phase, sampled directly in the autoclave reactor at typical process conditions (i.e., d < 106 μm, T = 100 °C, p_{CO2} = 19 bar, L/S = 10 kg/kg, n = 1000 rpm, t = 30 min). For this purpose, the reactor was equipped with a

dedicated sampling device, which included an in-line filter that allowed instantaneous filtration of the steel slag suspension.

2.2.2   Materials Characterization

The carbonate content of the fresh and carbonated samples was determined with two different analytical methods: (1) thermal decomposition (TGA-MS) and (2) acidification (C-analyser).

TGA-MS analyses were performed in duplicate in a thermal gravimetrical analysis system (Mettler-Toledo TGA/SDTA 851e) coupled with a mass spectrometer (Pfeiffer, Thermostar) (TGA-MS). Samples (10-20 mg) (<106 μm) were heated in aluminium oxide ceramic cups under an oxygen atmosphere at 40 °C/min from 25 to 1000 °C. Weight loss was measured by the TGA, while the evolved gas was analysed for CO_2 and H_2O by the MS. Three weight fractions were distinguished: (1) 25-105 °C; (2) 105-500 °C; (3) 500-1000 °C. These fractions represent: (1) moisture, (2) organic, elemental carbon and (if present) $MgCO_3$, and (3) $CaCO_3$ (inorganic carbon), respectively. During heating of the samples, samples were kept isothermally at 105 and 500 °C for 15 min to obtain a good discrimination between the weight fractions. The third weight fraction of the TGA curve ($\Delta m_{500\text{-}1000°C}$) based on dry weight ($m_{105°C}$) was used as the calcium carbonate content, expressed in terms of CO_2 [wt%]:

$$CO_2[\text{wt\%}] = \frac{\Delta m_{500\text{-}1000°C}}{m_{105°C}} \times 100 \qquad\qquad \text{(eq 2.5)}$$

Total inorganic carbon (TIC) was determined with the solid sample module of a Shimadzu TOC 5000A C-analyser (TOC-SSM). A 0.75 mL volume of 1:1 diluted HCl was added to a 50-100 mg sample (<106 μm) and heated to 200 °C. The evolved gas was analysed for CO_2 with a nondispersive infrared detector (NDIR). Since the C-analyser measures total inorganic carbon and TGA-MS determines $CaCO_3$, the difference between the two measurements was used to verify that no carbonates other than $CaCO_3$ had formed.

For determination of the total composition, a fresh steel slag sample was ground (<106 μm) and, subsequently, digested and analysed with inductively coupled plasma atomic emission spectrometry (ICP-AES) for Al, As, B, Ba, Ca, Cd, Co, Cr, Cu, Fe, Ge, K, La, Li, Mg, Mn, Mo, Na, Ni, P, Pb, S, Sb, Se, Sn, Sr, V, W, Y, and Zn (digestion with $HNO_3/HClO_4$) and Si and Ti ($HNO_3/HClO_4/HF$). In addition, Cl was determined coulometrically after heating of a solid steel slag sample at 1200 °C in an oven and subsequent trapping of the evolved gases.

The carbonation degree (ζ_{Ca}) can be determined from the total Ca content of the fresh steel slag (Ca$_{total}$), the molar weights of Ca (MW$_{Ca}$) and CO$_2$ (MW$_{CO2}$), and the carbonate content measured with TGA-MS, corrected for the weight increase due to carbonation. In eq 2.6, it is assumed that only Ca is carbonated during the carbonation process, that the initial carbonate content of the (fresh) steel slag is negligible, and that no significant mass is lost due to leaching in the autoclave reactor:

$$\zeta_{Ca}[\%] = \frac{\dfrac{CO_2[wt\%]}{100 - CO_2[wt\%]} \times \dfrac{MW_{Ca}[kg/mol]}{MW_{CO_2}[kg/mol]}}{Ca_{total}[kg/kg]} \times 100 \qquad \text{(eq 2.6)}$$

Significant formation of other carbonates (mainly MgCO$_3$) is improbable because of the relatively low Mg content of steel slag and the very limited Mg conversion expected due to the relatively low CO$_2$ pressure and short reaction times (Chapter 1) applied in the experiments (see below for verification). Typical process conditions needed to carbonate Mg silicates via the aqueous carbonation route, without addition of extra chemicals or additional pre-treatment steps other than grinding, include p$_{CO2}$ > 100 bar and a reaction time in the order of hours (O'Connor et al., 2005).

The leaching characteristics of Ca and Si from the original steel slag were determined in a pH$_{stat}$ system, to obtain additional information on the available Ca species in the steel slag. Eight suspensions of a ground steel slag sample (d < 106 μm) and Nanopure-demineralised water at a liquid-to-solid ratio of 10 kg/kg were stirred in closed Teflon reaction vessels for 48 h at room temperature. For seven vessels, the pH was controlled automatically at a preset pH value by the addition of 1 or 5 M HNO$_3$ and 1 M NaOH. One vessel was left at the native pH of the sample. After 48 h, the pH of the suspensions was measured and the suspensions were filtered through 0.2 μm membrane filters. The clear filtrates were acidified with concentrated HNO$_3$ and, subsequently, analysed for Ca and Si by ICP-AES. The leaching of other elements was also measured. These data and geochemical modelling of the pH$_{stat}$ leaching curves are the subject of Chapter 3.

To determine the native pH of samples that had been carbonated in the autoclave, L/S = 10 kg/kg suspensions in Nanopure-demineralised water were prepared and stirred open to the atmosphere for 24 h. The pH was recorded continuously, and the pH value reached after stabilization was reported. Particle size distribution and volume-based mean particle size (D[4,3]) of samples were measured by laser diffraction (Malvern Mastersizer 2000) using ethanol (96%)

as dispersing agent. The BET single point method with N_2 was used to measure the specific surface area. Mineralogical composition was determined using powder X-ray diffraction (XRD) (Bruker, D8 advance). Samples were studied with a scanning electron microscope (SEM) with energy-dispersive X-ray (EDX) spot analysis. Finally, geochemical equilibrium calculations were performed with The Geochemist's Workbench 4.0 (GWB) (Bethke, 2002).

2.3   Results and Discussion

2.3.1   Feedstock Analysis

The bulk total composition of the steel slag used is shown in Table 2.1. The slag is rich in Fe originating from the processed iron ore and Ca from the addition of limestone in the steel production process to remove impurities (e.g. Si and P). The slag is very suitable for mineral CO_2 sequestration because of its high Ca content and high alkalinity (pH 12.6). The maximal CO_2 sequestration capacity is 0.25 kg of CO_2/kg of steel slag on the basis of the total Ca content, which would be equivalent to a carbonate content of the product of 20 wt% CO_2. The native pH of the fresh slag is in good agreement with the theoretical pH of a saturated portlandite ($Ca(OH)_2$) solution (pH 12.4 calculated with GWB), the presence of which was confirmed by XRD analysis. The acid neutralizing capacity of the fresh slag is 4.0 mol of HNO_3/kg on the basis of the total acid consumption in the pH_{stat} at pH 8 (i.e., approximating the pH of a calcium carbonate saturated system in equilibrium with the atmosphere). This value corresponds to a CO_2 sequestration capacity of 0.09 kg/kg. Since this value is based on the amount of Ca that is available for leaching at 25 °C, it is lower than the capacity based on the total composition.

Table 2.1: *Composition of fresh steel slag expressed in terms of oxides.*

Element [a]	Composition [wt%]
Fe_2O_3	35.5
CaO	31.7
SiO_2	9.1
MgO	6.0
MnO	3.4
Al_2O_3	1.6
TiO_2	1.3

[a] Only elements present at >1 wt% are shown.

The size distribution, mean particle size, and carbonate content of the different batches of fresh steel slag that were used for the carbonation experiments are

shown in Annex 2.1. All samples show a wide size distribution, which includes very small particles (<1 µm). The initial calcium carbonate content of the steel slag is significantly higher for the small size fractions and varies between 1.5 and 5.1 wt% CO$_2$, corresponding to a Ca conversion (eq 2.6) of 6 and 22%.

Table 2.2: *Identified minerals in fresh and carbonated steel slag (ζ_{Ca} = 60%, p_{CO2} = 20 bar, T = 150 °C, t = 30 min, d < 106 µm (batch 3), n = 500 rpm, L/S = 10 kg/kg) with analysis method.*

Element	Phase	Fresh steel slag	Carbonated steel slag
Ca	Ca(OH)$_2$ (portlandite)	XRD	ND [a]
	Ca-(Fe)-silicates	SEM	SEM
	Ca-Fe-O	SEM	SEM
	CaCO$_3$ (calcite)	TGA-MS (traces)	XRD, TGA-MS, SEM
Mg	Mg-Fe-O	SEM	SEM
	MgCO$_3$ (magnesite)	ND	XRD (traces)
other	SiO$_2$	ND	SEM
	FeO	SEM	SEM

[a] ND = not detected.

2.3.2 Mineralogy

Table 2.2 shows the mineralogical phases that were identified in a representative fresh and carbonated steel slag sample. Element mappings of Ca, Si, O, Fe, and Mg by SEM-EDX are shown in Annex 2.1. Calcite and traces of MgCO$_3$ (magnesite) were the only carbonates identified by XRD in the carbonated product. Comparison of the TGA-MS and TOC-SSM results (not shown) indicated that no significant amount of MgCO$_3$ was formed during the carbonation process, which confirmed that reaction conditions (i.e., particularly pressure) were insufficient to significantly carbonate Mg minerals. The same result was obtained for other degrees of carbonation. Therefore, the Ca conversion as defined by eq 2.6 can be applied to quantify the sequestration of CO$_2$ by the steel slag. For the further carbonation results presented in this paper only the TGA-MS results will be used.

2.3.3 Calcium Speciation

Three major phases of calcium in the fresh steel slag have been identified (Table 2.2): Ca(OH)$_2$, Ca-(Fe)-silicates, and Ca-Fe-O. The first two phases have been reported as minerals reacting with CO$_2$ in other alkaline solid residues (Reddy et al., 1994; Tawfic et al., 1995). A lower carbonation rate is expected for Ca silicates relative to Ca (hydr)oxides, on the basis of their solubility and previous carbonation experiments (see also Chapter 1) (Lackner et al., 1997).

Portlandite was converted completely to calcite at the applied carbonation conditions (Table 2.2).

Figure 2.1 shows the pH-dependent leaching of Ca and Si in a pH_{stat} system. At two pH values the leached amount of calcium shows a steep increase. The first step occurs between pH 11.1 and 9.6, and the calcium concentration at pH 9.6 is 6450.2 mg/L or 29.6% of the total calcium content. We define this part of the calcium as fraction I. The second step occurs between pH 5.1 and 3.5. At pH 3.5, 61.6% of the total Ca has been dissolved. Fraction II is defined as the increase in the second step (i.e., 32.0% of the total calcium content). This fraction includes the amount leached between pH 9.6 and 5.1. The rest (Ca fraction III, 38.4% of the total Ca) consists of Ca that is virtually insoluble or physically not available for leaching at this particular particle size and leaching time. Possibly, fraction III corresponds with the identified Ca-Fe-O phase.

Solubility products of $Ca(OH)_2$ (portlandite), amorphous SiO_2 (Allison et al., 1991), and CSH ($Ca_{1.1}SiO_7H_{7.8}$) (Gaucher et al., 2004) were used to calculate the solubility curves of these minerals, as shown in Figure 2.1. Ca fraction I probably consists mainly of portlandite and Ca silicates (similar to CSH) that are relatively easily leachable. Fraction II is assumed to consist of Ca silicates that are more difficult to dissolve, on the basis of the observed slight increase in Si leaching below pH 9.6.
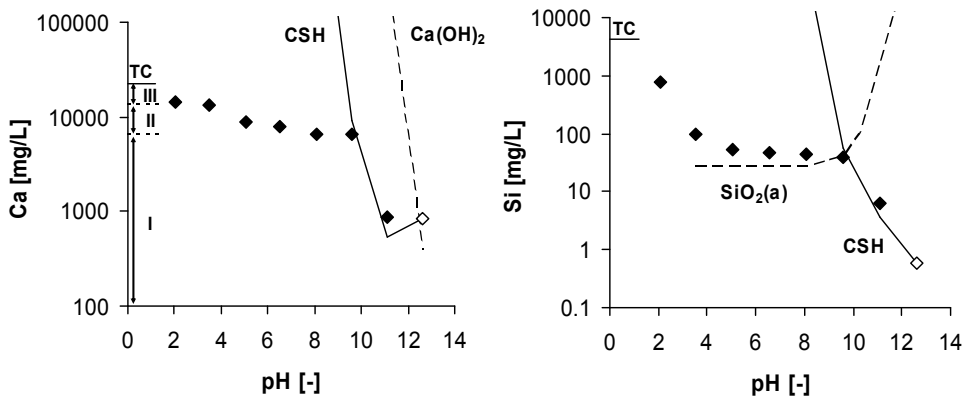

Figure 2.1: *Ca- and Si-leaching characteristics of fresh steel slag feedstock (<106 μm) and geochemical modelling of solubility control by specific minerals. Total content (TC) and Ca-fractions I-III are indicated. Open symbols indicate the native pH of the sample.*

2.3.4 Process Variables

Process conditions in the autoclave reactor were varied systematically to determine their influence on the Ca conversion and to identify the rate-limiting step in the carbonation of steel slag. Given equations 2.2 - 2.4, five different process steps can be distinguished: (1) diffusion of Ca toward the surface of the solid steel slag particles; (2) dissolution of Ca from the surface into the solution; (3) dissolution of gaseous CO$_2$; (4) conversion of dissolved CO$_2$ (aq) to the (bi)carbonate ion; (5) precipitation of CaCO$_3$. The main process variables are (1) reaction time (t), (2) temperature (T), (3) CO$_2$ pressure (p$_{CO2}$), (4) particle size (d), (5) stirring speed (n), and (6) liquid-to-solid ratio (L/S). These process variables were varied individually in six series of experiments. Ranges of process conditions were chosen such that a wide variation of conversions was obtained (20 - 80%). Because Ca fraction I was found to be carbonated very rapidly (see below), this study focuses particularly on the reaction mechanisms involved in the carbonation of Ca fraction II, and process conditions were selected accordingly. The results of the six series of experiments are shown in Figure 2.2 and will be discussed below.

In the following discussion, it is assumed that precipitation only occurs during the reaction at elevated temperature and pressure and that any possible formation of calcite upon depressurisation of the reactor is negligible. This assumption was tested by analysing a sample taken directly from the reactor at typical process conditions. Only 3% of Ca in the suspension was found to be dissolved just before depressurisation. It is unlikely that significant amounts of additional Ca are leached during the short depressurisation time (typically 1-2 min) and given the increasing pH. Therefore, no more that approximately 3% of the measured Ca conversion can be attributed to calcite formed during the depressurisation of the reactor.

Reaction Time. In the first 2 min over 40% of the calcium is carbonated (i.e., fraction I and 36% of fraction II), while only an extra 13% (or 39% of fraction II) reacts when the reaction time is increased to 30 min. This pattern is consistent with the observed calcium speciation in the fresh steel slag; first, a Ca fraction that is carbonated relatively easily (I), followed by a more difficult to convert fraction (II). Carbonation of fraction II is initially rapid and then declines gradually. The declining reaction rate shows that the precipitation of calcite is not rate-determining for this process. In that case, precipitated calcium carbonate would have enhanced further precipitation by serving as precipitation nuclei and a progressive increase of the conversion with reaction time would have resulted.
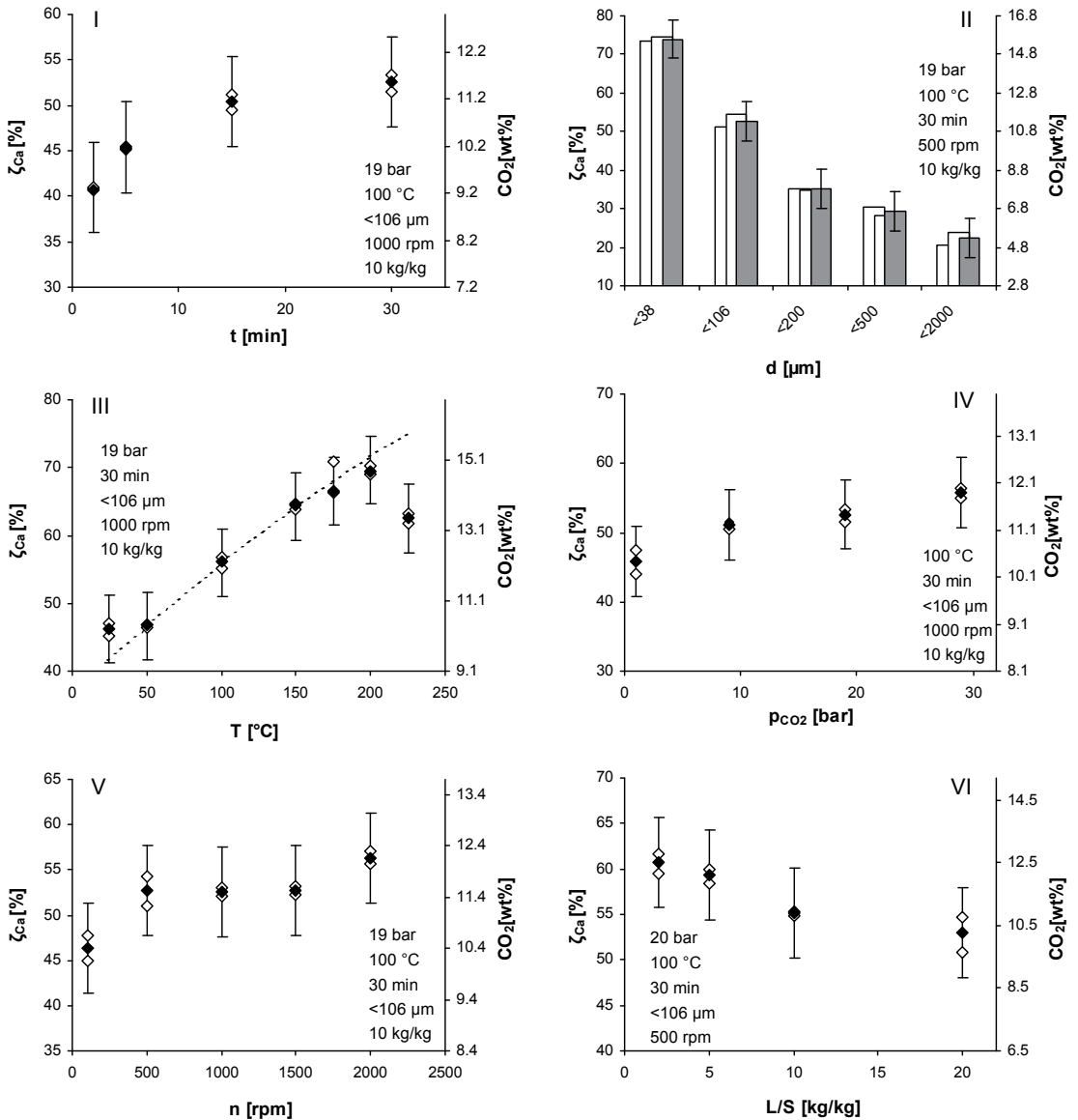
Figure 2.2: *Calcium-conversion (ζ_{Ca}) and carbonate content (CO_2) as a function of various process variables. For each carbonation experiment the duplicate TGA-analyses (open symbol) and the resulting mean conversion (solid symbol) are shown. Error bars are based on 5% absolute deviation of the Ca-conversion (as calculated in Chapter 3). (I) Reaction time, feedstock batch 2. (II) Particle size, sample <106 µm = batch 2. (III) Reaction temperature including Arrhenius-plot (dotted line) with A = 6.0 %Ca/min and E_a = 3.6 kJ/mol, batch 3. (IV) Carbon dioxide pressure, batch 2. (V) Stirring rate, batch 2. (VI) Liquid-to-solid ratio, batch 3.*

Particle Size. Reduction of particle size from <2 mm to <38 µm results in a large increase of the conversion from 24 to 74%. This observation suggests that reactions involving the solid particles contribute to the overall reaction rate. BET analyses performed on fresh steel slag samples 2 and 3 showed that steel slag particles are nonporous and, therefore, the specific surface area can be calculated directly from the D[4,3] value obtained from particle size analysis if we assume spherical particles. The conversion-particle size (D[4,3]) dependence measured at various reaction temperatures shows an exponential relation with a power of between -0.7 and -0.4. Thus, reducing the mean particle size by a factor of 2 increases the conversion relatively by 32 to 62%.

Temperature. The reaction temperature has two opposite effects on the carbonation rate. At higher temperatures leaching of Ca from the matrix is likely to proceed faster, but the solubility of carbon dioxide in the solution decreases. As shown in Figure 2.2, the carbonation increases toward higher temperatures between 25 and 175 °C. At temperatures above the optimum of around 200 °C, the conversion decreases when the temperature is increased further. Apparently, the lower carbon dioxide solubility limits the conversion at high temperatures. The observed temperature pattern and optimum correspond well with the reported pattern and optimal temperature (185 °C) for the aqueous carbonation of olivine (O'Connor et al., 2005). The calcium conversion between 50 and 150 °C shows an Arrhenius-type temperature dependence with ζ_{Ca}/t as pseudo-reaction rate for the carbonation of Ca-fraction II. The temperature influence shows that leaching of Ca is probably the rate-determining reaction step between 25 and 150 °C and that at temperatures above the optimum (i.e., >200 °C) a reaction step involving CO$_2$ becomes rate limiting.

Carbon Dioxide Pressure and Stirring Rate. At a reaction temperature below the temperature optimum, CO$_2$ pressure and stirring rate have a very limited influence on the reaction rate above a specific threshold value (i.e., 500 rpm and around 9 bar, respectively, as observed in preliminary experiments). These trends are also visible in Figure 2.2. Below this threshold, the Ca conversion decreases significantly due to inadequate mixing and a deficiency of dissolved CO$_2$, respectively. The presented carbonation experiments were typically conducted at conditions above these threshold values, and the reaction rate can, therefore, be considered independent of the stirring rate and CO$_2$ pressure. The insignificant effect of the CO$_2$ pressure shows that CO$_2$ mass transfer is not rate-determining and confirms that it is the leaching of Ca that controls the reaction rate. The leaching of Ca consists of two steps: (1) diffusion of Ca toward the surface of a particle; (2) dissolution of Ca from the surface into the solution. The negligible influence of the stirring rate on the conversion suggests that mass transfer from the particle's surface into the solution is relatively fast. Therefore,

the diffusion of calcium from the particle interior toward its surface is the likely reaction step that determines the overall carbonation rate.

Liquid-to-Solid Ratio. A decrease of the liquid-to-solid ratio results in a slight increase of the conversion, which might be explained by the higher ionic strength and, consequently, higher solubility of calcium. O'Connor et al. have shown that addition of salts could enhance the carbonation of Mg-silicates (O'Connor et al., 2005). L/S-ratios lower than two cannot be stirred sufficiently in the autoclave reactor that was used in this study and would result in poor CO_2 gas-liquid and Ca solid-liquid mass transfer rates. Therefore, we conclude that the optimal liquid-to-solid ratio in this type of reactor is 2 kg/kg.

2.3.5   Reaction Mechanisms

Figure 2.3 shows SEM micrographs of fresh and carbonated steel slag. Notable is the change in morphology of particle surfaces when comparing micrographs I and II. The carbonated particles contain a porous coating that is absent in the non-carbonated particles. The composition of this coating was identified as $CaCO_3$ by SEM/EDX analysis of polished samples embedded in resin (micrograph III). No separate calcium carbonate particles were identified in the carbonated sample. Further examination of the polished samples has revealed three other phases: (1) an iron-rich phase (indicated as Ca-Fe-O, Ca fraction III); (2) a calcium silicate phase (Ca fraction II); (3) a SiO_2 phase with traces of Ca. The first two phases are present in both the noncarbonated and the carbonated slag (Table 2.2). SiO_2 and $CaCO_3$ were only identified in the carbonated material. The formation of a carbonate coating and SiO_2 rim has also been reported for the carbonation of Mg ores (21).
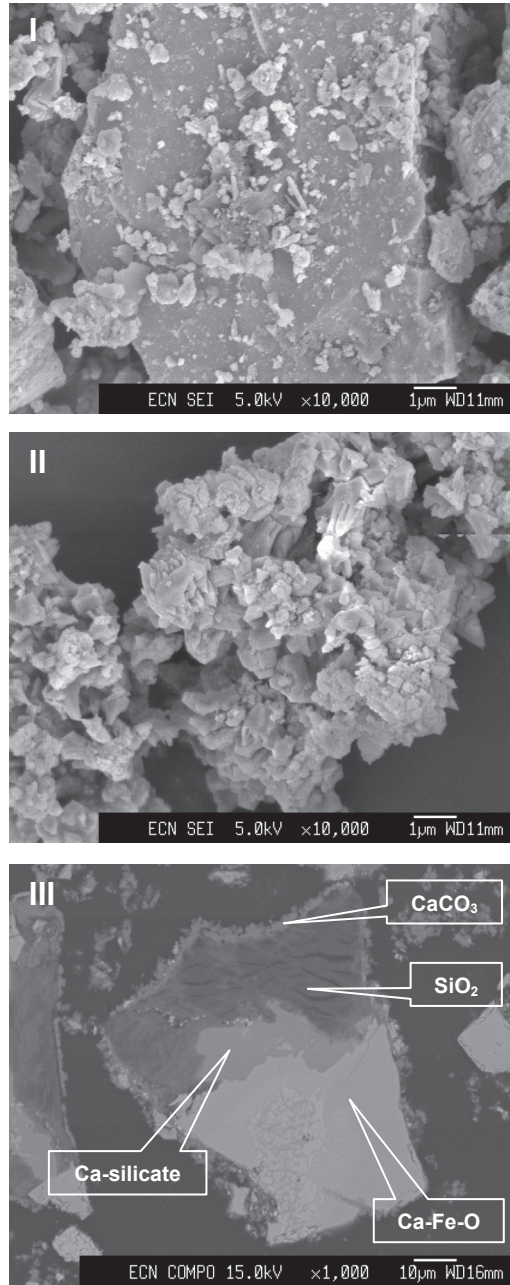
Figure 2.3: *SEM micrographs of fresh (I) and carbonated (II) steel slag (p$_{CO2}$ = 20 bar, T = 150 °C, t = 30 min, d < 106 μm (batch 3), n = 500 rpm, L/S = 10 kg/kg). SEM-BSE (backscatter electron) micrograph of polished carbonated steel slag particle embedded in resin with SEM-EDX analysis (III).*

The mineralogical changes taking place during carbonation resulted in a neutralization of the pH value. Figure 2.4 shows how the native pH of steel slag samples, measured after 24h stabilization, decreases with increasing carbonation degree for selected carbonation experiments at L/S = 10 kg/kg. The pH of the 74% carbonated slag (9.4) is still significantly higher than the pH of a solution saturated with calcite (8.3 calculated with GWB). Similar changes in mineralogy and pH values after carbonation have been reported for other alkaline residues (e.g. Reddy et al., 1991 & 1994; Tawfic et al., 1995). During the 24h pH measurement, the pH of carbonated steel slag suspensions was found to start around 8 after which it increased regressively before stabilizing. This behaviour suggests that the pH is controlled initially by calcite and at longer equilibration times by diffusion of residual alkalinity through the porous $CaCO_3$-coating.
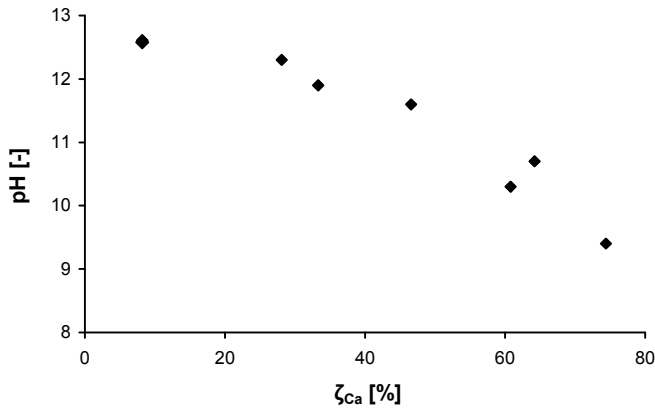
Figure 2.4: *Native pH of carbonated steel slag as a function of the degree of carbonation (L/S = 10 kg/kg, 24h).*

These observations and the influences of the process variables discussed above lead to the following conclusions on the carbonation mechanisms of steel slag:

(1) The carbonation of Ca takes place in two subsequent steps (i.e., dissolution and precipitation) rather than by solid-state conversion. After the initial rapid carbonation of the $Ca(OH)_2$ present in the fresh steel slag, calcium from the Ca silicate phase diffuses toward the surface of the particle and is subsequently leached (eq 2.3). The Ca in solution is carbonated and precipitates as calcite on the outer surface of the steel slag particles (eq 2.4).

(2) Among the various process steps, the diffusion of Ca toward the surface of steel slag particles probably determines the overall reaction rate at temperatures below an optimal conversion temperature (i.e., 200 °C for the

conditions presented). At higher temperatures or lower CO$_2$ pressures, a deficiency of dissolved CO$_2$ results in a decrease of the conversion.

(3) The leaching of Ca results in a withdrawing Ca silicate core surrounded by a Ca-depleted SiO$_2$ phase. This SiO$_2$ rim apparently hinders the diffusion of Ca from the particle interior resulting in a declining reaction rate.

Further enhancement of the carbonation rate could contribute to the development of a cost-effective CO$_2$ sequestration process and research efforts should focus particularly on the identified rate-controlling mechanisms.

Annex 2.1   Supporting Information[1]

Table A.2.1.1: *Definition, particle size, and carbonate content of the fresh steel slag batches.*

Batch	Size			TGA-MS
	Sieve class [µm]	$d_{0.5}$ [µm]	D[4,3] [µm]	$CaCO_3$ [wt% CO_2]
1	<38	11.6	14.6	5.1
2	<106	24.1	34.4	1.5
3	<106	19.7	32.6	2.0
4	<200	36.5	61.7	2.1
5	<500	45.3	97.4	1.7
6	<2000	ND [a]	ND	ND

[a] ND = not determined.
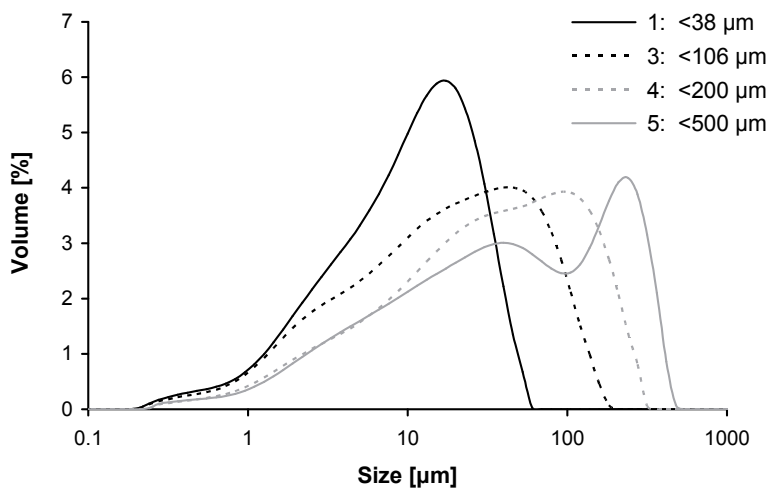
Figure A.2.1.1: *Particle size distribution of selected fresh steel slag batches.*

---

[1] Available at Environmental Science & Technology website, http://pubs.acs.org.
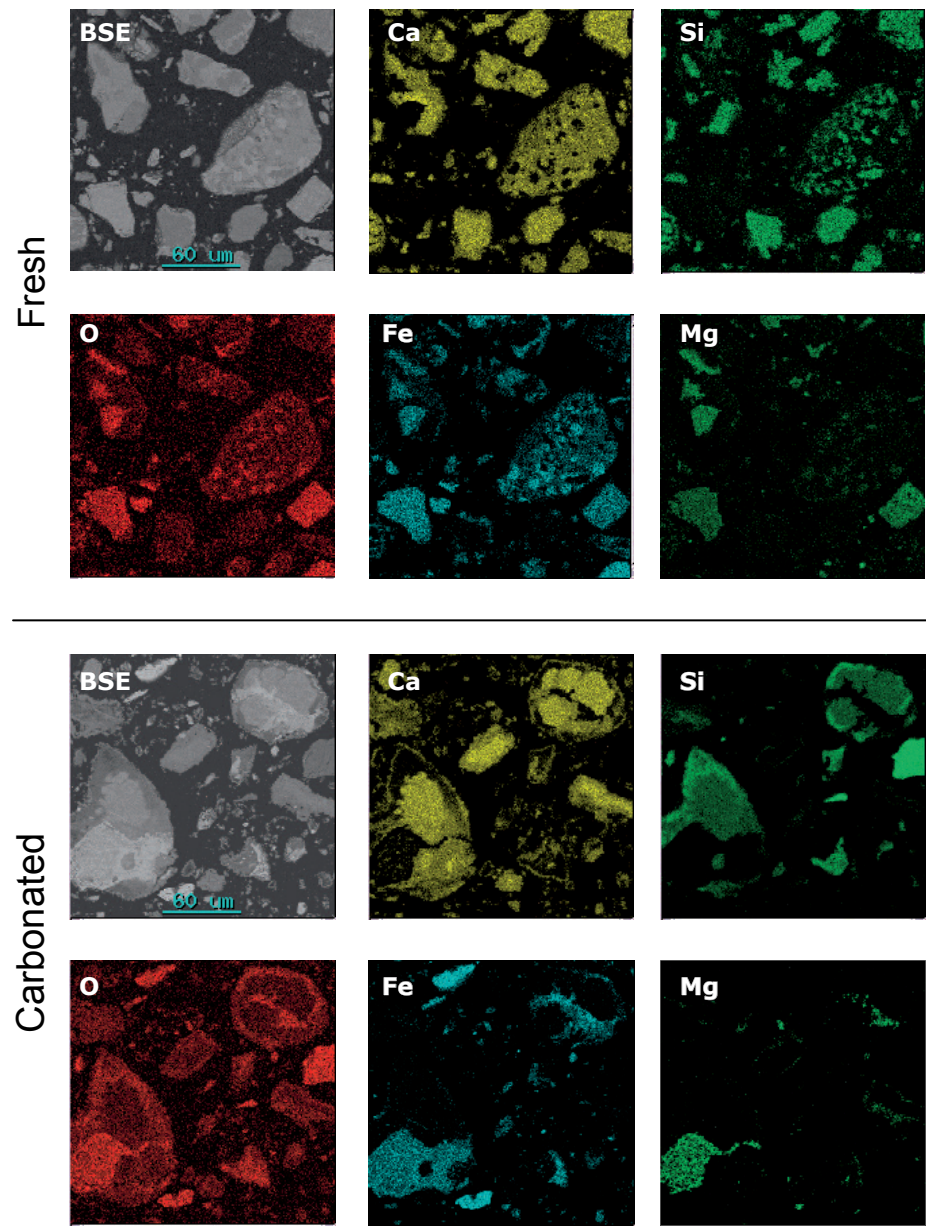
Figure A.2.1.2: *SEM-EDX image of fresh (top) and carbonated (bottom) steel slag samples.*

CHAPTER 3

CARBONATION OF STEEL SLAG FOR CO$_2$ SEQUESTRATION: LEACHING OF PRODUCTS AND REACTION MECHANISMS

Published in similar form as:

Huijgen, W.J.J. & Comans, R.N.J. (2006) *Carbonation of steel slag for CO$_2$ sequestration: leaching of products and reaction mechanisms*, Environmental Science and Technology, 40(*8*), 2790-2796.

CARBONATION OF STEEL SLAG FOR CO$_2$ SEQUESTRATION: LEACHING OF PRODUCTS AND REACTION MECHANISMS

Wouter J.J. Huijgen[1] & Rob N.J. Comans[1,2]

Carbonation of industrial alkaline residues can be used as a CO$_2$ sequestration technology to reduce carbon dioxide emissions. In this study, steel slag samples were carbonated to a varying extent. Leaching experiments and geochemical modelling were used to identify solubility-controlling processes of major and trace elements, both with regard to carbonation mechanisms and the environmental properties of the (carbonated) steel slag. Carbonation was shown to reduce the leaching of alkaline earth metals (except Mg) by conversion of Ca-phases, such as portlandite, ettringite, and Ca-(Fe)-silicates into calcite, possibly containing traces of Ba and Sr. The leaching of vanadium increased substantially upon carbonation, probably due to the dissolution of a Ca-vanadate. The reactive surface area of Al- and Fe-(hydr)oxides increased with the carbonation degree, which tends to reduce the leaching of sorption-controlled trace elements. Sorption on Mn-(hydr)oxides was found to be required to adequately model the leaching of divalent cations, but was not influenced by carbonation. Consideration of these three distinct reactive surfaces and possible (surface) precipitation reactions resulted in adequate modelling predictions of oxyanion and trace metal leaching from (carbonated) steel slag. Hence, these surfaces exert a major influence on the environmental properties of both fresh and carbonated steel slag.

---

[1] Energy Research Centre of The Netherlands.
[2] Wageningen University.

3.1 Introduction

Mineral CO_2 sequestration is a technology to reduce greenhouse gas emissions on the basis of the industrial carbonation of Ca/Mg-silicates (see Introduction and Chapter 1, and references therein). Its very large potential carbon sequestration capacity and the exothermic nature of the accompanying reactions have led to an increasing amount of research in this area in recent years (Chapter 1). In a previous paper, we have pointed to the use of alkaline solid residues as an inexpensive and directly available feedstock for mineral CO_2 sequestration, and we have studied the mechanisms of aqueous steel slag carbonation as a possible CO_2 sequestration process (Chapter 2).

Carbonation of alkaline solid residues is known to potentially affect the leaching of constituents from these materials. For example, reduced leaching of elements potentially harmful to the environment has been reported for residues such as municipal solid waste incineration (MSWI) bottom ash (Cu and Mo) (Meima et al., 2002), fly ash from coal fired power plants (Cd, Cu, Ni, Pb, Se, and Zn) (Reddy et al., 1994), and air pollution control residues (e.g., As, Cd, Cr, Pb, and Se) (Tawfic et al., 1995). In such studies, a number of (theoretical) mechanisms has been distinguished by which carbonation affects leaching, for example: (1) precipitation of carbonates, (2) pH-neutralization, (3) formation of minerals other than carbonates, (4) coprecipitation, and (5) sorption at freshly precipitated surfaces. In the literature, geochemical modelling has been successfully applied to identify the processes that control the leaching behaviour of constituents from (weathered) steel slag (Fällman, 2000; Apul et al., 2005). In this paper, we will perform geochemical modelling on the pH-dependent leaching behaviour of steel slag samples with a varying carbonation degree in order to further our understanding of the mechanisms of aqueous steel slag carbonation, particularly with respect to trace elements, which could not be studied by the methods used in the previous paper (Chapter 2) (i.e., varying process conditions and XRD and SEM analyses). In addition to its relevance for the identification of carbonation mechanisms, this combined leaching and geochemical modelling approach can provide insight into the binding mechanisms of (trace) elements. Finally, the leaching properties of secondary materials such as steel slag also form an important issue in assessments of their potential for beneficial utilization. Since an environmentally sound application of the carbonated products is a prerequisite for further process development of mineral CO_2 sequestration, this aspect will also be considered (see Annex 3.1).

3.2 Materials and Methods

3.2.1 Steel Slag Carbonation Experiments

Mineral CO_2 sequestration experiments were performed by carbonating steel slag analogously to the procedure applied in the previous paper (Chapter 2). In short, fresh steel slag was ground by a tungsten-carbide rotating disk pulveriser to pass a specific sieve size (d). A slurry of ground steel slag in Nanopure-demineralised water at a specific liquid-to-solid ratio (L/S) was carbonated in an autoclave reactor at elevated temperature (T) and CO_2 pressure (p_{CO2}). After the reaction time (t) had elapsed, the resulting slurry was filtered quantitatively through a 0.2 µm filter, after which the solid was dried overnight at 50 °C in an oven. The Ca-conversion to Ca-carbonate (ζ_{Ca}) (i.e., carbonation degree) was determined by measuring the carbonate content of the solid product by TGA-MS. For more details on the applied procedure, experimental setup, and analytical methods for the carbonation process, we refer to Chapter 2.

Carbonation experiments at identical conditions were repeated until sufficient material of the carbonated product was available for leaching experiments. The products of individual carbonation experiments were mixed homogeneously and, thus, three samples with a varying carbonation degree were obtained. Sample codes 30, 60, and 90 indicate the intended carbonation degree. In addition, two fresh steel slag samples with different particle sizes were prepared (sample code 0). The coarse sample (sample 0-c) was crushed to <2 mm. The fine sample (sample 0-f) was ground to a mean particle size similar to that of the feedstock used for the carbonation experiments. The definition, characteristics, and carbonation conditions of all five samples are shown in Table 3.1 and their particle size distributions measured by laser diffraction are given in Annex 3.1. All five samples originated from the same original fresh steel slag batch of which the total elemental composition has been given earlier in Chapter 2.

Repetition of carbonation experiments at identical conditions enabled determination of the experimental accuracy (see Annex 3.1). The absolute experimental error in the carbonation degree on the basis of two times the standard deviation (σ) is determined at 5.0%, at all process conditions.

During the preparation of samples 60 and 90, the process water remaining after the filtration of the slurry at the end of each carbonation experiment was stored for further analysis. The individual filtrates from repeated experiments at identical conditions were mixed, equilibrated with the atmosphere for 24h, and analysed, analogously to the pH_{stat} leachates (see below).

Table 3.1: *pH$_{stat}$ samples: characteristics, carbonation conditions, and Fe, Al, and Mn-selective chemical extraction data.*

Sample	0-c [a]	0-f [b]	30	60	90
Sample characteristics					
ζ_{Ca} [%]	ND [c]	8 ± 1	33 ± 5	62 ± 5	84 ± 5
CO_2 sequestered [g/kg] [d]	ND	NA [e]	76	154	210
pH [-]	ND	12.6	11.4	10.3	10.5
D[4,3] [μm] [f]	888	28	41	27	22
A_{spec} [g] [10^3 m^2/m^3]	33	836	NA	NA	NA
Process conditions					
Number of experiments	NA	NA	8	8	3
D[4,3]$_{feedstock}$ [μm]	NA	NA	37	33	38
T [°C]	NA	NA	30	150	200
p_{CO2} [bar]	NA	NA	2	20	30
t [min]	NA	NA	5	30	60
L/S [kg/kg]	NA	NA	10	10	3
n_{anchor} [rpm] [h]	NA	NA	500	500	500
Mean extraction results					
Fe-ASC [g/kg] [i]	ND	6.4 ± 0.2 [j]	18.0 ± 2.5	6.8 ± 1.6 [k]	7.1 ± 0.4 [j]
Fe-DITH [g/kg] [l]	ND	72.6 ± 3.2	78.4 ± 7.0	94.6 ± 4.9 [k]	99.0 ± 3.8
Al-OXA [g/kg] [m]	ND	1.5 ± 0.0	2.5 ± 0.1	2.4 ± 0.1 [k]	3.8 ± 0.1
Mn-DITH [g/kg] [n]	ND	12.7 ± 0.7	13.3 ± 1.6	12.8 ± 2.7 [k]	11.2 ± 0.2
Specific surface area					
Al+Fe [m^2/g]	ND	19.6 ± 0.8	31.7 ± 4.1	25.3 ± 2.7	28.8 ± 1.3
Al+Fe+Mn [m^2/g]	ND	40.0 ± 1.8	53.2 ± 6.6	45.9 ± 7.1	46.9 ± 1.5

[a] 'Coarse' sample 0; crushed to <2 mm. [b] 'Fine' sample 0; ground to mean particle size similar to that of feedstock used in carbonation experiments. [c] Not determined. [d] Per kg dried and calcinated fresh steel slag. [e] Not applicable. [f] Volume-based mean particle size. [g] Specific surface area assuming nonporous spherical particles. [h] Stirring rate of the anchor stirrer. [i] Ascorbine acid. Total content Fe: 248 g/kg. [j] Result based on two out of three measurements. [k] Extraction performed in duplicate instead of triplicate. [l] Dithionite. [m] Oxalate. Total content Al: 9 g/kg. [n] Total content Mn: 26 g/kg.

3.2.2 Characterization of Leaching Processes

The pH-dependent leaching characteristics of both the fresh and carbonated steel slag samples were determined in a pH$_{stat}$ system. Eight suspensions of a slag sample and Nanopure-demineralised water, at an initial liquid-to-solid ratio of 10 kg/kg, were stirred for 48h in closed Teflon reaction vessels at room temperature. For seven vessels, the pH was controlled automatically ±0.2 pH around a pre-set pH-value by the addition of 1 or 5 M HNO$_3$ and 1 M NaOH (pH: 2, 3.5, 5, 6.5, 8, 9.5, and 11 or 12.5). Final L/S ratios after pH adjustment were

typically between 10 and 12 kg/kg. For one vessel, the pH was not adjusted and leaching was performed at the native pH of the sample. After 48h, the pH and redox potential (sample 0-f and 60) of the suspensions were determined and the suspensions were filtered through 0.2 μm filters. The clear filtrate was divided into two fractions. One fraction was acidified with concentrated HNO_3 and analysed for Al, As, B, Ba, Ca, Cd, Co, Cr, Cu, Fe, K, Li, Mg, Mn, Mo, Na, Ni, P, Pb, S, Si, Sn, Sr, Ti, V, W, and Zn by ICP-AES. The other fraction was left untreated and analysed for Cl by ion-chromatography and for dissolved organic carbon (DOC) and dissolved inorganic carbon (DIC) with a C-analyser. P and S were assumed to represent PO_4 and SO_4, respectively. Element concentrations are reported at the final L/S ratios after pH adjustment.

3.2.3   Selective Chemical Extractions

Selective chemical extractions were performed in triplicate on the fresh and carbonated pH_{stat} samples to determine the amounts of Al-, Fe-, and Mn-(hydr)oxides. Extractions with dithionite (Kostka & Luther, 1994), ascorbic acid (Kostka & Luther, 1994), and oxalate (Blakemore et al., 1987) were used for total Fe-(hydr)oxides (Fe-DITH), amorphous Fe-(hydr)oxides (Fe-ASC), and total Al-(hydr)oxides (Al-OXA), respectively, following the approach of Dijkstra et al. (2004). The amount of crystalline Fe-(hydr)oxides was estimated from the difference in Fe extracted between the dithionite and the ascorbic acid extractions. The selective extractions used for Al- and Fe-(hydr)oxides were also applied for Mn. The dithionite and oxalate extractions gave similar results, but the ascorbic acid extraction resulted in much lower amounts of extracted Mn. The dithionite extraction was selected to determine the amount of Mn-(hydr)oxides (Mn-DITH), since dithionite extractions have been used previously for the (selective) chemical extraction of Mn-(hydr)oxides (e.g., Deming et al., 2001; Nearman et al., 2004).

3.2.4   Geochemical Modelling

Geochemical modelling was performed on the pH_{stat} leachates and the process water samples from the carbonation experiments to identify the leaching processes. For this purpose, two models were set up in the geochemical modelling framework ORCHESTRA (Meeussen, 2003), which are both discussed below.

Solubility Control. Solubility control modelling started by calculation of mineral saturation indices (SI), defined here as $\log(IAP/K_{sp})$ with IAP = ion activity product and K_{sp} = solubility product. The thermodynamic database used consisted of the MINTEQA2 database version 3.11 (Allison et al., 1991),

extended with minor modifications as described by Dijkstra et al. (2002) and with solubility constants for Ca-silicates (i.e., CSH-phases and zeolites) (Gaucher et al., 2004). Subsequently, potential solubility controlling minerals were selected on the basis of (1) the determined SI-values (i.e., closeness to zero), (2) likeliness of their presence in (carbonated) steel slag, and (3) the resemblance of the calculated solubility curve (see below) and the measured pH_{stat} data. Finally, the total element concentration in solution corresponding with solubility control by an infinite amount of a selected mineral was calculated, as explained in detail by Meima and Comans (1997).

Sorption on Metal(hydr)oxides. Sorption on metal-(hydr)oxides often controls the leaching of minor and trace elements, such as oxyanions and heavy metals (e.g., Dijkstra et al., 2004; Apul et al., 2005). Sorption of both cations (Co^{2+}, Ni^{2+}, Zn^{2+}, and Cr^{3+}) and oxyanions (CrO_4^{2-}, MoO_4^{2-}, and VO_4^{3-}) on Fe-, Al-, and Mn-(hydr)oxides was modelled, in the presence of concentrations in solution of main constituents (e.g., Ca, DIC), soluble constituents (e.g., Cl, Na, K) and elements competitive for sorption (e.g., P, S), using the diffuse layer model and parameters of Dzombak and Morel (1990). Sorption on amorphous and crystalline Fe-(hydr)oxides as well as Al-(hydr)oxides was modelled with sorption reactions on hydrous ferric oxide (HFO), following the approach of Dijkstra et al. (2004). In addition to sorption on Al- and Fe-(hydr)oxides, we have considered sorption on Mn-(hydr)oxides, given the relatively large amount of Mn present in steel slag (Chapter 2) and the known sorption ability of Mn-(hydr)oxides (Tonkin et al., 2004). The recent publication of specific sorption constants for divalent metal cations on Mn-surfaces by Tonkin et al. (2004) enabled direct incorporation of these processes in the generalized two-layer model of Dzombak and Morel (1990).

The amount of metal-(hydr)oxides determined by selective chemical extractions were used to calculate the surface area available for sorption, after correction for the dissolved amount of Al, Fe, and Mn at each specific pH. In these calculations, a specific surface area of 600 m^2/g was used for amorphous Fe-(hydr)oxide and Al-(hydr)oxide and 100 m^2/g for crystalline ferric (hydr)oxide, respectively (Dijkstra et al., 2004). As input for the reactive surface area of hydrous manganese oxide (HMO), a molar mass of 119 g_{HMO}/mol$_{Mn}$ and a specific surface area of 746 m^2/g_{HMO} were used in the model, following the approach of Tonkin et al. (2004).

The element concentrations in the leachates were modelled over the total pH range starting from a specific pH starting point at which the availability of the sorbate (i.e., the maximum fraction of an element that can be leached) is determined. For all sorbates except Mo, the concentration in the pH 2 leachate

was taken as an estimate of availability, since it is assumed that at this pH the element fraction that can potentially be leached, is in solution. For Mo, the highest concentration in the alkaline pH-range was taken (e.g., at pH 8 for sample 0-f). Verification of these assumptions by modelling with ORCHESTRA for each individual sorbate showed that at most 8% remained sorbed at pH 2 (or, e.g., pH 8 for Mo).

In both model definitions described above, the effect of binding to DOC on the speciation of elements was not considered in view of the low amount of DOC (i.e., ≤10 mg/L) measured in the pH_{stat} leachates (Annex 3.1). In addition, an oxidizing environment (pH + pe = 16) was assumed for all leachates on the basis of the redox potentials measured in the pH_{stat} leachates of samples 0-f and 60. Finally, the Davies equation was used for calculating the activities of solution species.

3.3   Results and Discussion

The pH_{stat} leaching curves of all elements analysed including DOC and DIC are given in Annex 3.1 for all five pH_{stat} samples. Figure 3.1 shows a selection of these data, i.e., the pH-dependent leaching of the major elements (Fe, Ca, Si, Mg, Mn, and Al) and a selection of trace elements (V, S, Cr, Sr, Ba, and Ni), for the finely ground fresh steel slag sample 0-f and the carbonated steel slag samples 30 and 60 (samples 60 and 90 have a similar native pH and show similar leaching). Figure 3.1 also shows the modelling results of element concentrations in the leachates for the most representative samples (i.e., sample 0-f for processes relevant for fresh steel slag and sample 60 for processes relevant for carbonated products). In Annex 3.1 similar graphs as Figure 3.1 are shown for Co, Zn, and Mo. In comparing modelling results with measured concentrations, it should be noted that the used 'infinite solid approach' (Meima & Comans, 1997) may overpredict leaching at pH-values where mineral solubility is very high (e.g., Mg, Sr, and Mn at low pH). The saturation indices of selected minerals are given in Table 3.2 for the leachates at native pH of samples 0-f, 30, 60, and 90 and for the process water samples resulting from the preparation of sample 60 and 90.

The grinding of the starting material and the experimental conditions (i.e., aqueous environment at elevated temperature and CO_2 pressure) result in significant leaching during the carbonation process itself. Therefore, both the effect of size reduction and the release of soluble constituents during the carbonation process are considered in Annex 3.1. For most elements, grinding does not significantly affect their leaching behaviour. The leachable amounts of

alkali metals, Cl, Mo, and S are reduced by prior leaching during the carbonation process.

The effect of carbonation on leaching and its implications for the reaction mechanisms during the carbonation process will be discussed for four categories of elements: (1) elements that play a role in the carbonation reactions determined previously (2) (i.e., Ca and Si), (2) other alkaline earth metals that can potentially be carbonated (i.e., Mg, Sr, and Ba), (3) elements providing reactive (hydr)oxide surfaces (i.e., Al, Fe, and Mn), and (4) (other) minor and trace elements (oxyanions and heavy metals) that are potentially harmful to the environment.

Table 3.2: *Saturation indices of selected minerals in pH_{stat} leachates at native pH and process water samples resulting from the carbonation experiments.*

Element	Mineral	pH_{stat} leachate [a]				Process water [b]	
	Sample	0-f	30	60	90	60	90
Ca	Portlandite, $Ca(OH)_2$	0.3	-2.9	-5.0	-4.8	-8.5	-8.6
	CSH_1.1, $Ca_{1.1}SiO_7H_{7.8}$	0.0	0.7	-0.4	-0.5	-3.5	-3.3
	Ettringite [c]	0.1	-6.9	-13.6	-13.4	-16.2	-15.9
	Calcite, $CaCO_3$	1.6	1.6	1.3	1.4	2.3	2.5
Si	CSH_1.1, $Ca_{1.1}SiO_7H_{7.8}$	0.0	0.7	-0.4	-0.5	-3.5	-2.3
	Silica, SiO_2 [d]	-5.6	-1.4	-0.1	-0.5	0.6	0.9
Mg	Brucite, $Mg(OH)_2$	0.5	0.4	-0.6	-0.7	-2.5	-2.6
	Magnesite, $MgCO_3$	-4.6	-1.5	-0.6	-0.9	2.0	2.1
Ba	Barite, $BaSO_4$	-0.9	-2.0	-2.7	-3.0	-1.1	-1.3
	Witherite, $BaCO_3$	-2.2	-3.2	-4.0	-4.0	-2.3	-2.3
Sr	Strontianite, $SrCO_3$	-0.9	-1.0	-1.8	-1.6	-0.5	-0.0

[a] pH_{stat} leachate at the sample's native pH. [b] Process water resulting from the carbonation experiments. pH of both process water samples is 8.3, corresponding with the theoretical pH of a solution saturated with calcite. [c] $Ca_6(Al)_2(OH)_{12}(SO_4)_3 \cdot 26H_2O$. [d] Amorphous.
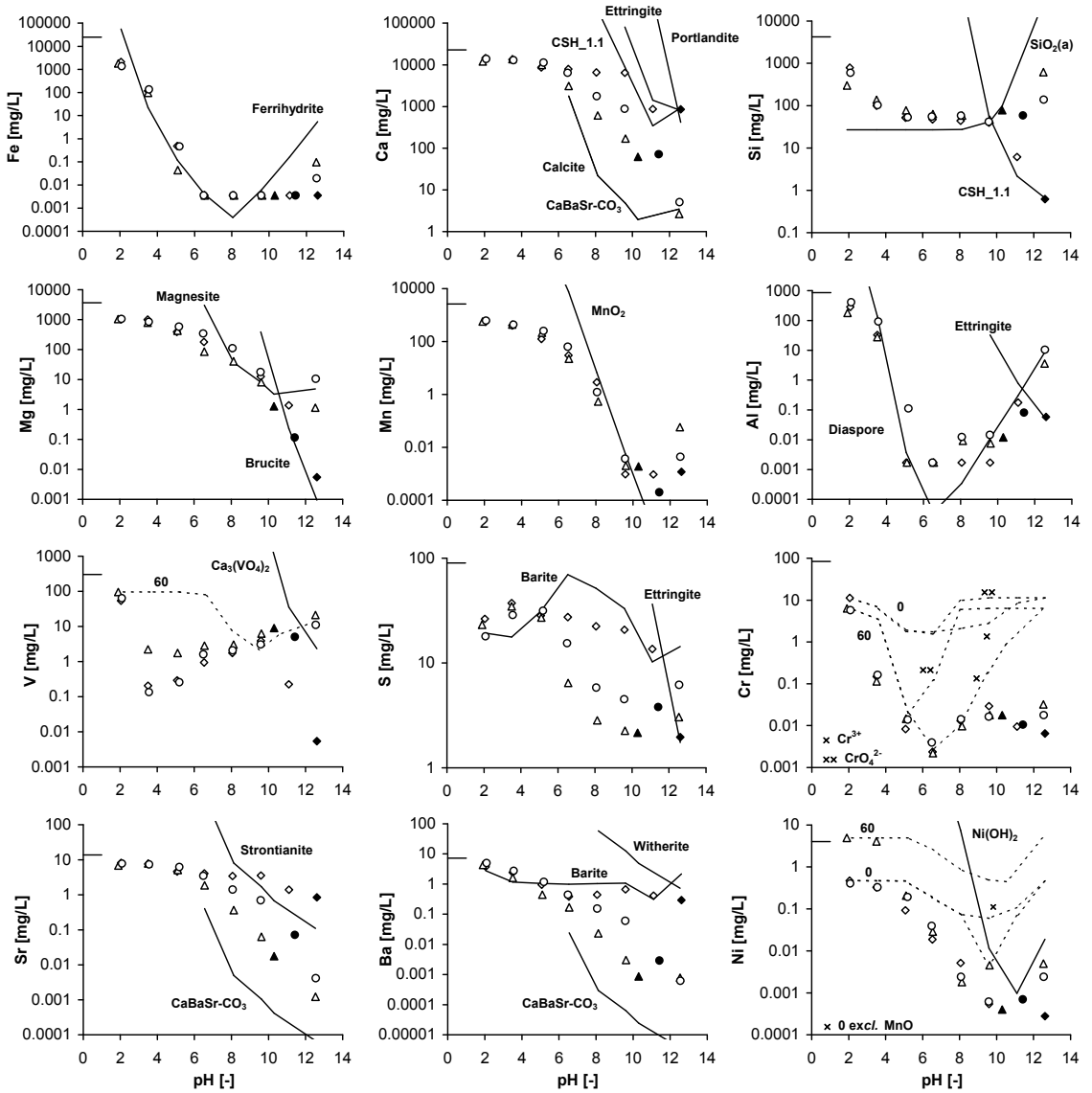
Figure 3.1: *pH$_{stat}$ leaching curves of main and selected trace elements for the 'fine' fresh steel slag sample 0-f (◇) and carbonated samples 30 (○) and 60 (△). Solid symbol: concentration in pH$_{stat}$ leachate at native pH. Data points below the detection limit (DTL) are shown as half of the DTL. Selected modelling results for the pH$_{stat}$ leachates of samples 0-f and 60; either on the basis of solubility control by a specific mineral or solid solution (——) or on sorption processes (- - -). Short horizontal lines represent the total amount present in the fresh steel slag.*

3.3.1 Calcium and Silicon

The fresh steel slag contains at least three Ca-mineral phases as shown in an earlier study (Chapter 2): $Ca(OH)_2$ (portlandite), Ca-(Fe)-silicates, and Ca-Fe-oxides. On the basis of its pH-dependent Ca-leaching profile (here shown in Figure 3.1), three Ca-fractions were defined with respect to their expected dissolution and carbonation rate: fraction I (i.e., 30% of the total Ca for a ground steel slag sample) was assumed to consist of portlandite and Ca-(Fe)-silicates that are relatively easily leachable, fraction II (32%) of Ca-(Fe)-silicates that are more difficult to dissolve and fraction III (38%) of Ca-Fe-oxides that are probably virtually insoluble at this particular particle size and leaching time (Chapter 2). Portlandite controls the slag's native pH of 12.6 and dissolves rapidly upon a pH decrease (Figure 3.1). A relatively easily leachable fraction of the Ca-(Fe)-silicates dissolves between pH 11 and 9.5 and causes a steep increase of the Ca-concentration in the pH_{stat} leachates between these pH-values (Figure 3.1). A number of specific Ca-silicates has been reported for fresh steel slag (Shi, 2004). Given the available Ca-silicate minerals in our thermodynamic database, the steep increase in Ca-concentration in the leachates and the corresponding Si behaviour can be described most adequately by the cement mineral CSH_1.1 ($Ca_{1.1}SiO_7H_{7.8}$) (Gaucher et al., 2004) (Figure 3.1). Geochemical modelling based on the total set of elements analysed shows that ettringite ($Ca_6(Al)_2(OH)_{12}(SO_4)_3 \cdot 26H_2O$) may also be present in the fresh steel slag, given a SI-value of 0.1 at native pH and the shape of the pH_{stat} leaching curves of Al, Ca, and S at pH 11-12.5 (Figure 3.1). Ettringite also dissolves rapidly upon a pH decrease (Figure 3.1), which makes it part of Ca fraction I. Therefore, ettringite might be responsible for the significant prior leaching of S during the mineral CO_2 sequestration experiments in the autoclave reactor.

During carbonation, the Ca-minerals are (partly) converted into calcium carbonate. Calcite is the only crystalline form of calcium carbonate detected by XRD in carbonated steel slag (Chapter 2). Calcite is less soluble than the original solubility-controlling Ca-phases and, therefore, the Ca-concentration in the leachates decreases significantly (Figure 3.1). The pH_{stat} leaching curves of samples 0-f, 30, and 60 develop toward the calcite solubility curve upon a higher degree of carbonation. However, both the leachates and process water samples remain 1-2 orders of magnitude oversaturated with respect to calcite (Table 3.2), a commonly observed phenomenon in leachates from (carbonated) secondary materials (see Meima & Comans (1997), and references therein).

The carbonation degrees of samples 30 and 60 suggest virtually complete conversion of the defined Ca-fractions I and I + II, respectively. Indeed, the leachates of the carbonated samples at their native pH and the process water

from the preparation of sample 60 are undersaturated by orders of magnitude with respect to portlandite and ettringite, which suggests that these Ca-phases have been converted into calcite. The absence of portlandite in carbonated steel slag could be confirmed by XRD by comparing a fresh and a carbonated sample. In addition, the leaching curves of Si show that (at least a part of) the Ca-silicate present in the fresh slag has been carbonated for all carbonated samples. During carbonation of Ca-silicates, a Ca-depleted silicate rim is formed around the steel slag particles (Chapter 2), which causes the solubility of Si to be controlled by amorphous SiO_2 instead of Ca-silicate minerals. This conversion results in increasing Si concentrations at high pH in the carbonated samples' leachates in contrast with the decreasing pattern for the fresh sample. The significant overestimation of Si concentrations at pH > 9.5 by the geochemical model used is probably due to the experimental leaching time (48h), which may be insufficient to reach solubility equilibrium with SiO_2, as was also observed earlier for weathered steel slag (Apul et al., 2005) and MSWI bottom ash (Kirby & Rimstidt, 1994). The Ca-silicate phase, however, does not seem to have been carbonated completely, since the leachates of samples 60 and 90 remain close to saturation with CSH_1.1 at native pH.

As stated above, samples 60 and 90 have a similar native pH and show generally similar leaching behaviour. These observations suggest that the mineralogical composition of the carbonated particle surfaces are similar at the two carbonation degrees, consistent with the earlier observed formation of a $CaCO_3$ coating and a SiO_2 rim (Chapter 2). The native pH of these largely carbonated samples is about two units higher than the pH of a calcite saturated system at atmospheric CO_2 pressure (i.e., 8.3). The remaining alkalinity probably originates predominantly from unconverted parts of the Ca-silicate phase in the interior of the particles, as discussed earlier (Chapter 2).

Summarizing, mineral formation during carbonation affects the Ca (and Si) leaching. The geochemical modelling results suggest that the following Ca-carbonation reactions have occurred during the carbonation of steel slag:

$$Ca(OH)_2 \text{ (portlandite)} + CO_2 \rightarrow CaCO_3 \text{ (calcite)} + H_2O \qquad \text{(eq 3.1)}$$
$$Ca_6(Al)_2(OH)_{12}(SO_4)_3 \cdot 26H_2O \text{ (ettringite)} + 6\ CO_2 \rightarrow$$
$$CaCO_3 \text{ (calcite)} + 2\ Al^{3+} + 3\ SO_4^{2-} + 32\ H_2O \qquad \text{(eq 3.2)}$$
$$\text{Ca-silicate (CSH)} + CO_2 \rightarrow$$
$$CaCO_3 \text{ (calcite)} + SiO_2 \text{ (amorphous silica)} \textit{ (partly)} \qquad \text{(eq 3.3)}$$
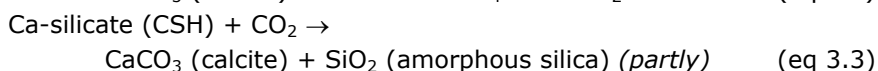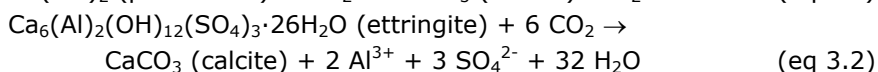
3.3.2 Magnesium, Strontium, and Barium

Alkaline earth metals other than Ca can potentially also form carbonates during aqueous steel slag carbonation. If an alkaline earth metal is carbonated, its concentration in the leachates decreases due to the formation of a less soluble carbonate, analogously to Ca.

For Mg, the pH_{stat} leaching curve hardly changes after carbonation, which implies that Mg has not been carbonated significantly. For the fresh steel slag at pH > 9.5, the leaching of Mg can be adequately modelled with solubility control by brucite $(Mg(OH)_2)$ (Figure 3.1). For the carbonated samples, the SI of brucite tends to undersaturation, while that of magnesite $(MgCO_3)$ increases toward zero with the carbonation degree (Table 3.2). The process water samples are two orders of magnitude undersaturated and oversaturated with respect to brucite and magnesite, respectively. Probably, during the 24h in which the process water samples were equilibrated with the atmosphere, magnesite has formed in the solution originally oversaturated with CO_2. The apparently slow formation of magnesite might explain its detection by XRD at trace levels in a carbonated steel slag sample (Chapter 2) and also the lack of any substantial magnesite formation at the process conditions applied, consistent with earlier observations (Chapter 2).

The concentrations of Ba and Sr in the leachates do decrease by several orders of magnitude upon carbonation. The leaching of Ba from the fresh steel slag seems to be controlled by the solubility of barite $(BaSO_4)$ at pH 2-11, as reported earlier for steel slag (Fällman, 2000). Solubility control by $Ba(SO_4,CrO_4)$ or $(Ba,Ca)SO_4$ solid solutions, as also suggested in the literature (Fällman, 2000; Apul et al., 2005), gives a less adequate description of the Ba leaching. After carbonation, the Ba concentrations in the leachates follow the $BaCO_3$ (witherite) solubility curve at pH ≥ 8, but the concentrations are orders of magnitude undersaturated. The same applies for Sr and $SrCO_3$ (strontianite). A possible explanation could be the formation of a (Ca,Ba,Sr)-carbonate solid solution. Incorporation of small amounts of Ba- and Sr-carbonate in a calcite structure reduces their activity coefficient and, thereby, their solubility, without significantly changing the solubility of calcite (i.e., Ca remains equally oversaturated). The composition of an ideal solid solution was determined for each individual data point with a model setup within ORCHESTRA (Meeussen, 2003) based on the relative activities of Ca, Ba, and Sr in solution and the solubility constants of the corresponding carbonate minerals. The calculated compositions lie within narrow margins between pH 8 and the native pH for all carbonated samples (e.g., sample 60: 99.86 - 99.94% Ca, 0.0005 - 0.0014% Ba, and 0.06 - 0.14% Sr). The solubility curves of the solid solution shown in

Figure 3.1 were determined by correcting the solubility constants of the three carbonate end members by the calculated mole fractions of Ca, Ba, and Sr at native pH.

3.3.3   Reactive Al-, Fe-, and Mn-(hydr)oxide Surfaces

The leaching curve of Al can be modelled adequately by the solubility of diaspore (AlOOH) for all samples, except at high pH for the non-carbonated sample where ettringite is probably present (Figure 3.1). Similarly, the leaching of Fe for all samples can be described by ferrihydrite ($Fe(OH)_3$). Analogously to Al, ferrihydrite significantly overestimates the leaching of Fe at high pH. Possibly, cementitious (Fe-containing) phases that are not present in our thermodynamic database are playing a role at strongly alkaline conditions. Carbonation leads to an increase of the amount of total Fe- and Al-(hydr)oxides determined by selective extraction (i.e., Fe-DITH and Al-OXA, respectively, in Table 3.1). Also Fe-ASC (amorphous Fe-(hydr)oxides) tends to increase with the carbonation degree (except sample 30). For samples 60 and 90, the Fe-(hydr)oxides formed upon carbonation are mainly crystalline (i.e., the amount of total Fe-(hydr)oxides extracted increases more strongly with the carbonation degree than that of amorphous Fe-(hydr)oxides). However, for sample 30 the formed Fe-(hydr)oxides seem to be mainly amorphous. The lower reaction temperature applied in the carbonation experiments of sample 30 (i.e., 30 °C vs. 150-200 °C for the higher carbonation degrees) may have prevented the formation of crystalline Fe-(hydr)oxides. Enhanced temperatures are generally required for the formation of crystalline Fe-(hydr)oxides within relatively short timescales; e.g., 60 °C for the synthesis of goethite (Hiemstra et al., 1989). Because amorphous Fe-(hydr)oxides have a larger specific surface area than crystalline Fe-(hydr)oxides (i.e., 600 vs. 100 m^2/g in the model), this observation suggests that carbonation at low temperature results in a higher reactive surface area. For all samples, the specific surface area for sorption provided by Al- and Fe-(hydr)oxides is higher after carbonation (i.e., up to 47%) (Table 3.1). The relative occurrence of Fe-ASC and Al-OXA in our more finely ground steel slag is very similar to those reported by Apul et al. (2005), although the absolute levels are substantially higher.

The concentration of Mn in the leachates of all samples increases steeply upon a pH decrease below pH 11, which can be adequately described by the solubility of MnO_2. Carbonation has no distinct effect on the amount of Mn-(hydr)oxides extracted (Table 3.1). Including Mn-(hydr)oxides in the sorption model results in a substantial increase of the total surface area available for sorption for the various samples (i.e., 18.1 - 21.5 m^2/g or 63 - 104 %) (Table 3.1). The total specific surface area for sorption including extractable Mn-(hydr)oxides is (still)

slightly higher for the carbonated steel slag samples than for sample 0-f (Table 3.1), although no apparent relation with the carbonation degree was found.

3.3.4 Oxyanions and Heavy Metals

Consideration of the leaching of potentially hazardous oxyanions and heavy metals, particularly V and Cr which are present in substantial amounts in steel slag (Proctor et al., 2000; Chapter 2), is important in evaluating potential reuse possibilities for (carbonated) steel slag (see also Annex 3.1). The leaching pattern of V from the fresh steel slag suggests the presence of Ca-phases in which V is incorporated, as reported earlier (Prelinger & Klepp, 2002). Between pH 12.5 and 9.5, these phases dissolve, following the shape of the solubility curve of $Ca_3(VO_4)_2$, although the leachates remain undersaturated. Vanadium solubility control by $Pb_3(VO_4)_2$ at neutral pH, as suggested by Apul et al. (2005), could not be confirmed. After carbonation, the leaching pattern of V at high pH has changed and V leaching around native pH is probably sorption controlled.

For Cr, no mineral in the thermodynamic database provided an adequate description of its leaching at any pH (see also discussion on Ba). Sorption of Cr was modelled assuming either (anionic) chromate (CrO_4^{2-}) or (cationic) Cr^{3+} as the dominant Cr species. Sorption of Cr^{3+} describes the Cr leaching from the carbonated samples better than chromate (Figure 3.1), despite the oxidizing environment in the pH_{stat} leachates. Cr is mainly present as Cr(III) in steel slag due to its reducing nature (Proctor et al., 2000) and, apparently, the (complete) oxidation of Cr(III) toward Cr(VI) has not occurred. For the fresh steel slag, the sorption model cannot describe the measured data adequately, given the high Cr availability of 0.22 mmol/L, relative to the available reactive (type I) surface sites in the model (0.18 mmol/L). This condition makes the model particularly sensitive to correct assumptions with regard to both the availability of Cr and that of the reactive surface sites. It should be noted that, for Cr^{3+}, the only surface complexation reaction in the model of Dzombak and Morel (1990) is defined for the high-affinity and low-capacity (type I) HFO-sites. In addition, no parameters for Cr sorption on Mn-(hydr)oxides have been provided by Tonkin et al. (2004).

The leaching of both Ni and Co from the fresh steel slag is adequately described by sorption, except at pH > 9.5 at which (hydr)oxides are likely to control leaching (Figure 3.1 and Annex 3.1). The extension of the sorption model compared to earlier studies such as Apul et al. (2005) with sorption on Mn-(hydr)oxides is required to adequately predict the leaching of both elements between pH 8 and 9.5. Upon carbonation, the pH-range in which Co shows significant sorption seems to become wider, which might be due to the increased

reactive surface area. This effect is not noticeable for other sorbates. Co shows a decreased availability after carbonation, while the availability of Ni increases at elevated carbonation temperature (samples 60 and 90).

The leaching of Zn was also modelled by sorption, because the Zn concentrations are orders of magnitude undersaturated with respect to solubility control by, e.g., ZnO (Annex 3.1). Since surface complexation of Zn on HFO and HMO could not adequately describe the Zn leaching at pH > 9.5, the sorption model was extended with surface precipitation reactions for Zn on Fe-(hydr)oxides as discussed by Dijkstra et al. (2004). This extension was tested for all divalent cations, but only for Zn an improvement of the modelling results was found. Overall, the decreased leaching of Zn after carbonation does not seem to be caused by the precipitation of metal carbonates as suggested by Reddy et al. for fly ash carbonation (Reddy et al., 1994), but solely by the decrease of the native pH. For Zn, the effect of surface complexation on HMO is less prominent than for Co and Ni.

Finally, the pH$_{stat}$ leaching curve of Mo was described adequately by the sorption model, for both samples 0-f and 60 (Annex 3.1). The Mo concentrations in the pH $\leq$ 5 leachates are below the detection limit for all pH$_{stat}$ samples (Annex 3.1). The reduced leaching after carbonation at alkaline conditions is probably mainly due to prior leaching during aqueous steel slag carbonation.

Consideration of the major reactive Al-, Fe-, and Mn-(hydr)oxide surfaces in steel slag, as well as possible surface precipitation reactions, enables adequate modelling predictions of oxyanion and trace metal leaching from both fresh and carbonated steel slag. Hence, these surfaces exert a major influence on the environmental properties of both fresh and carbonated steel slag, which warrants their explicit consideration in the environmental risk assessment of these materials.

Annex 3.1 Supporting Information[1]
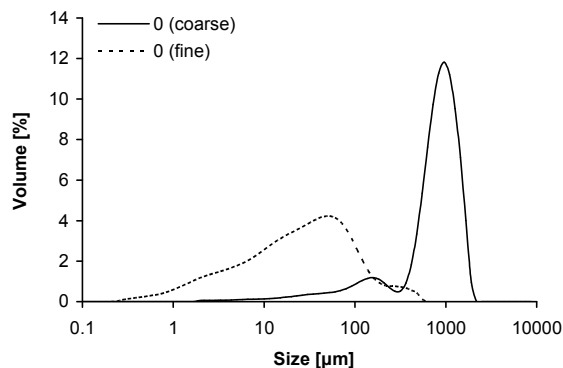
Sample	$d_{0.5}$	$D[4,3]$
0 (coarse)	895	888
0 (fine)	28	55
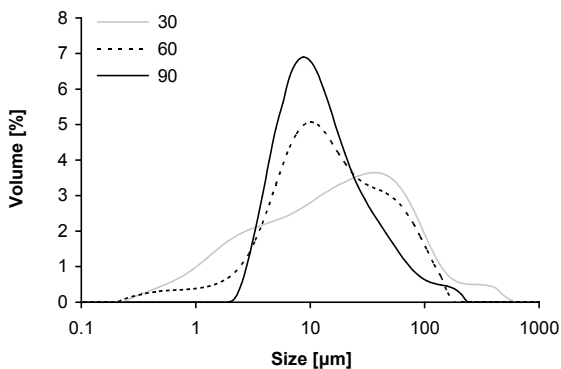
Sample	$d_{0.5}$	$D[4,3]$
30	18	41
60	14	27
90	12	22
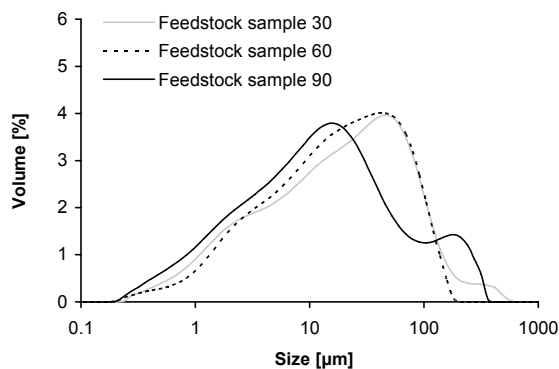
Feedstock sample	$d_{0.5}$	$D[4,3]$
30	18	37
60	20	33
90	13	38

Figure A.3.1.1: *Particle size distribution measured by laser diffraction (suspensions in ethanol, not vibrated) of fresh (top) and carbonated (middle) pH$_{stat}$ steel slag samples and of starting material used for the carbonation experiments (bottom). All sizes are given in µm. $d_{0.5}$ = number-based mean particle size. $D[4,3]$ = volume-based mean particle size.*

---

[1] Available at Environmental Science & Technology website, http://pubs.acs.org.
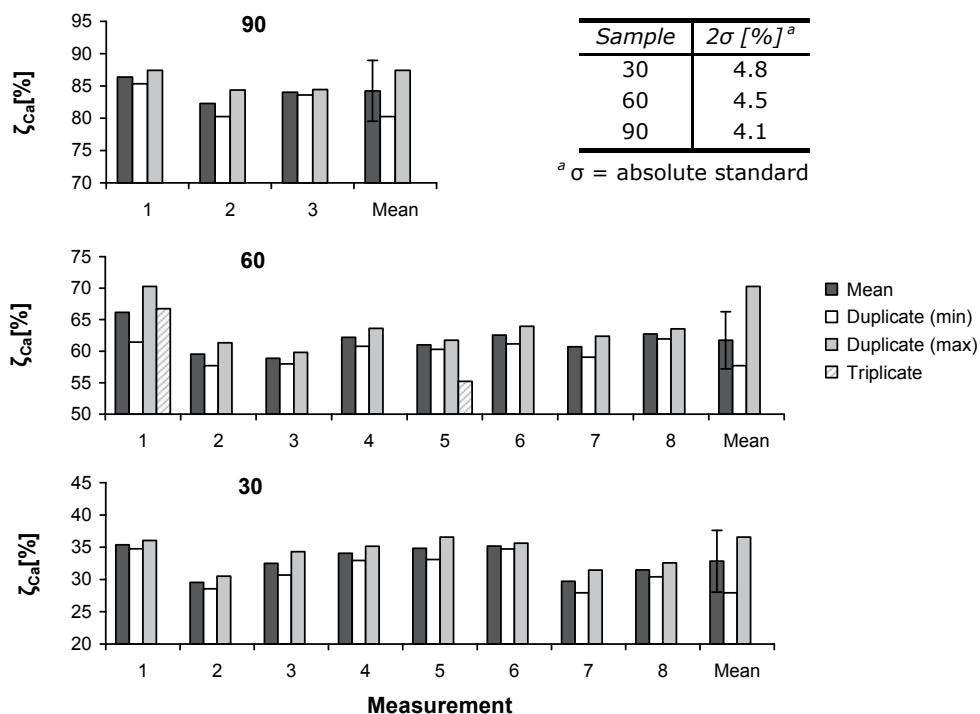
Figure A.3.1.2: *Experimental accuracy of carbonation degree measured (ζ_{Ca}) based on repetition of experiments at identical conditions for preparing pH_{stat} samples 30, 60, and 90. The carbonate content of carbonated products was analysed at least twice by TGA-MS. If the difference in conversion between the two analyses was larger than 2%., a third analysis was performed and with the help of Grubb's test potential outliers were excluded.*

A.3.1.1 Effect of Grinding

Grinding the crushed (<2 mm) fresh steel slag sample 0-c increases the specific surface area by an order of magnitude (Table 3.1) and increases the leaching of Co by 1-2 orders of magnitude, of Cr by 1 order of magnitude (at pH < 6) and of Mn (pH < 8), Pb (pH < 6), and W by less than 1 order of magnitude (Figure A.3.1.5). The increase in the amount of tungsten and cobalt leached might be attributed to the tungsten carbide grinding equipment, which may contain traces of Co. For the other elements, grinding does not significantly affect their leaching behaviour.

A.3.1.2 Effect of Prior Leaching in the Autoclave Reactor

The prior leaching of elements into the water phase during the aqueous steel slag carbonation experiments for preparation of samples 60 and 90 is shown in Figure A.3.1.3. For both samples, the most mobile elements are Cl (i.e., 69 and 80% of its total amount has dissolved for samples 60 and 90, respectively) and Na (55/45%). Other soluble elements are the other alkali metals (i.e., K (22/12%) and Li (19/32%)), S (18/6%), and Mo (16/4%). Of the other elements less than 10 and 3% of their total amount present has been leached during the carbonation experiments for sample 60 and 90, respectively. Due to the lower liquid-to-solid ratio applied during preparation of sample 90 (Table 3.1), the dissolution of most constituents during the mineral CO_2 sequestration experiments is less prominent than for sample 60.
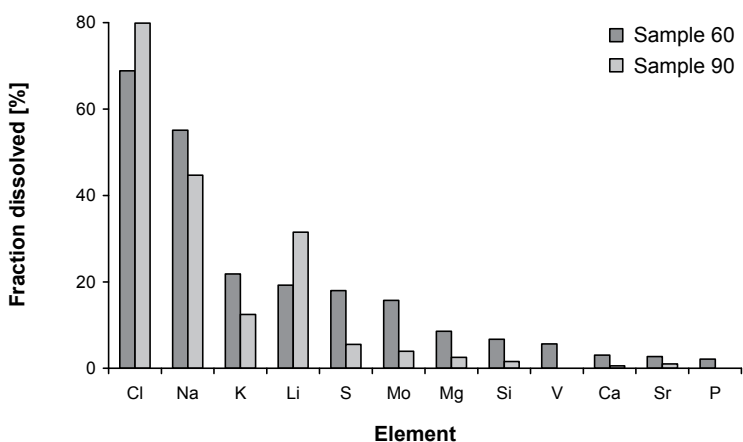
Figure A.3.1.3: *Fraction of the element's total amount present in the fresh steel slag that has dissolved into the process water during preparation of samples 60 and 90 in the autoclave reactor. Elements with fraction > 1% are shown.*

A.3.1.3 Implications of Leaching on the Re-use Possibilities of (Carbonated) Steel Slag

Environmentally sound reuse (or disposal) of the carbonated products seems essential for further process development of mineral carbonation for CO_2 sequestration. In addition, beneficial reuse of the products might reduce CO_2 sequestration costs. In order to assess the effect of carbonation on the reuse possibilities of the steel slag in construction, the pH_{stat} leaching curves of the fresh and carbonated steel slag samples were compared to the regulatory limits set by the Dutch building materials decree (1995) (category 1, application height 1 m) (Figure A.3.1.5). Since the regulatory limits used only apply to the Dutch context, their use and implications should be regarded as an example.

For the crushed fresh steel slag (<2 mm), the concentrations in the leachates of the majority of elements are orders of magnitude below their limit at native pH, while none of the elements analysed exceeds its limit at this pH. Please note that not all elements for which a regulatory limit exists have been analyzed (viz. Br, CN, F, Hg, Sb, and Se). The only critical elements are Ba and Mo, i.e., their concentration in the leachate at the sample's native pH is below but close to the corresponding regulatory limit. During carbonation, the native pH of steel slag decreases (Chapter 2). Possible effects of carbonation can be predicted from the pH_{stat} leaching curves of the fresh steel slag sample based on the expected native pH (i.e., pH 8-12) neglecting other meanwhile occurring processes, such as mineral neoformation and sorption. At pH 10, the Ba concentration in the leachates could potentially increase to levels above its regulatory limit. Sulphur may become critical if the native pH decreases towards 8 and V may already exceed its regulatory limit at only a slightly lower pH. Therefore, from a reuse point of view, Ba, S, V, and Mo are taken into account specifically in the discussion following.

Grinding the fresh steel slag does not form a barrier for the reuse of steel slag from an environmental quality point of view. Of the elements that show increased leaching after grinding, Cr, Mn, and Pb do not show altered leaching at either the native pH of the fresh steel slag or pH-values that can potentially be reached after carbonation (pH 8-12). Only Co and W show increased leaching after grinding over the entire pH-range, but no regulatory limits are exceeded. Prior leaching during the aqueous steel slag carbonation process has a beneficial effect on the environmental quality of the carbonated products, i.e., the potentially leachable amounts of, e.g., Cl, S, and Mo are reduced. Finally, carbonation itself reduces the leaching of (regulated) elements due to mineral neoformation (e.g., Ba, Ca, Sr), pH reduction (e.g., Al, Fe, Zn) and increased sorption at Al- and Fe-(hydr)oxides of trace elements (e.g., Co).

After carbonation, the concentrations in the leachates of the carbonated steel slag samples of almost all elements analysed are orders of magnitude below their limit at native pH. However, due to the dissolution of the Ca-vanadate phase upon the pH decrease and the subsequent carbonation of the Ca in the autoclave reactor, V is no longer solubility-controlled by Ca-vanadate and the leaching of V is enhanced such that its regulatory limit is significantly exceeded at native pH. This observation implies that the carbonated steel slag samples cannot be used directly for construction purposes within the Dutch context. A possible solution could be the application of the carbonated products as filler in concrete, which might reduce the leaching of oxyanions, such as vanadium, due to immobilization as alkaline Ca-phases. Further research on leaching and other aspects of specific reuse applications of carbonated products (e.g., civil engineering demands and possible value) is required for further process development of mineral CO_2 sequestration.
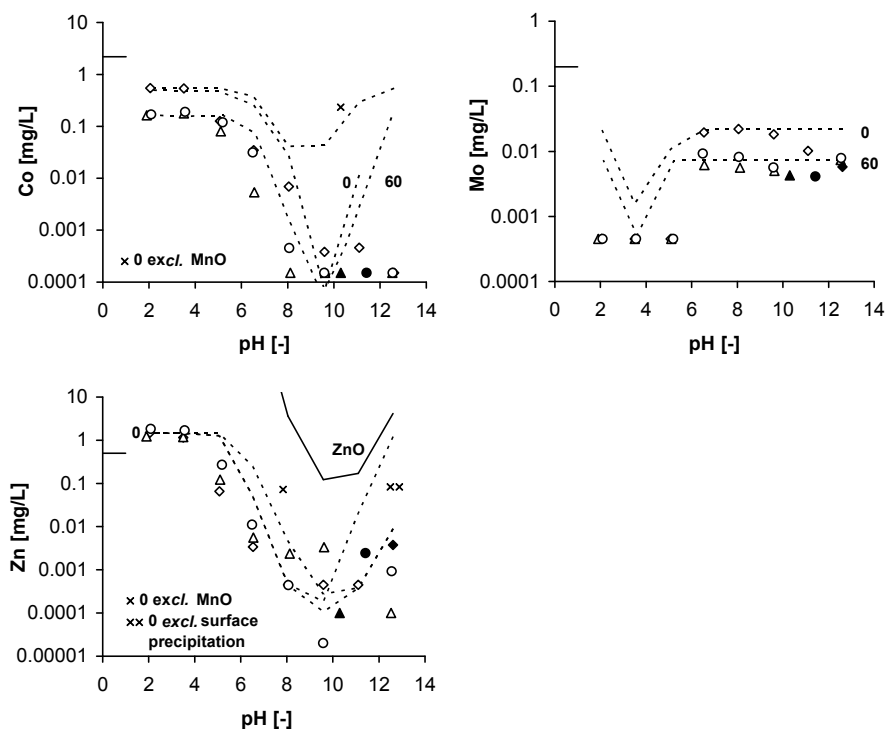
Figure A.3.1.4: *pH_{stat} leaching of selected trace elements for the fresh steel slag sample 0-f (◇) and carbonated samples 30 (○) and 60 (△). Solid symbol: concentration in pH_{stat} leachate at native pH. Data points below the detection limit (DTL) are shown as half of the DTL. Selected modelling results for the pH_{stat} leachates of samples 0-f and 60; either on the basis of solubility control by a specific mineral (——) or on sorption processes (········). Short horizontal lines represent the total amount present in the fresh steel slag.*
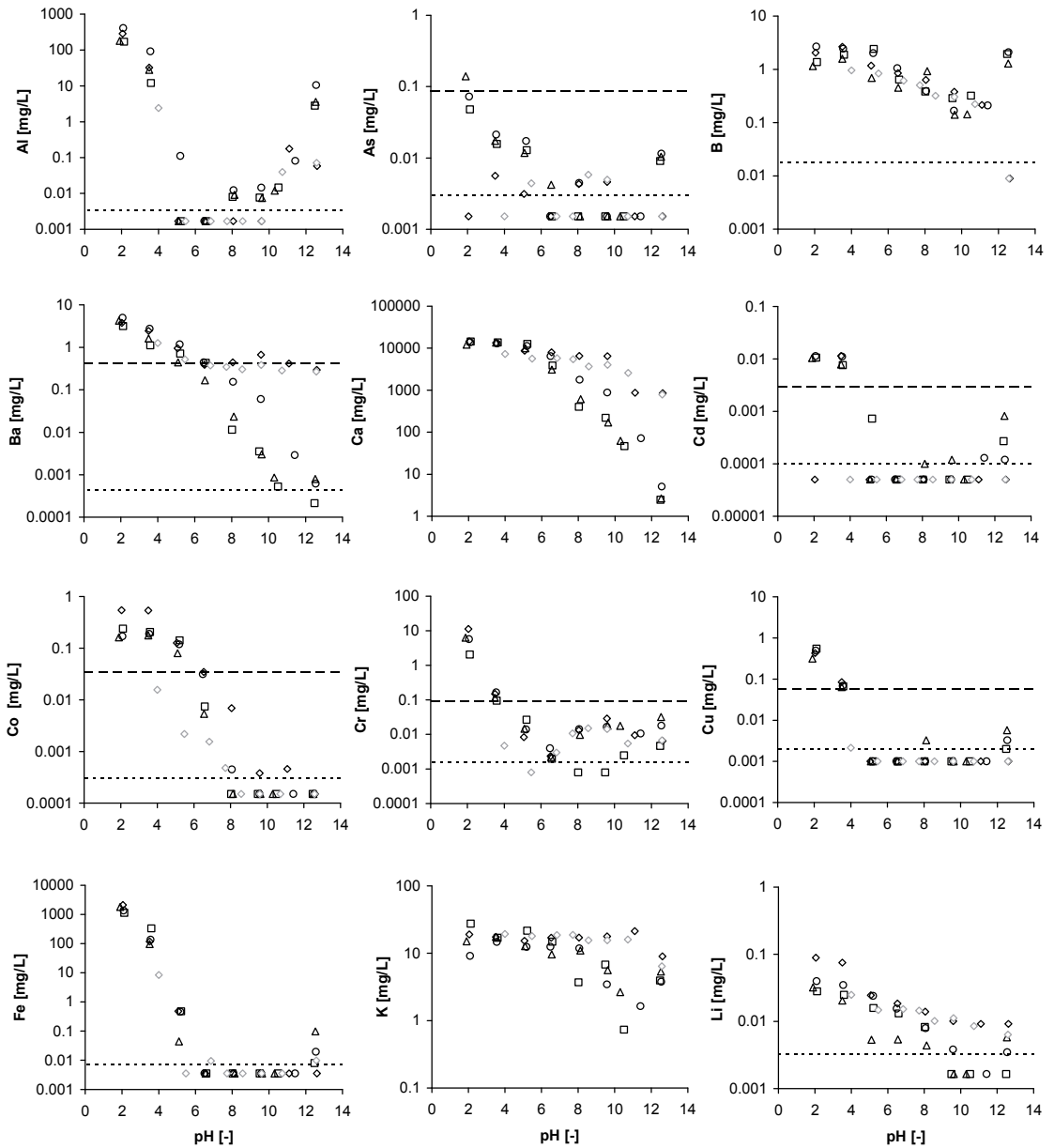
Figure A.3.1.5: *pH$_{stat}$ leaching curves of all elements analysed (except Na), DIC, and DOC from the fresh steel slag samples 0-c (◇) and 0-f (◇) and carbonated samples 30 (○), 60 (△), and 90 (□). ----: limit set by the Dutch building materials decree (1995) and ⋯⋯: detection limit (DTL). Na-data are not shown since NaOH is used as base in the pH$_{stat}$ leaching tests. Data below the DTL are shown as half of the DTL.*
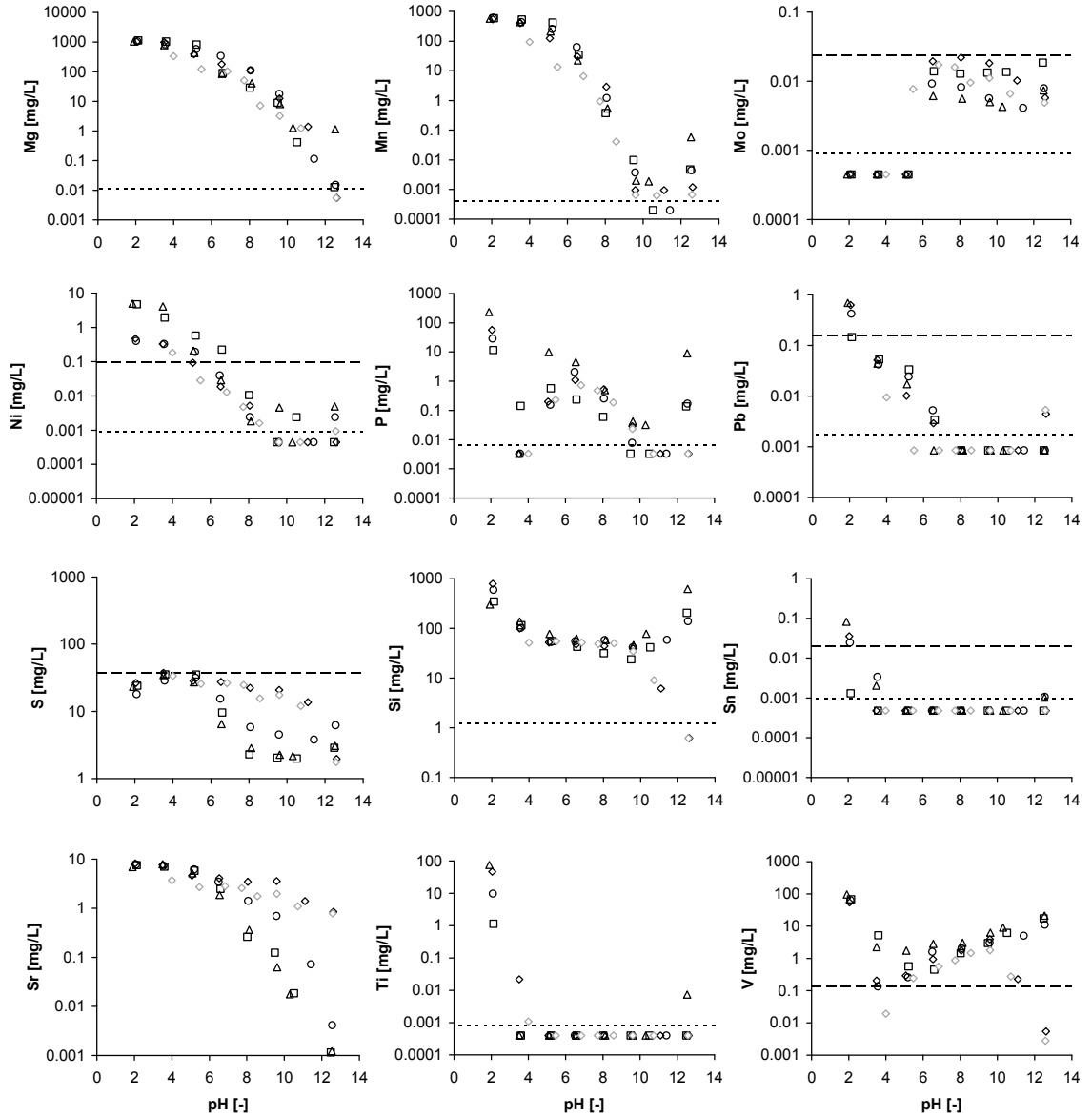
Figure A.3.1.5: *Continued.*
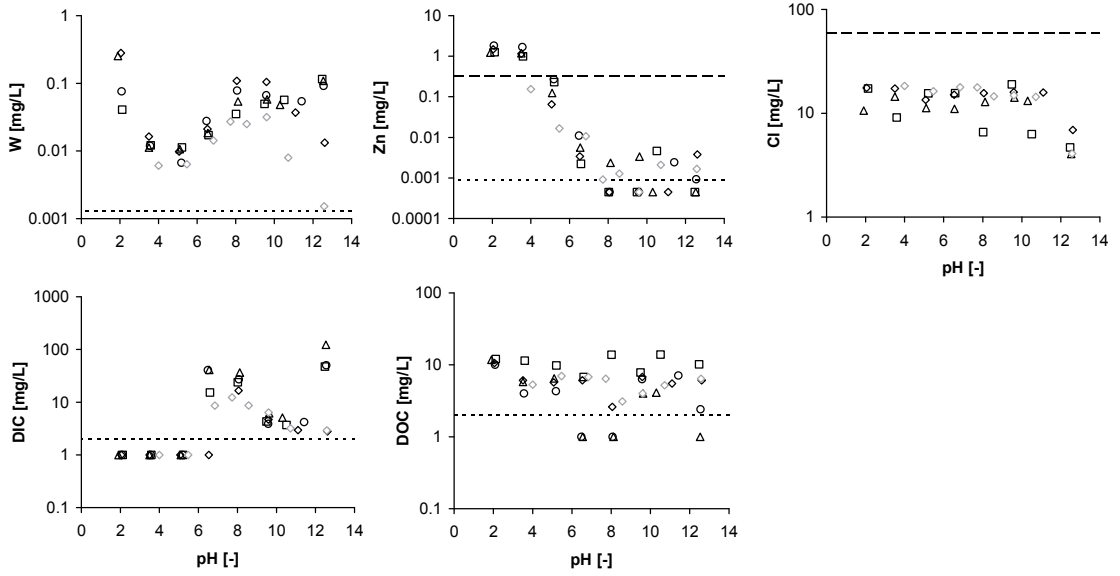
Figure A.3.1.5: *Continued.*

CHAPTER 4

MECHANISMS OF AQUEOUS WOLLASTONITE CARBONATION AS A POSSIBLE CO$_2$ SEQUESTRATION PROCESS

Published in similar form as:

Huijgen, W.J.J., Witkamp, G.J. & Comans, R.N.J. (2006) *Mechanisms of aqueous wollastonite carbonation as a possible CO$_2$ sequestration process*, Chemical Engineering Science, 61(*13*), 4242-4251.

MECHANISMS OF AQUEOUS WOLLASTONITE CARBONATION AS A POSSIBLE CO$_2$ SEQUESTRATION PROCESS

Wouter J.J. Huijgen[1]*, Geert-Jan Witkamp*[2] *& Rob N.J. Comans*[1,3]

The mechanisms of aqueous wollastonite carbonation as a possible carbon dioxide sequestration process were investigated experimentally by systematic variation of the reaction temperature, CO$_2$ pressure, particle size, reaction time, liquid-to-solid ratio, and agitation power. The carbonation reaction was observed to occur via the aqueous phase in two steps: (1) Ca leaching from the CaSiO$_3$ matrix and (2) CaCO$_3$ nucleation and growth. Leaching is hindered by a Ca-depleted silicate rim resulting from incongruent Ca-dissolution. Two temperature regimes were identified in the overall carbonation process. At temperatures below an optimum reaction temperature, the overall reaction rate is probably limited by the leaching rate of Ca. At higher temperatures, nucleation and growth of calcium carbonate are probably limiting the conversion, due to a reduced (bi)carbonate activity. The mechanisms for the aqueous carbonation of wollastonite were shown to be similar to those reported previously for an industrial residue and a Mg-silicate. The carbonation of wollastonite proceeds rapidly relative to Mg-silicates, with a maximum conversion in 15 min of 70% at 200 °C, 20 bar CO$_2$ partial pressure, and a particle size of <38 µm. The obtained insight in the reaction mechanisms enables the energetic and economic assessment of CO$_2$ sequestration by wollastonite carbonation, which forms an essential next step in its further development.

---

[1] Energy Research Centre of The Netherlands.
[2] Delft University of Technology.
[3] Wageningen University.

4.1   Introduction

Various carbon dioxide capture and storage technologies are being studied worldwide in order to mitigate global warming in the relatively short term. Mineral CO_2 sequestration is a chemical storage route in which carbon dioxide is bound in a carbonate mineral (e.g., Lackner, 1995 & 2002; Park & Fan, 2004; Chapter 1). The basic concept of this technology is deduced from the natural weathering of Ca/Mg-silicates. For wollastonite ($CaSiO_3$), the overall weathering reaction can be written as:

$$CaSiO_3 \text{ (s)} + CO_2 \text{ (g)} \rightarrow CaCO_3 \text{ (s)} + SiO_2 \text{ (s)} \qquad \text{(eq 4.1)}$$

Potential advantages of mineral CO_2 sequestration are the permanent and inherently safe storage of CO_2 due to the thermodynamically stable nature of the carbonate product formed and the vast sequestration capacity because of the widespread and abundant occurrence of suitable feedstock (Lackner, 2002). In addition, carbonation is an exothermic process, ΔH_r = -87 kJ/mol for wollastonite (Lackner et al., 1995), which potentially reduces the overall energy consumption and costs of carbon sequestration. However, natural weathering processes are slow with timescales at atmospheric conditions of thousands to millions of years. For industrial implementation, a reduction of the reaction time to the order of minutes has to be achieved by developing alternative process routes.

Ca/Mg-silicates that are suitable as feedstock for mineral CO_2 sequestration include primary minerals, such as wollastonite ($CaSiO_3$) and olivine (Mg_2SiO_4), and alkaline solid residues such as steel slag (Chapter 1). In a previous paper, we have reported the reaction mechanisms of mineral CO_2 sequestration by aqueous steel slag carbonation (Chapter 2). In the present study, we have extended our research to primary minerals. Wollastonite was selected as model feedstock for our carbonation experiments, because Ca-silicates tend to be more reactive towards carbonation than Mg-silicates (Lackner et al., 1997; Chapter 1), although suitable deposits are limited relative to the world-wide abundance of Mg-silicates (Lackner et al., 1995 & 1997). In addition, the choice for a Ca-silicate enables the direct comparison to the carbonation of Ca-rich alkaline solid residues such as steel slag.

Several process routes for industrial mineral CO_2 sequestration have been reported. The so-called aqueous carbonation route (O'Connor et al., 2005) has been selected as the most promising route in a recent review (Chapter 1). In this process, carbonation occurs in a gas-solid-water slurry, which increases the

reaction rate substantially compared to direct gas-solid carbonation. Process steps within the aqueous carbonation route are
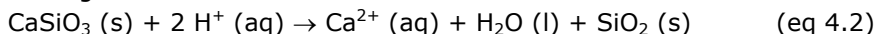
1. Leaching of Ca:
    $$CaSiO_3 \text{ (s)} + 2\ H^+ \text{ (aq)} \rightarrow Ca^{2+} \text{ (aq)} + H_2O \text{ (l)} + SiO_2 \text{ (s)} \qquad \text{(eq 4.2)}$$
2. Dissolution of CO_2 and subsequent conversion of (bi)carbonate species:
    $$CO_2 \text{ (g)} + H_2O \text{ (l)} \rightarrow H_2CO_3 \text{ (aq)} \rightarrow HCO_3^- \text{ (aq)} + H^+ \text{ (aq)} \qquad \text{(eq 4.3)}$$
3. Nucleation and growth of calcium carbonate:
    $$Ca^{2+} \text{ (aq)} + HCO_3^- \text{ (aq)} \rightarrow CaCO_3 \text{ (s)} + H^+ \text{ (aq)} \qquad \text{(eq 4.4)}$$
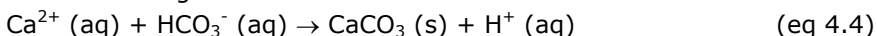
A limited number of studies on wollastonite carbonation for CO_2 sequestration has been published so far (Kojima et al., 1997; Wu et al., 2001; O'Connor et al., 2005). These studies have demonstrated that (1) the leaching of Ca from the $CaSiO_3$ matrix (eq 4.2) is the rate-limiting reaction step at the conditions applied and that (2) this step can be enhanced by e.g. increasing the specific surface area of the wollastonite. However, two of these studies (Kojima et al., 1997; Wu et al., 2001) focus on carbonation at low CO_2 pressure and low temperature and reported reaction times are, consequently, much too long for industrial application. O'Connor et al. (2005) have studied the carbonation of various silicate minerals at elevated temperature and pressure, including a limited number of experiments with wollastonite, which confirms the higher reactivity of Ca- relative to Mg-silicates.

In the present paper, we present an experimental study on the mechanisms of wollastonite carbonation at elevated temperature and pressure in support of the development of a rapid carbon dioxide sequestration process. The rate-determining reaction steps are identified and compared to those reported earlier for other feedstock. Finally, routes for further research on aqueous wollastonite carbonation are indicated.

4.2 Materials and Methods

4.2.1 Wollastonite Characteristics

Wollastonite with size class <7 mm (Casiflux A 7020) was obtained from Ankerpoort B.V., Maastricht, The Netherlands. The particle size distribution of the wollastonite was determined by laser diffraction (Malvern Mastersizer 2000) (Figure 4.1).

[µm]	Sieve	D[3,2]	D[4,3]
	<7000	55.1	375
	<500	23.5	159
	<106	12.8	51.1
	<38	7.9	16.1
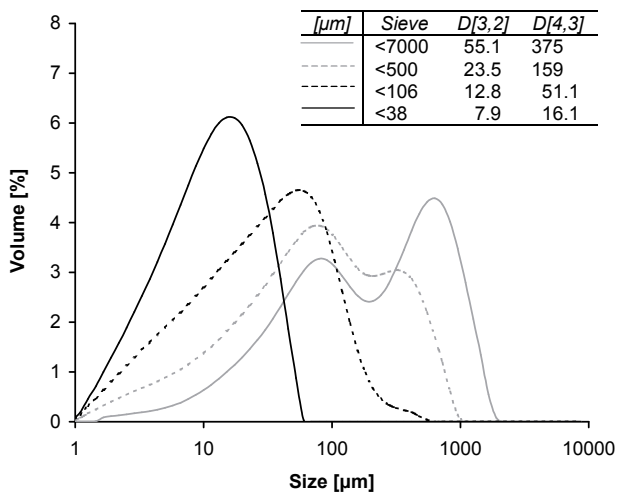
Figure 4.1: *Particle size distribution of original (<7000 µm) and ground wollastonite samples with size class, D[3,2] (surface area-based mean diameter), and D[4,3] (volume-based mean diameter) (suspensions in water, not vibrated).*

Scanning Electron Microscope (SEM) analysis of a wollastonite sample (<106 µm) showed needle-shaped particles consistent with its crystal structure. X-ray powder diffraction (XRD) (Bruker, D8 advance) identified (Fe)-wollastonite, with best fitting formula $(Ca_{0.96}Fe_{0.04})SiO_3$ and traces of lime (CaO) and calcite ($CaCO_3$), but no crystalline SiO_2 (Figure 4.2). The calcium carbonate content of the fresh wollastonite (<106 µm), expressed in terms of CO_2, was determined by TGA-MS (see below, eq 4.5). The lime content was estimated from the amount of dissolved Ca at pH 8.5 in the pH_{stat} leaching curve of the fresh wollastonite (see also below). The total composition of the wollastonite was determined by grinding a sub-sample to <106 µm. A part of the ground sub-sample was digested with concentrated $HNO_3/HClO_4/HF$ (in proportions of 5:0.5:4.5) in an autoclave at 190 °C for 10 h. The rest of the sample was digested in a lithium metaborate smelt at 1150 °C during 30 min (1 g at 0.1 g sample). Element concentrations in the resulting solutions were measured by ICP-AES. Table 4.1

shows the determined composition of the wollastonite. The maximum CO_2 sequestration capacity is 329 g CO_2 per kg wollastonite (i.e., if all calcium is carbonated). The resulting product would contain 24.8 wt% CO_2. The carbonation degree (ζ_{Ca}) of the starting material is 2.4% of the total amount of Ca, based on eq 4.6 below.
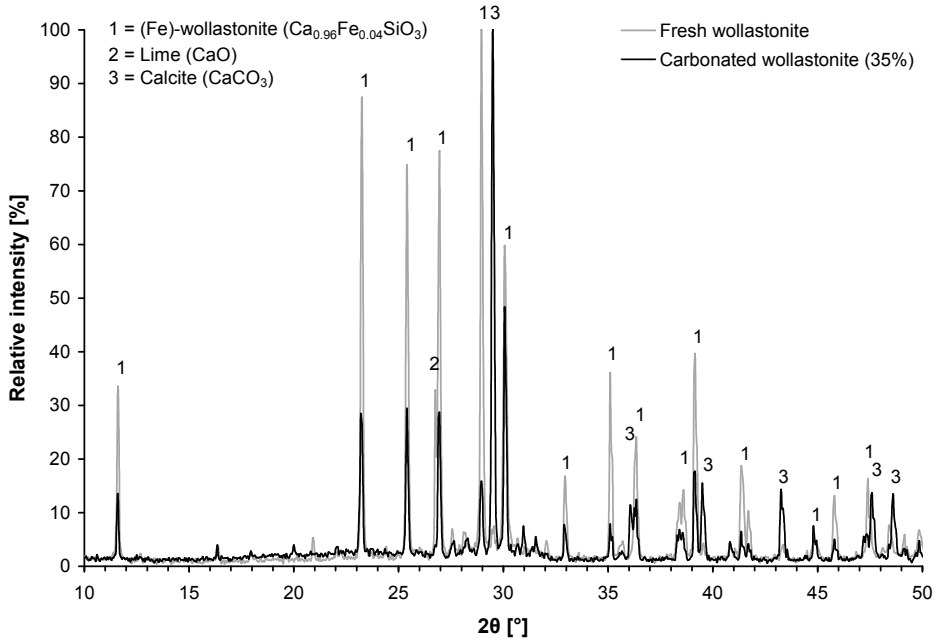
Figure 4.2: *XRD spectra for both fresh and 35% carbonated wollastonite (reference case) with peak identifications.*

Table 4.1: *Wollastonite composition based on XRD, TGA-MS, and pH$_{stat}$ analysis of solid and ICP-AES analysis after total digestion.*

Component	Content [%]
$CaSiO_3$	84.3
SiO_2	12.3
$MgSiO_3$	2.5
$CaCO_3$	1.8
CaO	0.3
Other (e.g., Mn, Fe)	0.9

The pH of a wollastonite-water slurry at a liquid-to-solid ratio of 10 kg/kg was determined at 10.6 (open to the atmosphere, after 24 h). This value is in good agreement with the natural pH of wollastonite (10.7) as calculated with The Geochemist's Workbench 4.0 (GWB) (Bethke, 2002). The leaching

characteristics of Ca and Si from fresh (and carbonated) wollastonite were measured in a pH$_{stat}$-system. Eight suspensions of ground wollastonite (<106 µm) and Nanopure-demineralised water at a liquid-to-solid ratio of 10 kg/kg were stirred at room temperature in closed Teflon reaction vessels. For seven vessels, the pH was controlled automatically within ±0.2 pH of a pre-set pH value by the addition of HNO$_3$ and NaOH. In one vessel, leaching occurred at the native pH of the sample (i.e., not adjusted by the addition of acid or base). After 48 h, the final pH of the suspensions was determined and the suspensions were filtered over 0.2 µm membrane filters. The clear filtrates were acidified with concentrated HNO$_3$ (pH < 3) and analysed for Ca and Si by ICP-AES. Solubility products of CaSiO$_3$ (wollastonite), amorphous SiO$_2$, and calcite (CaCO$_3$) were used to calculate the solubility curves of these minerals, as shown in Figure 4.3.
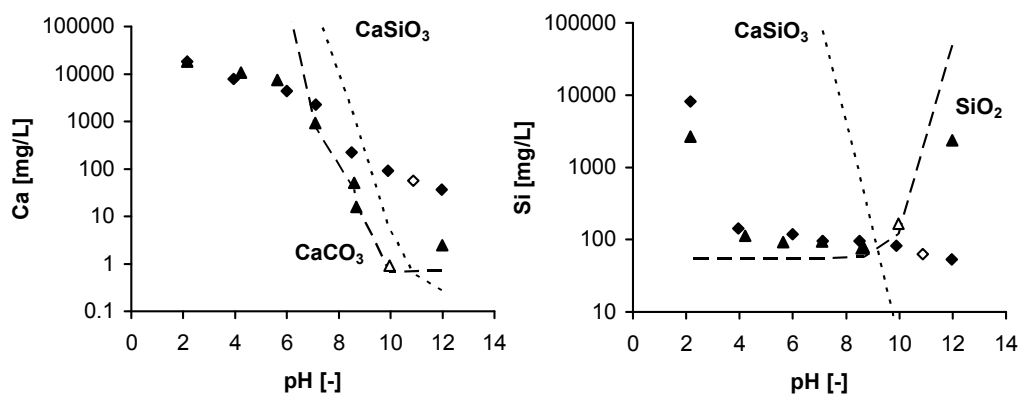
Figure 4.3: *Ca- and Si-leaching from fresh and carbonated (ζ$_{Ca}$ = 45%) wollastonite in Nanopure-demineralised water (pH$_{stat}$, L/S = 10 kg/kg, 48 h) and geochemical modelling of solubility control by specific minerals (CaSiO$_3$ = wollastonite, SiO$_2$ = amorphous silica, CaCO$_3$ = calcite). An open symbol indicates the native pH of the sample.*

4.2.2 Carbonation Experiments

Three representative wollastonite batches were ground quantitatively to a specific sieve size class using a tungsten-carbide vibratory ring pulveriser (<38, <106, and <500 µm). Figure 4.1 shows the resulting particle size distributions that were measured by laser diffraction. Homogeneous samples of each batch were taken with a sample splitter. For each carbonation experiment, a (ground) wollastonite sample was suspended in Nanopure-demineralised water in a 450 mL AISI316 autoclave reactor (Limbo 350, Büchi Glas Uster). The suspension was stirred using a three-bladed pitched turbine (D = 32×10^{-3} m) in order to suspend the solid wollastonite particles and disperse the CO$_2$ gas. The reactor was heated to a specific reaction temperature and, subsequently, CO$_2$ was

added directly into the slurry with the help of a compressor (a Haskel AG75 gas booster) until a pre-determined CO_2 pressure was reached. Subsequently, the pressure and temperature were kept at their set-point by replenishment of the consumed CO_2 and cooling of the reaction heat, respectively. After the reaction time had expired, the CO_2 addition was stopped and the autoclave was cooled down and depressurised (Figure 4.4). The suspension was immediately filtered quantitatively over a 0.2 µm membrane filter, the solid was dried and, finally, the carbonate content was analysed by thermal gravimetrical analysis (TGA-MS) to determine the conversion of the reaction.
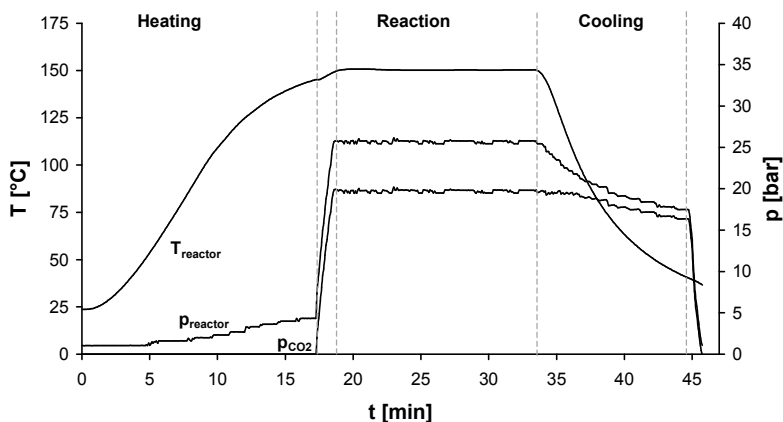
Figure 4.4: *Reactor temperature, total pressure, and CO_2 partial pressure during a typical carbonation experiment (reference case).*

The following process variables, which potentially influence the carbonation reaction, were varied systemically: (1) reaction time (t), (2) reaction temperature (T), (3) CO_2 partial pressure (p_{CO2}), (4) particle size of wollastonite feedstock (d), (5) liquid-to-solid ratio (L/S), and (6) agitation power determined by the stirring rate (n). Ranges of process conditions were chosen such that a wide range of conversions resulted (t = 5 - 60 min, T = 25 - 225 °C, p_{CO2} = 1 - 40 bar, d = <38 - <7000 µm, L/S = 2 - 10 kg/kg, n = 100 - 2000 rpm). The stirring rate, as adjusted experimentally, corresponds with a power input of 1×10^0, 1×10^2, and 8×10^3 W/m^3, for n = 100, 500, and 2000 rpm, respectively, assuming a power number (N_p) of 1 for all Reynolds numbers (calculations for 150 mL water at 200 °C).

TGA-MS analyses were performed in duplicate in a thermal gravimetrical analysis system (Mettler-Toledo TGA/SDTA 851e) coupled with a mass spectrometer (Pfeiffer, Thermostar) (TGA-MS). Samples (10-20 mg) were heated in aluminium oxide ceramic cups under an oxygen atmosphere at

40 °C/min from 30 to 1000 °C with one stop at 105 °C for 15 min (Figure 4.5). The TGA measured the weight loss caused by drying (30-105 °C) and by thermal decomposition of carbonates (105-1000 °C). The MS simultaneously analysed the evolved gas for CO_2 and H_2O. The amount of CO_2 sequestered as calcium carbonate of a sample was defined on the basis of its dry weight ($m_{105°C}$) and the weight loss between 105 and 1000 °C ($\Delta m_{105\text{-}1000°C}$):

$$CO_2[wt\%] = \frac{\Delta m_{105-1000°C}[kg]}{m_{105°C}[kg]} \times 100 \qquad (eq\ 4.5)$$

The carbonation degree (ζ_{Ca}) was determined by the carbonate content measured by TGA-MS, the total calcium content (Ca_{total}) and the carbonate content ($CO_{2,0}$) of the fresh wollastonite, assuming only Ca had been carbonated during the carbonation process and no significant mass had been lost due to leaching in the reactor.

$$\zeta_{Ca}[\%] = \frac{CO_2[wt\%] \times \dfrac{100 - CO_{2,0}[wt\%]}{100 - CO_2[wt\%]} \times \dfrac{MW_{Ca}[kg\,/\,mol]}{MW_{CO_2}[kg\,/\,mol]}}{Ca_{total}[kg\,/\,kg]} \qquad (eq\ 4.6)$$

If the absolute difference in carbonation degree between the duplicate analyses was larger than 2%, a third TGA-analysis was performed and potential outliers were identified with Grubb's statistical test. The resulting mean carbonate content and ζ_{Ca} are given in this paper. For a more detailed description of the experimental procedure see Chapter 2.

In the discussion of the results below, it is assumed that carbonation occurs exclusively during the reaction time (i.e., at elevated temperature and pressure) and not during heating, cooling or depressurisation of the reactor (Figure 4.4). First, the effect of the heating period on the carbonation degree is assumed to be negligible since (1) CO_2 is absent during heating of the reactor and (2) the amount of Ca that is leached during heating is probably relatively limited, because leaching is expected to proceed orders of magnitude faster after the addition of CO_2 due to the resulting pH decrease. Second, the effect of the cooling time is neglected since preliminary experiments have shown that carbonation rates have been reduced substantially at the end of the reaction time and these rates probably decrease even further during cooling due to the lowering of the reactor temperature. Therefore, although the heating and cooling times (max. 23 min and 15 min, respectively, at T = 225 °C) are significant compared to the reaction time (typically 15 min), their effect on the carbonation degree is neglected. Third, the amount of calcite that precipitates during the depressurisation of the autoclave is assumed to be negligible. Although

depressurisation results in an increase of the supersaturation of calcite (i.e., due to a pH increase), the amount of extra calcite that can precipitate during depressurisation is small. First, a limited fraction of the Ca is dissolved at the moment of depressurisation. Analysis of an aqueous solution sample taken directly from the autoclave at 20 bar CO_2 pressure and 150 °C (d < 106 µm, t = 15 min, L/S = 5 kg/kg, n = 500 rpm), using a sampling device with an in-line filter, showed that only 1% of the Ca was dissolved at the moment of depressurisation. Second, it is unlikely that a significant amount of additional Ca dissolves during depressurisation given the short time involved (typically, 1-2 min) and the increasing pH. Summarizing, we suggest that carbonation occurs exclusively during the reaction time at elevated temperature and pressure (Figure 4.4).

4.3 Results and Discussion

4.3.1 Reaction Mechanisms

A reference carbonation experiment at T = 150 °C, p_{CO2} = 20 bar, d < 106 µm, n = 500 rpm, L/S = 5 kg/kg, and t = 15 min resulted in a Ca-conversion of 35% and a native pH decrease to 9.1. Figure 4.4 shows the development of the temperature and the pressure during the reference carbonation experiment. A TGA-MS curve of the carbonation product is shown in Figure 4.5.
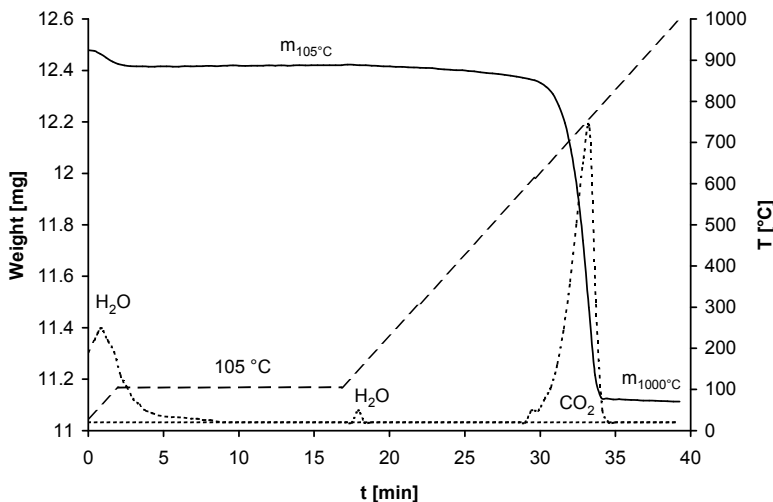
Figure 4.5: *TGA-MS curve of 35% carbonated wollastonite (reference case). Weight of sample (——), temperature (- - -), and MS-signals (··········) as a function of the measurement time.*

XRD (Figure 4.2) and SEM-EDX analyses (Figure 4.6) of fresh and carbonated wollastonite samples identified the reactants and products given in eq 4.1, with calcite as the only crystal form of calcium carbonate detected. The pH_{stat} leaching curves of fresh and carbonated wollastonite (Figure 4.3) confirm the formation of calcium carbonate and silica. For carbonated wollastonite, the leaching of Ca and Si seems to be controlled by the solubility of calcite and amorphous SiO_2, respectively. Figure 4.3 also shows that the leachates are not in equilibrium with wollastonite.
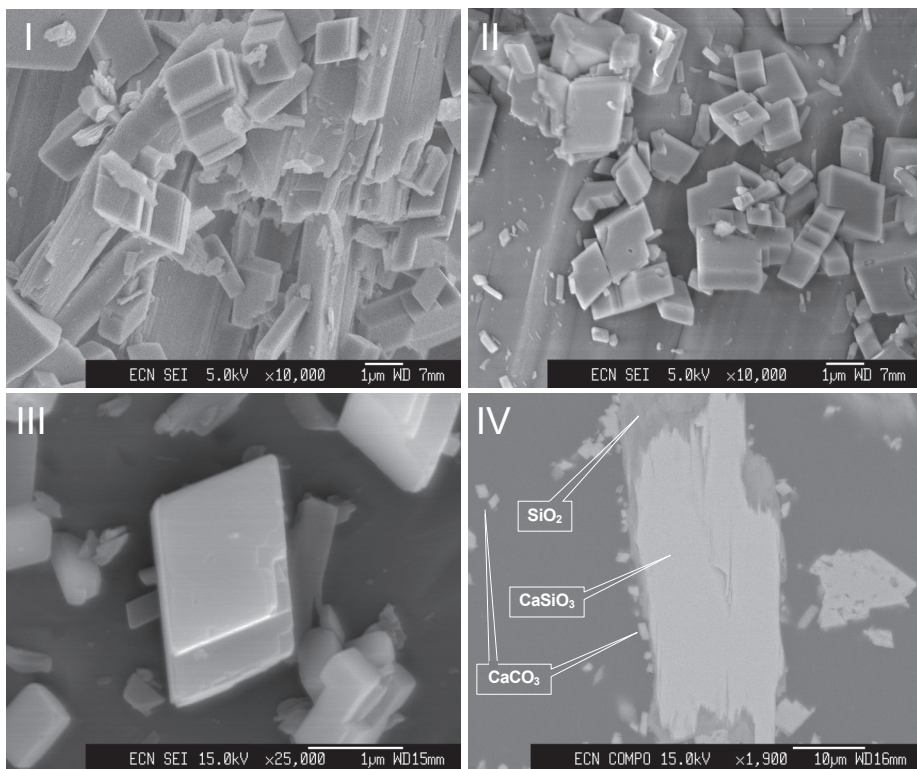
Figure 4.6: *Scanning electron micrographs. I: 35% carbonated wollastonite (reference case). II: 72% carbonated wollastonite (maximum conversion obtained). III: calcite crystal. IV: backscatter electron (BSE) micrograph of polished cross-section of 72% carbonated wollastonite embedded in resin with EDX spot analyses results.*

The dependency of the carbonation degree on the process variables is shown in Figure 4.7. The effect of the individual process variables on the degree of carbonation is discussed below.
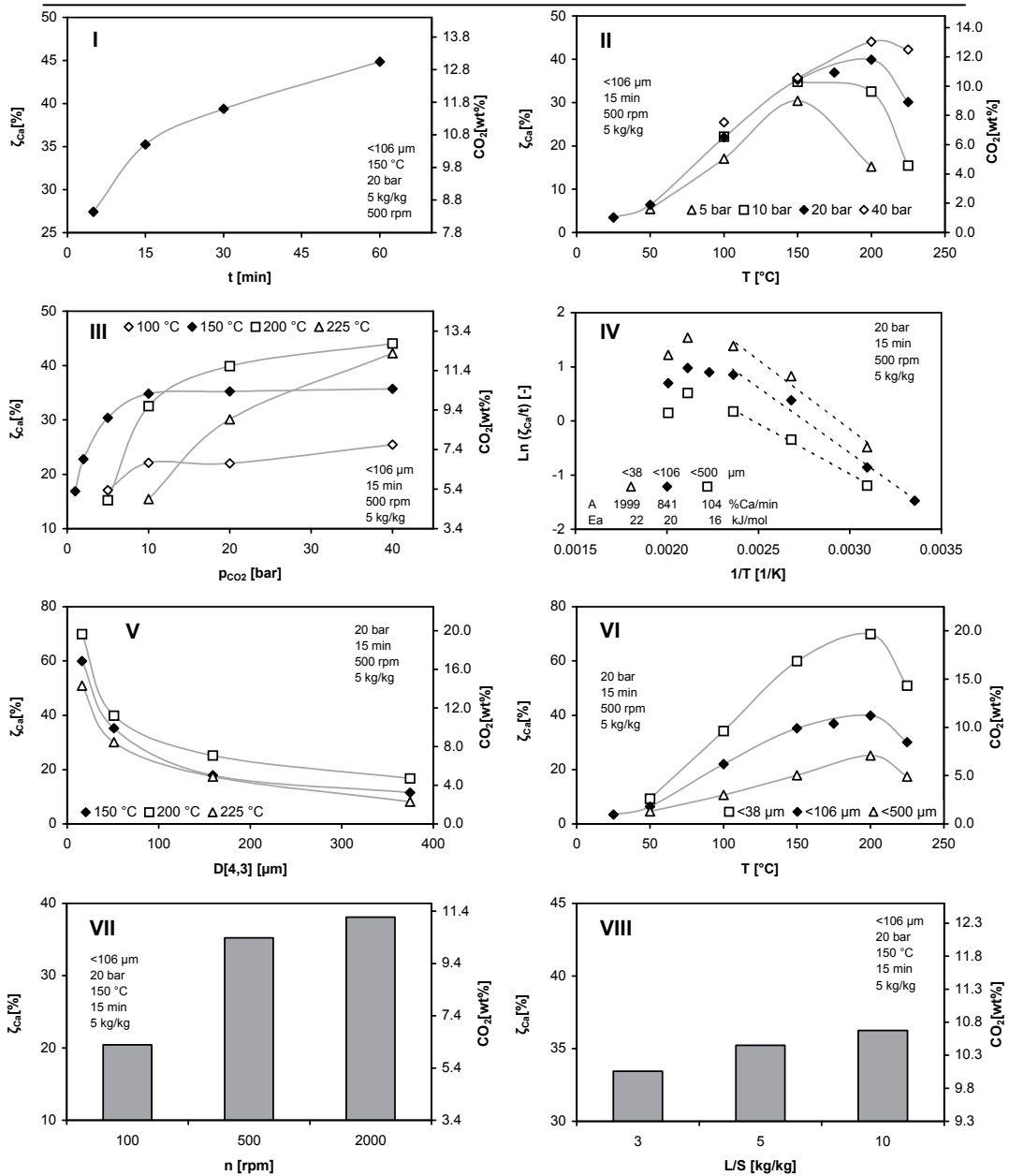
Figure 4.7: *Influence of various process variables on the Ca-conversion (ζ_{Ca}) and carbonate content (CO_2) of wollastonite. Data series including the reference case experiment (◆). (I) Reaction time. (II) Temperature at various CO_2 pressures. (III) CO_2 pressure at various temperatures. (IV) Arrhenius-plot for various particles sizes. Activation energy is based on data points with $T \leq 150$ °C. (V) Volume-based mean diameter at various temperatures. (VI) Temperature at various particle sizes. (VII) Agitation power determined by the stirring rate. (VIII) Liquid-to-solid ratio.*

Reaction Time. The carbonation rate decreases as the reaction time elapses (Figure 4.7.I). The SEM-micrographs suggest that this effect is caused by physical barriers that develop during the carbonation process (Figure 4.6). The scanning electron micrographs of a 35% and a 72% carbonated wollastonite sample (Figures 4.6.I and 4.6.II) show rhombohedral calcite crystals (Figure 4.6.III) that have precipitated during the carbonation of the needle-shaped wollastonite particles. These calcite crystals have been identified both at the surface of the wollastonite particles and as separate phases (Figure 4.6.IV). In addition, SEM-EDX analyses on the carbonated products show the formation of a Ca-depleted SiO_2-rim at the edges of the unconverted wollastonite (Figure 4.6.IV). This observation suggests preferential (incongruent) Ca-leaching relative to Si. Incongruent Ca leaching from $CaSiO_3$ is confirmed by the strong preferential dissolution of Ca relative to Si observed between pH 8 and 4 in the pH_{stat} experiment (Figure 4.3), given that 97% of the Ca in the fresh wollastonite ore is present as $CaSiO_3$ (Table 4.1). At these pH values, the leaching of Si seems to be controlled by the solubility of less-soluble amorphous silica.

The observations discussed above show that (1) carbonation actually takes place via the aqueous phase according to eq 4.2-4.4 and (2) (further) carbonation is hindered by the Ca-depleted SiO_2-rim formed during the process, at some locations accompanied by precipitated $CaCO_3$ particles on the wollastonite surface. Therefore, we consider the leaching of Ca from unconverted wollastonite (eq 4.2) to consist of the following steps: (1) diffusion of protons through the SiO_2 layer at the particle surface towards the unconverted $CaSiO_3$ core, (2) calcium release from the $CaSiO_3$ matrix, leaving solid SiO_2 behind and (3) diffusion of Ca ions (and H_2O formed) through the SiO_2 layer towards the solid/liquid interface. Subsequently, Ca^{2+} (aq) reacts with (bi)carbonate, either directly at the solid/liquid interface or in the bulk solution (eq 4.4).

Particle Size. Figure 4.7.V shows the influence of the volume-based mean particle size (D[4,3]) on the Ca-conversion at 150, 200, and 225 °C. Grinding the wollastonite sample as received to <38 μm (D[4,3] = 16.1 μm) results in an increase of the conversion from 12 to 60% at 150 °C and 20 bar CO_2. The conversion corresponds roughly with the reciprocal square root of the volume-based mean particle size at all temperatures ($\zeta \propto D[4,3]^n$ with n between 0.45 and 0.56). Probably, the specific surface area of the wollastonite particles controls the overall reaction rate, which can be demonstrated by the dependence of the wollastonite conversion on the surface-area based mean particle size (D[3,2]), i.e., $\zeta \propto D[3,2]^n$, resulting in n = 0.85, 0.72, and 0.93 at 150, 200, and 225 °C, respectively. The exponential factor n approximates the theoretical value of n = 1 even closer (0.93 - 1.11), when the low conversions

obtained with the <7000 µm particle size are left out of consideration, since the relative experimental error is largest for these experiments. In brief, size reduction is a key process step in increasing the reaction rate by means of an increase of the specific surface area.

Stirring Rate. The conversion is not influenced by the agitation power at high stirring rates (i.e., ≥500 rpm), which are typically used in the experiments (Figure 4.7.VII). However, lowering the stirring rate from 500 to 100 rpm at 150 °C and 20 bar CO_2 results in a large decrease of the conversion, suggesting that processes in the boundary layer at either the solid/liquid or gas/liquid interface become rate-determining at low stirring rates (e.g., transport of leached Ca from the wollastonite interface into the water phase).

Liquid-to-Solid Ratio. The influence of the liquid-to-solid ratio (Figure 4.7.VIII) seems to suggest that the conversion slightly increases if the system becomes more diluted. However, the effects are small compared to the (absolute) experimental error of the carbonation experiments, which was determined at 5% for steel slag carbonation in our experimental setup (Chapter 3). Based on the limited number of observations with regard to the effect of the L/S ratio, it is uncertain whether the observed slight increase in the conversion is significant.

Reaction Temperature and CO_2 Pressure. At 20 bar CO_2 pressure, the carbonation rate increases with reaction temperature between 25 and 150 °C (Figure 4.7.II). However, after a further increase of the temperature, the conversion stabilises and, subsequently, decreases, resulting in a maximum conversion around 200 °C. This behaviour is probably a result of two opposite temperature effects; raising the reaction temperature increases reaction and mass transfer rates (e.g., leaching of Ca), but on the other hand reduces the activity of (bi)carbonate in water. A simulation of demineralised water saturated with CO_2 at p_{CO2} = 20 bar showed a decrease of the log activity for CO_3^{2-} from -10.3 at 25°C to -11.1 at 225 °C and for HCO_3^- from -3.3 to -4.2 (GWB). The decrease of the (bi)carbonate activity apparently becomes dominant above 200 °C causing a net decrease of the conversion. This effect can also be demonstrated in a pressure dependency plot (Figure 4.7.III). At 150 °C, the conversion remains constant between 10 and 40 bar; the (bi)carbonate activity is sufficient. Only a further decrease of the CO_2 partial pressure below 10 bar reduces the (bi)carbonate activity such that a decline of the reaction rate results. At 200 and 225 °C, however, increasing the CO_2 pressure from 20 to 40 bar results in a rise of the conversion. Apparently, at 20 bar, a deficiency of (bi)carbonate activity occurs when the temperature is increased from 150 to 200 °C. In the GWB simulation discussed above, the log HCO_3^- activity at 150 °C and 20 bar CO_2 is -3.8. At 5, 10, and 40 bar CO_2, the calculated temperatures at

which the same activity occurs are 85, 116, and 179 °C, respectively. The calculated p,T-dependency of the HCO_3^- activity seems consistent with the observed conversion patterns shown in Figure 4.7.II. The reaction temperature of maximum conversion and the accompanying maximum conversion itself both increase with a higher CO_2 pressure (Figure 4.7.II). In other words, the reaction temperature and, thus the conversion, can be increased further at higher CO_2 pressures before the adverse effect of the reduced (bi)carbonate activity becomes dominant. A similar influence of the temperature and CO_2 pressure can be observed in the data on aqueous wollastonite carbonation presented by O'Connor et al. (2005), although the temperature effect in that study is less evident since the conversion approaches the theoretical maximum already at T = 100 °C mainly due to the smaller particle size used.

The conversion-temperature plot at 20 bar CO_2 for various particles sizes (Figure 4.7.VI) shows that the maximum conversion increases with decreasing particle size, but that the shape of the curve and the optimum reaction temperature remain roughly the same. Apparently, the decreasing (bi)carbonate activity has a similar influence on the conversion for all particle sizes. The temperature-profiles can be plotted analogously to an Arrhenius-plot using ζ_{Ca}/t as a pseudo-reaction rate (Figure 4.7.IV). The resulting pseudo-activation energies (E_a) are 22, 20, and 16 kJ/mol for the <38, <106, and <500 µm batches, respectively, based on the carbonation results at 25-150 °C (i.e., the conditions at which the (bi)carbonate activity is not influencing the conversion). The activation energies determined should only be used qualitatively, since no actual reaction rates were measured. Actual activation energies reported in the literature are significantly higher, e.g., 72 kJ/mol as used by Brady (1991).

Based on the temperature profiles, two regimes of process conditions can be defined: regime I at a temperature below the optimum reaction temperature and regime II at higher temperatures. The reaction mechanisms in both regimes will be discussed in more detail below.

Regime I. In regime I, reaction steps involving CO_2 or (bi)carbonate are unlikely to be rate determining, since no dependency of the conversion on the CO_2 pressure was measured. In addition, increasing the specific surface area of wollastonite was found to result in a substantially higher carbonation rate. Therefore, it can be concluded that the leaching of Ca (eq 4.2) is probably the rate-determining reaction step in regime I. The limited influence of the stirring rate on the conversion at the conditions typically applied in regime I suggests that the Ca-leaching rate is probably determined by the Ca-diffusion rate through the silicate rim, rather than by the boundary layer at the solid/liquid interface.

Regime II. In regime II, where the conversion was found to depend on the CO_2 pressure, processes in which CO_2 or (bi)carbonate is involved are likely to dominate the carbonation rate. Four process steps in which CO_2 is (in)directly involved can be distinguished: (1) dissolution of CO_2, (2) conversion of dissolved CO_2 to the (bi)carbonate-ion, (3) leaching of Ca, influenced by pH as controlled by the amount of dissolved CO_2, and (4) nucleation and growth of calcium carbonate.

Since the particle size has a similar influence on the conversion in regimes I and II (Figure 4.7.V), it is likely that the conversion in regime II is limited by process steps in which Ca is also involved (i.e., process steps 3 or 4). The influence of a change in CO_2 solubility on pH and Ca-leaching could not be studied directly in the experimental setup used, since it was not possible to adequately measure the pH in situ. Chemical equilibrium modelling (GWB) of 20 bar CO_2 saturated demineralised water (i.e., without wollastonite present) resulted in a pH of 4.0 and 4.1 at 200 and 225 °C, respectively. A similar simulation with wollastonite present at L/S = 5 kg/kg resulted in a pH of 5.3 at both 200 and 225 °C. These simplified calculations suggest that the pH increase between 200 and 225 °C is small relative to the large decrease in conversion that is observed between these temperatures. Therefore, it seems more probable that nucleation and growth of $CaCO_3$ (i.e., process step 4) limit the conversion in regime II, rather than (pH-dependent) leaching of Ca (i.e., process step 3).

4.3.2   Comparison to Other Carbonation Feedstock

As stated in the introduction, the use of a Ca-silicate for the mineral carbonation experiments enables the direct comparison of the carbonation mechanisms to that of steel slag as reported earlier (Chapter 2). Figure 4.8 shows the influence of the reaction temperature on the conversion of the Ca-silicates wollastonite and steel slag. The shape of the curve and the optimum temperature are similar for both materials. Steel slag, however, shows a higher conversion, especially at low temperatures, which confirms the tendency of alkaline thermal residues to be more susceptible to weathering due to their (geo)chemical instability, as suggested in Chapter 2. The carbonation of wollastonite, on the other hand, shows a stronger temperature dependency, i.e., pseudo-Ea $\approx$ 20 vs. 4 kJ/mol for steel slag (Chapter 2). As a result, the amount of CO_2 reacted with wollastonite at higher temperatures approaches that of steel slag.

The mechanisms for the aqueous carbonation of the Ca-silicates wollastonite (this study and O'Connor et al., 2005) and steel slag (Chapter 2) are generally similar to those reported for the Mg-silicate olivine (e.g., O'Connor et al., 2002 & 2005). The influence of the reaction temperature and the optimum temperature

for the Ca-silicates correspond roughly with those reported for the Mg-silicate olivine (185 °C, O'Connor et al., 2005). The formation of a SiO_2-rim was also observed for the aqueous carbonation of olivine by O'Connor et al. (2002) and Chizmeshya et al. (2004). A possible difference in the mechanisms reported, which warrants further investigation, is the location of carbonate formation (see also IEA GHG, 2005). In our experiments on steel slag carbonation, the calcite was observed to precipitate on the particle surfaces (Chapter 2), whereas O'Connor et al. (2002 & 2005) reported that magnesite forms as separate particles. For wollastonite, we have observed both situations for the precipitation of calcium carbonate (Figure 4.6.IV). Finally, comparison of both ores (i.e., wollastonite and olivine) shows that the CO_2 pressure required to carbonate wollastonite via the aqueous carbonation route, without the use of additives or pre-treatment steps other than conventional grinding, is significantly lower than for Mg-silicates, i.e., typically 10-40 bar vs. > 100 bar for olivine, as was also observed by O'Connor et al. (2005).
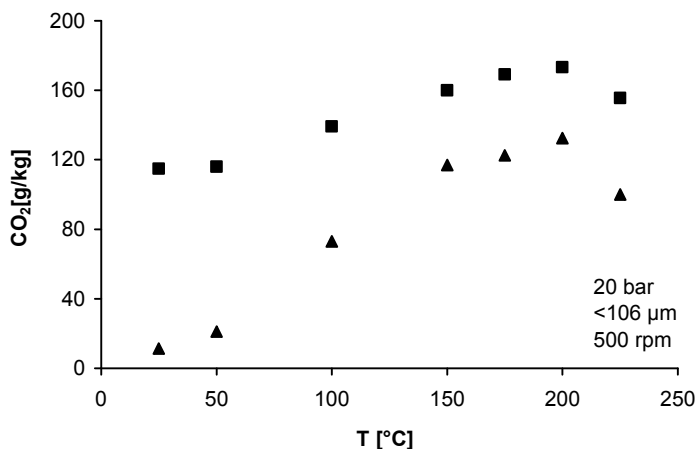
Figure 4.8: *Influence of reaction temperature on calcium carbonate content, expressed in terms of CO₂ of carbonated wollastonite (▲) (t = 15 min, L/S = 5 kg/kg) (Figure 4.3) and steel slag (■) (t = 30 min, L/S = 10 kg/kg) (Chapter 2).*

4.3.3 Process Improvement

The maximum conversion that was obtained within the ranges of process conditions applied is 72% by combining each process parameter's optimum value (d < 38 μm, T = 200 °C, p_{CO2} = 40 bar, t = 60 min, L/S = 10 kg/kg, and n = 500 rpm). Studies aiming at a further increase of the wollastonite carbonation rate, which might be required for cost-effective CO_2 sequestration, should focus on surmounting the factors limiting the reaction rate, as identified in this paper. Application of reaction conditions outside the ranges studied (e.g.,

further grinding or a higher temperature in combination with a higher pressure) could enhance the carbonation rate, but the energy consumption and sequestration costs do then also increase. An alternative might be the use of an extraction agent such as acetic acid (Kakizawa et al., 2001) or additives to enhance the calcium leaching (e.g., NaCl and $NaHCO_3$ (O'Connor et al., 2005) or $NaNO_3$ (Geerlings et al., 2002)).

4.4   Conclusions

The aqueous carbonation of wollastonite for mineral CO_2 sequestration occurs in two subsequent steps via the aqueous phase (i.e., Ca-leaching and $CaCO_3$ precipitation). A key process variable is the specific surface area of the wollastonite particles. The applied CO_2 pressure determines the optimum reaction temperature at which maximum conversion is reached. At temperatures below the optimum, the overall reaction rate is probably limited by the leaching of Ca from wollastonite into the water phase, which is suggested to be controlled by diffusion of Ca through a Ca-depleted silicate rim formed by incongruent leaching. At higher temperatures, a reduction of the bi(carbonate) activity probably causes the nucleation and growth of calcium carbonate to limit the conversion.

The aqueous carbonation mechanisms of wollastonite, olivine, and steel slag were shown to be generally similar. Wollastonite carbonates rapidly compared to Mg-silicates, with a maximum conversion in 15 min of 70% at relatively mild conditions (d < 38 μm, T = 200 °C, and p_{CO2} = 20 bar). However, resources of wollastonite are limited, relative to those of Mg-silicates. The process conditions required to sequester CO_2 by the aqueous carbonation of wollastonite seem technically feasible. However, the energy consumption and costs associated particularly with the grinding to a small particle size (e.g., <38 μm or D[3,2] = 7.9 μm) are likely to be substantial. Therefore, an essential step in the further development of this process is an assessment of the energetic and economic feasibility of aqueous wollastonite carbonation as a possible CO_2 sequestration process.

Annex 4.1   pH$_{stat}$ of (Carbonated) Wollastonite

The leachates resulting from the pH$_{stat}$ analyses as described in §4.2.1 were analysed for an additional set of (trace) elements, in addition to Ca and Si (Figure 4.3). Figure A.4.1.1 shows the resulting pH$_{stat}$ leaching graphs for selected elements as well as the geochemical modelling curves of potentially solubility-controlling minerals. This modelling was performed as described in §3.2.4 for steel slag.
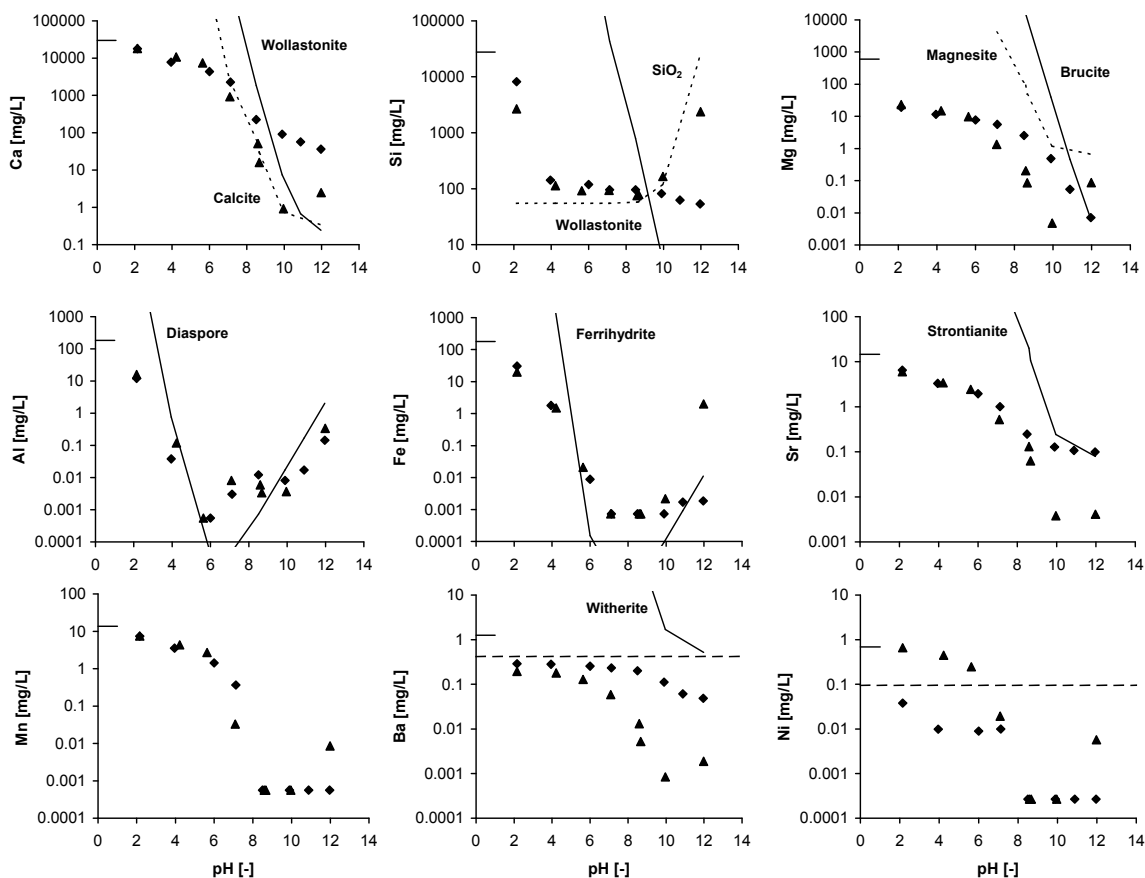
Figure A.4.1.1: *Leaching of selected elements from fresh (♦) and carbonated (▲, ζ_{Ca} = 45%) wollastonite in Nanopure-demineralised water (pH$_{stat}$, L/S = 10 kg/kg, 48h) including geochemical modelling curves of potentially solubility-controlling minerals. Data points below the detection limit (DTL) are shown as half of the DTL. ‒‒‒: limit set by the Dutch building materials decree (1995). Short horizontal lines represent the total amount present in the fresh wollastonite.*

Largely similar effects of carbonation on the leaching of (trace) elements were observed for wollastonite as those described for steel slag (§3.3). For example, also in the case of wollastonite, Ca, Ba, and Sr show reduced leaching after carbonation due to carbonate formation, which probably results in a solid solution of carbonates. However, in contrast to what was found for steel slag (§3.3.2), also Mg shows altered leaching behaviour after wollastonite carbonation, which might indicate that Mg has been carbonated to some extent. The effect of sorption of trace elements on Fe, Al, and Mn-(hydr)oxides places a negligible role in the case of wollastonite given the limited amount of Fe, Al, and Mn present. Finally, for steel slag (§3.3.4), the availability of Ni was reported to increase after carbonation. This effect was also found for wollastonite. Possibly, the Ni originates from the material of construction of the autoclave reactor (AISI 316).

Annex 4.2   Effect of Salts

In the literature, addition of specific salts such as NaCl, NaHCO$_3$, and NaNO$_3$ was reported to enhance the aqueous carbonation rate of Mg-silicates by adjusting the pH and/or reducing the Mg-activity due to an increase of the ionic strength and/or the formation of Mg-complexes (Geerlings et al., 2002; O'Connor et al., 2005) (see also §1.3.2). In this annex, the effect of addition of these sodium salts on the aqueous carbonation of wollastonite is studied.

The procedure for the carbonation experiments as described in §4.2.1 was modified on two points.
First, at the beginning of the carbonation experiments, a salt (NaCl, NaHCO$_3$ or NaNO$_3$; 0-1.5M) was dissolved into the Nanopure-demineralised water before the fresh wollastonite was suspended in the solution.
Second, the TGA method was modified, since the addition of a salt was found to affect the TGA curve in some cases. In the case of NaCl, an extra mass loss occurs between 780-950 °C, during which no CO$_2$ is released. Therefore, an extra stop in the heating of the TGA was introduced at 700 °C in order to separate this mass loss from the calcination step and eq 4.5 was changed into:

$$CO_2[wt\%] = \frac{\Delta m_{105-700°C}[kg]}{m_{105°C}[kg]} \times 100 \qquad \text{(eq 4.7)}$$

In the case of addition of NaNO$_3$, an extra mass loss and CO$_2$ peak occur between 400 and 600 °C, possibly indicating another form of calcium carbonate formed. This mass loss was included in the carbonate-content determined and eq 4.5 remained the same.

Figure A.4.2.1 shows the effect of addition of NaCl and NaNO$_3$ on the aqueous carbonation of wollastonite. It can be concluded that the addition of these salts enhances the carbonation rate. Above a maximum concentration level (0.5 and 1M in the case of NaCl and NaNO$_3$, respectively), the effect of further addition seems to diminish and the carbonation rate is not enhanced further.
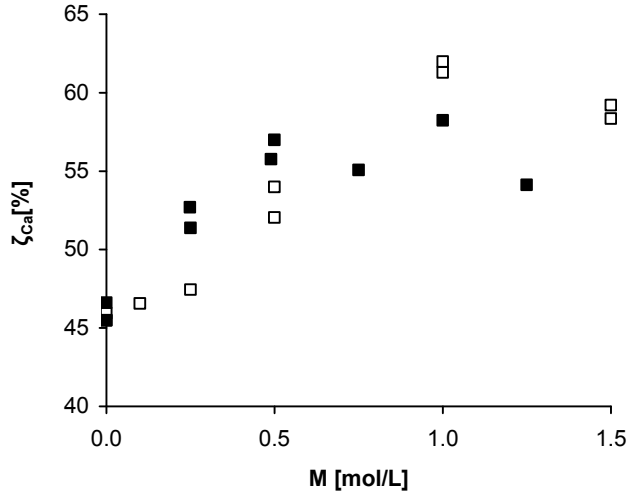
Figure A.4.2.1: *Carbonation experiments with the addition of NaNO$_3$ (□) and NaCl (■). d < 106 µm (D[4,3] = 45 µm), p$_{CO2}$ = 20 bar, T = 150 °C, t = 15 min, n = 500 rpm, and L/S = 5 kg/kg.*

Addition of NaHCO$_3$ (0-1M) as well as 0.64M NaHCO$_3$ in combination with 0.5 or 1M NaCl, as used in the literature to enhance the carbonation of olivine (O'Connor et al., 2005), did not result in a significant enhancement of the carbonation rate (results not shown).

Annex 4.3 Development of Aqueous Wollastonite Carbonation Process

In order to obtain a better insight in the carbonation process, the autoclave reactor was equipped with an in-situ sampling device including an in-line filter. Thus, liquid and solid samples could be taken at in-situ process conditions. The liquid samples were analysed for Ca and Si with ICP-AES. The solid samples were dried and analysed for their carbonate content by TGA-MS (§4.2.2).

Dissolution of Wollastonite

First, the dissolution of wollastonite was examined. Therefore, the autoclave was filled with a wollastonite-water slurry (d < 106 µm, L/S = 5 kg/kg) and heated to a specific temperature set-point (T, 50-200 °C). When this set-point was reached, a liquid sample was taken from the autoclave reactor. The time required to heat up the autoclave reactor was found to increase from 6.5 min at 50 °C to 24.8 min at 200 °C. Figure A.4.3.1 shows the measured Ca and Si concentrations as well as the pH of the liquid samples. In addition, the Si concentration corresponding with congruent wollastonite dissolution was calculated on the basis of the measured Ca concentration and is also shown in Figure A.4.3.1.
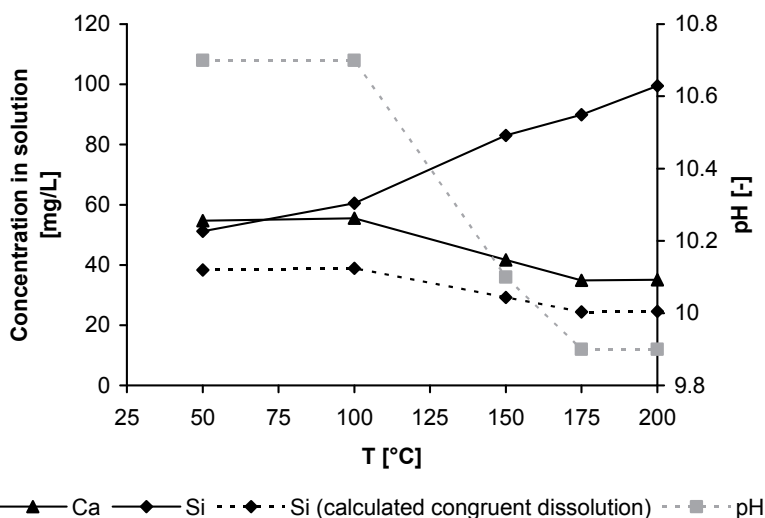
Figure A.4.3.1: *Dissolution measurements of wollastonite (d < 106 µm, n = 500 rpm, L/S = 5 kg/kg).*

Figure A.4.3.1 shows that the dissolution of wollastonite occurs incongruently. Si is leached preferentially at the conditions occurring during heating the reactor. A temperature increase enhances the dissolution of Si even further, while it decreases the solubility of Ca. At 200 °C, the dissolution ratio of Ca:Si is 0.9:3.5 mmol/L.

This effect can be demonstrated by the solubility products of the relevant minerals. The dissolution reaction of wollastonite is:

$$CaSiO_3 \text{ (s)} + H_2O \text{ (l)} \rightarrow Ca^{2+} \text{ (aq)} + SiO_2 \text{ (aq)} + 2 \text{ } OH^- \text{ (aq)} \qquad \text{(eq 4.7)}$$
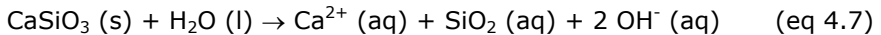
Calculations with GWB (Bethke, 2002) show that the solubility product of wollastonite increases from log K = -14.3 at 25 °C to -13.7 at 100 °C and subsequently decreases to -14.1 at 200 °C. In addition, amorphous SiO_2 (s) is more dissolvable at higher temperatures (log K = -2.7 at 25 °C and -1.8 at 200 °C):

$$SiO_2 \text{ (s)} \rightarrow SiO_2 \text{ (aq)} \qquad \text{(eq 4.8)}$$

The preferential leaching of Ca that was observed during the carbonation experiment (§4.3.1) seems to be due to the pH decrease resulting form the addition of CO_2 (see also Figures A.4.3.2 and A.4.3.3).

Carbonation of Wollastonite

In a second series of experiments, samples were taken during carbonation experiments (at 50, 100, and 150 °C, last two shown in Figure A.4.3.2). Both liquid and solid samples were taken at three different moments during the reaction: after heating the reactor and after 5 and 15 minutes of reaction. In addition, the carbonate content of the fresh and carbonated wollastonite was measured. Finally, the composition of the process water resulting from the carbonation experiment was analysed as well as a solution at 25 °C within a few minutes after being brought into contact with fresh wollastonite.

Figure A.4.3.2 shows the temperature, CO_2 pressure, and the carbonation degree during the carbonation experiment. In addition, the Ca and Si concentrations as well as the pH are shown. During the carbonation experiment the carbonation degree increases with time, following a similar pattern as shown in Figure 4.7.I. Figure A.4.3.2 seems to suggest that the carbonation degree slightly decreases during cooling and depressurisation of the reactor. However, as discussed in §4.2.2, if these stages of the carbonation experiments would have any effect at all, it would be an increase of the carbonation degree.

Therefore, this apparently decreasing effect observed in the experiments is probably due to a preferential sampling of relatively small particles by the sampling device (note: the last but one carbonation degree is based on a sub-sample taken with the sampling device, the very last on the entire sample). Thus, it seems that the use of the sampling device would lead to an overestimation of the carbonation degree.
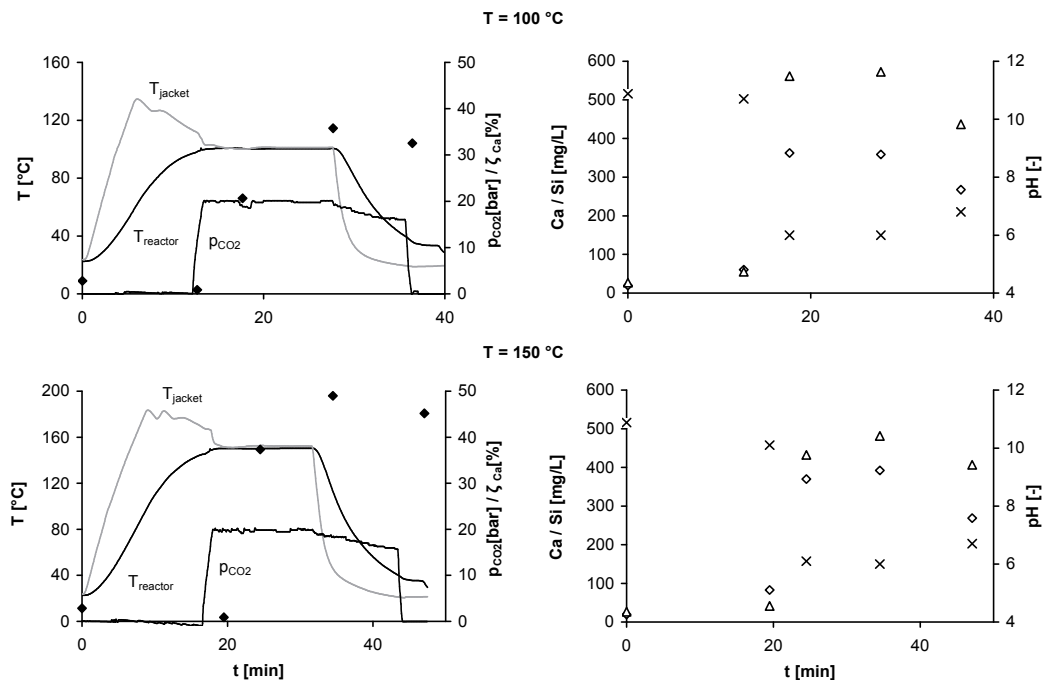
Figure A.4.3.2: *Carbonation experiments of wollastonite (T = 100 °C (left) / 150 °C (right), p_{CO2} = 20 bar, t = 15 min, d < 106 µm, n = 500 rpm, L/S = 5 kg/kg). In the bottom graphs, the temperatures (T_{jacket}, $T_{reactor}$), CO₂ pressure (p_{CO2}), and the carbonation degree (♦,ζ_{Ca}) are shown during the experiment. In the top graphs, the Ca (△) and Si (◇) concentrations as well as the pH (×) are shown.*

The pH of the solution decreases, as expected, due to the addition of CO_2 and slightly increases again upon depressurisation. It should be noted that the process water resulting from the carbonation experiment was not equilibrated with the atmosphere (i.e., the pH was measured directly after filtration of the carbonation slurry). Thus, the pH is lower than what would be expected from solubility-equilibrium with calcite (8.3). Furthermore, the measured pH during the carbonation experiment is probably somewhat higher than the actual in-situ pH, since some CO_2 is inevitably released into the atmosphere. Geochemical simulations of demineralised water in equilibrium with a 20 bar CO_2 gas atmosphere at 150 °C resulted in pH 3.8 (GWB). A similar simulation of a

solution saturated with wollastonite gave pH 5.2. The measured value at 150 °C is pH 6.0.

Based on these measured concentrations in solution and pH values, the solubility indices of wollastonite ($CaSiO_3$) and amorphous SiO_2 were calculated (Figure A.4.3.3).
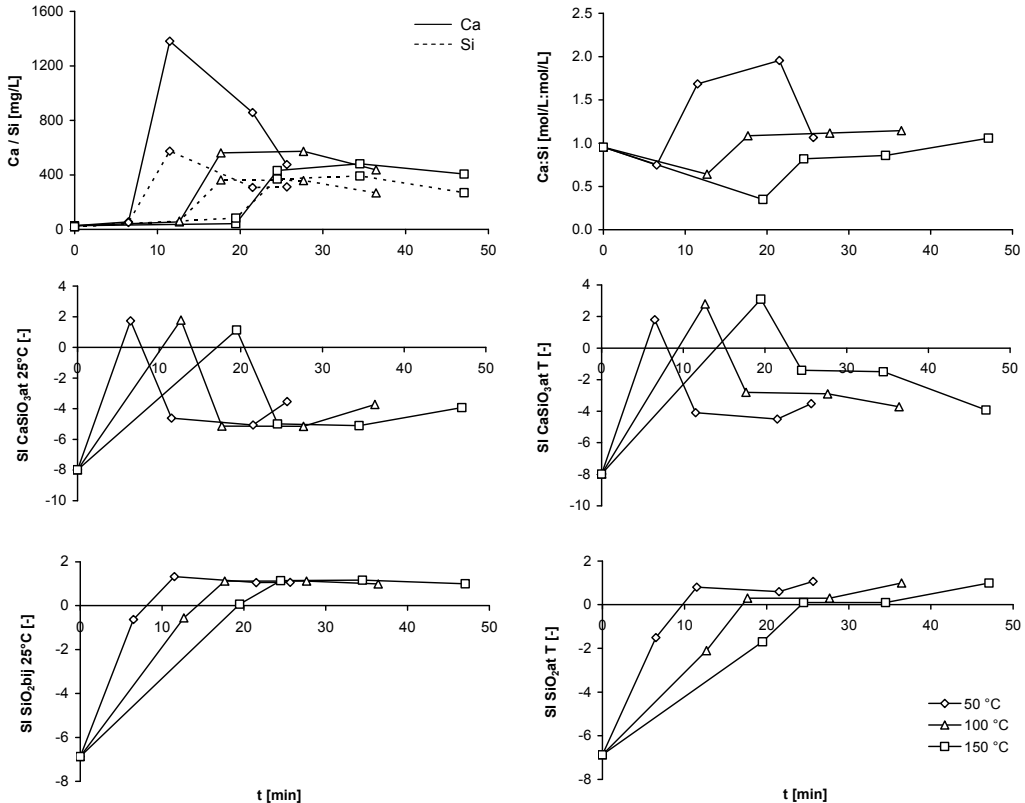
Figure A.4.3.3: *Ca and Si concentrations in solution and saturation indices of $CaSiO_3$ and SiO_2 during carbonation experiments (p_{CO2} = 20 bar, t = 15 min, d < 106 µm, n = 500 rpm, L/S = 5 kg/kg).*

For a proper interpretation of the carbonation process, the total inorganic carbon (TIC) content of the liquid samples should be measured and the solubility indices for calcite ($CaCO_3$) should be calculated. Preliminary experiments showed that direct analysis of TIC in liquid samples taken with the sampling device is inaccurate due to (calcite) precipitation in the samples and CO_2 release during handling. Therefore, it would be better to, e.g., directly mix the liquid sample with a saturated $BaCl_2$-solution so that TIC is fixed in precipitated $BaCO_3$. Subsequently, the barium carbonate can be filtered and analysed.

Further study of the carbonation reaction with the help of the in-situ sampling device might be useful to obtain a more-detailed insight in the carbonation mechanisms. Thus, additional possibilities to further enhance the carbonation rate might be identified.

CHAPTER 5

ENERGY CONSUMPTION AND NET CO$_2$ SEQUESTRATION OF AQUEOUS MINERAL CARBONATION
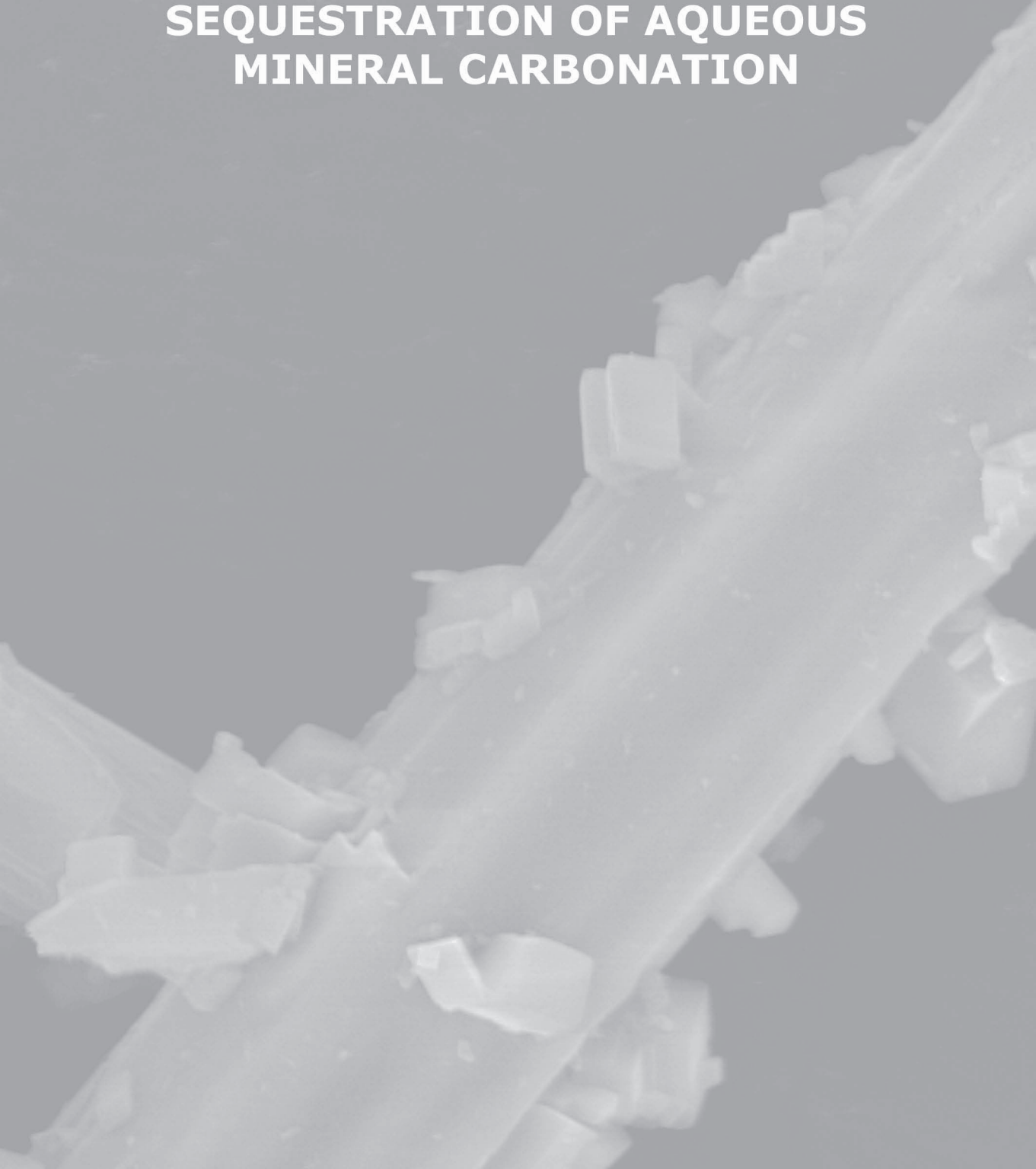
Will be published in similar form as:

Huijgen, W.J.J., Ruijg, G.J., Comans, R.N.J. & Witkamp, G.J. (2006) *Energy consumption and net CO$_2$ sequestration of aqueous mineral carbonation*, Industrial & Engineering Chemistry Research (in press).

ENERGY CONSUMPTION AND NET CO$_2$ SEQUESTRATION OF AQUEOUS MINERAL CARBONATION

Wouter J.J. Huijgen[1], Gerrit Jan Ruijg[1],
Rob N.J. Comans[1,2] & Geert-Jan Witkamp[3]

Aqueous mineral carbonation is a potentially attractive sequestration technology to reduce CO$_2$ emissions. The energy consumption of this technology, however, reduces the net amount of CO$_2$ sequestered. Therefore, the energetic CO$_2$ sequestration efficiency of aqueous mineral carbonation was studied in dependence of various process variables using either wollastonite (CaSiO$_3$) or steel slag as feedstock. For wollastonite, the maximum energetic CO$_2$ sequestration efficiency within the ranges of process conditions studied was 75% at 200 °C, 20 bar CO$_2$, and a particle size of <38 µm. The main energy-consuming process steps were the grinding of the feedstock and the compression of the CO$_2$ feed. At these process conditions, a significantly lower efficiency was determined for steel slag (69%), mainly because of the lower Ca content of the feedstock. The CO$_2$ sequestration efficiency might be improved substantially for both types of feedstock by, e.g., reducing the amount of process water applied and further grinding of the feedstock. The calculated energetic efficiencies warrant a further assessment of the (energetic) feasibility of CO$_2$ sequestration by aqueous mineral carbonation on the basis of a pilot-scale process.

---

[1] Energy Research Centre of The Netherlands.
[2] Wageningen University.
[3] Delft University of Technology.

5.1   Introduction

Mineral carbonation is a potentially attractive CO$_2$ sequestration technology to mitigate possible climate change, on the basis of industrially mimicked natural weathering processes (Wu et al., 2001; IPCC, 2005; Chapter 1). Potential feedstocks for mineral CO$_2$ sequestration include primary Ca/Mg-silicates, such as wollastonite (CaSiO$_3$) (O'Connor et al., 2005; Chapter 4) and olivine (Mg$_2$SiO$_4$) (O'Connor et al., 2002 & 2005), and industrial residues, such as steel slag (Chapter 3) and waste cement (Iizuka et al., 2004). A number of different process routes has been reported, of which the aqueous mineral carbonation route was selected as the most promising in a recent review (Chapter 1, see also references therein), e.g., for wollastonite:

$$CaSiO_3 \text{ (s)} + CO_2 \text{ (g)} \xrightarrow{H_2O, \, T\uparrow, \, p_{CO2}\uparrow} CaCO_3 \text{ (s)} + SiO_2 \text{ (s)} \qquad \text{(eq 5.1)}$$
$$\Delta H_r = -87 \text{ kJ/mol \& } \Delta G_r = -44 \text{ kJ/mol (Lackner et al., 1995)}$$
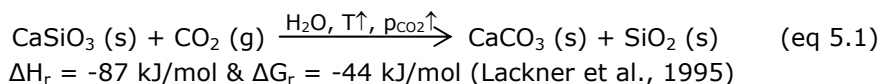
The key issue in mineral carbonation research is the enhancement of the carbonation reaction, which is typically very slow at natural conditions (IPCC, 2005; Chapter 1). In previous papers, we have studied the aqueous carbonation of two Ca-silicates, wollastonite (Chapter 4) and steel slag (Chapters 2 & 3), and shown that the carbonation rate could be increased significantly by, e.g., grinding the feedstock and elevating the temperature and CO$_2$ pressure in the process. The process conditions required for substantial conversion seem technically feasible (i.e., typically, 175 - 200 °C, 10 - 40 bar CO$_2$, a particle size of <38 μm, and a reaction time of 15 - 30 min). However, all the measures required to increase the reaction rate consume energy and reduce the net amount of CO$_2$ sequestered because of extra CO$_2$ emissions caused. On the other hand, the exothermic mineral carbonation reaction may potentially generate usable heat. Overall, an energetic CO$_2$ sequestration efficiency (η_{CO2}) of the mineral carbonation process can be defined on the basis of the amount of CO$_2$ sequestered in the carbonation reactor (CO$_{2,sequestered}$) and the net overall amount of CO$_2$ sequestered by the mineral carbonation process (CO$_{2,avoided}$):

$$\eta_{CO2}[\%] = \frac{CO_{2,avoided}}{CO_{2,sequestered}} \times 100 = 100 - \frac{E_{power} \times \varepsilon_{power} + E_{heat} \times \varepsilon_{heat}}{CO_{2,sequestered}} \times 100$$

$$\text{(eq 5.2)}$$

The extra CO$_2$ emissions associated with the mineral carbonation process are determined by the power and heat consumption of the process (taking the reaction heat into account) (E$_{power}$ and E$_{heat}$, respectively) and the conversion

factors of the power and heat consumption into CO_2 emissions (ε_{power} and ε_{heat}, respectively). The energy consumption of the mineral carbonation process is influenced by the conditions in the carbonation reactor both directly as well as indirectly through their effect on the carbonation conversion. Therefore, a system study of the aqueous mineral carbonation process is required to determine its overall energetic CO_2 sequestration efficiency and to optimize this efficiency on the basis of its dependence on the reactor conditions.

A number of (preliminary) system studies on different approaches for CO_2 sequestration by mineral carbonation has been published (e.g., Kakizawa et al., 2001; O'Connor et al., 2005; Teir et al., 2005), including the aqueous mineral carbonation route (O'Connor et al., 2005). However, the results presented for wollastonite in the latter system study by the Albany Research Center (ARC) have been predicted on the basis of a carbonation process designed for olivine. In addition, the study does not include the use of industrial residues as feedstock for mineral carbonation. Although their availability is relatively limited, residues might be of interest since no mining is required and residues tend to be more reactive with regard to carbonation than ores at relatively mild process conditions (Chapters 2 & 4).

The aim of the present study is to determine and optimize the energetic performance of CO_2 sequestration by aqueous carbonation of Ca-silicates, both an ore and an industrial residue. A mineral carbonation process will be designed and the CO_2 sequestration efficiency will be determined at various sets of process conditions. A sensitivity analysis will be performed in order to assess the accuracy of the energetic efficiency determined and to indicate routes for further improvement of the CO_2 sequestration efficiency.

5.2 Methods and Assumptions

5.2.1 Process Simulation

A block diagram of a CO_2 sequestration process on the basis of mineral carbonation is shown in Figure 5.1 including the system boundaries of the present study. The mineral carbonation plant is assumed to be located at the source of the solid feedstock. The mineral carbonation process step, which is subject of this study, includes the compression of the CO_2 feed and the grinding of the feedstock (Figure 5.1).
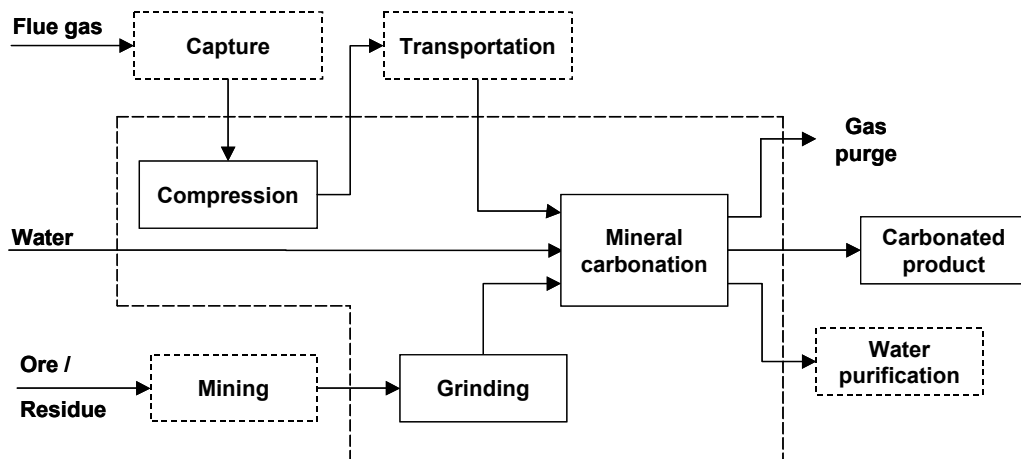
Figure 5.1: *Block diagram of mineral carbonation process for CO_2 sequestration together with system boundaries of the present study.*
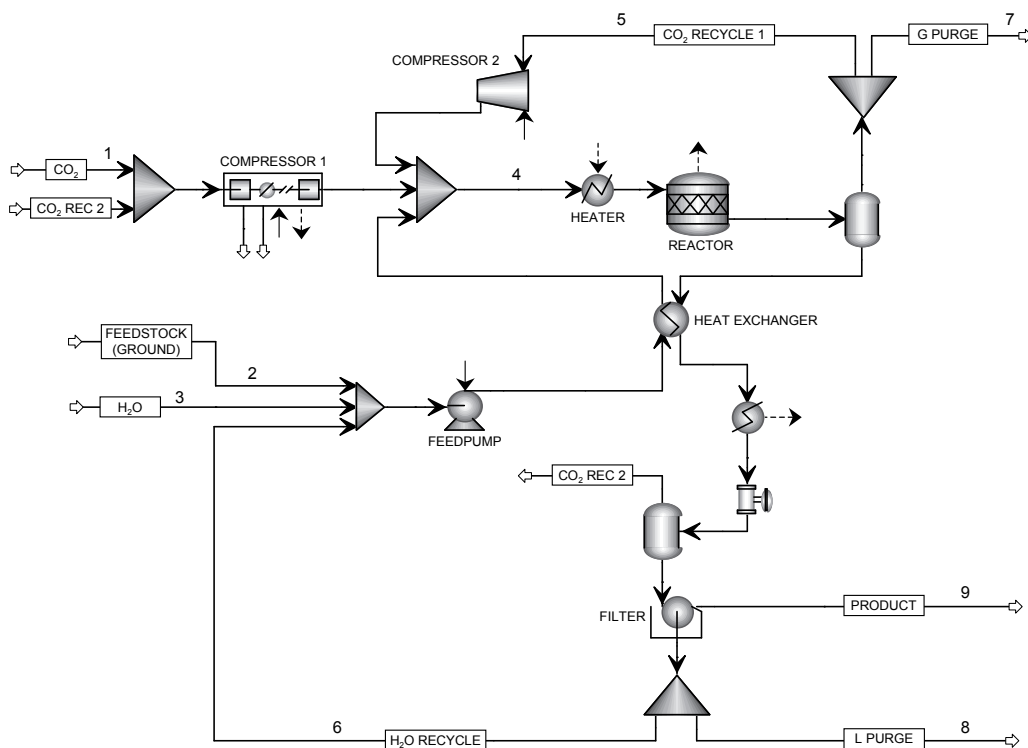
Figure 5.2: *Simplified ASPEN flow diagram of an aqueous mineral carbonation process. At the points indicated, the temperature, pressure, and composition of streams are given in the table (next page). Process conditions: T = 200 °C, p_{CO2} = 20 bar, batches W1 and S1 (d < 38 μm), and L/S = 5 kg/kg (ζ_{CaSiO3} = 69% and 67% for wollastonite and steel slag, respectively). Heat (→) and power (-→) flows are indicated.*

Stream number	1	2	3	4	5	6	7	8	9
Wollastonite									
T [°C]	25	25	25	180	200	39	40	39	39
p [bar]	1.0	1.0	1.0	35.5	34.5	1.0	1.0	1.0	1.0
Mass flow [ton/ton CO_2 seq]									
$CaSiO_3$		3.8		3.8					1.2
$CaCO_3$		0.1		0.1					2.4
SiO_2		0.6		0.6					2.0
H_2O			1.0	22.7	0.0	21.6	0.0	0.0	1.0
CO_2	1.0			1.8	0.1	0.3	0.0	0.0	0.0
Steel slag									
T [°C]	25	25	25	181	200	39	40	39	39
p [bar]	1.0	1.0	1.0	35.5	34.5	1.0	1.0	1.0	1.0
Mass flow [ton/ton CO_2 seq]									
$CaSiO_3$		3.9		3.9					1.3
$CaCO_3$		0.5		0.5					2.8
SiO_2									1.4
FeO		2.4		2.4					2.4
H_2O			1.4	34.4	0.0	33.0	0.0	0.0	1.4
CO_2	1.0			1.7	0.1	0.4	0.0	0.0	0.0

Figure 5.2: *Continued.*

ASPEN Plus flow-sheeting software (2005) was used to simulate the continuous mineral carbonation process, for which the flowsheet is shown in Figure 5.2. In the process, the solid feedstock, after being ground to a specific particle size (d) (§5.2.2), is mixed with water at a specific liquid-to-solid ratio (L/S) and the resulting slurry is pumped to the reactor pressure (p). Subsequently, the slurry is heated with the carbonation reactor outlet in a heat exchanger to 20 °C below the reactor temperature (T). CO_2 is pressurized in a multiple-stage compressor to the reactor pressure and added to the slurry. The mixture is heated to the reactor temperature, and the carbonation reaction takes place in a continuous (cooled) carbonation reactor at isothermal conditions during the reaction time (t). The total pressure in the reactor equalled the sum of the partial CO_2 pressure (p_{CO2}) and the H_2O vapour pressure (p_{H2O}) as determined by ASPEN at the reactor temperature (e.g., p_{H2O} = 16 bar at 200 °C). After the reactor, the non-reacted gaseous CO_2 is separated from the solid-liquid slurry and recycled to the reactor. The slurry is depressurized to 1 atm after being cooled to 40 °C in two steps (first, in a heat exchanger by exchanging heat with the reactor feed and, second, in a cooler with cooling water). The CO_2 released from the slurry upon depressurization is recycled to the compressor in a second CO_2 recycle. The solid product is separated from the slurry by filtration, and the remaining process water is recycled. A purge is used in both the liquid and the main gas

recycles to avoid possible accumulation of (inert) impurities (i.e., soluble salts leached from the feedstock and gaseous impurities in the (captured) CO$_2$ feed, such as N$_2$). In the compressor, moisture present in the second CO$_2$-recycle stream might condense. This condensate is separated and added to the water recycle. Table 5.1 shows additional assumptions used for the various unit operations.

Table 5.1: *Assumptions used within the ASPEN simulations for the unit operations.*

Unit operation	Assumptions
Pump	Pump efficiency = 0.8. Single-stage centrifugal pump.
Compressor 1	Three-stage centrifugal compressor with intermediate cooling between subsequent stages to 40 °C. Isentropic operation with an efficiency of 0.8 for each stage. Condensed water added to process water recycle. [a]
Compressor 2	Single-stage blower. Isentropic operation with an efficiency of 0.8.
Reactor	Isothermal operation. Pressure drop = 1 bar. Amount of CO$_2$ sequestered = 1 ton/h. [b]
Filter	Centrifugal filter. Atmospheric operation. Separation efficiency of solids = 100%. Mass fraction of solids in cake = 0.85.
Flash drums	Isothermal and isobaric. Top flash carbonation reactor outlet = 0.1 ton/h of CO$_2$. [c]
Valves	Adiabatic operation.
Splitters [d]	0% purge fractions for both CO$_2$ recycle 1 and H$_2$O recycle.
Other	All starting materials enter the process at 25 °C and 1 atm. Product and purge streams leave the process at 1 atm.

[a] The number of stages is selected such that the pressure ratio per stage for the highest outlet pressure simulated (i.e., 65.5 bar) is between 3:1 and 5:1 (Perry and Green, 1998). [b] The difference between the amount of CO$_2$ present in the reactor in- and outlet. Only defined for simulation purposes, since the CO$_2$ sequestration efficiency is independent of the scale of the process. [c] At the end of the carbonation reaction, remaining gaseous CO$_2$ has to be present in the reactor outlet to ensure that the slurry in the reactor has been saturated with dissolved CO$_2$ during the entire carbonation reaction. Therefore, 10% of the amount of CO$_2$ sequestered in the reactor was specified to come over the top in the flash after the reactor. [d] In a final plant design, the CO$_2$ purge fraction is determined by the composition of the gas stream resulting after CO$_2$ capture. The H$_2$O purge fraction depends on the composition of the water recycle stream. Both are yet unknown, and the purge fractions are, therefore, set at 0.

The thermodynamic property set used for the ASPEN simulations, 'Peng-Robinson with Huron-Vidal 2 mixing rules' (PRMHV2), was selected according to Carlson (1996) on the basis of a polar non-electrolyte system at pressures > 10 bar. The influence of ions (generated by leaching from solids and dissolution of

gaseous CO_2) on the thermodynamic properties of the system was neglected. However, the effect of dissolved ions on the carbonation reaction (Chapters 2 & 4) is implicitly included in the definition of the conversion in the carbonation reactor (§5.2.3). The ASPEN components defined for the wollastonite carbonation process were 'carbon-dioxide' (CO_2), 'water' (H_2O), and the solids 'wollastonite' ($CaSiO_3$), 'silicon-dioxide' (SiO_2), and 'calcium-carbonate-calcite' ($CaCO_3$). The composition used for the wollastonite feedstock was 84.3 wt% $CaSiO_3$, 13.9 wt% SiO_2, and 1.8 wt% $CaCO_3$ (Chapter 4), assuming all other (inert) components were present as SiO_2. The only reaction taken into account was the carbonation reaction (eq 5.1), which was assumed to occur exclusively in the carbonation reactor (see §5.2.3). The steel slag feedstock consisted mainly of Ca and Fe phases (Chapter 2). In previous work, the various Ca phases and their carbonation reactions have been identified (Chapters 2 & 3). However, the contribution of each phase and reaction could not be quantified. Therefore, as a simplification, the composition of the steel slag (Chapter 2) was defined in terms of the same Ca components as used for wollastonite plus 'ferrous-oxide' (FeO) (56.8 wt% $CaSiO_3$, 7.7 wt% $CaCO_3$, and 35.5 wt% FeO). It was assumed that all Ca was present as either $CaSiO_3$ or $CaCO_3$ (based on the carbonate content in §5.2.3) and that the rest of the feedstock consisted of FeO. FeO was considered to be inert, since no significant amount of carbonate minerals other than calcite was formed at the process conditions applied in the steel slag carbonation experiments (Chapter 2). Analogously to wollastonite, the Ca carbonation reaction of steel slag was assumed to be represented by eq 5.1 (see also §5.3.3).

5.2.2 Feedstock Batches

Table 5.2 shows the definition of the wollastonite and steel slag feedstock batches used in this study. For each batch, the corresponding power required for grinding (W) was calculated with Bond's equation (Bond, 1961):

$$W = 0.01 \times W_i \times \left(\frac{1}{\sqrt{d_1}} - \frac{1}{\sqrt{d_0}} \right) \qquad \text{(eq 5.3)}$$

with the original particle size of the feedstock (d_0), the imaginary sieve size through which 80 wt% of the ground feedstock passes (d_1), and the standard Bond's working index (W_i) (as reported in the literature for $d_0 = \infty$ and $d_1 = 100$ µm (Perry and Green, 1998)). In the case of a grinding step with final particle size < 70 µm, an extra multiplier of $(10.6 \times 10^{-6} + d_1)/1.145d_1$ was applied to eq 5.3, as used by ASPEN (2005) (see also Perry & Green (1998)). The fresh wollastonite ore was assumed to be supplied to the grinding equipment as uniform particles of 0.1 m (d_0). The standard Bond's working index (W_i) of wollastonite was set at 14 kWh/ton (i.e., mean of working indices

of limestone (11.6 kWh/ton) and silica sand (16.5 kWh/ton) (Perry and Green, 1998)). The ore grade of the wollastonite ore was assumed to be 50% (O'Connor et al., 2005). Following the approach taken by the Albany Research Center (O'Connor et al., 2005), the wollastonite ore was assumed to be first ground to <200 mesh (roughly 75 μm) and, subsequently, concentrated to the composition assumed for the wollastonite feedstock by removing the gangue (see §5.2.1). Finally, the concentrated ore is ground to its final particle size. If the final particle size is >75 μm, grinding was performed in a single step. The energy penalty for the beneficiation (i.e., ore concentrating) step was assumed to be 4 kWh/ton (O'Connor et al., 2005). Because ore grade is no issue for steel slag, this feedstock is ground in a single step. For this material, the standard Bond's working index available for blast furnace slag of 12 kWh/ton (Perry and Green, 1998) was used. In addition, a particle size of 0.02 m was selected as a representative size for freshly produced steel slag. The 80 wt% passing size of the individual wollastonite and steel slag batches was estimated on the basis of the particle size distribution measured by laser diffraction (Chapters 2 & 3) (Table 5.2).

5.2.3   Carbonation Degree

The conversion in the carbonation reactor defined the required supply of fresh solid feedstock (i.e., the amount of CO_2 sequestered is fixed; see Table 5.1). The influence of the following six process variables on the carbonation degree (ζ) had been studied previously in a lab-scale autoclave reactor for both wollastonite and steel slag: temperature, CO_2 pressure, particle size, stirring rate (n), residence time, and liquid-to-solid ratio (Chapters 2 & 4). These data sets were applied as an estimation of the conversion in the continuous large-scale carbonation reactor used in this system study. For simulation purposes, the Ca carbonation degree as measured in the lab-scale autoclave reactor (ζ_{Ca}) (Chapters 2 & 4) was expressed in terms of the $CaSiO_3$ fraction in the reactor inlet (ζ_{CaSiO_3}). In the case of steel slag, conversion data reported earlier (Chapter 2) were first corrected for the carbonate content of the fresh steel slag (3.4 wt%) similarly to the approach reported for wollastonite (Chapter 4).

For the specific purpose of this system study, three series of additional carbonation experiments were performed in the autoclave reactor following the experimental approach described earlier (Chapters 2 & 4). For these additional experiments, two extra feedstock batches were prepared and analyzed as reported in previous work (Chapters 2 & 4) (batches W2 (<106 μm) and S2 (<38 μm); see Table 5.2). In the first series of experiments, steel slag was carbonated in duplicate at the same process conditions at which the maximum energetic efficiency was found for wollastonite (see §5.3.1; d <38 μm, T =

200 °C, p_{CO2} = 20 bar, t = 15 min, n = 500 rpm, and L/S = 5 kg/kg). In the other two series of experiments, the effect of process water recycling on the carbonation degree and the composition of the process water was studied for both wollastonite and steel slag (see Annex 5.1).

Table 5.2: *Definition, particle size data, and grinding energy of wollastonite and steel slag feedstock batches.*

Batch	Sieve [μm]	D[4,3] [μm] [a]	d_1 [μm] [b]	W [kWh/ton feedstock] [c]			
				G-1	B	G-2	Total
Wollastonite							
W1	<38	16	20	31 [d]	4 [e]	20 [f]	56
W2	<106	45	60	31	4	3	38
W3	<106	51	69	31	4	1	36
W4	<500	159	240	17	4		21
W5	<7000	375	631	10	4		14
Steel slag							
S1	<38	14	23				31 [g]
S2	<38	15	23				31
S3	<106	33	52				17
S4	<106	34	52				17
S5	<500	97	158				9
S6	<2000	582	832				3

[a] Volume-based mean particle size. [b] 80wt% passing sieve size (see eq 5.2).
[c] W = grinding energy. In the case of wollastonite, the grinding energy consists of three steps: first-stage grinding (G-1), beneficiation (B), and second-stage grinding of the concentrated ore (G-2). In the case of steel slag, grinding takes place in a single step.
[d] First grinding step from 0.1 m to 75 μm; ore grade = 50%; W_i = 14 kWh/ton. [e] Energy penalty for beneficiation. [f] Second grinding step from 75 μm to final particle size; W_i = 14 kWh/ton. [g] d_0 =0.02 m and W_i = 12 kWh/ton (Perry and Green, 1998).

5.2.4 CO₂ Sequestration Efficiency

For each set of reactor conditions, the ASPEN flowsheet of the mineral carbonation process as given in Figure 5.2 was simulated. The outcome consisted of the composition, temperature, and pressure of the process streams and the power and heat consumption of the unit operations. Subsequently, the CO_2 sequestration efficiency was calculated on the basis of eq 5.2. The power consumption of the mineral carbonation process (E_{power}) consisted of power consumption for compression, pumping, and grinding. The (possible) power consumption of the reactor and the filter were neglected. E_{heat} was the net process heat (i.e., the heat required for heating the reactants minus the reaction

heat). In the case of a possible surplus of process heat, a useful application of this heat was assumed outside the system boundaries of this study and the negative CO$_2$ emissions associated were taken into account in the energetic CO$_2$ efficiency. The reaction heat of the carbonation reaction (eq 5.1) was calculated by ASPEN for each reactor temperature and pressure (e.g., -84 kJ/mol at standard conditions). The conversion factor of the power required in the process into CO$_2$ emissions (ϵ_{power}) was set at 0.60 kg CO$_2$/kWh as an estimation of the average value in The Netherlands (cf. representative values for a natural gas combined cycle and a powder coal power plant of 0.36 and 0.80 kg CO$_2$/kWh, respectively (Rubin et al., 2004)). The conversion factor of the heat consumption in the process into CO$_2$ emissions was based on the combustion of methane (ΔH_r = -803 kJ/mol (Perry and Green, 1998) or ϵ_{heat} = 0.20 kg CO$_2$/kWh).

In the simulations, the influence of the process variables reactor temperature, CO$_2$ partial pressure, and particle size on the CO$_2$ sequestration efficiency was studied. The ranges within which these variables could be varied were slightly restricted compared to the carbonation experiments (Chapters 2 & 4). Because of the pressure drop over the reactor (1 bar), simulations on the basis of carbonation measurements at p$_{CO2}$ = 1 bar were performed with p$_{CO2}$ = 1.5 bar to enable simulation. In addition, processes with a reactor temperature below 60 °C could not be simulated because of the assumptions given in Table 5.1 (T$_{H2O-recycle}$ = 40 °C and $\Delta T_{heat-exchanger}$ = 20 °C).

The possible influence on the CO$_2$ sequestration efficiency of the other process variables studied experimentally, i.e., residence time, agitation rate, and L/S-ratio (Chapters 2 & 4), was (initially) not taken into account in this study. A longer residence time increases the energy consumption of the process that must be kept at elevated temperature and pressure for a longer time. However, these energy losses are not taken into account in the current assessment, since they cannot be quantified at the current stage of process development. The possible minimum agitation rate and the accompanying power input required to obtain sufficient mixing in the continuous carbonation reactor are also currently unknown. For reasons of comparison, all wollastonite and steel slag simulations were (initially) performed at L/S = 5 kg/kg, although the steel slag conversions were actually measured at L/S = 10 kg/kg (Chapter 2). The consequences of this assumption will be discussed in §5.3.3. The L/S-ratio was defined in the ASPEN flowsheet on the basis of all solids present in the reactor feed.

Finally, a sensitivity analysis was performed on the CO$_2$ sequestration efficiency of aqueous wollastonite carbonation at the energetically optimum reactor conditions (§5.3.1). In this analysis, a selection of assumptions and input

variables for the ASPEN simulations and the CO_2 emission calculations were varied within possible limits. For steel slag, a similar analysis was performed at identical conditions.

5.3   Results and Discussion

5.3.1   Wollastonite

Figure 5.3 shows the influence of the particle size, reactor temperature, and CO_2 pressure on (1) the measured carbonation degree of wollastonite (Chapter 4), expressed in terms of the $CaSiO_3$ fraction in the reactor feed (ζ_{CaSiO3}), and (2) the corresponding simulated CO_2 sequestration efficiencies (η_{CO2}).

In general, differences between the ζ_{CaSiO3} and η_{CO2} curves appear at low carbonation degrees, since a low conversion has a strong reducing effect on the sequestration efficiency. Substantially more energy is required for both grinding the feedstock and heating the wollastonite-water slurry.

The influence of process variables on the energetic sequestration efficiency shown in Figure 5.3 consists of a direct effect of the process variables on the energy consumption as well as an indirect effect through their influence on the carbonation degree. To be able to distinguish between both effects, Table 5.3 shows the influence of the same process variables on the sequestration efficiency at constant conversion (arbitrarily kept at 69%; see below). It should be noted that the simulations presented in Table 5.3 are performed for the specific purpose of eliminating the *indirect* effect of the process conditions on the energetic efficiency, thus allowing an assessment of only the *direct* effect of these conditions on the energy consumption.

Figure 5.3.I.b shows that increasing the conversion by size reduction is favourable with regard to the CO_2 sequestration efficiency, within the ranges of process conditions studied (d = <38 - <7000 μm). Grinding leads to a higher carbonation degree because of an increased specific surface area (Chapter 4) and, thereby, a reduction of the amount of feedstock that has to be processed (Figure 5.3.I.a). On the other hand, the grinding energy per kilogram of feedstock increases substantially for smaller particle sizes (Table 5.2), which has a reducing effect on the energetic efficiency (Table 5.3). Figure 5.3.I.b shows that the effect of the increased conversion on the energetic efficiency is larger than the extra energy consumption, within the range of particle sizes studied. However, the cases simulated for small particle sizes are less favourable from an energetic point of view than from a conversion point of view (Figure 5.3.I.b),

and an optimum in CO_2 sequestration efficiency probably occurs when the wollastonite is further ground to particle sizes smaller than <38 μm (d_1 = 20 μm; see Table 5.2).
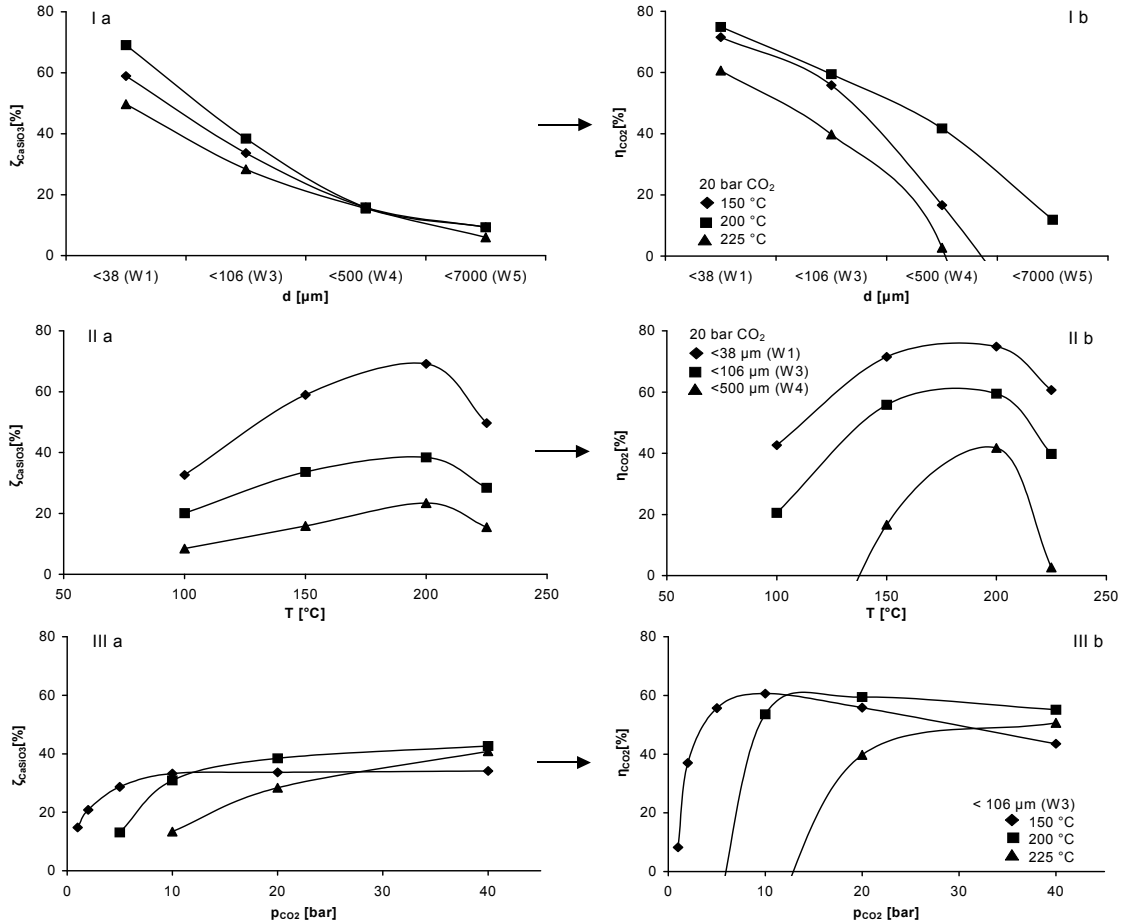
Figure 5.3: *Measured carbonation degree (ζ_{CaSiO3}) (Chapter 4) and the corresponding calculated CO_2 sequestration efficiency (η_{CO2}) as a function of various process variables for wollastonite. Simulations were performed at L/S = 5 kg/kg. Conversion measurements in lab-scale autoclave reactor were performed at t = 15 min, n = 500 rpm, and L/S = 5 kg/kg. (I) Particle size at various reactor temperatures; (II) reactor temperature at various particle sizes; and (III) CO_2 pressure at various temperatures.*

The reactor temperature shows an optimum carbonation rate (Figure 5.3.II.a) and energetic efficiency (Figure 5.3.II.b) around 200 °C. The occurrence of a maximum carbonation degree is caused by two opposite temperature effects: (1) a higher dissolution rate of Ca upon a temperature increase and (2) a retardation of the $CaCO_3$ precipitation due to decreased CO_2 activity in solution (Chapter 4). The influences of the reactor temperature on the CO_2 sequestration

efficiency and the $CaSiO_3$ conversion are similar, although the influence is less significant for the efficiency (Figure 5.3.II, d < 38 μm). Apparently, the extra CO_2 emissions associated with an increase of the reactor temperature to 200 °C are smaller than the extra amount of CO_2 sequestered. These extra CO_2 emissions are caused both by the increased temperature itself as well as by the temperature effect on the water vapour (and total) pressure. Table 5.3 shows calculations at both constant and adjusted total pressure. The influence of the temperature at constant total pressure will be discussed first.

Table 5.3: *Direct influence of process variables on the power and heat consumption and CO_2 sequestration efficiency for wollastonite.[a]*

Variable	Feedstock batch	Reactor conditions				ζ_{CaSiO3} [%] [b]	Power [kWh / ton CO_2 seq]		Heat [kWh / ton CO_2 seq]		η_{CO2} [%]
		d [μm]	T [°C]	p_{H2O} [bar]	p_{CO2} [bar]	p [bar]		I [c]	II [d]	III [e]	IV [f]	
d	W1	<38	200	16	20	36	69	253	150	-799	752	75
	W3	<106	200	16	20	36	69	165	150	-799	752	80
	W4	<500	200	16	20	36	69	96	150	-799	752	84
	W5	<7000	200	16	20	36	69	65	150	-799	752	86
p_{CO2}	W1	<38	200	16	10	26	69	253	101	-994	934	78
	W1	<38	200	16	20	36	69	253	150	-799	752	75
	W1	<38	200	16	30	46	69	253	202	-724	690	72
	W1	<38	200	16	40	56	69	253	256	-679	658	69
T	W1	<38	100	16	20	36	69	253	367	-197	556	70
	W1	<38	150	16	20	36	69	253	225	-505	597	73
	W1	<38	175	16	20	36	69	253	185	-629	643	74
	W1	<38	200	16	20	36	69	253	150	-799	752	75
T + p_{H2O}	W1	<38	100	1	20	21	69	253	198	-373	564	77
	W1	<38	150	5	20	25	69	253	151	-572	618	77
	W1	<38	175	9	20	29	69	253	147	-672	670	76
	W1	<38	200	16	20	36	69	253	150	-799	752	75

[a] In the simulations, conversion is kept constant at 69%. Corresponding starting process conditions: batch W1 (d < 38 μm), T = 200 °C, and p_{CO2} = 20 bar. Simulations were performed at L/S = 5 kg/kg. [b] Conversion was kept constant to eliminate the indirect effect of the process conditions on the energetic efficiency through their influence on the conversion. [c] Grinding. [d] Compression & pumping. [e] Heater. [f] Reactor heat.

At constant carbonation degree and water vapour pressure, a higher reactor temperature would increase the energy required to heat the CO_2 gas (Table 5.3). However, changing the reactor temperature has no direct effect on the energy consumption of the heater used for heating the liquid-solid slurry. The

slurry is heated to 20 °C below the reactor temperature in the heat exchanger independently of the actual reactor temperature. As an indirect effect of a higher reactor temperature, the amount of dissolved CO$_2$ in the reactor outlet decreases because of a solubility decrease. Thus, less CO$_2$ is recycled in the second CO$_2$ recycle and would have to be recompressed (stream 'CO$_2$ REC 2' in Figure 5.2). Finally, the reactor temperature affects the reactor heat (Table 5.3). Overall, an increase of the reactor temperature at constant total pressure and carbonation degree would have an increasing effect on the CO$_2$ sequestration efficiency (Table 5.3). Apparently, the effect on the amount of dissolved CO$_2$ dominates the other temperature effects.

If the temperature effect on the water vapour pressure is included (Table 5.3), the effects of reactor temperature and pressure on the energetic efficiency occur in combination (see below for more detail). The power required for compression shows a minimum for the 175 °C case (two counter-effective effects occur: a higher energy consumption for compression due to the higher total pressure and a smaller amount of CO$_2$ that has to be compressed) (Table 5.3). Overall, elevation of the reactor temperature has a slightly decreasing direct effect on the CO$_2$ sequestration efficiency caused by the increase of the water vapour pressure (Table 5.3).

Finally, elevation of the CO$_2$ pressure has, in most cases, a favourable effect on the CO$_2$ sequestration efficiency (Figure 5.3.III). However, cases with only a small positive effect of the CO$_2$ pressure on the conversion form an exception (i.e., 150 and 200 °C lines in Figure 5.3.III.b). A higher CO$_2$ pressure, in principle, increases the carbonation degree because of an increase of the CaCO$_3$ precipitation rate (Chapter 4) (Figure 5.3.III.a). However, above a specific (temperature-dependent) CO$_2$ pressure, the carbonation degree becomes independent of the CO$_2$ pressure since the (bi)carbonate activity in solution is no longer rate-limiting (Chapter 4) (Figure 5.3.III.a). The direct effect of a higher p_{CO2} on the energetic efficiency consists not only of increased power consumption for compression but also of a changed heat balance of the process (Table 5.3). A higher CO$_2$ pressure increases the temperature of the CO$_2$ gas outlet stream of the compressor and, thus, lowers the energy consumption of the heater. In addition, the reactor heat decreases upon an increasing CO$_2$ pressure. The actual reactor heat of -799 kWh/ton CO$_2$ sequestered at 200 °C and 20 bar CO$_2$ consists of the standard reaction heat as specified at standard conditions (-528 kWh/ton CO$_2$ sequestered at 25 °C and 1 bar) corrected for the actual reactor temperature and pressure. The extra CO$_2$ emission caused by increased compression is larger than the influence of the heat balance of the process, and overall, an increase of the CO$_2$ pressure has a direct reducing effect on the CO$_2$ sequestration efficiency (Table 5.3). Overall, this extra CO$_2$ emission due to elevating the CO$_2$ pressure is generally smaller than the extra CO$_2$

sequestered at a higher CO_2 pressures (Figure 5.3.III). However, cases with only a small effect of a higher CO_2 pressure on the conversion might become energetically less favourable for the higher pressures (i.e., 150 and 200 °C lines in Figure 5.3.III.b). Therefore, the optimum CO_2 pressure can only be determined by additional carbonation experiments and simulations at the optimum reactor temperature (200 °C) and particle size.

The maximum energetic efficiency of CO_2 sequestration by wollastonite carbonation found within the ranges of process conditions studied is 75%. The corresponding set of conditions is T = 200 °C, p_{CO2} = 20 bar, and d < 38 µm with a carbonation degree (ζ_{CaSiO3}) of 69%. In the rest of this thesis, we refer to this set as the 'energetically optimum' process conditions, although more favourable conditions may occur outside the range of experimental data that this study is based on. For this set of conditions, Figure 5.2 shows the stream properties for the aqueous wollastonite carbonation process and Table 5.4 shows the accompanying heat and power flows. The largest fraction of the total power required is for grinding, followed by that for compression of the CO_2 feed. The power required for recompression of the CO_2 recycle and for pumping the slurry is very small. The overall heat balance of the process is slightly negative at these reactor conditions (see §5.3.3.4).

Table 5.4: *Heat and power consumption of process equipment and their individual effect on the CO_2 sequestration efficiency for wollastonite (batch W1) and steel slag (S1).[a]*

Process equipment		Wollastonite				Steel slag			
		E [kWh/ ton CO_2 seq]		$\Delta\eta_{CO2}$ [%] [b]		E [kWh/ ton CO_2 seq]		$\Delta\eta_{CO2}$ [%]	
Power	Compressor 1	118	(*96*)	-7	(*-6*)	137	(*104*)	-8	(*-6*)
	Compressor 2	0	(*0*)	-0	(*-0*)	0	(*0*)	-0	(*-0*)
	Pump	33	(*13*)	-2	(*-1*)	50	(*20*)	-3	(*-1*)
	Grinding	253	(*253*)	-15	(*-15*)	213	(*213*)	-13	(*-13*)
	Sum	403	(*362*)	-24	(*-22*)	400	(337)	-24	(*-20*)
Heat	Reactor	-752	(*-757*)	+15	(*+15*)	-747	(*-755*)	+15	(*+15*)
	Heater	799	(*462*)	-16	(*-9*)	1101	(*588*)	-22	(*-12*)
	Sum	47	(*-295*)	-1	(*+6*)	354	(*-167*)	-7	(*+3*)
Total efficiency loss				-25	(*-16*)			-31	(*-17*)
η_{CO2} [%]				75	(*84*)			69	(*82*)

[a] Process conditions: d < 38 µm, T = 200 °C, and p_{CO2} = 20 bar (ζ_{CaSiO3} = 69% (wollastonite) and 67% (steel slag)). Standard calculations were performed at L/S = 5 kg/kg, and alternative calculations shown between brackets were performed at L/S = 2 kg/kg. [b] CO_2 sequestration efficiency loss.

5.3.2 Steel Slag

Figure 5.4 shows the carbonation degree of steel slag in dependence of the reactor temperature, CO$_2$ pressure, and particle size on the basis of data presented earlier (Chapter 2). In addition, the corresponding calculated CO$_2$ sequestration efficiencies are shown. The carbonation mechanisms of steel slag have been reported to be similar to those of wollastonite (Chapter 4). Therefore, the influence of the three process variables on the carbonation degree and the CO$_2$ sequestration efficiency of both Ca-silicate feedstocks are generally similar. However, the differences in sequestration efficiency are smaller in the case of steel slag (Figures 5.3 & 5.4) as a result of the smaller differences in conversion due to its relatively rapid carbonation at mild process conditions (Chapter 4). The limited set of data shown in Figure 5.4 suggests that, similarly to wollastonite, the energetically optimum reactor temperature is 200 °C. In addition, the optimum particle size also seems to be smaller than the minimum particle size of <38 µm at which carbonation experiments were performed. However, the optimum CO$_2$ pressure seems to be lower than in the case of wollastonite, but this difference might be due to the lower temperature at which the measurements were performed (see also Figure 5.3).

The set of conversion data reported earlier for aqueous steel slag carbonation (Chapter 2) is too limited to determine a representative maximum CO$_2$ sequestration efficiency for this feedstock. In addition, the steel slag carbonation experiments were conducted at other sets of process conditions (particularly, reaction time and liquid-to-solid ratio) than the wollastonite carbonation experiments, which hinders the direct comparison of both feedstocks. An additional carbonation experiment with steel slag (batch S1) at the energetically optimum process conditions of wollastonite (d < 38 µm, T = 200 °C, p_{CO2} = 20 bar, L/S = 5 kg/kg, n = 500 rpm, and t = 15 min) resulted in ζ_{CaSiO3} = 67% and η_{CO2} = 69%. The stream properties at these process conditions are shown in Figure 5.2 and the corresponding heat and power streams are shown in Table 5.4. At these process conditions, the energetic efficiency in the case of steel slag is significantly lower than that in the case of wollastonite. As Table 5.4 shows, this difference is particularly caused by a more negative overall reactor heat ($\Delta\eta_{CO2}$ = -7 vs. -1%, for steel slag and wollastonite, respectively). Given that the conversions obtained for both feedstocks are similar, this effect is caused by the lower Ca content of the steel slag feedstock (i.e., 23 wt% (Chapter 2) vs. 30 wt% (Chapter 4)), which results in a larger amount of slurry that has to be heated to the reactor temperature (L/S-ratio is kept constant).
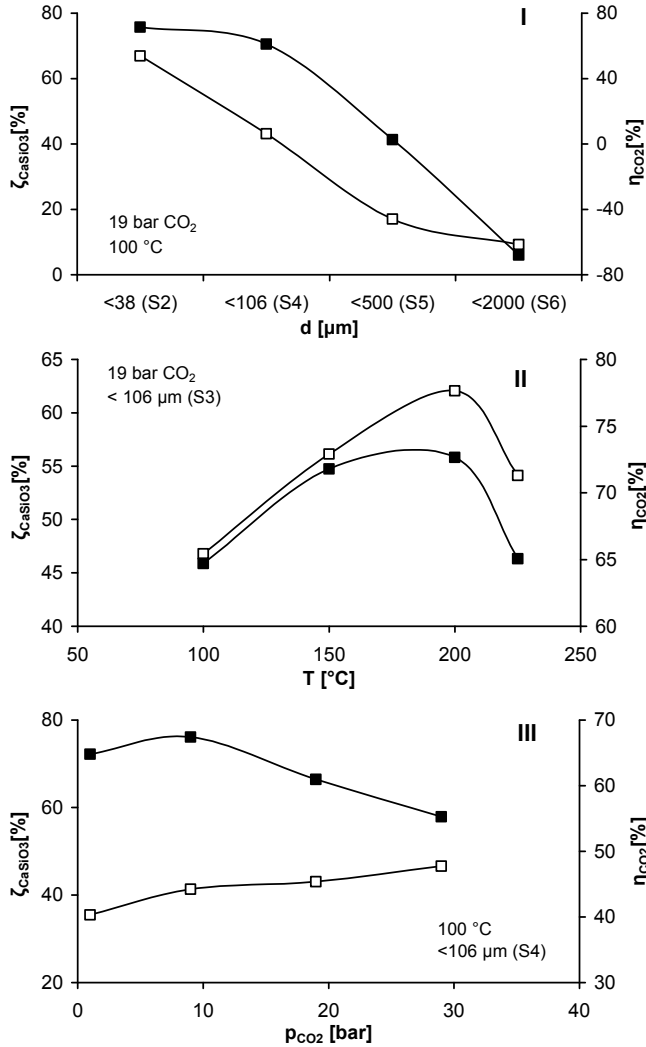
Figure 5.4: *Measured carbonation degree (ζ_{CaSiO3}) (Chapter 2) (open symbols) and the corresponding calculated CO_2 sequestration efficiency (η_{CO2}) (solid symbols) as a function of various process variables for steel slag. Simulations were performed at L/S = 5 kg/kg. Conversion measurements in lab-scale autoclave reactor were performed at t = 30 min, n = 500 (I) / 1000 (II & III) rpm, and L/S = 10 kg/kg. (I) Particle size; (II) reactor temperature; and (III) CO_2 pressure.*

It should be noted that the energetic efficiency of steel slag carbonation at the energetically optimum process conditions found for wollastonite (i.e., 69%) is not the maximum efficiency calculated for steel slag. The maximum efficiency at <38 µm in Figure 5.4.I is 72% and that at 200 °C in Figure 5.4.II is even 73%. However, these values are based on carbonation degrees measured at a reaction

time of 30 min instead of 15 min. A longer reaction time increases the conversion (Chapter 2), while it has no direct effect on the energy consumption of the process, as taken into account in the current assessment. Therefore, a longer reaction time directly improves the energetic efficiency. The optimum energetic efficiency of steel slag carbonation can only be determined on the basis of a more extensive set of carbonation experiments that fully takes into account the relatively rapid carbonation of this feedstock at mild process conditions (Chapter 4).

5.3.3 Sensitivity Analysis

Figure 5.5 shows the outcome of the sensitivity analysis on the CO$_2$ sequestration efficiency of wollastonite carbonation at energetically optimum reactor conditions.
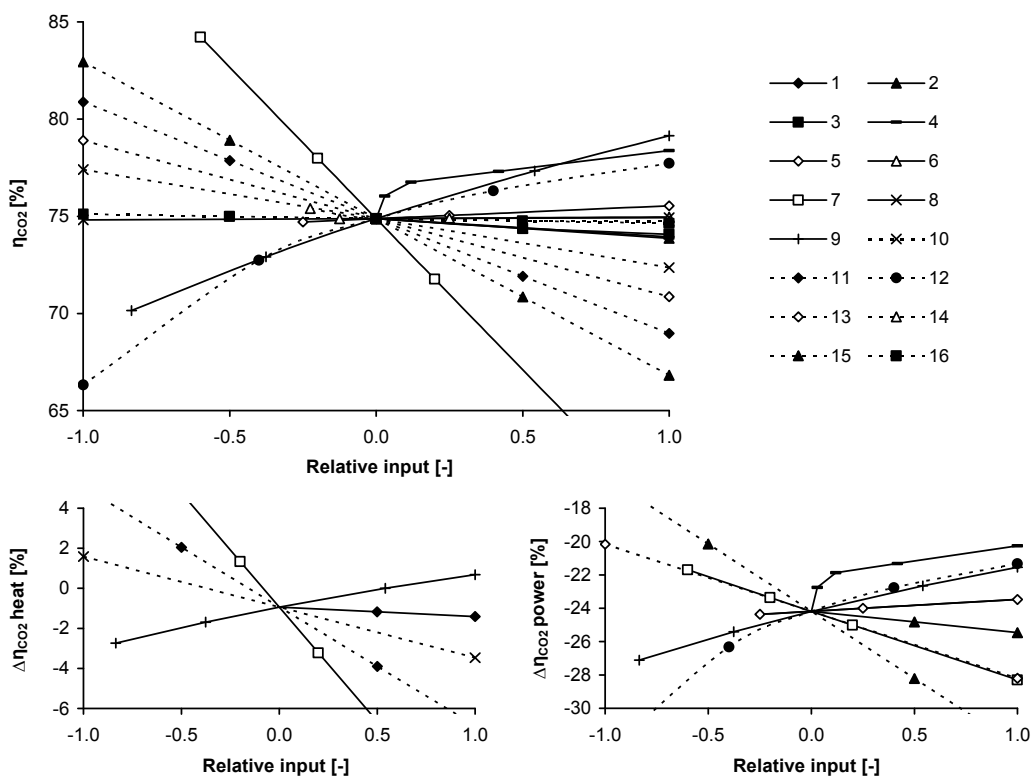
Figure 5.5: *Sensitivity analysis of CO$_2$ sequestration efficiency (η_{CO2}) by wollastonite carbonation for the parameters shown in the table (next page) at energetically maximum reactor conditions (ζ_{CaSiO3} = 69%, T = 200 °C, p$_{CO2}$ = 20 bar, d < 38 μm (batch W1)) and L/S = 5 kg/kg. In the graphs at the right, the energetic efficiency loss ($\Delta\eta_{CO2}$) due to the heat and power consumption is shown for a selection of parameters.*

#	Variable	Standard	Min	Max
1	Purge factor CO_2 [-]	0 (0)[a]	0 (0)	1 (1)
2	Purge factor H_2O [-]	0 (0)	0 (0)	1 (1)
3	Temperature H_2O recycle [°C][b]	40 (0)	40 (0)	80 (1)[c]
4	Pressure H_2O recycle [bar]	1 (0)	1 (0)	34.5 (1)[d]
5	Pressure drop reactor [bar]	1 (0)	0 (-0.25)	5 (1)
6	Excess gaseous CO_2 supply reactor [%]	10 (0)	5 (-0.13)	50 (1)
7	L/S-ratio reactor feed [kg/kg][e]	5 (0)	2 (-0.6)	10 (1)
8	Filter; solid content filter cake [kg/kg]	0.85 (0)	0.7 (-1)	1.0 (1)
9	Carbonation degree (ζ_{CaSiO3}) [%]	69 (0)	60 (-0.83)	80 (1)
10	Heat of reaction (ΔH_r) [kJ/mol]	84 (0)[f]	64 (-1)	104 (1)
11	$\Delta T_{heat-exchanger}$ [°C]	20 (0)[g]	10 (-1)	30 (1)
12	Ore grade [%]	50 (0)	25 (-1)	75 (1)
13	Bond's working index [kWh/ton]	14 (0)	10 (-1)	18 (1)
14	Initial particle size feedstock [m]	0.1 (0)	0.01 (-0.2)	0.5 (1)
15	ε_{power} [kg/kWh][h]	0.60 (0)	0.40 (-1)	0.80 (1)
16	ε_{heat} [kg/kWh]	0.20 (0)	0.15 (-1)	0.25 (1)

[a] Numbers between brackets are the relative input values used for the graphs. [b] For these simulations, the ASPEN flowsheet was extended with a cooler, which cools the 'CO$_2$ REC 2' stream to 40 °C in order to avoid an increase of the gas volume that compressor 1 has to compress. [c] In principle, the maximum temperature of the H_2O recycle is $T_{reactor}$. However, this value could not be simulated because the process water is recycled at atmospheric pressure. [d] Maximum pressure = $p_{reactor}$ - pressure drop over reactor. [e] In the sensitivity analysis the possible effect of the L/S-ratio on the conversion has been neglected. For wollastonite, a limited effect of the L/S-ratio was reported earlier (Chapter 4). For steel slag, a reduction of the L/S-ratio seems to slightly increase the conversion measured at lab-scale (Chapter 2). [f] Heat of reaction as determined by ASPEN. [g] Temperature difference at the hot side of the heat exchanger. At the cold side of the heat exchanger the ΔT is slightly larger (e.g., 25 vs. 20 °C), since the reactor outlet slurry has a larger heat capacity than the reactor inlet slurry due to the presence of dissolved CO_2. [h] Representative values for a natural gas combined cycle and a powder coal power plant are 0.36 and 0.80 kg CO_2/kWh, respectively (Rubin et al., 2004).

Figure 5.5: *Continued.*

Most variables have a relatively small influence on the sequestration efficiency within the ranges studied (<1.5%). Eight variables have a relatively large influence on the energetic efficiency: the liquid-to-solid ratio, the specific CO_2 emission associated with power consumption, the temperature difference at the hot side of the heat exchanger, the carbonation degree, the pressure of the water recycle, the Bond's working index, the ore grade, and the reaction heat assumed. Some of these factors will be discussed in more detail below.

Heat Exchanger Performance. The heat integration of the mineral carbonation process (particularly, the performance of the heat exchanger) has a large influence on the CO$_2$ sequestration efficiency, since the amount of heat both exchanged in the heat exchanger and cooled away in the cooler of the water recycle is large. At the energetically optimum reactor conditions and under the assumptions made, the heat generated by the carbonation reaction is smaller than the amount of heat required to heat up the reactants (Table 5.4). The energy required to heat the reactor feed directly depends on the temperature difference assumed to be required for (cost-efficient) heat exchange between the reactor outlet and inlet slurries within the heat exchanger. For example, assuming a minimally feasible temperature difference in the heat exchanger of 10 °C, the CO$_2$ sequestration efficiency would increase to 81% and the process would generate a net surplus of reaction heat (253 kWh/ton CO$_2$ sequestered) (for steel slag, 101 kWh/ton CO$_2$ sequestered and η_{CO2} = 78% at $\Delta T_{\text{heat-exchanger}}$ = 10 °C). However, by reducing the driving force for heat exchange, the surface area required and, thereby, the investment costs of the heat exchanger would increase. Therefore, the optimum temperature difference can only be determined economically.

Liquid-to-Solid Ratio. A reduction of the L/S-ratio leads to a substantial improvement of the heat balance of the process and, thus, the CO$_2$ sequestration efficiency (Figure 5.5 & Table 5.4). First, the energy required to pump and heat up the slurry is reduced. Second, less CO$_2$ has to be compressed by compressor 1 since less CO$_2$ dissolves into the slurry. Other possible energetic benefits, not taken into account in the present study, are a smaller reactor that has to be heated to the reactor temperature and the production of 'less-diluted' heat by the exothermic carbonation reaction. Therefore, the aqueous mineral carbonation process should, in principle, be designed at the minimum feasible L/S-ratio. However, if the L/S-ratio becomes too low, pumping and stirring problems might arise because of an increased viscosity, which would result in a large decrease of the conversion (Chapters 2 & 4). The minimum feasible L/S-ratio depends on the final reactor and process design. The minimum L/S-ratio that could be stirred adequately in the lab-scale autoclave reactor used for the carbonation experiments is 2 kg/kg (Chapter 2). Reduction of the L/S-ratio from 5 to 2 kg/kg (solids content of the reactor = 17 and 33wt%, respectively) would increase the CO$_2$ sequestration efficiency by wollastonite carbonation to 84% (steel slag: η_{CO2} = 83% at L/S = 2 kg/kg). Table 5.4 shows that, at L/S = 2 kg/kg, the process has a net surplus of reaction heat for both feedstocks. A dedicated industrial process might be operated at even lower L/S-ratios down to 1 kg/kg, which may further improve the CO$_2$ sequestration efficiency of the process. Further experimental research in a continuous pilot-

scale reactor is recommended to study the carbonation degree as a function of the L/S-ratio and, thus, to determine the minimally feasible L/S-ratio.

Water Recycle (Temperature and Pressure). The temperature of the water recycle has a remarkably small effect on the energetic efficiency of the process (Figure 5.5). The heat consumption of the heater is largely independent of the temperature of the water recycle because of the performance of the heat exchanger. However, it should be noted that, in the mineral carbonation process in Figure 5.2, the heat duty of the heat exchanger is very large (e.g., 3971 and 1690 kWh/ton CO_2 sequestered at L/S = 5 and 2 kg/kg, respectively, for wollastonite), Thus, the investment costs for the heat exchanger may be substantial. Therefore, an increase of the water recycle temperature may be considered from an economic point of view.

In contrast to its temperature, the pressure of the water recycle does have a significant effect on the energetic sequestration efficiency. The water recycle is depressurized to 1 atm in order to enable filtration at atmospheric conditions and facilitate the addition of fresh feedstock to the slurry. By recycling the water at a higher pressure, less energy is required for pumping the slurry. In addition, less CO_2 in the 'CO$_2$ REC 2' stream has to be (re)compressed, since less CO_2 is released from the slurry upon depressurization. A relatively limited increase of the water recycle pressure to 2 bar has the largest effect on the CO_2 sequestration efficiency without causing extra costs for high-pressure equipment.

Carbonation Reaction (Carbonation Degree and Reaction Heat). Obviously, the CO_2 sequestration efficiency depends strongly on the carbonation degree and, thereby, on the assumption that the conversion in the large-scale continuous reactor equals the conversion obtained in a lab-scale autoclave reactor (§5.2.3). At least two effects can be distinguished, which might cause a difference between these conversions.

First, the reactor type might affect the reaction rate because of physical effects (e.g., abrasion and mixing intensity). An increase of the carbonation degree of particularly coarse particles has been reported for Mg-silicates in a pilot-scale flow-loop reactor, compared to a laboratory autoclave reactor, probably because of intensified mixing and removal of the carbonation rate-limiting SiO_2-rim (O'Connor et al., 2005).

Second, the carbonation degree might be influenced by the recycling of the process water. Preliminary experiments with regard to the effect of process water recycling on the carbonation of wollastonite and steel slag seem to suggest that the carbonation degree increases slightly because of process water recycling (Annex 5.1), possibly because of an increase of the ionic strength

(Chapter 2). Given the major effect of the carbonation degree on the CO$_2$ sequestration efficiency, research on further enhancement of the carbonation process, while not decreasing the energetic efficiency, is warranted (see also §5.3.1).

In addition to the carbonation degree, the reaction heat assumed has a significant influence on the energetic efficiency (e.g., for steel slag, η_{CO2} = 66 and 72% at ΔH_r = -64 and -104 kJ/mol, respectively). Since both the composition and the occurring carbonation reactions have been simplified in the case of steel slag (see §5.2.1), further study to improve this input for the steel slag simulations, and thereby to increase the accuracy of the calculated CO$_2$ sequestration efficiencies, seems warranted. The carbonation of, for example, portlandite (Ca(OH)$_2$) (ΔH_r = -68 kJ/mol (Lackner et al., 1995)) present in fresh steel slag (Chapter 2) might cause the actual reaction heat to differ from the assumed one (ΔH_r = -84 kJ/mol), which would then also change the energetic efficiency.

Grinding (Bond's Working Index and Ore Grade). Given the dominant effect of the energy consumption for grinding on the CO$_2$ sequestration efficiency (Table 5.4), the Bond's working index and ore grade are major influential parameters. Therefore, these parameters should be verified by measurements to enable further improvement of the sequestration efficiency calculations.

5.3.4 Discussion

In the Supporting Information, a comparison of energetic efficiencies reported in this and other mineral carbonation studies is given. From the results of the other system study on aqueous mineral carbonation (O'Connor et al., 2005), a CO$_2$ sequestration efficiency for aqueous wollastonite carbonation of 82% can be deduced. It is difficult to directly compare the results of this study by the Albany Research Centre (ARC) with the present study because of the large number of different assumptions made in the assessment of the energetic efficiency (Nilsen & Penner, 2001; O'Connor et al., 2005). At a specific CO$_2$ emission of 0.85 kg CO$_2$/kWh for a powder coal power plant and L/S = 2.33 kg/kg as used in the ARC study (O'Connor et al., 2005), our model resulted in a slightly lower CO$_2$ sequestration efficiency of 75%. This difference is particularly caused by the recycling of non-converted solid feedstock as applied in the ARC study (Nilsen & Penner, 2001; O'Connor et al., 2005). The possible separation and recycling of non-converted feedstock present in the reactor outlet might cause a substantial increase of the CO$_2$ sequestration efficiency. However, the feasibility of continuous large-scale separation of non-carbonated and carbonated Ca-silicate

particles is presently unclear (see discussion in Chapter 4). Further research on this subject is warranted.

In determining the CO_2 sequestration efficiency of the entire sequestration process (Figure 5.1), it should be kept in mind that, in system studies on CO_2 capture technologies, compression is typically (already) included, since CO_2 has to be compressed for transportation (typically, p > 80 bar) (IPCC, 2005). The maximum CO_2 sequestration efficiency of the aqueous wollastonite carbonation process, without the energy consumption due to compression of the CO_2 feed, is 82 and 90% at L/S = 5 and 2 kg/kg, respectively (steel slag: η_{CO2} = 73 and 87%, respectively). In addition, the lower CO_2 pressure required for the aqueous carbonation of Ca-silicates, compared to other CO_2 storage options, such as storage in depleted gas fields, as well as Mg-silicate carbonation processes (both, typically, p > 100 bar (IPCC, 2005; O'Connor et al., 2005)), may give an energetic benefit that should be taken into account when comparing different CO_2 storage technologies.

Overall, application of the process conditions used for lab-scale carbonation experiments would lead to a mineral carbonation process that would consume a substantial amount of extra energy ($\Delta\eta_{CO2} \approx$ 25-30%). However, the CO_2 sequestration efficiency of aqueous Ca-silicate carbonation might substantially improve if the options that are identified in this study could be implemented. Therefore, pilot-scale research on mineral carbonation is recommended to determine the feasibility of the suggested reduction of the L/S-ratio, and to verify the energetic efficiency calculations with respect to the carbonation degree. In addition, a cost evaluation study on CO_2 sequestration by aqueous mineral carbonation is required for final optimization of the process conditions (including reaction time) and the heat integration of the process. Final assessments of the energetic feasibility of CO_2 sequestration by mineral carbonation should be made for specific locations (particularly, with respect to ε_{power}) and should include the energy consumption of (possible) CO_2 capture, mining, and transportation.

5.4   Conclusions

Increasing the carbonation rate of wollastonite or steel slag by either grinding the feedstock, elevating the reaction temperature, or increasing the CO_2 partial pressure was shown to also improve the energetic CO_2 sequestration efficiency. Within the ranges of process conditions studied, energetic optima were found between the carbonation degree and the associated extra energy consumption, for both the temperature and the CO_2 pressure. The maximum CO_2

sequestration efficiency for wollastonite at a liquid-to-solid ratio of 5 kg/kg and a reaction time of 15 min was 75% at 200 °C, 20 bar CO$_2$, and a particle size of <38 μm. The grinding of the feedstock ($\Delta\eta_{CO2}$ = -15%) and the compression of the carbon dioxide (-7%) were identified as the main energy-consuming process steps. At these process conditions, a significantly lower CO$_2$ sequestration efficiency was found for steel slag, 69%, mainly due to the lower Ca content of the feedstock. Further grinding (particularly, wollastonite) or reducing the CO$_2$ partial pressure (steel slag) can potentially improve the CO$_2$ sequestration efficiency. In addition, a sensitivity analysis has shown that the CO$_2$ sequestration efficiency may be increased substantially by, e.g., improving the heat integration of the process and reducing the amount of process water applied. The options that have been identified to improve the energetic efficiency warrant a further assessment of the (energetic) feasibility of CO$_2$ sequestration by aqueous mineral carbonation on the basis of a pilot-scale process.

Annex 5.1   Supporting Information[1]

A.5.1.1 Purge Fraction of Process Water Recycling

The feasible purge fraction for the H_2O recycle primarily depends on the amount of impurities leached from the solids. In two series of experiments, the effect of process water recycling on the carbonation degree and the composition of the process water was studied for both wollastonite and steel slag. First, a carbonation experiment was executed in Nanopure-demineralised water. In each subsequent experiment, carbonation was performed in a mixture containing 50% Nanopure-demineralised water and 50% process water resulting from the previous experiment. Four subsequent carbonation experiments were performed, corresponding with a H_2O recycle purge factor of 1 - 0.125. The composition of the process water resulting from each carbonation experiment was determined by ICP-AES and ion-chromatography (IC).

Figure A.5.1.1 shows that leached concentrations of groups of elements are affected differently by recycling. Leached concentrations of mobile elements such as Na, Cl, and S simply accumulate due to recycling, since these elements do not reach solubility limits. For steel slag, elements that show reduced leaching after carbonation (Chapter 3) also show a decreasing concentration profile upon recycling of the process water (e.g., Ca and Ba). Analogously, the concentration of elements that show increased leaching after carbonation (Chapter 3), such as V, increases. The leaching of the vast majority of elements does not seem to affect the feasibility of water recycling. However, for steel slag elements such as Cl, S, and V might hinder process water recycling by extra costs for, e.g. corrosion protection and/or wastewater treatment. Further study of this issue by continuous mineral carbonation experiments on pilot-scale seems warranted.

---

[1] Available at Industrial & Engineering Chemistry Research website, http://pubs.acs.org.
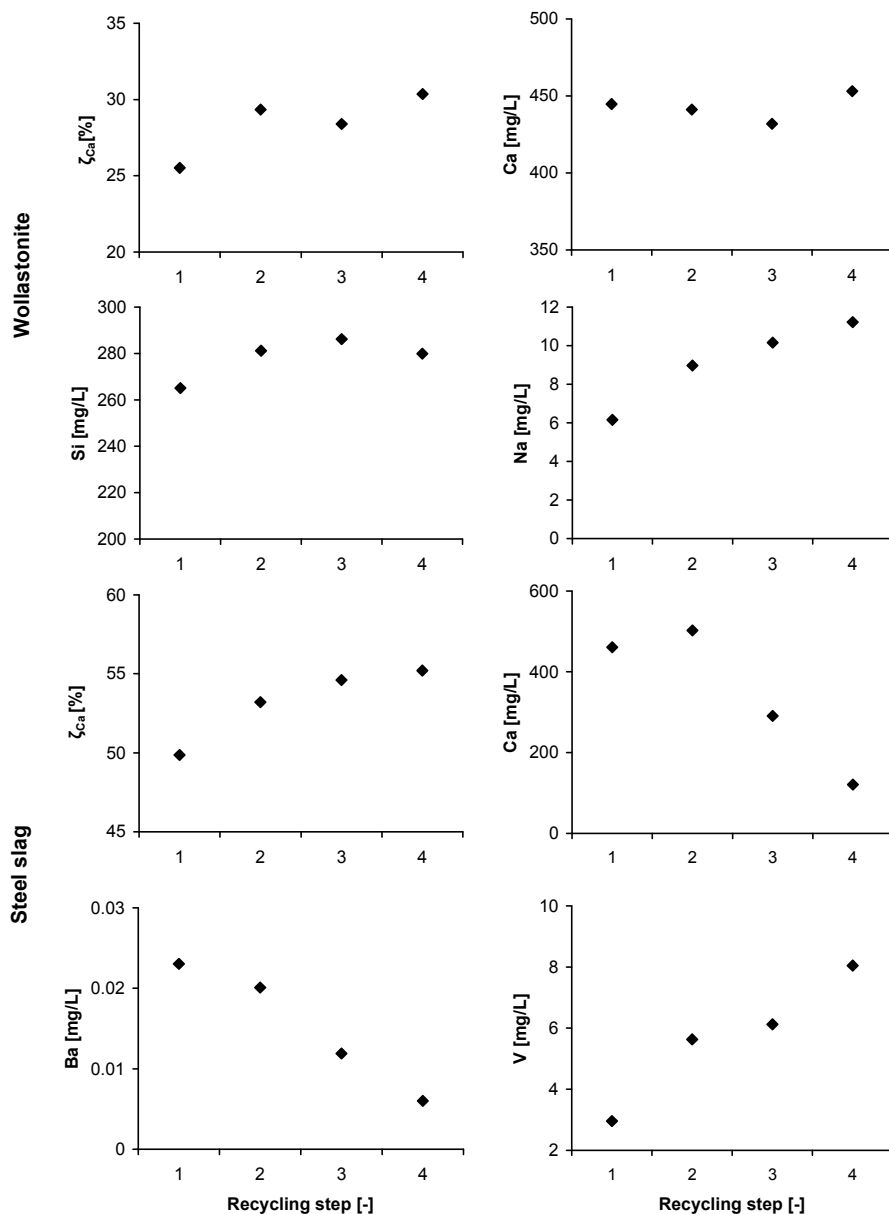
Figure A.5.1.1: *Effect of process water recycling on the Ca carbonation degree in a lab-scale autoclave reactor (ζ$_{Ca}$) and the leaching of selected elements. Experimental reactor conditions: d < 106 μm (batches W2 and S3), T = 100 °C, p$_{CO2}$ = 10 bar (S3) or 20 bar (W2), n = 500 rpm, t = 15 min, and L/S = 5 kg/kg (W2) or 10 kg/kg (S3). The absolute standard deviation determined for the carbonation degree of steel slag is 5% conversion (Chapter 2).*

A.5.1.2 CO$_2$ Loss

The definition for the CO$_2$ sequestration efficiency (eq 5.2) used in this study does not take into account the CO$_2$ loss in the process. This loss might influence the energetic efficiency of the entire CO$_2$ sequestration process since a larger amount of CO$_2$ has to be captured. The CO$_2$ loss consists of CO$_2$ that is purged and CO$_2$ that is entrained with the H$_2$O purge and the product stream. The actual purge fractions are unknown at the current stage of process development, although these fractions will probably be small (see also above). In the simulations presented, the CO$_2$ loss only consist of CO$_2$ lost through the product stream and this loss is negligible (e.g., for wollastonite carbonation at energetically optimum reactor conditions, 98.8% of the CO$_2$ feed is sequestered).

A.5.1.3 Comparison to Other Process Studies and Feedstock

Table A.5.1.1 shows reported CO$_2$ sequestration efficiencies (η_{CO2}) for different types of mineral carbonation processes and feedstock. The efficiencies reported are generally similar in magnitude. With regard to the indirect process routes, it should be noted that the energy consumption caused by the recycling of the extraction agent may be substantial and is not always included adequately in the assessments.

Because of the significance of the carbonation degree (see §5.3.3), or more precisely the amount of feedstock required per ton of CO$_2$ sequestered, the use of Mg-silicates as alternative feedstock for mineral carbonation might be considered. Both the molar weight of Mg and the typical Mg-content of Mg-ores make that, for example, potentially less olivine (Mg$_2$SiO$_4$) has to be processed relative to Ca-silicates. In addition, the amount of both wollastonite and steel slag is limited relative to the worldwide abundance of Mg-silicates. On the other hand, the process conditions required to substantially carbonate Ca-silicates are milder than those for Mg-silicates, which has resulted in a higher energetic CO$_2$ sequestration efficiency reported in an earlier study (O'Connor et al., 2005) for wollastonite than for olivine (Table A.5.1.1).

Table A.5.1.1: *Comparison of CO₂ sequestration efficiencies reported (excl. CO₂ capture).*

η_{CO2} [%]	Feedstock	Process route [a]	Extraction agent	Reference
82	wollastonite	direct	water	(O'Connor et al., 2005)
75	wollastonite	direct	water	this study
69	steel slag	direct	water	this study
72	olivine	direct	water [b]	(O'Connor et al., 2005)
82	serpentine	direct	water [b]	(O'Connor et al., 2005)
70 [c]	Mg-silicate	direct	molten MgCl₂	(IEA GHG, 2000)
80	waste cement	indirect	water	(Iizuka et al., 2004)
85 [d]	wollastonite	indirect	acetic acid	(Kakizawa et al., 2001)
<0	Mg-silicate	indirect	HCl	(IEA GHG, 2000)

[a] Direct route: Ca/Mg-extraction and carbonation take place in a single process step. Indirect route: Ca/Mg is first extracted and, subsequently, carbonated in a second process step. For more information on process routes and extraction agents, see Chapter 1. [b] Salts added: 0.64M NaHCO₃, 1M NaCl. [c] Without energy consumption for production of make-up MgCl₂. [d] Energy consumption associated with production and recycling of acetic acid is not taken into account.

CHAPTER 6

COST EVALUATION OF CO$_2$ SEQUESTRATION BY AQUEOUS MINERAL CARBONATION
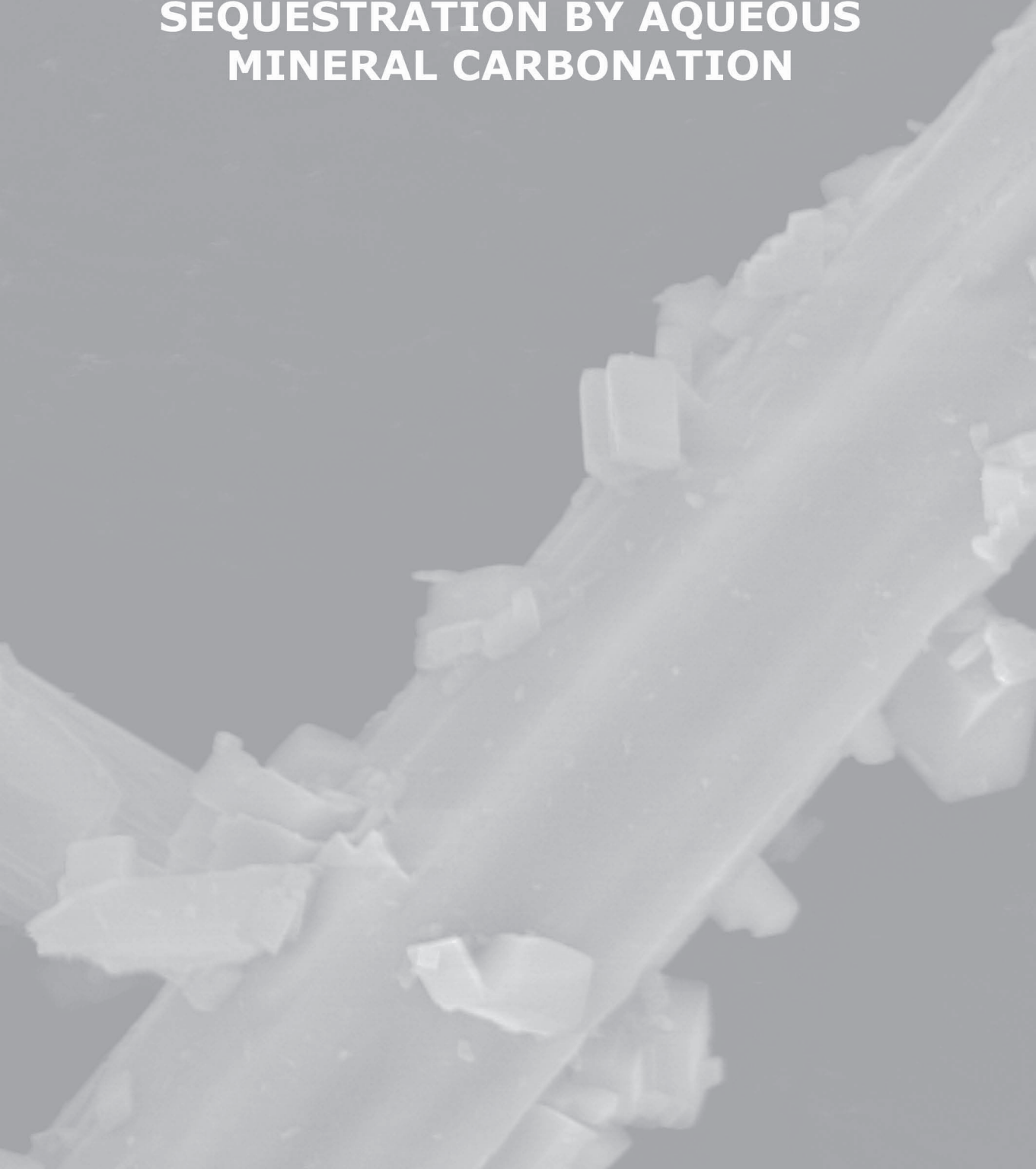
Submitted for possible publication in similar form to Energy Conversion and Management.

COST EVALUATION OF CO$_2$ SEQUESTRATION BY AQUEOUS MINERAL CARBONATION

Wouter J.J. Huijgen[1]*, Rob N.J. Comans*[1,2] *& Geert-Jan Witkamp*[3]

A cost evaluation of CO$_2$ sequestration by aqueous mineral carbonation has been made, using either wollastonite (CaSiO$_3$) or steel slag as feedstock. First, the process was simulated to determine the properties of streams as well as the power and heat consumption of the process equipment. Second, a basic design was made for the major process equipment and total investment costs were estimated with the help of publicly available literature and a factorial cost estimation method. Finally, the sequestration costs were determined on the basis of the depreciation of investments and variable and fixed operating costs. Estimated costs are 102 and 77 €/ton CO$_2$ net avoided for wollastonite and steel slag, respectively. For wollastonite, major costs are associated with the feedstock and the electricity consumption for grinding and compression (54 and 26 €/ton CO$_2$ avoided, respectively). A sensitivity analysis showed that additional influential parameters in the sequestration costs include the liquid-to-solid ratio in the carbonation reactor and the possible value of the carbonated product. The sequestration costs for steel slag are significantly lower due to the absence of costs for the feedstock. Although various options for potential cost reduction have been identified, CO$_2$ sequestration by current aqueous carbonation processes seems expensive relative to other CO$_2$ storage technologies. The permanent and inherently safe sequestration of CO$_2$ by mineral carbonation may justify higher costs, but further cost reductions are required, particularly in view of (current) prices of CO$_2$ emission rights. (Niche) applications of mineral carbonation with a solid residue such as steel slag as feedstock and/or a useful carbonated product hold the best prospects for an economically feasible CO$_2$ sequestration process.

---

[1] Energy Research Centre of The Netherlands.
[2] Wageningen University.
[3] Delft University of Technology.

6.1   Introduction

Carbon dioxide sequestration by mineral carbonation is a potentially attractive route to mitigate possible global warming on the basis of industrial imitation of natural weathering processes (Lackner et al., 1997; IPCC, 2005; Chapter 1). Potentially suitable feedstock for mineral carbonation include Ca- and Mg-silicate ores, such as wollastonite ($CaSiO_3$) and olivine (Mg_2SiO_4), and industrial residues such as steel slag and municipal solid waste incinerator bottom ash (Kojima et al., 1997; Stolaroff et al., 2004; Chapter 1). For example, the (overall) carbonation process for wollastonite can be given as:

$$CaSiO_3 \text{ (s)} + CO_2 \text{ (g)} \rightarrow CaCO_3 \text{ (s)} + SiO_2 \text{ (s)} \qquad \text{(eq 6.1)}$$
$$\Delta H_r = -87 \text{ kJ/mol \& } \Delta G_r = -44 \text{ kJ/mol (Lackner et al., 1995)}$$
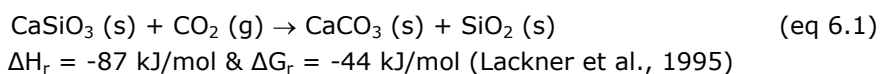
Benefits compared to other CO_2 capture and storage (CCS) technologies (e.g., storage in depleted gas fields and oceans) include the permanent and inherently safe character of the CO_2 sequestration and its potentially vast storage capacity (IPCC, 2005; Chapter 1). However, weathering processes are slow at natural conditions, and, therefore, various approaches have been studied to increase the mineral carbonation rate such that the process can be implemented industrially (IPCC, 2005; Chapter 1). One of the possible process routes reported is direct aqueous mineral carbonation, in which carbonation takes place in a single process step in an aqueous suspension. The presence of water is known to accelerate the carbonation reaction (Chapter 1). In Chapters 2 & 4, we have experimentally studied the aqueous carbonation of the Ca-silicates steel slag and wollastonite in a lab-scale autoclave reactor in dependence of the major process conditions, i.e., reactor temperature (T), partial CO_2 pressure (p_{CO2}), reaction time (t), particle size of the feedstock (d), liquid-to-solid ratio (L/S), and stirring rate (n). It has been shown that these Ca-silicates can be carbonated substantially within industrially realistic reaction times (≤30 min) by finely grinding the feedstock (typically, <38 µm) and moderately elevating the reactor temperature (150-200 °C) and CO_2 pressure (10-40 bar) (Chapters 2 & 4). The potentially costly use of additives and a CO_2 pressure over 100 bar, as typically applied to enhance the carbonation of Mg-silicates (O'Connor et al., 2005), was found not to be required for Ca-silicates (Chapter 4).

Although CO_2 sequestration by aqueous carbonation of Ca-silicates seems technically feasible, the grinding, heating, and compression required to increase the carbonation rate cause an energy penalty and increase the sequestration costs. The energy penalty reduces the net fraction of CO_2 sequestered due to

the power and heat consumption of the mineral carbonation process. The energetic sequestration efficiency (η_{CO2}) is defined as:

$$\eta_{CO2} = \frac{CO_{2,avoided}}{CO_{2,sequestered}} = \frac{CO_{2,sequestered} - \left(CO_{2,power} + CO_{2,heat}\right)}{CO_{2,sequestered}} \quad \text{(eq 6.2)}$$

with the amount of CO_2 sequestered in the process ($CO_{2,sequestered}$), the net amount of CO_2 avoided ($CO_{2,avoided}$), and the extra CO_2 emissions due to heat ($CO_{2,heat}$) and power consumption ($CO_{2,power}$). In Chapter 5, optimum energetic CO_2 sequestration efficiencies of 83 and 84% have been reported for aqueous carbonation of both steel slag and wollastonite (T = 200 °C, p_{CO2} = 20 bar, d < 38 µm, and assuming a reduced liquid-to-solid ratio of 2 kg/kg). Taking into account the various possibilities identified to potentially further increase the CO_2 sequestration efficiency, it was concluded that aqueous mineral carbonation of Ca-silicates is potentially energetically feasible (Chapter 5). However, an economic assessment of mineral carbonation is required for final evaluation of the feasibility of this CO_2 sequestration technology.

Various (preliminary) studies on the sequestration costs of mineral carbonation processes have been published (e.g., IEA GHG, 2000; Kakizawa et al., 2001; Iizuka et al., 2004; O'Connor et al., 2005; Teir et al., 2005). To the best of our knowledge, only one previous cost evaluation of the aqueous mineral carbonation process has been published in the open literature (O'Connor et al., 2005). In that study, sequestration costs of 93 €/ton CO_2 avoided were reported for wollastonite (conversion rate: 1.2 $ = 1 €) (O'Connor et al., 2005). These costs seem substantially higher than other possible technologies for carbon capture and storage (e.g., costs of geological are storage typically 0.5-7 €/ton CO_2 injected (IPCC, 2005)). Unfortunately, the sequestration costs reported for aqueous wollastonite carbonation were estimated on the basis of a carbonation process designed for olivine (O'Connor et al., 2005). A system study on a dedicated wollastonite carbonation process, fully taking into account its relatively mild process conditions (Chapter 4), is required to obtain a better insight in the cost breakdown of CO_2 sequestration by wollastonite carbonation. Moreover, industrial residues were not considered as a possible feedstock in the previous study (O'Connor et al., 2005), while these materials potentially offer a cost benefit compared to ores, since mining and transportation are no longer required because of their availability in industrial areas near CO_2 sources.

The aim of the present paper is an assessment of CO_2 sequestration costs by aqueous Ca-silicate carbonation. For both wollastonite and steel slag as feedstock, a basic design of an aqueous mineral carbonation process will be

made to estimate the investment and depreciation costs. Subsequently, the remaining fixed costs (e.g., for labour and maintenance) and the variable costs (e.g., for feedstock and electricity consumption) will be assessed to determine the CO_2 sequestration costs. Finally, a sensitivity analysis will be performed to investigate how the process conditions and the assumptions made affect the overall sequestration costs and to identify routes for cost reduction.

6.2   Materials and Methods

6.2.1   Mineral Carbonation Process

Figure 6.1 shows a block diagram of a CO_2 sequestration process on the basis of mineral carbonation together with the system boundaries of the present cost evaluation. The process was assumed to be located at the source of the solid feedstock and therefore no transport of Ca-silicates is required.

Within the system boundaries, a flowsheet of a mineral carbonation process was developed (Figure 6.2) for simulations with ASPEN Plus flowsheeting software (2005). The wollastonite carbonation process was designed to sequester all CO_2 emitted from a 100 MW power plant (i.e., 60,000 kg/h or 480 kton/yr CO_2 assuming a specific CO_2 emission of 0.60 kg/kWh, as used in Chapter 5, and an operational time of 8000 hr/yr). For steel slag, a significantly smaller carbonation process was designed in view of the relatively limited availability of steel slag; 15,000 kg/h or 120 kton/yr CO_2, consistent with the approximate amount of CO_2 that can potentially be sequestered in the steel slag produced in The Netherlands (Huijgen and Comans, 2005). Simulations of both the wollastonite and steel slag carbonation processes were performed using the methods and assumptions reported previously (Chapter 5). The conversions (ζ_{CaSiO3}) measured in a lab-scale autoclave reactor (Chapters 2 & 4) were used as input for the continuous carbonation reactor (see also Chapter 5). In addition, the process conditions corresponding with the maximum energetic efficiency found earlier were used (i.e., d < 38 μm, T = 200 °C, and p_{CO2} = 20 bar). The corresponding conversions (ζ_{CaSiO3}) are 69% and 67% for wollastonite and steel slag, respectively (Chapter 5). Finally, simulations were performed at L/S = 2 kg/kg, i.e., the minimum L/S-ratio that allowed adequate stirring of the suspension in the lab-scale autoclave reactor that was used for the carbonation experiments (Chapter 2)) (see also §6.3.1.3 and Chapter 5). The resulting composition and physical properties of the streams as well as the power and heat flows are given in Figure 6.2. At these conditions, the total power and heat consumptions in the case of wollastonite are 296 and -295 kWh/ton CO_2 sequestered, respectively (steel slag: 337 and -167 kWh/ton CO_2). The

corresponding energetic efficiencies (η_{CO2}) are 84 and 83% for wollastonite and steel slag, respectively (as indicated above; see Chapter 5 for further details).
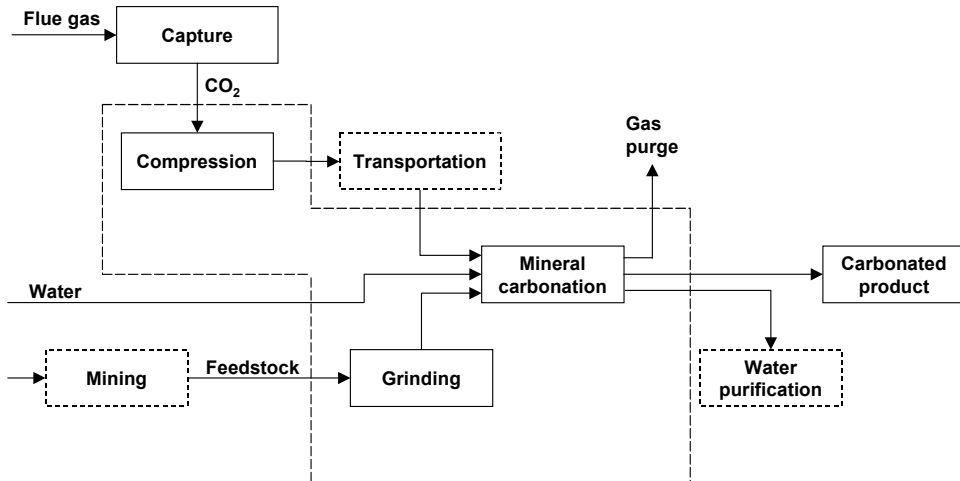
Figure 6.1: *Block diagram of a CO₂ sequestration process on the basis of mineral carbonation. System boundaries of the present study are indicated by the broken lines.*

Table 6.1: *Assumptions used for estimation of operating costs.*

Operating costs	Reference	
Variable		
Wollastonite	10 €/ton	
Steel slag	0 €/ton	
Water (softened)	0.35 €/m^3	(DACE, 2005)
Cooling water	0.05 €/m^3	(DACE, 2005)
Natural gas [a]	0.12 €/m^3	(DACE, 2005)
Electricity	0.06 €/kWh	(DACE, 2005)
Fixed		
Operating labour	300/yr k€/operator [b]	
Wollastonite	3 operators	
Steel slag	2 operators	
Plant overheads	50 % operating labour	(Sinnott, 1997)
Laboratory	20 % operating labour	(Sinnott, 1997)
Supervision	20 % operating labour	(Sinnott, 1997)
Maintenance	5 % fixed capital	(Sinnott, 1997)
Local taxes	1 % fixed capital	(Sinnott, 1997)
Insurance	1 % fixed capital	(Sinnott, 1997)

[a] Only applicable, if heat flow reactor (f in Figure 6.2) < heater (e). Not the case at energetically optimum conditions (Figure 6.2). [b] Assumed nominal wages operator: 30.000 €/yr. Full continuous operation = 5 shifts/day. Surcharge factor of 2 is used to include taxes and insurance.
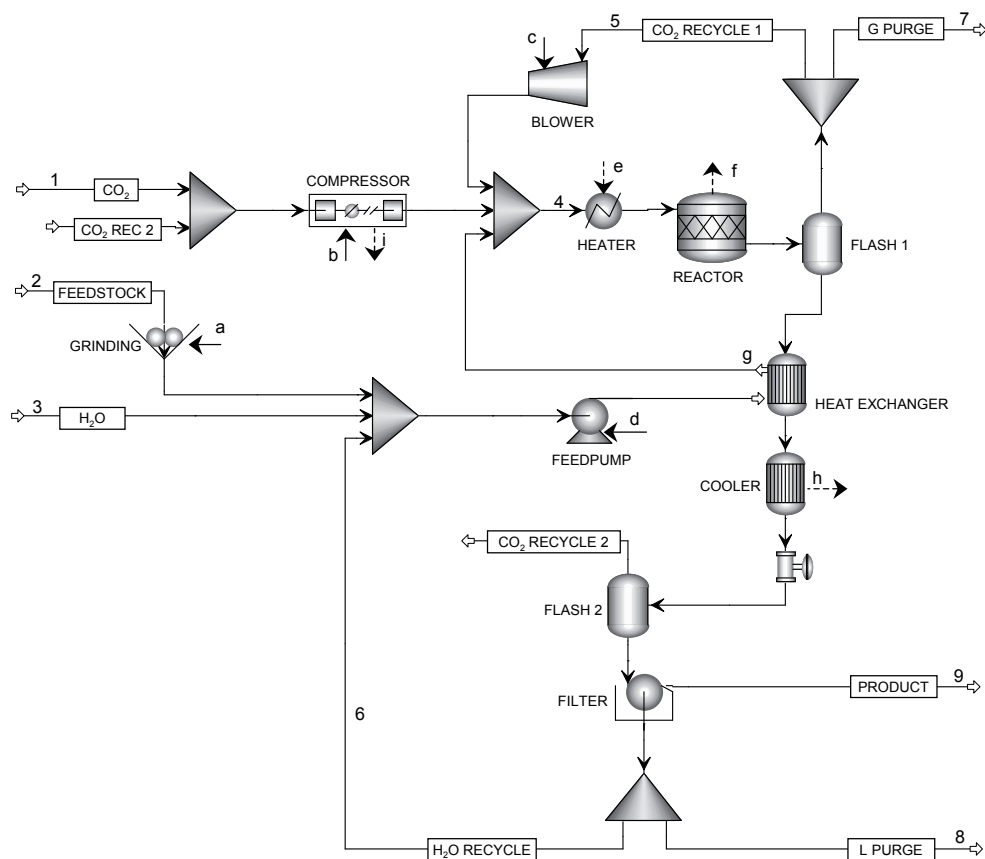
6.2.2 Cost Evaluation

On the basis of the simulated mineral carbonation process shown in Figure 6.2, the variable and fixed sequestration costs were estimated. Costs were calculated for an assumed new plant located in The Netherlands and constructed in the 3rd quarter of 2004 (i.e., corresponding with the major source used for price information (DACE, 2005)) All costs are given in the euro currency, using a conversion rate of 1.2 \$ = 1 € for prices given in dollars.

Investment Costs. The investment costs were estimated using a detailed factorial cost estimation method as described by Sinnott (1997). First, the price of each major unit operation in the mineral carbonation process (Figure 6.2) was calculated as follows:

Stream number		1	2	3	4	5	6	7	8	9
T [°C]	W	25	25	25	176	200	39	40	39	39
	S	25	25	25	178	200	39	40	39	39
p [bar]	W	1.0	1.0	1.0	35.5	34.5	1.0	1.0	1.0	1.0
	S	1.0	1.0	1.0	35.5	34.5	1.0	1.0	1.0	1.0
Mass flow [ton/h]										
$CaSiO_3$	W		229.2 [a]		229.2					70.8
	S		58.7		58.7					19.1
$CaCO_3$	W		4.9		4.9					141.3
	S		8.0		8.0					42.1
SiO_2	W		37.8		37.8					119.7
	S									20.5
FeO	W									
	S		36.7		36.7					36.7
H_2O	W			56.8	543.7	2.4	484.3			56.8
	S			20.3	206.8	0.6	215.3			20.3
CO_2	W	61.8			54.4	6.0	6.1			1.8
	S	15.6			23.0	1.5	2.6			0.6

Power & heat flows		a	b	c	d	f-e [b]	g [c]	h	i	
E [MW]	W	11.2	5.7	0.0	0.8	-17.7	101.5	-17.0	-3.8	
	S	1.9	1.6	0.0	0.3	-2.5	38.4	-6.1	-1.1	

[a] Excluding gangue. [b] Net reaction heat. [c] Amount of heat transferred within heat exchanger.

Figure 6.2: *Simplified ASPEN flow diagram of an aqueous mineral carbonation process, indicating heat streams (- -➤) and power input (⟶). The properties and composition of the mass streams and the power and heat flows at the points indicated are given in the table. Reactor conditions: d < 38 μm, T = 200 °C, p_{CO2} = 20 bar, and t = 15 min (wollastonite: ζ_{CaSiO3} = 69% and η_{CO2} = 84%; steel slag: ζ_{CaSiO3} = 67% and η_{CO2} = 83%). Simulations were performed at L/S = 2 kg/kg. W = wollastonite; S = steel slag.*

(1) A basic design of the unit operation was made to determine equipment type, main dimensions, and possibly wall thickness. Because of possible corrosion due to the presence of carbonic acid at low pH and of dissolved trace elements such as Cl, AISI 316 stainless steel was selected for the construction of all process equipment, except for the grinding equipment and the compressor. It was assumed that carbon steel was a suitable material of construction for the compressor.

(2) Reference equipment was selected for which price information was available in public literature (Peters and Timmerhaus, 1991; DACE, 2005). The size of the reference equipment was chosen as close as possible to the actual designed equipment size.

(3) The cost of the reference equipment was adjusted for the actual size of the equipment type using an apparatus-specific scale factor, which was calculated from the costs data available in the public literature (Table 6.3) (Peters and Timmerhaus, 1991; DACE, 2005).

(4) If required, the price of the scaled reference equipment was corrected for the operating pressure as well as the material of construction. On the basis of data presented in (Sinnott, 1997), a factor of 2 was assumed for conversion of prices specified for carbon steel equipment into stainless steel equipment (AISI 316). Prices given for equipment operating at atmospheric pressure were corrected by a factor of 1.6 in the case of an operating pressure around 35 bar. Possible corrections for time and location relevant for the price of the reference equipment were carried out with the 'chemical engineering plant cost index' (DACE, 2005).

After calculation of the costs for the major process equipment, these costs were first multiplied individually with specific factors to include direct associated costs (Table 6.2). Direct associated costs taken into account were equipment erection, instrumentation, piping, process buildings, storages, utilities, ancillary buildings, and site development costs. For each major unit operation, the sum of the costs for the equipment and the direct associated investments (the 'total physical equipment costs') was determined. Subsequently, these physical equipment costs were extended with the associated indirect costs (i.e., design & engineering costs, contractor's fee, and contingency) (Table 6.2). For all equipment except the grinding equipment, general numbers available in the literature for a fluid-solid plant were used (Sinnott, 1997) (Table 6.2). For the grinding equipment, the costs reported for the reference equipment already included a number of associated investments (Peters and Timmerhaus, 1991) and the surcharge factors were adjusted accordingly (Table 6.2). The direct physical equipment costs and the indirect associated investments were added up resulting in the 'total fixed capital costs' (Sinnott, 1997). Finally, 10% of the total fixed capital costs was reserved as working capital and the investment costs of the mineral carbonation plant were determined as the sum of the fixed and working capital (Sinnott, 1997).

Table 6.2: *Surcharge factors used for various equipment.*

Surcharges		Equipment [a]	
		General	*Grinding*
Direct associated investments [% equipment cost]	Equipment erection	45	0 [b]
	Instrumentation [c]	25	0 [b]
	Piping	45	20 [d]
	Process buildings	10	5 [d]
	Storages	20	10 [d]
	Utilities	45	20 [d]
	Ancillary buildings	20	10 [d]
	Site development	5	5
	Sum	*215*	*70*
Indirect associated investments [e] [% total physical equipment cost]	Design & engineering	25	10 [d]
	Contractor's fee	5	0 [b]
	Contingency	10	10
	Sum	*40*	*20*

[a] General numbers for fluid-solid plant (Sinnott, 1997). [b] Included in the reference equipment price (Peters and Timmerhaus, 1991). [c] Includes electrical costs. [d] Assumed to be partially included in the reference equipment price (Peters and Timmerhaus, 1991). [e] Consists of equipment cost and direct associated investment costs.

Sequestration Costs. The sequestration costs consisted of depreciation costs and variable and fixed operating costs. The depreciation costs were determined by linear depreciation of the total fixed capital costs over a period of 10 years. The variable operating costs consisted of costs for feedstock and utilities. Table 6.1 shows the relevant prices assumed. The price of wollastonite ore mined on a large scale is uncertain. For lump wollastonite, which is nowadays mined on a limited scale, a minimum commercial price of 42 €/ton has been reported (Teir et al., 2005). If wollastonite would be mined on a significantly larger scale, its price would probably decrease, but to what extent is uncertain. As a first estimate, 10 €/ton was used and the influence of a change in the wollastonite ore price on the sequestration costs was studied in a sensitivity analysis (§6.3.1.3). For steel slag, a price of 0 €/ton was assumed since it is generated as a residue during the production of steel. The utilities required for aqueous mineral carbonation were electricity for e.g. the crushers, compressors and pumps, (possibly) natural gas to heat the reactants and (cooling) water. In the calculations, the sales price of the carbonated product was set at 0 €/ton for both wollastonite and steel slag, since it is unclear if beneficial application of the product is feasible. Moreover, it was assumed that no costs were required for possible disposal of the carbonated product.

The fixed operating costs consisted of costs for operating labour, maintenance, plant overheads, laboratory, supervision, local taxes and insurance. The

assumptions used in determining the fixed operating costs are also shown in Table 6.1.

In order to determine the sequestration costs, the depreciation costs, and the variable and fixed operating costs were added up, resulting in the costs per ton CO_2 physically sequestered in the carbonation reactor. Subsequently, the sequestration costs were divided by the energetic CO_2 sequestration efficiency (eq 6.2) in order to convert the costs per ton of CO_2 sequestered into costs per ton of CO_2 net avoided.

Finally, the sensitivity analysis of the CO_2 sequestration costs comprised both the influence of the assumptions made as well as the effect of the major process parameters (i.e., temperature, pressure, particle size). The latter was done to verify that the economically optimum set of process conditions corresponds with the energetically optimum set (e.g., for wollastonite, 200 °C, 20 bar CO_2, <38 μm, Chapter 5), as implicitly assumed in §6.2.1.

6.3   Results and Discussion

6.3.1   Wollastonite

6.3.1.1 Investment Costs

Table 6.3 shows the calculation of the investment costs of the wollastonite carbonation process shown in Figure 6.2. The costs of the reference equipment selected for the major unit operations and possible scale and other correction factors used are specified. The total investment costs of the wollastonite carbonation plant are 45 M€ of which 41 M€ fixed capital. Total process equipment costs are 11 M€ of which the most expensive process equipments are the grinding equipment (3.1 M€), the compressor (2.5 M€), the reactor (2.2 M€), and the heat exchanger (2.0 M€). Among the grinding equipment, the fine grinding step in the ball mill is by far the most expensive grinding step (2.9 M€). The costs of the second compressor, the feed pump, and the flash tanks are negligible compared to the other investment costs.

Below, a short discussion on the selection, design, and cost estimation of each major unit operation is given.

Grinding Equipment. The grinding equipment is required to crush and grind 272 ton/h wollastonite ore (Figure 6.2) from an initial particle size of 0.1 m to <38 μm (D[4,3] = 16 μm) (Chapters 4 & 5). On the basis of the cost

information available (Peters and Timmerhaus, 1991) and the specifications of various grinding equipment (Walas, 1988), two types of reference grinding equipment were selected for the cost estimation of the mineral carbonation process: a cone crusher for initial size reduction, followed by a ball mill. Possible investment costs associated with the inpurity of the wollastonite ore (Chapter 5) have been neglected in this study.

Compressor, Blower, and Pump. In the flowsheet simulations, a multi-stage compressor was assumed for the compression of the CO_2 feed. Three stages were assumed to be required, on the basis of the ratio between the inlet- and outlet pressure (isentropic operation with an efficiency of 0.8) (Chapter 5). However, price information was only available for a single-stage (screw) compressor (DACE, 2005). Therefore, for cost estimation purposes, three of these single-stage compressors were assumed to be placed in series on a single axis and the whole was scaled to the gas volume that had to be compressed. One electro-motor was assumed to be sufficient to drive the axis.

The costs of the blower, used in the 'CO_2 recycle 1' to compensate for the pressure drop over the reactor (1 bar) (see Figure 6.2), were estimated by taking the costs of two blowers in series, with a pressure increase of 0.5 bar each (DACE, 2005) (Table 6.3).

The costs for the feed pump of the slurry was estimated on the basis of the costs of a (virtual) number of single-stage centrifugal fluid pumps in series. The (virtual) number of pumps in series was determined by the total pressure increase required and the pressure increase of a single centrifugal pump (i.e., 4.3 pumps, 34.5 bar, and 8 bar, respectively). Since the pumping of a slurry causes much higher costs for sealing and material of construction, compared to the pumping of a fluid, a correction factor of 4 was applied. The feed pumps were assumed to be driven by a single electro-motor.

Separation Equipment. Two types of separation equipment were used: flash tanks to separate gas streams from slurries and a filter to separate solids from the product slurry. The costs of the two flash tanks were estimated on the basis of the available prices for a cylindrical tank. A hold-up time of 10s was assumed to be sufficient for effective separation. The required wall thickness (d) was estimated with (Sinnott, 1997):

$$d = \frac{1.1 \times \dfrac{p}{10} \times D}{2f \times 1.1 \times \dfrac{p}{10}} \qquad \text{(eq 6.3)}$$

Table 6.3: *Determination of investment costs for wollastonite carbonation process. For steel*

| Flowsheet | Reference equipment from literature | | | | Flow-sheeting |
	Equipment type	Price [a] [k€]	Relevant size	Material	Relevant size
Compressor	Single-stage compressor	183	8800 m³/h	Steel	40353 (10966) m³/h
	Electro-motor	64	630 kW	NA [b]	5742 (1556) kW
	Sum				
Blower	Blower, 500 mbar	10 (7)	350 (70) m³/h	Steel	277 (69) m³/h
Feedpump	Single-stage centrifugal pump [d]	11	250 m³/h	AISI 316	724 (274) m³/h
	Electro-motor	10	132 kW		776 (296) kW
	Sum				
Flash tank 1	Cylindrical tank, 16 mm	20 (10)	5 (1) m³	Steel	3.3 (1.1) m³ [f]
Flash tank 2	Cylindrical tank, 3 mm	12 (8)	20 (5) m³	Steel	17.4 (6.7) m³ [f]
Filter	Rotating vacuum tumbler filter [g]	206	50 m²	AISI 316	141 (46) m² [h]
Heat exchanger	Shell and tube heat exchanger	342	1000 m²	AISI 316	4316 (1726) m²
Cooler	Shell and tube heat exchanger	252 (134)	700 (300) m²	AISI 316	695 (255) m²
Grinding equipment	Cone crusher	65	60 ton/h		272 (103) ton/h
	Ball mill	300	8 ton/h		272 (103) ton/h
	Sum				
Reactor	Stirred tank with jacket	138	30 m³	AISI 316	63-120 (49-105) m³
Sum Fixed capital Working capital Investment					

[a] All prices were obtained from the DACE price booklet (DACE, 2005), except for the grinding equipment (Peters and Timmerhaus, 1991). [b] Not applicable. [c] Material of construction. [d] 2900 rpm. [e] The pumping of a slurry imposes additional requirements for material of construction and sealings. [f] Hold-up = 10 s. [g] Although the filter is not operated at vacuum conditions, this is the only continuous filter for which price information was available in (DACE, 2005). [h] Estimated by ASPEN assuming a 1 bar pressure drop and a

with f = 120 N/mm² for stainless steel AISI 316, a safety margin of 1.1, the operating pressure (p) and a height-to-diameter (D) ratio of 2. Thus, a required wall thickness of 16 and 1 mm was determined for the flash tank in the reactor outlet and in the water recycle, respectively. The nearest wall thickness for which price information was available was 16 and 3 mm, respectively (DACE, 2005).

slag, deviating numbers are given between brackets.

Results Pressure [bar]	Number in series	Correction factors			Price [M€] Equipment	Surcharges Direct	Indirect
		Scale	Pressure	Other			
1-35.5	3	0.72			1.64 (0.64)		
NA	1	1.17			0.85 (0.18)		
					2.49 (0.83)	5.36 (1.78)	3.14 (1.04)
34.5-35.5	2	0.41		2 [c]	0.04 (0.03)	0.08 (0.06)	0.05 (0.04)
1-35.5	4.3	0.14		4 [e]	0.21 (0.19)		
NA	1	1.00			0.06 (0.02)		
					0.27 (0.21)	0.57 (0.44)	0.34 (0.26)
34.5	1	0.41		2 [c]	0.03 (0.02)	0.07 (0.05)	0.04 (0.03)
1	1	0.37		2 [c]	0.02 (0.02)	0.05 (0.04)	0.03 (0.02)
1	1	0.66	1 [i]		0.41 (0.19)	0.88 (0.42)	0.51 (0.24)
34.5-35.5	1	0.78	1.6	1.15 [j]	1.98 (0.96)	4.25 (2.07)	2.49 (1.22)
34.5/1	1	0.78	1.6	1.15 [j]	0.46 (0.22)	0.99 (0.47)	0.58 (0.27)
NA	1	0.73		1.29 [k]	0.25 (0.12)		
NA	1	0.57		1.29 [k]	2.89 (1.66)		
					3.14 (1.79)	2.20 (1.25)	1.07 (0.61)
35.5-34.5	5	0.45	1.6	1.2 [l]	2.17 (2.01)	4.67 (4.32)	2.74 (2.53)
					11.0 (6.3)	19.1 (10.9)	11.0 (6.3)
							41.1 (23.4)
							4.1 (2.3)
							45.2 (25.8)

cake resistance of $6.22 \cdot 10^{10}$ m/kg for $CaCO_3$ in water (Anon., 2006a). For the compressibility and porosity of the filter cake the standard ASPEN values of 0 and 0.45 were used, respectively. The mass fraction of water within the filter cake was set at 0.85 (Chapter 5). [i] Compared to vacuum. [j] U-type heat exchanger (DACE, 2005). [k] Price correction 1990-2004 (DACE, 2005). [l] To include bubble disperser (DACE, 2005).

Heat Exchangers. For both heat exchangers (i.e., the heat exchanger between the reactor outlet and inlet as well as the cooler in which the reactor outlet is cooled further with cooling water), a U-type shell and tube heat exchanger was selected. A heat transfer coefficient (U) of 1000 W/m²°C was assumed on the basis of data presented Sinnott (1997). The logarithmic mean temperature difference (ΔT_{lm}) was 23.5 and 24.4 °C for heat exchanger 1 and 2, respectively (cooling water assumed to enter at 15 °C and leave at 40 °C). Thus, the heat-exchanging surface areas $\left(A = \dfrac{Q}{U \Delta T_{lm}} \right)$ required were 4316 and 695 m² on the

basis of a heat duty (Q) of 101.5 and 17.0 MW, respectively (Figure 6.2). The required amount of cooling water was 585 m^3/h.

Reactor. The designed reactor comprised the mixer, heater, and reactor in the ASPEN flowsheet (Figure 6.2). The final design of the reactor was difficult to determine given the current state of research. As a first approach, a continuous version of a scaled-up autoclave reactor was used, i.e., a series of stirred tank reactors with a heating/cooling jacket. The slurry inlet flow was 892 m^3/h and the residence time 15 min resulting in a total slurry volume of the reactor of

223 m^3. The ratio of the gas and slurry volume flows $\left(\dfrac{\Phi_G}{\Phi_{L+S}} \right)$ was 1.9 and 0.3 at

the reactor inlet and outlet, respectively (gaseous CO_2 was consumed by the carbonation reaction). Assuming a series of 5 tank reactors and a (simplified) linear development of the conversion (i.e., gas consumption), the volumes of the five reactors were: 120, 106, 92, 78, and 63 m^3 (on the basis of a H:D-ratio of 1, D = 5.4, 5.1, 4.9, 4.6, and 4.3 m).

6.3.1.2 Mineral CO_2 Sequestration Costs

The net calculated sequestration costs for wollastonite carbonation are 102 €/ton CO_2 avoided (Table 6.4). These costs consist of the total sequestration costs of 86 €/ton CO_2 sequestered corrected for the energetic CO_2 sequestration efficiency of 84% as determined earlier at L/S = 2 kg/kg (Chapter 5). Table 6.4 shows the depreciation costs and variable and fixed operating costs both per ton of sequestered and avoided CO_2. The largest costs are associated with the feedstock (54 €/ton CO_2 avoided) and the electricity required (26 €/ton CO_2 avoided). The depreciation (10 €/ton CO_2 avoided) and total fixed operating costs (11 €/ton) are relatively limited. The electricity is mainly required for grinding of the feedstock (18 €/ton CO_2 avoided) and compression of the CO_2 feed (8 €/ton CO_2 avoided).

Table 6.4: *CO_2 sequestration costs for wollastonite and steel slag carbonation (excluding possible costs for CO_2 capture).*

Costs [€/ton CO_2]	Wollastonite		Steel slag	
	Sequestered	Avoided	Sequestered	Avoided
Depreciation [a]				
Compressor, blower, and pump	2	3	3	4
Reactor	2	2	6	8
Grinding equipment	2	3	6	7
Heat exchangers	2	2	4	4
Other equipment	0	0	1	1
Variable				
Feedstock	45	54	0	0
(Cooling) water	1	1	1	1
Electricity grinding	15	18	13	15
Electricity other	7	8	7	9
Fixed				
Staff	2	2	5	6
Maintenance	4	5	10	12
Other	3	4	8	10
Sum	*86*	*102*	*64*	*77*

[a] Including depreciation of direct and indirect associated investment costs.

6.3.1.3 Sensitivity Analysis and Process Optimisation

The sensitivity analysis given in Figure 6.3 shows the relative effect of selected parameters on the CO_2 sequestration costs of wollastonite carbonation. Within the ranges studied, the largest uncertainties in the reported sequestration costs are associated with the value of the carbonated product (36-168 €/ton CO_2 avoided), the wollastonite ore price (48-156 €/ton), the conversion in the carbonation reactor (88-119 €/ton), and the liquid-to-solid ratio (94-127 €/ton). As discussed above, the sequestration costs for the standard case are 102 €/ton.

Wollastonite
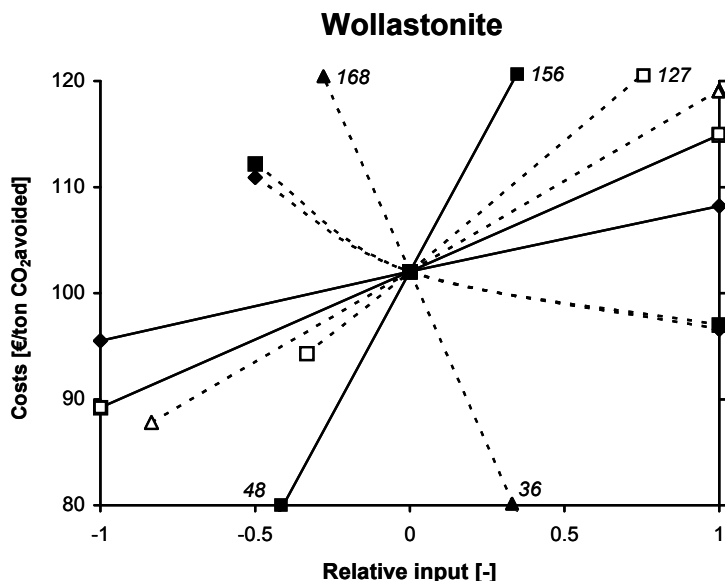
#	Variable	Wollastonite		
	Parameters cost evaluation	Standard	Min	Max
1	Water [€/m³]	0.35 (0) [a]	0.2 (-1)	0.5 (1)
2	Feedstock [€/ton]	10 (0)	0 (-1)	20 (1)
3	Cooling water [€/m³]	0.05 (0)	0.03 (-1)	0.07 (1)
4	Electricity [€/kWh]	0.06 (0)	0.03 (-1)	0.09 (1)
5 [b]	Reactor [M€]	2.2 (0)	1.1 (-1)	3.3 (1)
6 [b]	Grinding equipment [M€]	3.1 (0)	1.6 (-1)	4.7 (1)
7 [b]	Compressor, blower, and pump [M€]	2.8 (0)	1.4 (-1)	4.2 (1)
8 [b]	Heat exchangers [M€]	2.4 (0)	1.2 (-1)	3.7 (1)
9 [b]	Filter and flash tanks [M€]	0.5 (0)	0.2 (-1)	0.7 (1)
10	Surcharge factors (general & grinding equipment) [-] [c]	4.4 & 2.0 (0)	2.7 & 1.5 (-1)	6.1 & 2.5 (1)
11	Operating labour [-]	3 (0)	1 (-1)	5 (1)
12	Maintenance [%]	5 (0)	0 (-1)	10 (1)
13	Staff, Laboratory & Supervision [%]	90 (0)	45 (-1)	135 (1)
14	Local taxes & Insurance [%]	2 (0)	0 (-1)	4 (1)
15	Depreciation period [yr]	10 (0)	5 (-0.5)	20 (1)
16	Operational time [hr/yr]	8000 (0)	7500 (-1)	8500 (1)
17	Product price [€/ton]	0 (0)	-10 (-1)	10 (1)
	Parameters process simulation [d]			
18	Scale [ton CO₂/hr]	60 (0)	30 (-0.5)	120 (1)
19	Liquid-to-solid ratio [kg/kg]	2 (0)	1 (-0.33)	5 (1)
20	Temperature of H₂O recycle [°C] [e]	40 (0)		100 (1)
21	Carbonation degree (ζ_{CaSiO3}) [%]	69.1 (0)	60 (-0.8)	80 (1)

Figure 6.3: *Sensitivity analysis of CO₂ sequestration costs for wollastonite and steel slag carbonation for the parameters shown in the table. Table: in case of different values for the wollastonite and steel slag calculations, the values are given as wollastonite / steel*
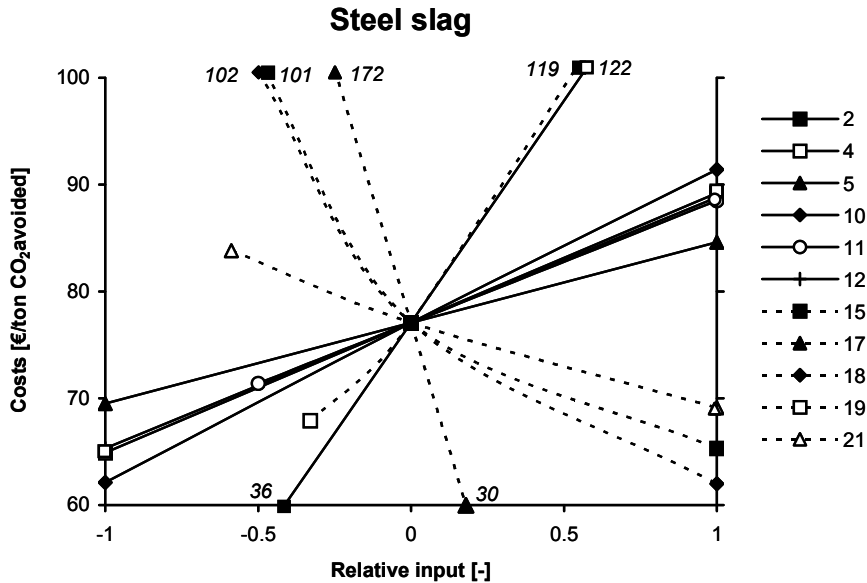
Steel slag

Steel slag Standard	Min	Max
0.35 (0)	0.2 (-1)	0.5 (1)
0 (0)	-5 (-1)	5 (1)
0.05 (0)	0.03 (-1)	0.07 (1)
0.06 (0)	0.03 (-1)	0.09 (1)
2.0 (0)	1.0 (-1)	3.0 (1)
1.8 (0)	0.9 (-1)	2.7 (1)
1.1 (0)	0.5 (-1)	1.6 (1)
1.2 (0)	0.6 (-1)	1.8 (1)
0.2 (0)	0.1 (-1)	0.3 (1)
4.4 & 2.0 (0)	2.7 & 1.5 (-1)	6.1 & 2.5 (1)
2 (0)	1 (-0.5)	4 (1)
5 (0)	0 (-1)	10 (1)
90 (0)	45 (-1)	135 (1)
2 (0)	0 (-1)	4 (1)
10 (0)	5 (-0.5)	20 (1)
8000 (0)	7500 (-1)	8500 (1)
0 (0)	-10 (-1)	5 (0.5)
15 (0)	7.5 (-1)	30 (1)
2 (0)	1 (-0.33)	5 (1)
40 (0)		100 (1)
67.4 (0)	60 (-0.6)	80 (1)

[a] Numbers between brackets are the relative input values, defined as:

$$\text{Rel. Value} = \frac{\text{Abs. Value} - \text{Standard}}{\text{Max} - \text{Standard}}, \text{ as used}$$

for the graphs.

[b] Including design parameters, price of reference equipment and price correction factors used (i.e., all assumptions given in Table 6.3).

[c] Multiplication factor based on all individual direct and indirect surcharge factors.

[d] Including possible effect on the energetic efficiency (η_{CO2}) (Chapter 5).

[e] For these simulations, the ASPEN flowsheet was extended with a cooler, which cools the second CO_2 recycle stream in order to avoid an increase of the gas volume that has to be compressed.

slag. Graph: for reasons of clarity, only the parameters with an influence ≥ 5 €/ton CO_2 avoided are shown. For variables with a minimum / maximum value outside the range of the graph, the values are indicated at the borders.

The price of wollastonite not only has a large influence on the sequestration costs, but also is among the most uncertain parameters (see §6.2.4). Thus, the economic feasibility of CO_2 sequestration by wollastonite carbonation depends largely on the feedstock price. Also the value of the carbonated product is an important parameter, since the mass of carbonated product is 5.5 or 7.9 times larger than the mass of CO_2 sequestered (in the case of wollastonite and steel slag, respectively). However this parameter is also uncertain, since no thorough assessments of possible markets have been reported so far (possible markets may include calcium carbonate for the paper industry and slaked lime for e.g. soda and steel production). In the current cost evaluation, it was assumed that the process did not yield a saleable product. In other cost evaluation studies on mineral carbonation processes, prices of 10-15 €/ton of product were assumed (Iizuka et al., 2004; Teir et al., 2005), which would reduce the sequestration costs substantially (e.g., from 102 €/ton CO_2 avoided to 36 €/ton at 10 €/ton product, see Figure 6.3). It should be noted that beneficial re-use of the carbonated product may impose the need of a drying step, which is not included in the current process design (Figure 6.2). A reduction of the L/S-ratio results in smaller streams that have to be processed and, thereby, less expensive equipment. In addition, the energetic efficiency of the process improves (Chapter 5), which reduces the sequestration costs per ton of CO_2 avoided.

Finally, it should be noted that the temperature of the water recycle does not have a significant influence on the sequestration costs (Figure 6.3). In the current process design, the heat duty of the heat exchanger is large, i.e. 101 MW due to among other factors the low temperature of the water recycle (40 °C) (Chapter 5). This value is of comparable magnitude as the size of the power plant which CO_2 emissions are sequestered (100 MW). Although an increase of the temperature of the process water recycle would reduce the deprecation costs for the heat exchanger, the effect on the overall sequestration costs is apparently very limited. Thus, the estimated sequestration costs seem also valid for a mineral carbonation process, which is further optimised with respect to the temperature of the water recycle.

Figure 6.4 shows the influence of the temperature, pressure, and particle size on, successively, the $CaSiO_3$ carbonation degree measured in a lab-scale autoclave reactor (Chapter 4) (I), the energetic efficiency simulated following Chapter 5 (II), and the sequestration costs per ton of CO_2 sequestered (III) and per ton of CO_2 avoided (IV) for wollastonite carbonation. It can be concluded that the economically optimum set of process conditions corresponds with the energetically optimum set, as implicitly assumed in §6.2.1. In fact, optimisation of the aqueous wollastonite carbonation process with respect to the carbonation degree leads more or less directly to minimum sequestration costs, as a result of

the dominant effect of the wollastonite feedstock on the overall sequestration costs.
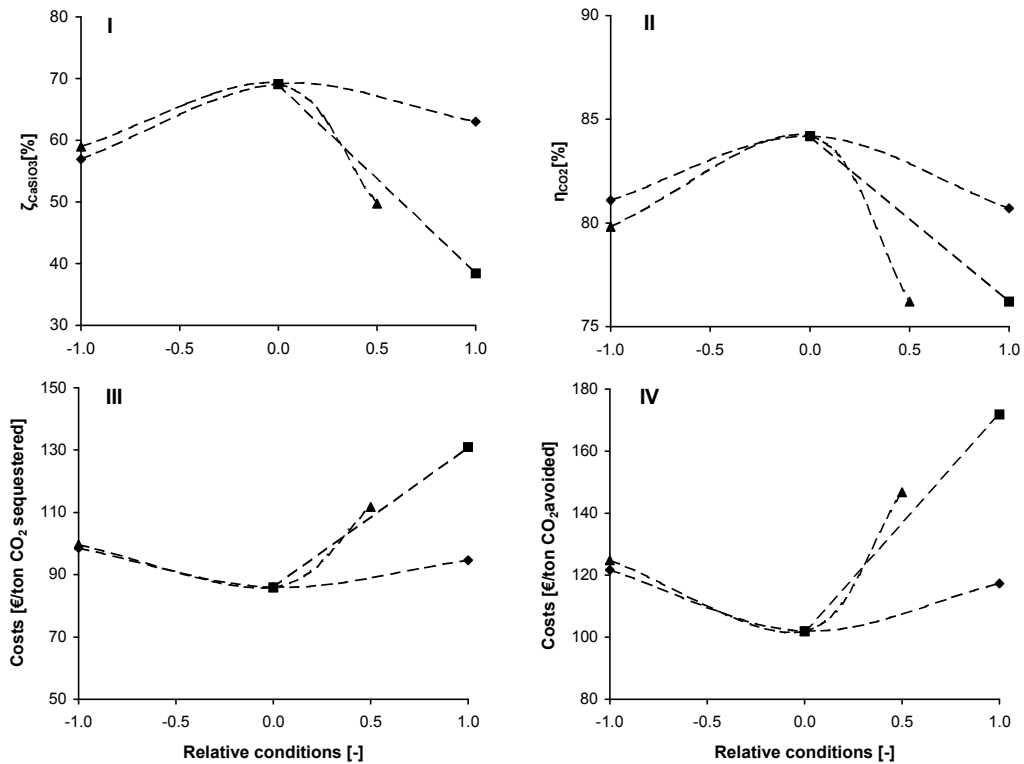
Variable	Standard [a]		Min	Max
Particle size	— ■ —	<38 (0)	NA	<106 (1)
Reactor temperature	— ▲ —	200 (0)	150 (-1)	225 (0.5)
CO_2 pressure	— ◆ —	20 (0)	10 (-1)	30 (1)

[a] Values between brackets are the relative input values used for the graphs.

Figure 6.4: *Influence of process conditions on $CaSiO_3$ conversion (ζ_{CaSiO3}) (I), energetic CO_2 sequestration efficiency (η_{CO2}) (II), and costs per ton of CO_2 sequestered (III) and per ton of CO_2 avoided (IV). Simulations were performed at L/S = 2 kg/kg.*

6.3.2 Steel Slag

The total sequestration costs by steel slag carbonation are 64 €/ton CO_2 sequestered or 77 €/ton CO_2 avoided sequestration costs (Table 6.4). The variable operating costs are substantially lower than for wollastonite because of the absence of feedstock costs. However, these reductions are partially annulled by the higher depreciation costs (23 €/ton CO_2 avoided) and fixed operating

costs (28 €/ton) (Table 6.1). These higher costs are caused by the smaller scale of the process and the larger grinding equipment and reactor relative to the amount of CO_2 sequestered, since more feedstock has to be processed mainly due to the lower Ca content of the feedstock (23 vs. 30% for wollastonite (Chapters 2 & 4)). The total investment costs are with 26 M€ lower than for wollastonite due to the smaller scale of the process (the design of the major process equipment and the estimation of the investment costs were performed similarly to wollastonite, see §6.3.1.1).

A potential additional cost benefit of the use of industrial residues as feedstock for mineral CO_2 sequestration is the generation of feedstock and CO_2 at the same location. The cost saving thus obtained is not taken into account in the numbers presented since it is outside the system boundaries, but transportation costs of CO_2 are typically in the range of 1-8 €/ton CO_2 (transport distance 250 km) (IPCC, 2005).

The influences of the various assumptions on the sequestration costs by steel slag carbonation (Figure 6.3) show that, since the scale of the process is smaller and the feedstock cost no longer dominates the overall sequestration costs, as in the case of wollastonite, also parameters concerning the estimation of the investment costs now have a significant influence. Within the ranges studied, the largest uncertainties in the sequestration costs are associated with the (possible) value of the carbonated product (30-172 €/ton), the possible costs of the feedstock (36-119 €/ton CO_2 avoided), the scale of the sequestration process (62-102 €/ton), the depreciation period (65-101 €/ton), and the liquid-to-solid ratio (68-122 €/ton). It is noteworthy that the conversion has a smaller influence on the sequestration costs than in the case of wollastonite. The scale of the process affects the sequestration costs in two ways: (1) scale-effect on the investment costs (see also Table 6.3) and (2) relative change of the number of operators required and, thereby, of the fixed operating costs. The depreciation period only virtually changes the sequestration costs, since the investment costs are spread out over different time periods.

6.3.3   Comparison to Other Cost Analyses

For the direct aqueous wollastonite carbonation process studied in this paper, the Albany Research Centre (ARC) calculated sequestration costs of 76 €/ton CO_2 sequestered or 93 €/ton CO_2 avoided (η_{CO2} = 82%, 1€ = 1.2$) (O'Connor et al., 2005). Comparison of the ARC results with the results of this study is complicated since: (1) in the ARC study, the wollastonite carbonation costs were estimated on the basis of a process designed for olivine carbonation and (2) the cost methodology itself has not been published (Nilsen and Penner, 2001;

O'Connor et al., 2005). In addition, the process design is different with regard to a number of aspects, e.g., (1) the partial recycling of the unconverted feedstock in the ARC process (Nilsen and Penner, 2001) (see also discussion in Chapter 5) and (2) the scale of the process (i.e., 1100 (O'Connor et al., 2005) vs. 60 ton/hr CO_2 sequestered in this study). Enlarging the current scale of the process to a scale comparable with that of the ARC study (a 1.3 GW coal-fired power plant (O'Connor et al., 2005)) would lower the sequestration costs for reasons of 'economy of scale' (Figure 6.3). However, given the very large solid material streams involved, a more modest scale for a mineral carbonation plant seems appropriate. In spite of the differences between these studies, the similar sequestration costs for aqueous wollastonite carbonation resulting from the ARC and this study (Table 6.5) are noteworthy.

In addition to cost estimates for the direct aqueous wollastonite carbonation route, Table 6.5 shows sequestration costs reported for other mineral carbonation processes. This limited set of cost estimates suggests that: (1) current direct carbonation routes (such as the direct aqueous route discussed in this paper) are less expensive than indirect carbonation routes and (2) mineral carbonation processes using solid residues as feedstock tend to be less expensive than processes using ores (see also a previously published comparison of process routes (Chapter 1)). Overall, the direct aqueous carbonation processes using either steel slag or olivine (Mg_2SiO_4) seem to have the lowest sequestration costs among the currently available mineral carbonation processes.

Finally, Table 6.5 also shows the costs of other CCS-technologies such as geological storage. In cost estimates of CO_2 storage options other than mineral carbonation, compression is typically left out of consideration, since compression for transportation purposes is generally already included in the CO_2 capture step. Mineral carbonation costs excluding compression decrease to 85 and 58 €/ton CO_2 avoided for wollastonite and steel slag, respectively, due to the absence of both investment costs for the compressor and electricity costs for compression as well as an increase of the sequestration efficiency to 90 and 89%. However, even excluding compression, the sequestration costs of current mineral carbonation technologies are high relative to the costs of geological CO_2 capture and storage options. Although the permanent and inherently safe sequestration of CO_2 by mineral carbonation may justify higher costs than those of geological storage, further cost reductions are required, particularly in view of (current) prices of CO_2 emission rights within the EU emissions trading scheme (20-25 €/ton, 2nd half 2005 (Anon., 2006b)).

Table 6.5: *Comparison of sequestration costs reported for mineral carbonation processes and other carbon capture & storage (CCS)-technologies (excluding possible costs for CO_2 capture).*

Costs mineral carbonation [€/ton CO_2 avoided]	Feedstock	Process route [a]	Extraction agent	Reference
93	wollastonite	direct	water	(O'Connor et al., 2005)
102	wollastonite	direct	water	This study
77	steel slag	direct	water	This study
65	olivine	direct	water [b]	(O'Connor et al., 2005)
258	serpentine [c]	direct	water [b]	(O'Connor et al., 2005)
95 [d]	Mg-silicate	direct	molten $MgCl_2$	(IEA GHG, 2000)
25 [e]	waste cement	indirect	water	(Iizuka et al., 2004)
57 [e]	wollastonite	indirect	acetic acid	(Kakizawa et al., 2001)
>150	Mg-silicate	indirect	HCl	(IEA GHG, 2000)
Other CCS-technologies [€/ton CO_2 injected]	Storage type	Costs type		
0.5 - 7	geological	storage		(IPCC, 2005)
0.1 - 0.3/yr		monitoring costs		(IPCC, 2005)
4 - 25	oceanic			(IPCC, 2005)

[a] For more information on process routes and extraction agents see a previously published literature review (Chapter 2). Direct route: Ca/Mg-extraction and carbonation takes place in a single process step. Indirect route: Ca/Mg is first extracted and, subsequently, carbonated in a second process step. [b] Salts added: 0.64M $NaHCO_3$, 1M NaCl.
[c] Heat-treated. [d] Assuming make-up $MgCl_2$ is not produced on-site, but has to be imported.
[e] Comprises only power costs and, in the case of waste cement, a revenue for selling $CaCO_3$.

6.3.4 Discussion

In this paper, we have presented a cost estimate of CO_2 sequestration by aqueous carbonation of Ca-silicates. In order to improve the accuracy of the cost estimate, it is recommended to study a number of assumptions made in the economic evaluation of the mineral carbonation process in further detail, in particular, the factors discussed in §6.3.1.3. First, pilot-scale experimental research on the carbonation process in a continuous reactor can provide a better insight in the carbonation process under industrial conditions. Research should particularly focus on the carbonation degree under those conditions as well as on the minimum L/S-ratio that is required for processing and carbonating. Second,

specific cost evaluations should be made for individual potential locations for a mineral carbonation plant taking into account, among other factors, the specific scale of the sequestration process. In addition, assessments of the relevant feedstock price and possible markets for the carbonated product should be made for each specific location.
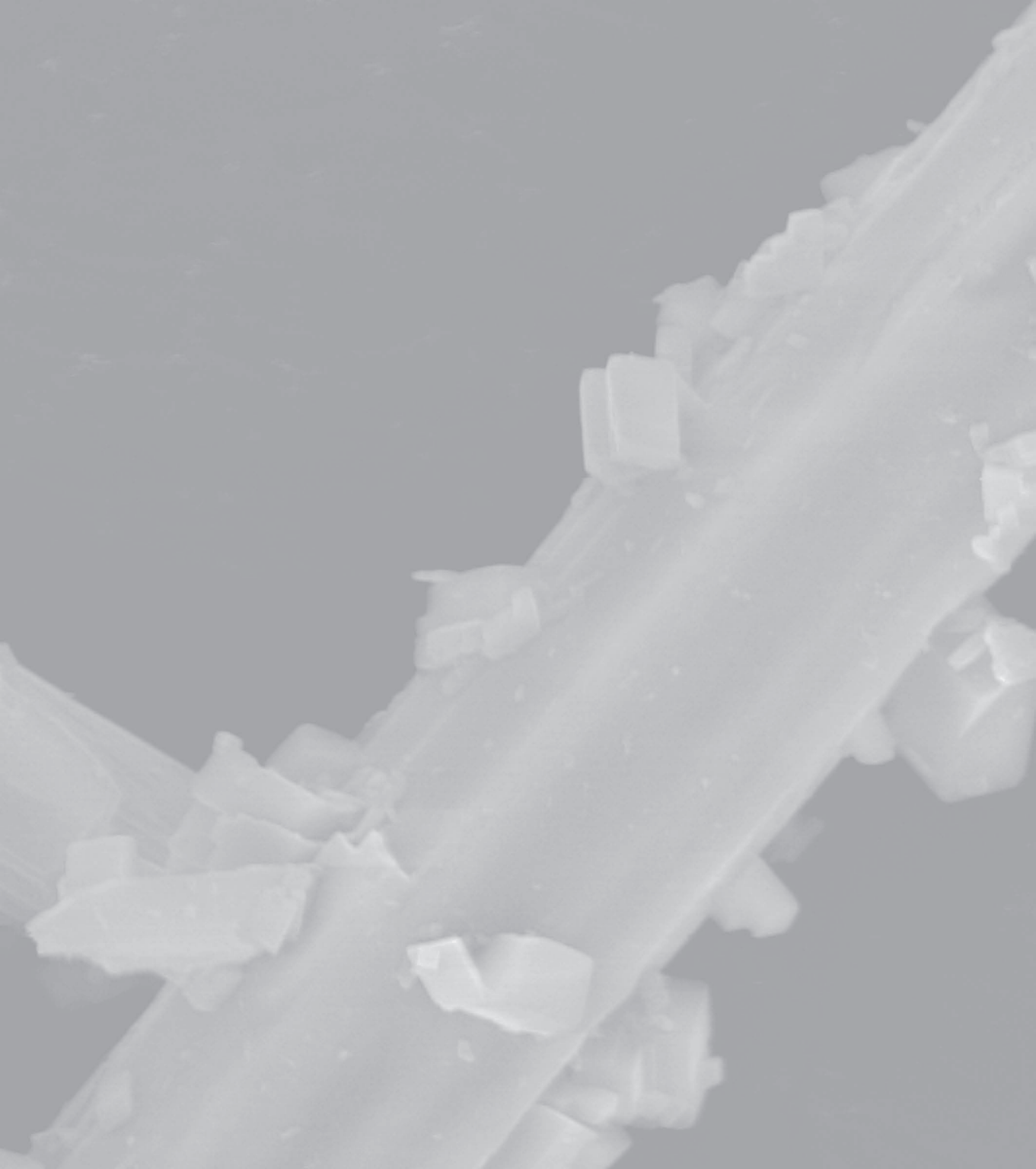
As noted in section 6.3.3, the estimated sequestration costs of state-of-the-art mineral carbonation are high relative to both the costs of other CO_2 capture and storage options as well as (current) CO_2 emission right trade prices within the EU. Research on cost reduction should focus on the major costs identified in this paper. For wollastonite carbonation, measures to further increase the carbonation degree are especially desirable given the large contribution of the ore costs to the overall sequestration costs (e.g., by further grinding (Chapters 4 & 5) and/or application of additives (Chapter 1)). Also, recycling of the unconverted feedstock may be considered, although the feasibility of separating the carbonated material from the fresh feedstock seems unclear (Chapter 5). An alternative might be the use of a Mg-silicate instead of wollastonite, since the costs of Mg-silicates are generally relatively low due to their widespread abundance. For residue carbonation processes, optimisation of the carbonation degree is less important since the material is assumed to be available for negligible costs (Figure 6.3). Therefore, carbonation at milder process conditions might be considered to reduce, e.g., the electricity consumption and the investment cost. For both types of feedstock, possibilities to increase the energetic performance (e.g., an increase of the pressure at which the water is recycled (Chapter 5)) of the process may also reduce the sequestration costs. Finally, in order to possibly reduce the overall sequestration costs of mineral carbonation substantially and to create a cost benefit compared to other CCS technologies, research on the possibilities to integrate mineral carbonation processes with the CO_2 capture process step (Figure 6.1) is recommended. CO_2 capture costs are substantial in the overall costs of 'carbon capture and storage'-technologies. Representative figures reported for different types of power plants range from 19 to 44 €/ton CO_2 on the basis of current technologies (IPCC, 2005).

6.4   Conclusions

A cost estimation of CO_2 sequestration by aqueous wollastonite and steel slag carbonation has resulted in sequestration costs of 102 and 77 €/ton CO_2 net avoided, respectively. For wollastonite, the major costs were found to be associated with the feedstock and the electricity consumption for grinding and compression (54 and 26 €/ton CO_2 avoided, respectively). In addition to the

electricity costs, the significantly lower sequestration costs for steel slag were largely determined by the depreciation and fixed operating costs (23 and 28 €/ton CO_2 avoided, respectively) due to the absence of costs for the feedstock and the smaller scale of the process. Sensitivity analyses have shown that influential parameters in the sequestration costs are the possible value of the carbonated product, the price of the feedstock (wollastonite), the liquid-to-solid ratio, the conversion in the reactor (wollastonite), and the scale of the process (steel slag). Although various options for potential cost reduction have been identified, CO_2 sequestration by current aqueous carbonation processes seems expensive relative to other CO_2 storage technologies. The permanent and inherently safe sequestration of CO_2 by mineral carbonation may justify higher costs, but further cost reductions are required, particularly in view of (current) prices of CO_2 emission rights. (Niche) applications of mineral carbonation with a solid residue as feedstock and/or a useful carbonated product hold the best prospects for an economically feasible CO_2 sequestration process.

EPILOGUE

EPILOGUE

Conclusions Individual Chapters

The **aim** of this thesis was to investigate the technical, energetic, and economic feasibility of CO_2 sequestration by mineral carbonation (see **Introduction**). A review of published literature (**Introduction** & **Chapter 1**) showed that mineral CO_2 sequestration has a number of fundamental advantages compared to other CO_2 storage technologies, including a vast potential CO_2 sequestration capacity and an inherently safe and permanent CO_2 storage. The key challenge in enabling the application of mineral carbonation as a CO_2 sequestration technology was found to be the realisation of an increase of the reaction rate in order to obtain an industrially viable process. With this objective in mind, two types of solid feedstock were selected for further research, the industrial residue steel slag and the mineral ore wollastonite ($CaSiO_3$) (**Chapter 1**). As a process route, the aqueous carbonation route (i.e., direct carbonation in an aqueous suspension) was selected as the most promising process route for further investigation.

The experimental studies in **Chapters 2** & **4** on the carbonation of steel slag and wollastonite, respectively, in a lab-scale autoclave reactor have shown that substantial carbonation degrees can be obtained at process conditions that seem technically feasible. For wollastonite, the maximum conversion reached within 15 min was 70% at 20 bar CO_2 pressure, 200 °C, and a particle size of <38 μm (**Chapter 4**). For steel slag, a maximum Ca carbonation degree of 74% was reached within 30 minutes at 19 bar CO_2 pressure, 100 °C, and a particle size of <38 μm (**Chapter 2**). Ca-silicates such as wollastonite and steel slag were found to react rapidly relative to published reaction rates for Mg-silicates, thus eliminating the need for either an energy-consuming heat-treatment step or CO_2 pressures >100 bar. Among the two studied Ca-silicates, steel slag was shown to react more rapidly, particularly at mild conditions (i.e., low temperature and CO_2 pressure).

The aqueous carbonation mechanisms of wollastonite and steel slag were shown to be generally similar (**Chapters 2** & **4**). The carbonation of Ca was shown to take place in two subsequent steps (i.e., dissolution and precipitation). Calcium from the Ca-silicate phase diffuses towards the surface of the particle and is leached. Subsequently, the Ca in solution is carbonated and precipitates as calcite on the outer surface of the steel slag particles. Grinding the solid feedstock was found to increase the carbonation rate substantially due to the

creation of a larger specific reactive surface area. In addition, an optimum reaction temperature, which depended on the applied CO_2 pressure, was found at which maximum conversion is reached (roughly, 200 °C at 20 bar CO_2). At temperatures below this optimum, the overall reaction rate is probably limited by the leaching rate of Ca into the water phase. Ca-leaching was suggested to be controlled by diffusion of Ca through a Ca-depleted silicate rim, which is formed by incongruent leaching. At higher temperatures, it was concluded that a reduction of the bi(carbonate) activity in solution probably limits nucleation and growth of calcium carbonate and thus the carbonation rate.

Leaching experiments on (carbonated) steel slag and geochemical modelling described in **Chapter 3** were used to identify solubility-controlling processes of elements both with regard to carbonation mechanisms and the environmental properties of the (carbonated) steel slag. Carbonation was shown to reduce the leaching of alkaline earth metals (except Mg) by conversion of Ca-phases into calcite, possibly containing traces of Ba and Sr. The following Ca-phases were identified in the fresh steel slag: portlandite ($Ca(OH)_2$), ettringite, and Ca-(Fe)-silicates. Portlandite and some of the Ca-silicates dissolve easily and, therefore, cause the relatively easy carbonation of steel slag. The leaching of vanadium was found to increase substantially upon carbonation, probably due to the dissolution of a Ca-vanadate mineral. The reactive surface area of Al- and Fe-(hydr)oxides was shown to increase upon carbonation, which tends to reduce the leaching of sorption-controlled trace elements.

In the second part of this thesis, a system study was performed to estimate the energy consumption (**Chapter 5**) and sequestration costs (**Chapter 6**) of an aqueous mineral carbonation plant. The net amount of CO_2 sequestered was found to be reduced due to extra CO_2 emissions associated with the energy consumption of the mineral carbonation process (i.e., the power and heat consumption of the process were larger than the exothermic reaction heat) (**Chapter 5**). Within the ranges of process conditions studied, an optimum CO_2 sequestration efficiency (η_{CO2}) of 74% was found for wollastonite at 200 °C, 20 bar CO_2, and a particle size of <38 µm. The main energy-consuming process steps were shown to be the grinding of the feedstock ($\Delta\eta_{CO2}$ = -15%) and the compression of the carbon dioxide (-7%). In the case of steel slag, the lower Ca content of the feedstock was found to significantly reduce the energetic efficiency to 69% at similar conditions. Finally, it was shown that the CO_2 sequestration efficiency might be improved substantially for both types of feedstock by, e.g., reducing the amount of process water applied, improving the heat-integration of the process and further grinding of the feedstock.

The cost analysis (**Chapter 6**) showed that state-of-the-art mineral CO_2 sequestration is a relatively expensive CO_2 emission reduction technology. The net sequestration costs determined for wollastonite are 102 €/ton CO_2 avoided and include the depreciation costs of the investments and variable and fixed operating costs. Major costs were found to be associated with the feedstock and the electricity consumption for grinding and compression (54 and 26 €/ton CO_2 avoided, respectively). The sequestration costs for steel slag were shown to be significantly lower (77 €/ton CO_2 net avoided) due to the absence of costs for the feedstock. Additional influential parameters in the sequestration costs were found to include the liquid-to-solid ratio in the carbonation reactor and the possible value of the carbonated product. Although various possibilities for potential cost reduction were identified, CO_2 sequestration by current aqueous wollastonite carbonation processes was found to be relatively expensive compared to both other CO_2 storage technologies and (current) CO_2 market prices. (Niche) applications of mineral carbonation with either a solid residue such as steel slag as feedstock or a useful carbonated product were identified to hold significantly better prospects for economic feasibility.

Discussion & Conclusion

On the basis of the conclusions of the individual chapters, it is concluded that the aqueous carbonation of Ca-silicates seems to be a technically feasible technology for CO_2 emission reduction. The energy consumption of current mineral carbonation processes was found to be substantial, but various options to significantly reduce this energy consumption were identified. Although the feasibility of these suggestions has to be studied in further research (see below), aqueous mineral carbonation can be considered as potentially energetically feasible. The main barrier for further implementation of mineral carbonation as a CO_2 sequestration technology are its relatively high costs.

In Chapter 6, it was concluded that CO_2 sequestration by current aqueous mineral carbonation processes is relatively expensive compared to both other CO_2 storage technologies and (current) EU CO_2 market prices. Figure 7.1 provides a comparison of *current* costs of (1) electricity generation by fossil fuels with CO_2 emission reduction by mineral carbonation, (2) electricity generation by fossil fuels with geological CO_2 storage, and (3) electricity generation by renewable energy sources. Although the costs of each individual technology may vary strongly, largely depending on specific factors such as location, mineral carbonation seems more expensive than CO_2 emission reduction by geological storage and renewable energy sources such as biomass and geothermal energy.

However, the costs of mineral carbonation seem comparable with those of thermal solar energy and (the high-end) of offshore and onshore wind energy.
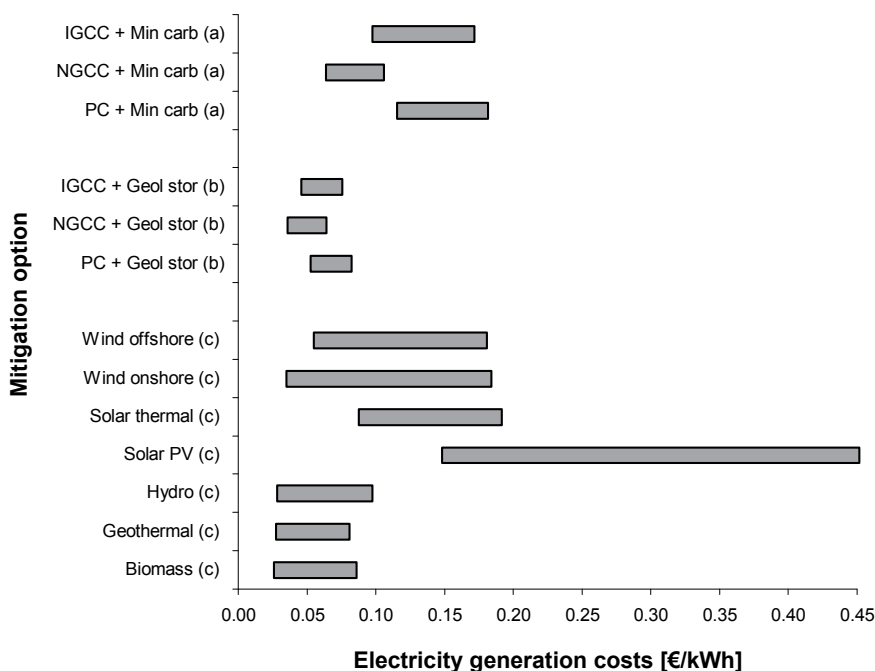

Figure 7.1: *Electricity generation costs by fossil fuels together with CO_2 emission reduction by mineral carbonation or geological CO_2 storage and electricity generation costs by various renewable energy sources. [a] Capture costs obtained from IPCC (2005). Amount of CO_2 captured 0.67-0.94 (IGCC), 0.36-0.41 (NGCC), and 0.82-0.97 (PC) kg CO_2/kWh (IPCC, 2005). Mineral carbonation costs obtained from Chapter 6. NGCC = natural gas combined cycle, IGCC = integrated gasification combined cycle & PC = pulverised coal power plant. [b] Prices of capture and geological storage obtained from IPCC (2005). [c] Prices obtained from IEA (2006). Reported prices are for 2002 (IPCC), 2004 (this thesis), and 2005 (IEA). Conversion rate used: 1€ = 1.2$.*

When comparing different 'carbon capture and storage' technologies, the higher cost of mineral carbonation relative to other (geological) CO_2 storage options should be held against the more permanent and safer CO_2 storage. At its current state of development, mineral CO_2 sequestration is a longer-term option compared to other CO_2 storage technologies. Further technology development and cost reduction are required for mineral CO_2 sequestration to be considered as part of a broad portfolio of employable CO_2 mitigation possibilities, including CO_2 storage technologies.

However, mineral CO_2 sequestration is a relatively new research area and large progress has been made in recent years in enhancing the carbonation rate and reducing energy consumption and costs. Given the development of the technology, the permanent character of the CO_2 sequestration, and the large sequestration potential, further research on mineral CO_2 sequestration is warranted, and specific suggestions are given below.

Further Research

Further research on mineral carbonation should focus particularly on reducing the sequestration costs. More specifically, the following recommendations can be given:

Aqueous Mineral Carbonation Process

– *Re-use of Carbonation Products.* Research on the re-use possibilities of carbonation products is recommended, particularly with regard to determination of value and volume of possible markets. The beneficial utilisation of these products can contribute to a substantial reduction of sequestration costs (**Chapter 6**). In fact, it might well turn out that mineral CO_2 sequestration can only be cost-effective if the product can be usefully applied. Beneficial re-use of carbonated products might especially facilitate the realisation of the first mineral CO_2 sequestration (demonstration) plants.
– *Pilot-scale Research.* An important next step in aqueous mineral carbonation research is a pilot-scale study of the carbonation reaction under continuous conditions and at a larger scale. Pilot-scale research should provide more insight in the technically feasible range of reactor conditions, particularly the minimum amount of process water required for adequate mixing and processing, which is important for reducing the energy consumption and costs of the current process (**Chapters 5** & **6**). In addition, preliminary research with a continuous pilot-scale carbonation reactor has been published showing that the reactor type may have a positive effect on the carbonation degree due to physical effects, such as abrasion, on the (rate-limiting) silica-rim (**Chapter 5**).
– *Carbonation of Industrial Solid Residues.* Further research on carbonation of industrial solid residues seems warranted given the significantly lower CO_2 sequestration costs (**Chapter 6**). Such research may include carbonation of other potentially suitable residue streams, such as construction and demolition waste (i.e., waste concrete and cement) and municipal solid waste incinerator bottom ash (**Chapter 1**). Given the relatively rapid carbonation of residues at mild process conditions and the absence of

feedstock costs, also research on direct gas-solid carbonation with moisturised CO_2 might be considered. The sequestration costs of this approach are probably substantially lower than that of the aqueous carbonation route studied in this thesis, although it should be stressed that the amount of CO_2 that can sequestered through this process route will be (very) limited (**Chapter 1**).

– *Improvement of System Study.* The system study in **Chapters 5** & **6** can be used for further (economic) optimisation of the process conditions (including reaction time) as well as the heat-integration of the process. In addition, site-specific assessments of the energetic and economic performance of CO_2 sequestration by mineral carbonation should be made and include the (possible) CO_2 capture, mining, and transportation process steps. Finally, research on the possible separation and recycling of unconverted Ca-silicate particles is recommended given its large potential effect on the energy consumption and sequestration costs (**Chapters 5** & **6**).

– *Carbonation Mechanisms.* Further insight in carbonation mechanisms, e.g. by studying the dissolution and carbonation mechanisms in-situ at elevated temperature and pressure (see **Annex 4.1**), may help to further our knowledge on the rate-limiting process steps. This insight might help to realise a further increase of the carbonation rate and, consequently, reduce the energy consumption and sequestration costs.

– *Mg-silicates.* Although the research presented in this thesis is based on Ca-silicates only, the further development of large-scale carbonation plants should also consider Mg-silicates as feedstock, given their lower costs (**Chapter 6**) and widespread abundance (**Chapter 1**). Based on current knowledge, it seems that, despite the more severe process conditions required to carbonate Mg-silicates compared to Ca-silicates (**Chapter 1**), the overall CO_2 sequestration costs are lower in the case of Mg-silicates (**Chapter 6**).

– *Additives.* The application of additives may enhance the dissolution of Ca from the solid matrix, similarly to the use of e.g. NaCl/NaHCO$_3$ in direct aqueous Mg-silicate carbonation processes (**§1.3.2**). It may be worthwhile to further study their effect on the carbonation rate, energy consumption, and sequestration costs in the case of wollastonite carbonation (see also **Annex 4.2**).

New Mineral Carbonation Concepts

Given the relative complexity of the mineral carbonation process compared to other CO_2 storage technologies, mineral carbonation will probably remain more expensive than geological storage despite further process optimisation. Two approaches to achieve a possible breakthrough in cost reduction are proposed:

- *Integration of Capture and Carbonation.* The overall CO_2 storage costs of e.g. geological storage are largely determined by the energy consumption and costs for CO_2 capture. A potential cost benefit of mineral CO_2 sequestration compared to other CO_2 storage options might come from a reduction of the costs for CO_2 capture through a (partial) integration of the capture and sequestration steps.
    - A first step might be heat-integration of the capture and sequestration processes. After process optimisation, the aqueous mineral carbonation process has a net overall exothermic reaction heat (**Chapter 6**). This heat might possibly be used in the CO_2 capture process to reduce its heat consumption.
    - In case of CO_2 capture by absorption, further integration of capture and storage might possibly be achieved by using the CO_2 loaded solvent resulting from the absorption step directly for carbonation, thus avoiding the energy-consuming stripping. This suggestion has, however, not yet been experimentally verified.
    - Finally, since aqueous Ca-silicate carbonation can be executed at low CO_2 pressures relative to e.g. storage in depleted gas fields (typically, 10-20 vs 100 bar), it might be worthwhile to investigate the effects of less excessive CO_2 purification or the possibility to skip the capture step and directly use the flue gas.
- *Sub-surface Carbonation.* This thesis has focused on aboveground carbonation. Its results might also be used to further explore sub-surface carbonation.
    - *In-situ Carbonation of Ores.* The relatively high sequestration costs of ex-situ ore carbonation processes are directly related to the need to enhance the carbonation rate and to the mining of the ore. In the case of underground in-situ ore carbonation, the ore would not have to be mined and longer reaction times can be permitted than in an industrial setting. Therefore, in-situ mineral carbonation holds perspective for CO_2 sequestration at lower costs and might be interesting to explore further.
    - *Mineral Trapping during Geological CO_2 Storage.* The research on aboveground mineral carbonation concepts might provide useful insights in sub-surface mineral carbonation processes relevant for the risk assessment of geological CO_2 storage. In studies on the long-term behaviour of geologically stored carbon dioxide, various trapping mechanisms are distinguished including mineral trapping (i.e., binding of gaseous CO_2 by carbonation reactions with surrounding rocks). The similarities in reactions and reaction conditions enable a mutual use of research results, which might be further explored than is done to date.

NOTATION
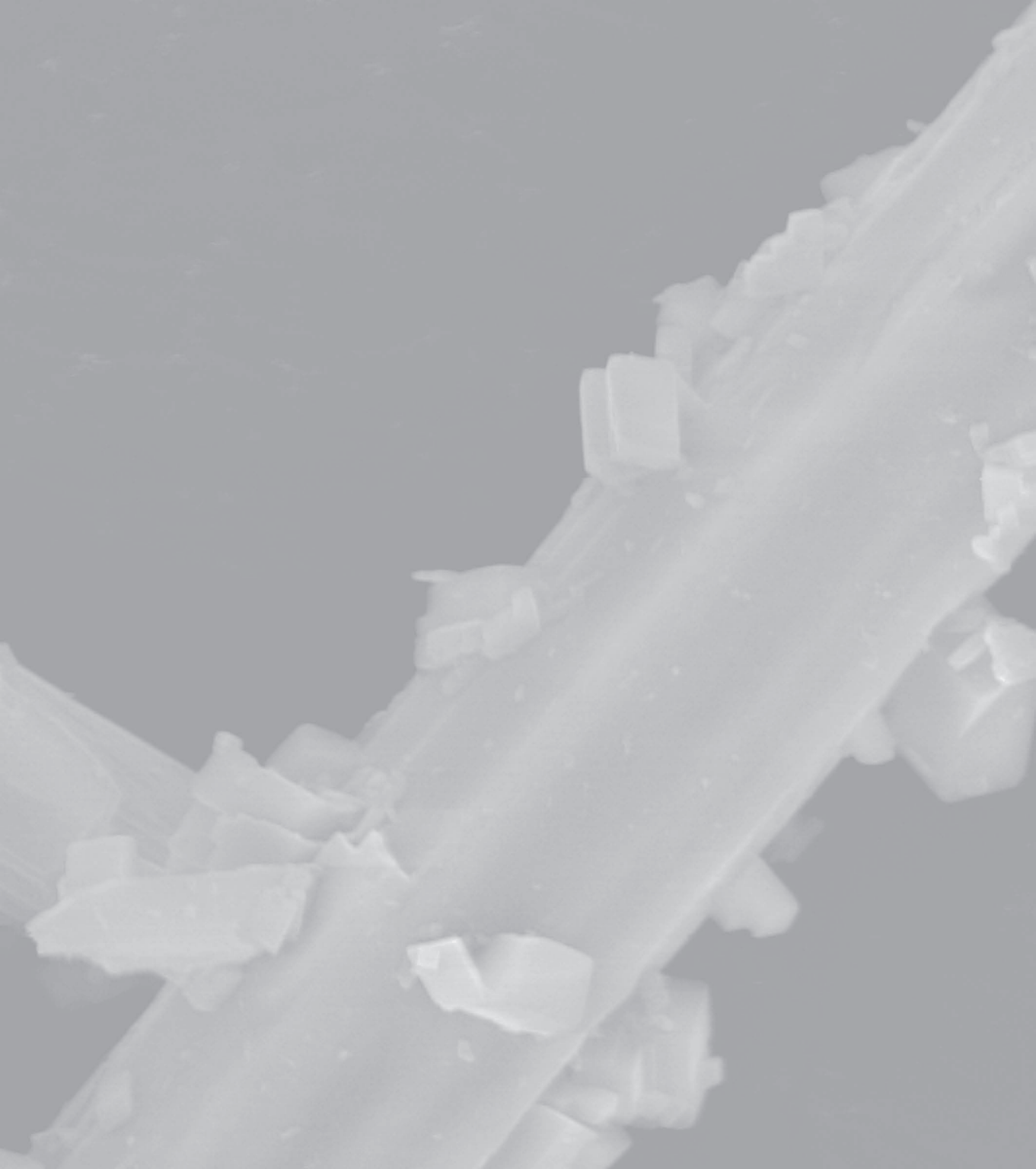
NOTATION

A	Heat-exchanging surface area	m^2
A	Pre-exponential factor Arrhenius equation	%/min
A_{spec}	Specific surface area	m^2/m^3
Ca_{total}	Total calcium content feedstock	kg/kg
CO_2	Carbonate content, expressed in terms of CO_2	wt%
$CO_{2,avoided}$	Net amount CO_2 avoided	kg/h
$CO_{2,extra}$	Extra CO_2 emission caused by mineral carbonation	kg/h
$CO_{2,sequestered}$	Amount CO_2 sequestered in reactor	kg/h
$CO_{2,heat}$	Extra CO_2 emission due to heat consumption	kg/h
$CO_{2,power}$	Extra CO_2 emission due to power consumption	kg/h
D	Diameter reactor	m
d	Particle size	µm
d	Wall thickness	m
D[3,2]	Surface area-based mean diameter	µm
D[4,3]	Volume-based mean diameter	µm
d_0	Initial particle size before grinding	m
d_1	Final particle size after grinding	m
$d_{0.5}$	Median particle size	µm
DTL	Detection limit	mg/L
E_a	Activation energy	kJ/mol
E_{heat}	Heat consumption of process	kWh
E_{power}	Power consumption of process	kWh
H	Height reactor	m
IAP	Ion activity product	mol^n/L^n
K_{sp}	Solubility product	mol^n/L^n
L/S	Liquid-to-solid ratio	kg/kg
$m_{105°C}$	Dry weight of TGA sample	kg
MW	Molar weight	kg/mol
n	Stirring rate	rpm
p	Pressure	bar
p_{CO2}	CO_2 partial pressure	bar
p_{H2O}	H_2O partial pressure	bar
Q	Heat	W
SI	Saturation index	-
t	Reaction time	min
T	Temperature	°C
TC	Total content	mg/kg
TIC	Total inorganic carbon	wt%

U	Heat transfer coefficient	W/m^{2}K
W	Energy consumption grinding	kWh/ton
W_i	Bond's work index	kWh/ton
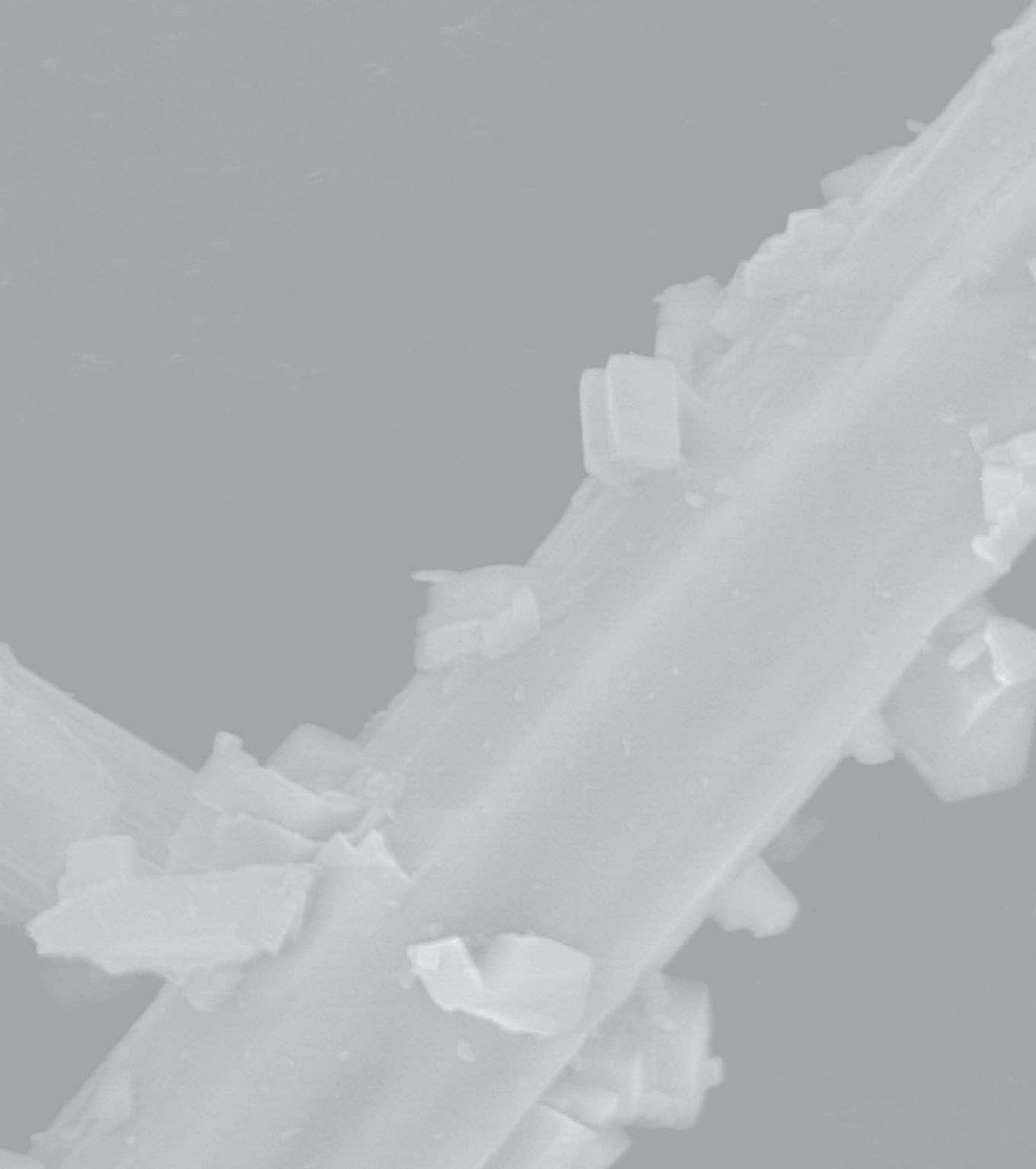
Greek characters

ΔG_r	Reaction Gibbs energy	kJ/mol
ΔH_r	Reaction enthalpy	kJ/mol
$\Delta m_{105-1000°C}$	Weight loss TGA between 105 and 1000 °C	kg
ΔP	Pressure drop	bar
ΔT	Temperature difference heat exchanger	°C
ΔT_{lm}	Logarithmic mean temperature difference	°C
$\Delta \eta_{CO2}$	CO_2 sequestration efficiency loss	%
ε_{heat}	Specific CO_2 emission heat	kg/kWh
ε_{power}	Specific CO_2 emission power	kg/kWh
ζ	Conversion	%
ζ_{Ca}	Conversion of total calcium content feedstock	%
ζ_{CaSiO3}	Conversion of $CaSiO_3$ fraction in the reactor inlet	%
η	Viscosity	kg/ms
η_{CO2}	Energetic CO_2 sequestration efficiency	%
σ	Standard deviation	%
Φ	Flow rate	m^3/h

Superscripts and subscripts

0	Fresh feedstock
Ca	Calcium
CO_2	Carbon dioxide
g	Gas
l	Liquid

REFERENCES

REFERENCES

Abanades, J.C. (2002) *The maximum capture efficiency of CO_2 using a carbonation/calcination cycle of CaO/CaCO$_3$*, Chemical Engineering Journal 90(*3*), 303-306.

Allison, J.D., Brown, D.S. & Novo-gradac, K.J. (1991) *MINTEQA2/PRODEFA2, Geochemical assessment model for environmental systems: version 3.11 databases and version 3.0 user's manual,* Environmental Research Laboratory, U.S. EPA, Athens, GA, USA.

Anon. (1995) *Bouwstoffenbesluit bodem- en oppervlaktewateren-bescherming (Dutch building material decree)* in Staatsblad van het Koninkrijk der Nederlanden (Official journal of the Kingdom of the Netherlands), No. 567 *(in Dutch)*.

Anon. (2005) *Aspen Plus 2004.1,* Aspen Technology Inc., Cambridge, MA, USA.

Anon. (2006a), http://www.filtration-and-separation.com.

Anon. (2006b), *PointCarbon (EU CO_2 emission right trade prices)*, http://www.pointcarbon.com.

Apul, D.S., Gardner, K.H., Eighmy, T.T., Fällman, A.-M. & Comans, R.N.J. (2005) *Simultaneous application of dissolution / precipitation and surface complexation / surface precipitation modeling to contaminant leaching,* Environmental Science and Technology 39(*15*), 5736-5741.

Bearat, H., McKelvy, M.J., Chizmeshya, A.V.G., Sharma, R. & Carpenter, R.W. (2002) *Magnesium hydroxide: dehydroxylation / carbonation reaction processes: implications for carbon dioxide mineral sequestration,* Journal of American Ceramic Society 85(*4*), 742-748.

Bethke, C.M. (2002) *The Geochemist's Workbench,* version 4.0*,* University of Illinois, IL, USA.

Blakemore, L.C., Searle, P.L. & Daly, B.K. (1987) *Methods for chemical analysis of soils*, NZ Soil Bureau, Science Report 80, Lower Hutt, New Zealand.

Blencoe, J.G., Anovitz, L.M., Palmer, D.A. & Beard, J.S. (2003) *Carbonation of calcium silicates for long-term CO_2 sequestration*, 2nd Annual Conference on Carbon Sequestration, Alexandria, VA, USA.

Blencoe, J.G., Palmer, D.A., Anovitz, L.M. & Beard, J.S. (2004) *Carbonation of metal silicates for long-term CO$_2$ sequestration*, patent number WO200409043.

Bond, F.C. (1961) *Crushing and grinding calculations. Part I,* British Chemical Engineering 6(*6*), 378-385.

Bond, G.M., Liu, N., Abel, A., McPherson, B.J. & Stringer, J. (2004) *Early results from a laboratory-scale pilot-plant demonstration of enzyme-catalyzed CO$_2$ sequestration with produced waters as cation source*, 7th International Conference on Greenhouse Gas Control Technologies, Vancouver, BC, Canada.

Bond, G.M., Stringer, J. & Brandvolk, D.K. (2001) *Development of integrated system for biomimetic CO$_2$ sequestration using the enzyme carbonic anhydrase,* Energy & Fuels 15(*2*), 309-316.

Brady, P.V. (1991) *The effect of silicate weathering on global temperature and atmospheric CO$_2$,* Journal of Geophysical Research 96(*B11*), 18101-18106.

Butt, D.P., Lackner, K.S. & Wendt, C.H. (1998) *The kinetics of binding carbon dioxide in magnesium carbonate*, 23rd International Conference on Coal Utilization and Fuel Systems, Clearwater, FL, USA.

Butt, D.P., Lackner, K.S., Wendt, C.H., Conzone, S.D., Kung, H., Lu, Y.-C. & Bremser, J.K. (1996) *Kinetics of thermal dehydroxylation and carbonation of magnesium hydroxide,* Journal of American Ceramic Society 79(*7*), 1892-1898.

Carey, J.W., Rosen, E.P., Bergfeld, D., Chipera, S.J., Counce, D.A., Snow, M.G., Ziock, H.-J. & Guthrie, G.D. (2003) *Experimental studies of the serpentine carbonation reaction*, 28th International Technical Conference on Coal Utilization & Fuel Systems, Coal Technology Association, Clearwater, FL, USA, 331-340.

Carlson, E.C. (1996) *Don't gamble with physical properties for simulations,* Chemical Engineering Progress 92(*10*), 35-46.

Chizmeshya, A.V.G., McKelvy, M.J., Gormley, D., Kocher, M., Nunez, R., Kim, Y.-C. & Carpenter, R. (2004) *CO$_2$ mineral carbonation processes in olivine feedstock: insights from the atomic scale simulation*, 29th International Technical Conference on Coal Utilization & Fuel Systems, Coal Technology Association, Clearwater, FL, USA.

Chizmeshya, A.V.G., McKelvy, M.J., Wolf, G., Sharma, R., Sankey, O.F., Bearat, H., Diefenbacher, J. & Carpenter, R.W. (2003) *Quantum simulation studies of olivine mineral carbonation*, 28th International Technical Conference on Coal Utilization & Fuel Systems, Coal Technology Association, Clearwater, FL, USA.

Chizmeshya, A.V.G., Sankey, O.F., McKelvy, M.J., Sharma, R., Carpenter, R.W., Wolf, G.H., Bearat, H. & Diefenbacher, J. (2002) *Atomic-level understanding of CO_2 mineral carbonation mechanisms from advanced computational modelling*, 27th International Technical Conference on Coal Utilization and Fuel Systems, Coal Technology Association, Clearwater, FL, USA.

Dahlin, D.C., O'Connor, W.K., Nilsen, D.N., Rush, G.E., Walters, R.P. & Turner, P.C. (2000) *A method for permanent CO_2 sequestration: supercritical CO_2 mineral carbonation*, 17th Annual International Pittsburgh Coal Conference, Pittsburgh, PA, USA.

Deming, D., Yu, L., Baiyu, Z., Xiuyi, H. & Baohua, Y. (2001) *Selective chemical extraction and separation of Mn, Fe oxides and organic material in natural surface coatings: application to the study of trace metal adsorption mechanisms in aquatic environments,* Microchemical Journal 69(*1*), 89-94.

Devoldere, K., Weyten, H., Vrancken, K. & Ginneken van, L. (2000) *Accelerated weathering of MSWI bottom ash by means of liquid and supercritical CO_2*, 7th Meeting on Supercritical Fluids, Antibes, France.

Dijkstra, J.J., Meeussen, J.C.L. & Comans, R.N.J. (2004) *Leaching of heavy metals from contaminated soils: an experimental and modeling study,* Environmental Science and Technology 38(*16*), 4390-4395.

Dijkstra, J.J., Sloot van der, H.A. & Comans, R.N.J. (2002) *Process identification and model development of contaminant transport in MSWI bottom ash,* Waste Management 22, 531-541.

Dunsmore, H.E. (1992) *A geological perspective on global warming and the possibility of carbon dioxide removal as calcium carbonate mineral*, Energy Conversion and Management 33, 565-572.

Dutch Association of Cost Engineers (DACE) (2005) *DACE price booklet (DACE prijzenboekje, in Dutch),* ed. 24*,* Elsevier, The Netherlands.

Dziedzic, D., Gorski, G.R., Gross, K.B. & Johnson, J.T. (2004) *Sequestration of carbon dioxide*, patent number US2004219090.

Dzombak, D.A. & Morel, F.M.M. (1990) *Surface complexation modeling: hydrous ferric oxide,* John Wiley & Sons, New York, USA.

Ecke, H. (2003) *Sequestration of metals in carbonated municipal solid waste incineration (MSWI) fly ash*, Waste Management 23(*7*), 631-640.

Fällman, A.-M. (2000) *Leaching of chromium and barium from steel slag in laboratory and field tests - a solubility controlled process,* Waste Management 20(*2-3*), 149-154.

Fauth, D.J., Baltrus, J.P., Knoer, J.P., Soong, Y., Howard, B.H., Graham, W.J., Maroto-Valer, M.M. & Andresen, J.M. (2001) *Conversion of silicate minerals with carbon dioxide producing environmentally benign and stable carbonates,* Preprints of Papers, Division of Fuel Chemistry, American Chemical Society 46(*1*), 278-279.

Fauth, D.J., Goldberg, P.M., Knoer, J.P., Soong, Y., O'Connor, W.K., Dahlin, D.C., Nilsen, D.N., Walters, R.P., Lackner, K.S., Ziock, H.-J., McKelvy, M.J. & Chen, Z.-Y. (2000) *Carbon dioxide storage as mineral carbonates*, Preprints of Symposia, American Chemical Society, Division Fuel Chemistry 45(*4*), 708-712.

Fauth, D.J., Soong, Y. & White, C.M. (2002) *Carbon sequestration utilizing industrial solid residues*, Preprints of Symposia, American Chemical Society, Division Fuel Chemistry 47(*1*), 37-38.

Fujii, M., Yamasaki, A., Kakizawa, M. & Yanagisawa, Y. (2001) *Reduction of CO_2 emission by treatment of waste concrete via an artificial process,* Preprints of Symposia, American Chemical Society, Division Fuel Chemistry 46(*1*), 75-77.

Gaucher, E.C., Blanc, P., Matray, J.-M. & Michau, N. (2004) *Modeling diffusion of an alkaline plume in a clay barrier,* Applied Geochemistry 19, 1505-1515.

Geerlings, J.J.C., Mesters, C.M.A.M. & Oosterbeek, H. (2002) *Process for mineral carbonation with carbon dioxide*, patent number WO02085788.

Gerdemann, S.J., Dahlin, D.C. & O'Connor, W.K. (2002) *Carbon dioxide sequestration by aqueous mineral carbonation of magnesium silicate minerals*, 6th International Conference on Greenhouse Gas Control Technologies, Kyoto, Japan.

Gerdemann, S.J., Dahlin, D.C., O'Connor, W.K., Penner, L.R. & Rush, G.E. (2004) *Factors affecting ex-situ aqueous mineral carbonation using calcium and magnesium silicate minerals*, 29th International Technical Conference on

Coal Utilization & Fuel Systems, Coal Technology Association, Clearwater, FL, USA.

Ginneken van, L., Dutre, V., Adrianses, W. & Weyten, H. (2002) *Effect of supercritical carbon dioxide treatment on the leaching performance of a cement-stabilised waste-form*, 8th Meeting on Supercritical Fluids.

Goff, F., Chipera, S., Counce, D. & Kluk, E. (2002) *Evaluation of ultramafic diatremes and related volcanic rocks as sources of magnesium for carbon dioxide sequestration in the United States*, LA-13921-MS, Los Alamos National Laboratory, Los Alamos, NM, USA.

Goff, F. & Lackner, K. S. (1998) *Carbon dioxide sequestering using ultramafic rocks,* Environmental Geosciences 5, 89-101.

Goldberg, P. & Walters, R. (2002) *A program to develop CO_2 sequestration via mineral carbonation*, 6th International Conference on Greenhouse Gas Control Technologies, Kyoto, Japan.

Haywood, H.M., Eyre, J.M. & Scholes, H. (2001) *Carbon dioxide sequestration as stable carbonate minerals - environmental barriers,* Environmental Geology 41, 11-16.

Hiemstra, T., Wit de, J.C.M. & Riemsdijk van, W.H. (1989) *Multisite proton modeling at the solid/solution interface of (hydr)oxides: A new approach, II. Application to various important (hydr)oxides,* Journal of Colloid and Interface Science 133, 488-508.

Huijgen, W.J.J. & Comans, R.N.J. (2005) *Mineral CO_2 sequestration by carbonation of industrial residues. Literature review and selection of residue*, ECN-C--05-074, Energy research Centre of the Netherlands, Petten, The Netherlands.

Iizuka, A., Fujii, M., Yamasaki, A. & Yanagisawa, Y. (2004) *Development of a new CO_2 sequestration process utilizing the carbonation of waste cement,* Industrial and Engineering Chemistry Research 43(*24*), 7880-7887.

Intergovernmental Panel on Climate Change (IPCC) (2001) *IPCC 3rd assessment report - Climate change*, Cambridge University Press, Cambridge, United Kingdom and New York, NY, USA.

Intergovernmental Panel on Climate Change (IPCC) (2005) *IPCC special report on carbon capture and storage*, Cambridge University Press, Cambridge, United Kingdom.

International Energy Agency (IEA) Coal Research (1999) *CO$_2$ reduction - prospects for coal.*

International Energy Agency (IEA) (2006) *Energy Technology Perspectives, Scenarios & Strategies to 2050,* ISBN 92-64-10982-X.

International Energy Agency - Greenhouse Gas R&D Programme (IEA-GHG) (2000) *CO$_2$ storage as carbonate minerals*, prepared by CSMA Consultants Ltd, PH3/17, Cheltenham, United Kingdom.

International Energy Agency - Greenhouse Gas R&D Programme (IEA-GHG) (2001) *Putting carbon back into the ground*, ISBN 1 898373 28 0, prepared by Davison et al., Cheltenham, United Kingdom.

Isoo, T., Takahashi, T. & Fukuhara, M. (2000) *Development of large steelmaking slag blocks using a new carbonation process*, Advances in Cement Research 12, 97-101.

Johnson, D.C. (2000) *Accelerated carbonation of waste calcium silicate materials*, SCI Lecture Paper Series 108, 1-10.

Johnson, D.C., MacLeod, C.L., Carey, P.J., & Hills, C.D. (2003) *Solidification of stainless steel slag by accelerated carbonation*, Environmental Technology 24(*7*), 671-678.

Jones, J.R., Knoer, J., Soong, Y., Harrison, D.K. & Fauth, D. (2000) *Low temperature - low pressure experimental design to form carbonate minerals under saturated CO$_2$ conditions*, 17th Annual International Pittsburgh Coal Conference, Pittsburgh, PA, USA.

Kakizawa, M., Yamasaki, A. & Yanagisawa, Y. (2001) *A new CO$_2$ disposal process using artificial rock weathering of calcium silicate accelerated by acetic acid,* Energy 26, 341-354.

Kirby, C.S. & Rimstidt, J.D. (1994) *Interaction of municipal solid waste ash with water,* Environmental Science and Technology 28(*3*), 443-451.

Kohlmann, J. & Zevenhoven, R. (2004) *Mineral carbonation in Finland, an approach to implementation*, 29th international technical conference on coal utilization & fuel systems, Coal Technology Association, Clearwater, FL, USA.

Kojima, T., Nagamine, A., Ueno, N. & Uemiya, S. (1997) *Absorption and fixation of carbon dioxide by rock weathering,* Energy Conversion and Management 38, S461-466.

Koljonen, T., Siikavirta, H., Zevenhoven, R. & Savolainen, I. (2004) *CO$_2$ capture, storage and reuse potential in Finland,* Energy 29, 1521-1527.

Kostka, J.E. & Luther III, G.W. (1994) *Partitioning and speciation of solid phase iron in saltmarsh sediments,* Geochimica et Cosmochimica Acta 58(*7*), 1701-1710.

Lackner, K.S. (2002) *Carbonate chemistry for sequestering fossil carbon,* Annual Review of Energy and the Environment 27, 193-232.

Lackner, K.S., Butt, D.P. & Wendt, C.H. (1997) *Progress on binding CO$_2$ in mineral substrates,* Energy Conversion and Management 38, S259-264.

Lackner, K.S., Wendt, C.H., Butt, D.P., Joyce, E.L. & Sharp, D.H. (1995) *Carbon dioxide disposal in carbonate minerals,* Energy 20(*11*), 1153-1170.

Lide, D.R. (2002) *Handbook of Chemistry and Physics*, ed. 83, CRC Press.

Maroto-Valer, M.M., Fauth, D.J., Kuchta, M.E., Zhang, Y., Andresen, J.M. & Soong, Y. (2001) *Study of magnesium rich minerals as carbonation feedstock materials for CO$_2$ sequestration*, 18th Annual International Pittsburgh Coal Conference, Newcastle, Australia.

Maroto-Valer, M.M., Kuchta, M.E., Zhang, Y. & Andrésen, J.M. (2002a) *Integrated carbonation: a novel concept to develop a CO$_2$ sequestration module for power plants*, 6th International Conference on Greenhouse Gas Control Technologies, Kyoto, Japan.

Maroto-Valer, M.M., Kuchta, M.E., Zhang, Y., Andresen, J.M. & Fauth, D.J. (2004a) *Comparison of physical and chemical activation of serpentine for enhanced CO$_2$ sequestration,* Preprints of symposia - American Chemical Society, Division Fuel Chemistry 49(*1*), 373-375.

Maroto-Valer, M.M., Zhang, Y., Kuchta, M.E. & Andresen, J.M. (2002b) *Activation of serpentine minerals for enhanced CO$_2$ sequestration*, 19th Annual International Pittsburgh Coal Conference, Pittsburgh, PA, USA.

Maroto-Valer, M.M., Zhang, Y., Kuchta, M.E., Andresen, J.M. & Fauth, D.J. (2004b) *Process for sequestering carbon dioxide and sulfur oxide*, patent number WO2004098740.

McKelvy, M.J., Bearat, H., Chizmeshya, A.V.G., Nunez, R. & Carpenter, R.W. (2003) *Understanding olivine CO$_2$ mineral sequestration mechanisms. The atomic level: optimizing reaction process design*, final report DE-FG26-01NT41282, Arizona State University, Tempe, AZ, USA.

McKelvy, M.J., Sharma, R., Chizmeshya, A.V.G., Carpenter, R.W. & Streib, K. (2001) *Magnesium hydroxide dehydroxylation: in situ nanoscale observations lamellar nucleation and growth,* Chemistry of Materials 13(*3*), 921-926.

Meeussen, J.C.L. (2003) *ORCHESTRA: An object-oriented framework for implementing chemical equilibrium models,* Environmental Science and Technology 37, 1175-1182.

Meima, J.A. & Comans, R.N.J. (1997) *Geochemical modeling of weathering reactions in municipal solid waste incinerator bottom ash,* Environmental Science and Technology 31, 1269-1276.

Meima, J.A., Weijden van der, R.D., Eighmy, T.T. & Comans, R.N.J. (2002) *Carbonation processes in municipal solid waste incinerator bottom ash and their effect on the leaching of copper and molybdenum,* Applied Geochemistry 17(*12*), 1503-1513.

Nearman, A., Mouélé, F., Trolard, F. & Bourrié, G. (2004) *Improved methods for selective dissolution of Mn oxides: applications for studying trace element associations,* Applied Geochemistry 19(*6*), 973-979.

Nelson, M.G. (2004) *Carbon dioxide sequestration by mechanochemical carbonation of mineral silicates*, final report DOE FG26-02NT41547, University of Utah, Salt Lake City, UT, USA.

National Energy Technology Laboratory (NETL) (2001) *Workshop NETL Mineral CO$_2$ Sequestration*.

Nilsen, D.N. & Penner, L.R. (2001) *Reducing greenhouse gas emissions: engineering and cost assessment of direct mineral carbonation technology (process development information for the olivine process)*, DOE/ARC-TR-01-015, Albany Research Center, Albany, OR, USA.

O'Connor, W.K., Dahlin, D.C., Gerdemann, S.J., Rush, G.E. & Penner, L.R. (2004) *Energy and economic considerations for ex-situ aqueous mineral carbonation*, 29th International Technical Conference on Coal Utilization & Fuel Systems, Coal Technology Association, Clearwater, FL, USA.

O'Connor, W.K., Dahlin, D.C., Nilsen, D.N., Gerdemann, S.J., Rush, G.E., Walters, R.P. & Turner, P.C. (2001a) *Research status on the sequestration of carbon dioxide by direct aqueous mineral carbonation*, 18th Annual International Pittsburgh Coal Conference, Newcastle, Australia.
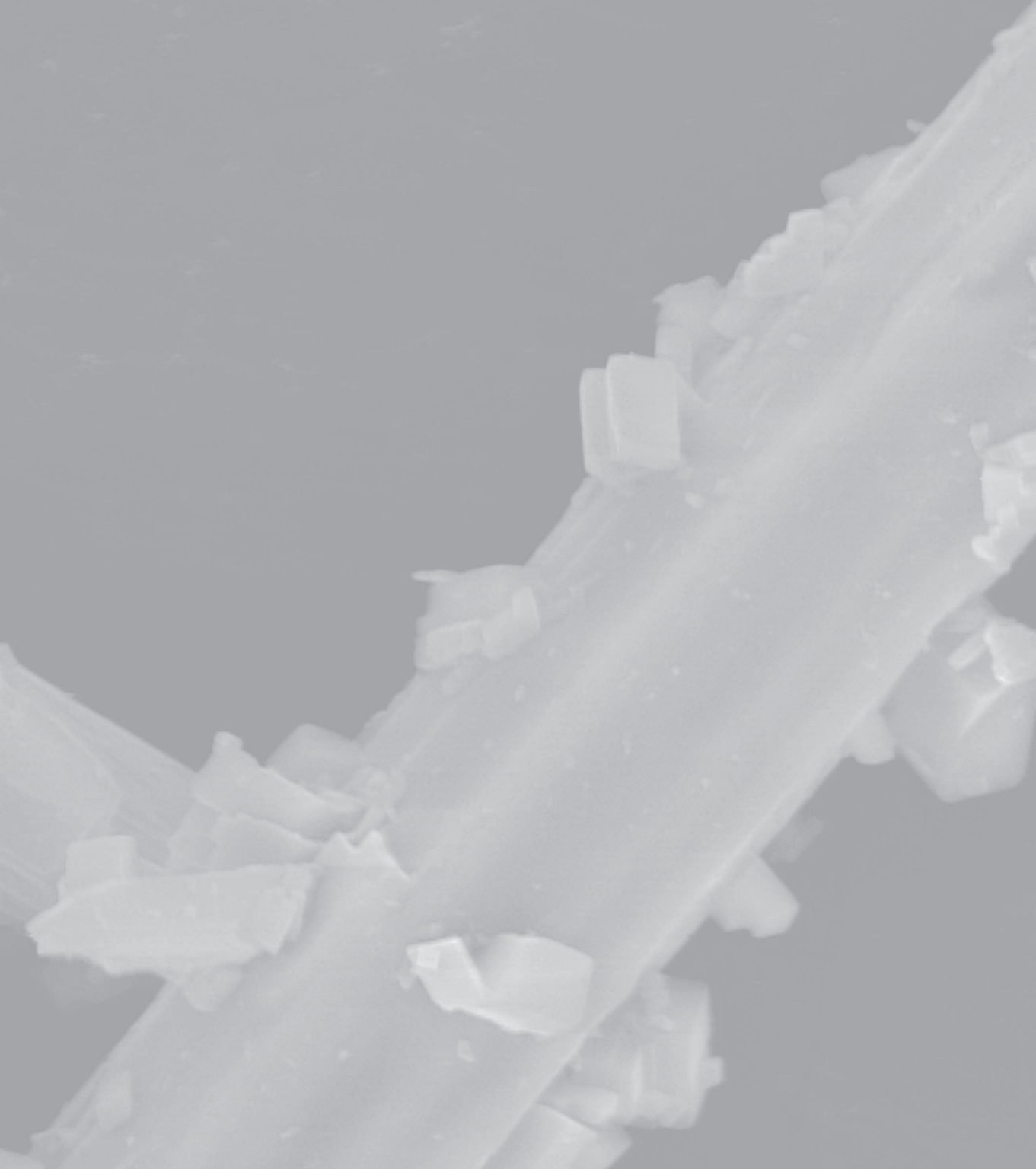
O'Connor, W.K., Dahlin, D.C., Nilsen, D.N., Rush, G.E., Walters, R.P. & Turner, P.C. (2001b) *Carbon dioxide sequestration by direct mineral carbonation: results from recent studies and current status*, 1st National Conference on Carbon Sequestration, Alexandria, VA, USA.

O'Connor, W.K., Dahlin, D.C., Nilsen, D.N., Walters, R.P. & Turner, P.C. (2000b) *Carbon dioxide sequestration by direct mineral carbonation with carbonic acid*, 25th International Technical Conference on Coal Utilization and Fuel Systems, Clearwater, FL, USA.

O'Connor, W.K., Dahlin, D.C., Rush, G.E., Dahlin, C.L. & Collins, W.K. (2002) *Carbon dioxide sequestration by direct mineral carbonation: process mineralogy of feed and products,* Minerals & Metallurgical Processing 19(*2*), 95-101.

O'Connor, W.K., Dahlin, D.C., Rush, G.E., Gerdemann, S.J., Penner, L.R. & Nilsen, D.N. (2005) *Aqueous mineral carbonation: mineral availability, pretreatment, reaction parametrics and process studies*, DOE/ARC-TR-04-002, Albany Research Center, Albany, OR, USA.

O'Connor, W.K., Dahlin, D.C., Nilsen, D.N., Gerdemann, S.J., Rush, G.E., Walters, R.P., & Turner, P.C. (2002a) *Continuing studies on direct aqueous mineral carbonation for CO_2 sequestration*, 27th International Technical Conference on Coal Utilization, Clearwater, FL, USA.

Park, A.-H.A. & Fan, L.-S. (2004) *CO_2 mineral sequestration: physically activated dissolution of serpentine and pH swing process,* Chemical Engineering Science 59(*22-23*), 5241-5247.

Park, A.-H.A., Jadhav, R. & Fan, L.-S. (2002) *Environmentally benign disposal of carbon dioxide: CO_2 mineral sequestration through carbonation of Mg-bearing minerals*, 19th Annual International Pittsburgh Coal Conference, Pittsburgh Coal Conference, University of Pittsburgh, Pittsburgh, PA, USA.

Park, A.-H.A., Jadhav, R. & Fan, L.-S. (2003a) *CO_2 mineral sequestration in a high-pressure, high temperature three-phase fluidised bed reactor*, 20th Annual International Pittsburgh Coal Conference, Pittsburgh, PA, USA.

Park, A.-H.A., Jadhav, R. & Fan, L.-S. (2003b) *CO_2 mineral sequestration: chemically enhanced aqueous carbonation of serpentine,* Canadian Journal of Chemical Engineering 81(*3*), 885-890.

Penner, L.R., O'Connor, W.K., Dahlin, D.C., Gerdemann, S.J. & Rush, G.E. (2004) *Mineral carbonation: Energy costs of pretreatment options and*

insights gained from flow loop reaction studies, 3rd Annual Conference on Carbon Sequestration, Alexandria, VA, USA.

Perry, R.H. & Green, D.W. (1998) *Perry's Chemical Engineers' Handbook,* ed. 7*,* McGraw-Hill, New York, USA.

Peters, M.S. & Timmerhaus, K.D. (1991) *Plant design and economics for chemical engineers,* McGraw-Hill, New York, USA.

Prelinger, H. & Klepp, K.O. (2002) *Vanadium in converter slags,* Steel research 73(*12*), 522-525.

Proctor, D.M., Fehling, K.A., Shay, E.C., Wittenborn, J.L., Green, J.J., Avent, C., Bigham, R.D., Connolly, M., Lee, B., Shepker, T.O. & Zak, M.A. (2000) *Physical and chemical characteristics of blast furnace, basic oxygen furnace, and electric arc furnace steel industry slags,* Environmental Science and Technology 34, 1576-1582.

Reddy, K.J., Gloss, S.P. & Wang, L. (1994) *Reaction of CO_2 with alkaline solid wastes to reduce contaminant mobility,* Water Research 28(*6*), 1377-1382.

Reddy, K.J., Drever, J.I. & Hasfurther, V.R. (1991) *Effects of a CO_2 pressure process on the solubilities of major and trace elements in oil shale solid wastes*, Environmental Science and Technology 25(*8*), 1466-1469.

Rubin, E.S., Rao, A.B. & Chen, C. (2004) *Comparative assessments of fossil fuel power plants with CO_2 capture and storage*, Proceedings of the 7th International Greenhouse Gas Technology Conference, Vancouver, BC, Canada, Volume I, 285-293.

Schulze, R.K., Hill, M.A., Field, R.D., Papin, P.A., Hanrahan, R.J. & Byler, D.D. (2004) *Characterization of carbonated serpentine using XPS and TEM,* Energy Conversion and Management 45(*20*), 3169-3179.

Seifritz, W. (1990) *CO_2 disposal by means of silicates,* Nature 345, 486.

Sharma, R., McKelvy, M.J. & Bearat, H. (2004) *In-situ nanoscale observations of the $Mg(OH)_2$ dehydroxylation and rehydroxylation mechanisms,* Philosophical Magazine A 84(*25-26*), 2711-2729.

Shi, C.J. (2004) *Steel slag - its production, processing, characteristics, and cementitious properties,* Journal of Materials in Civil Engineering 16(*3*), 230-236.

Short, N.R., Purnell, P. & Page, C.L. (2000) *Preliminiary investigations into the supercritical carbonation of cement pastes*, Journal of Material Science 36(*1*), 35-41.

Simsek-Ege, F.A., Bond, G.M. & Stringer, J. (2002) *Chapter 10, Polyelectrolyte cages for a novel biomimetic CO_2 sequestration system,* In Environmental Challenges and Greenhouse Gas Control For Fossil Fuel Utilization in the 21st Century*,* eds. Maroto-Valer, M.M., Song, C. & Soong, Y., Kluwer Academic / Plenum Publishers, New York, pp. 133-146.

Sinnott, R.K. (1997) *Chemical Engineering Design, Coulson & Richardson's Chemical Engineering, Volume 6,* ed. 2*,* Butterworth-Heinemann Ltd.

Stolaroff, J.K., Lowry, G.V. & Keith, D.W. (2004) *Using CaO- and MgO-rich industrial waste streams for carbon sequestration,* Energy Conversion and Management 46(*5*), 687-699.

Tang, Z., Maroto-Valer, M.M., Zhang, Y., Kuchta, M.E., Andresen, J.M. & Bair, S.A. (2002) *Simultaneous coal gasification and CO_2 sequestration using a fluidised bed of activated serpentine,* Preprints of Symposia - American Chemical Society, Division of Fuel Chemistry 47(*1*), 169-170.

Tawfic, T.A., Reddy, K.J. & Drever, J.I. (1995) *Reaction of CO_2 with clean coal technology ash to reduce trace element mobility,* Water, Air and Soil Pollution 84, 385-398.

Teir, S., Eloneva, S. & Zevenhoven, R. (2005) *Production of precipitated calcium carbonate from calcium silicates and carbon dioxide,* Energy Conversion and Management 46(*18-19*), 2954-2979.

Teir, S., Raiski, T., Kavaliauskaite, I., Denafas, G. & Zevenhoven, R. (2004) *Mineral carbonation and Finnish pulp and paper industry*, 29th international technical conference on coal utilization and fuel systems, Clearwater, FL, USA.

Tonkin, J.W., Balistrieri, L.S. & Murray, J.W. (2004) *Modeling sorption of divalent metal cations on hydrous manganese oxides using the diffuse double layer model,* Applied Geochemistry 19, 29-53.

Voormeij, D.A., Simandl, G.J. & O'Connor, W.K. (2004) *A systematic assessment of ultramafic rocks and their suitability for mineral sequestration of CO_2*, 7th international conference on greenhouse gas control technologies, Vancouver, BC, Canada.

Walas, S.M. (1988) *Chemical process equipment selection and design,* Butterworths, Boston.

Wendt, C.H., Butt, D.P., Lackner, K.S. & Ziock, H.-J. (1998a) *Thermodynamic calculations for acid decomposition of serpentine and olivine in $MgCl_2$ melts I, II, III*, LA-UR-98-4528 / 4529 / 5633, Los Alamos National Laboratory, Los Alamos, NM, USA.

Wendt, C.H., Butt, D.P., Lackner, K.S. & Ziock, H.-J. (1998b) *Thermodynamic considerations of using chlorides to accelerate the carbonate formation from magnesium silicates*, LA-UR-98-3612, Los Alamos National Laboratory, Los Alamos, NM, USA.

Wesker, E. & Geerlings, J.J.C. (2004) *Process for removal of carbon dioxide from flue gases*, patent number US2004126293.

Wu, J.C.S., Sheen, J.-D., Chen, S.-Y. & Fan, Y.-C. (2001) *Feasibility of CO_2 fixation via artificial rock weathering,* Industrial and Engineering Chemistry Research 40(*18*), 3902-3905.

Yegulalp, T.M., Lackner, K.S. & Ziock, H.J. (2001) *A review of emerging technologies for sustainable use of coal for power generation,* International Journal of Surface Mining Reclamation and Environment 15(*1*), 52-68.

Zevenhoven, R. & Kavaliauskaite, I. (2004) *Mineral carbonation for long-term CO_2 storage: an exergy analysis,* International Journal of Thermodynamics 7(*1*), 24-31.

Zevenhoven, R. & Kohlmann, J. (2002) *CO_2 sequestration by magnesium silicate mineral carbonation in Finland*, Recovery, Recycling & Re-integration, Geneva, Switzerland.

Zevenhoven, R. & Teir, S. (2004) *Long-term storage of CO_2 as magnesium carbonate in Finland*, 3rd Annual Conference on Carbon Capture and Sequestration, Alexandria, VA, USA.

DANKWOORD

DANKWOORD

Hoewel er maar één naam op de voorkant van dit boekje staat, hebben vele mensen, ieder op hun eigen wijze, bijgedragen aan de totstandkoming van dit proefschrift. Ik wil iedereen hiervoor hartelijk bedanken, zowel op het werk als privé. Een aantal mensen wil ik graag in het bijzonder noemen.

Allereerst wil ik Rob bedanken voor het begeleiden van mijn promotie. Bedankt voor het vertrouwen dat je vanaf het begin in mij gesteld hebt en de ruimte die je mij gegeven hebt om mijn eigen weg te gaan. De afgelopen jaren heb ik veel geleerd van jouw wetenschappelijke en nauwgezette manier van werken, in het bijzonder wanneer het gaat om het kritisch bekijken van eigen werk. Bedankt voor de tijd die je ondanks een volle agenda voor mij hebt vrijgemaakt om samen aan manuscripten te werken.

Uiteraard wil ik hier ook Geert-Jan bedanken. Hoewel je pas halverwege bij mijn promotie betrokken raakte en mij vanaf afstand moest begeleiden, heb ik veel aan je bijdragen gehad. Bedankt voor de stimulerende bijeenkomsten en je suggesties voor mijn onderzoek. Ik heb je praktische instelling met betrekking tot het publicatie- en promotieproces altijd erg gewaardeerd.

Van mijn collega's wil ik allereerst mijn oud-kamergenoten Andre en Joris bedanken. Betere kamergenoten kon ik me niet wensen! Ik vond het de afgelopen jaren erg fijn dat we alledrie in hetzelfde promotieschuitje zaten. Ook buiten het werk heb ik ons samenzijn tijdens etentjes, PD-sessies etc. altijd erg gewaardeerd. Behalve gezelligheid, heb ik ook voor mijn werk veel aan jullie gehad. Andre, dank voor je hulp met de TGA en vele andere praktische en experimentele zaken. Joris, bedankt voor het geduldig beantwoorden van al mijn vragen met betrekking tot het geochemisch modelleerwerk.

Petra, bedankt voor al je hulp op het lab en voor het uitvoeren van een deel van het experimentele werk. Het was fijn samenwerken! Hans M. dank voor je hulp bij het gebruik van ORCHESTRA en dank voor je goede suggesties tijdens het schrijven van wat nu hoofdstuk 3 geworden is. Uiteraard mogen ook de overige collega's (Hans vd S., Jantine, Remko) en oud-collega's (Chanelle, Daniëlle, Dirk, Esther, Gerlinde, Hein) binnen de groep Risicobeoordeling Milieuverontreiniging hier niet ontbreken. Al met al was het werken in de portocabin altijd erg gezellig en heb ik ECN-RISMIL als een leuke en hechte club ervaren.

Ook binnen de rest van ECN hebben diverse mensen hun bijdrage geleverd aan dit onderzoek. Allereerst wil ik Gerrit Jan en Jan Wilco bedanken voor hun bijdragen aan de systeemstudies die in hoofdstukken 5 en 6 staan. Zonder jullie specialistische kennis met betrekking tot ASPEN simulaties was het me niet gelukt dit programma iets zinnigs uit te laten rekenen. Daan en Jan

Willem bedankt voor het verzorgen van de (financiële) randvoorwaarden die het mij mogelijk hebben gemaakt dit onderzoek te doen. Mijn nieuwe collega's binnen ECN-Biomassa en in het bijzonder René en Hans wil ik bedanken voor hun begrip en flexibiliteit ten aanzien van mijn urenbesteding tijdens het afronden van dit proefschrift. Fijn dat er zo een redelijk soepele overgang tussen mijn oude en nieuwe werk mogelijk was.

Robin, tijdens je stage in najaar 2004 heb je een mooie basis neergelegd voor wat nu hoofdstukken 5 en 6 zijn geworden. Dank hiervoor! Het was leuk je te mogen begeleiden. Tot slot wil ik Jan de Graauw bedanken voor zijn waardevolle suggesties voor de kostenevaluatie (hoofdstuk 6).

Gezelligheid en steun van familie, vrienden en kennissen buiten het werk is minstens net zo belangrijk geweest in de totstandkoming van dit proefschrift. Ik ga hier niet iedereen noemen, maar jullie belangstelling voor mijn promotie-bezigheden is voor mij erg belangrijk geweest. Een speciaal woord is nog wel op zijn plaats voor Paul en Richard. Dat de keuze voor twee paranimfen op jullie is gevallen is voor mij een vanzelfsprekende zaak. Dank voor jullie vriendschap gedurende al zo vele jaren.

Joost enorm bedankt voor je ontwerp van dit boekje. Ik vind het resultaat er prachtig uitzien! Pap en mam, met dit proefschrift sluit ik een school- en studietraject af van zo'n 25 jaar, een traject dat jullie mede mogelijk hebben gemaakt. Dank voor alles wat jullie voor mij gedaan hebben en voor alles wat jullie voor mij betekenen.
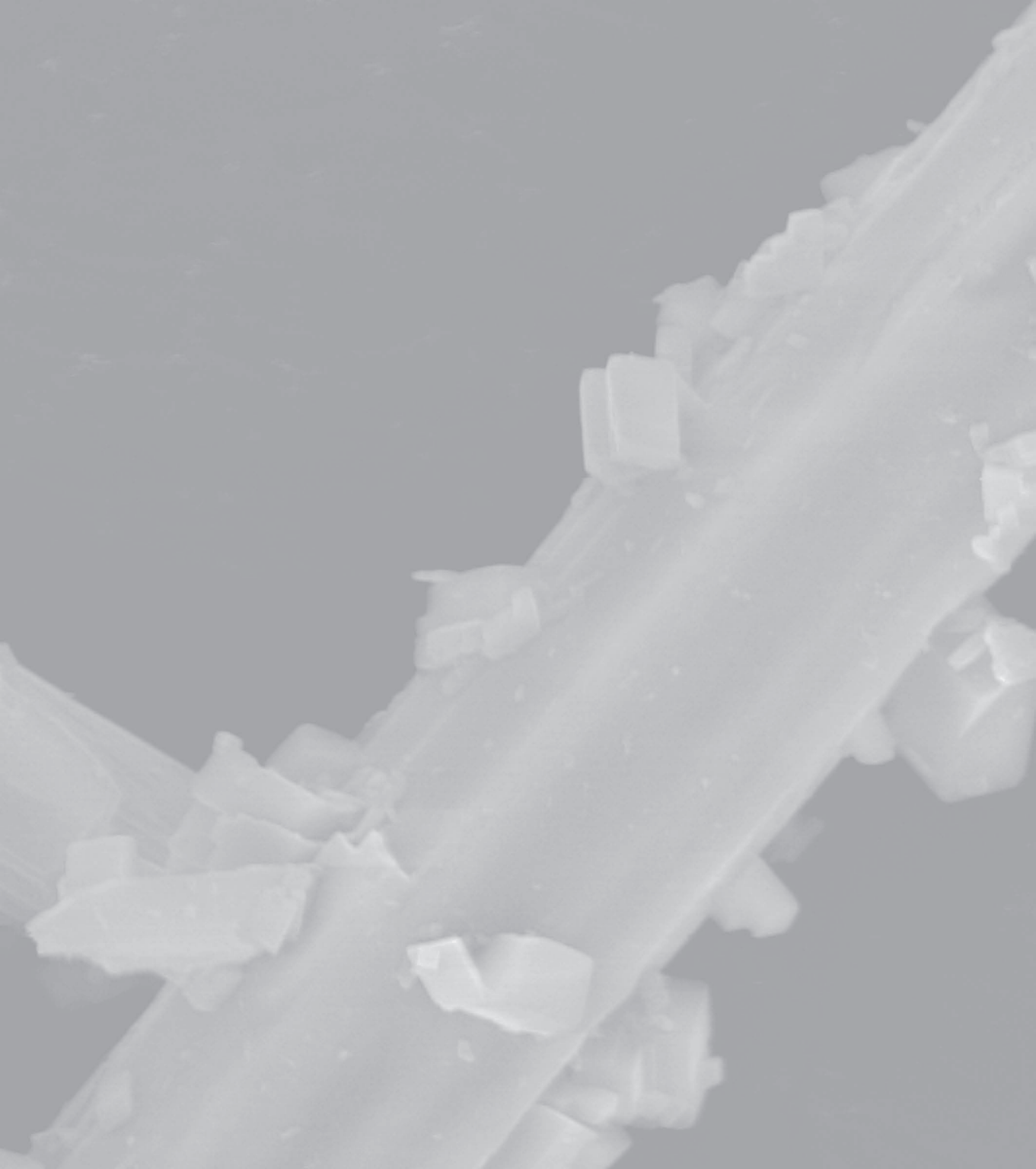
Floortje, de gewoonte in het schrijven van dankwoorden van proefschriften wil dat jij pas als laatste genoemd wordt, maar het moge duidelijk zijn dat dat geheel ten onrechte is. Samenwonen met iemand die een promotie doet moet af en toe irritant zijn; weer diezelfde verhalen over irritant trage processen en (ogenschijnlijk) verspilde dagen. Ontzettend bedankt voor al je liefde gedurende de afgelopen jaren. Zonder jou was dit boekje er misschien wel helemaal nooit gekomen.

Zo en nu op naar de verdediging. Om alvast de lastigste vraag te beantwoorden die mij tijdens de verdediging van mijn afstudeerscriptie (vanuit de zaal) gesteld werd: 'Wat vind je hier *nou* leuk aan?' ... Tja, ruim vijf jaar later kom ik nog steeds niet verder dan mijn toenmalige antwoord: onderzoek doen is gewoon leuk. Maar laat ik daar nu aantoevoegen: dat is een mooi onderwerp voor vervolgonderzoek!
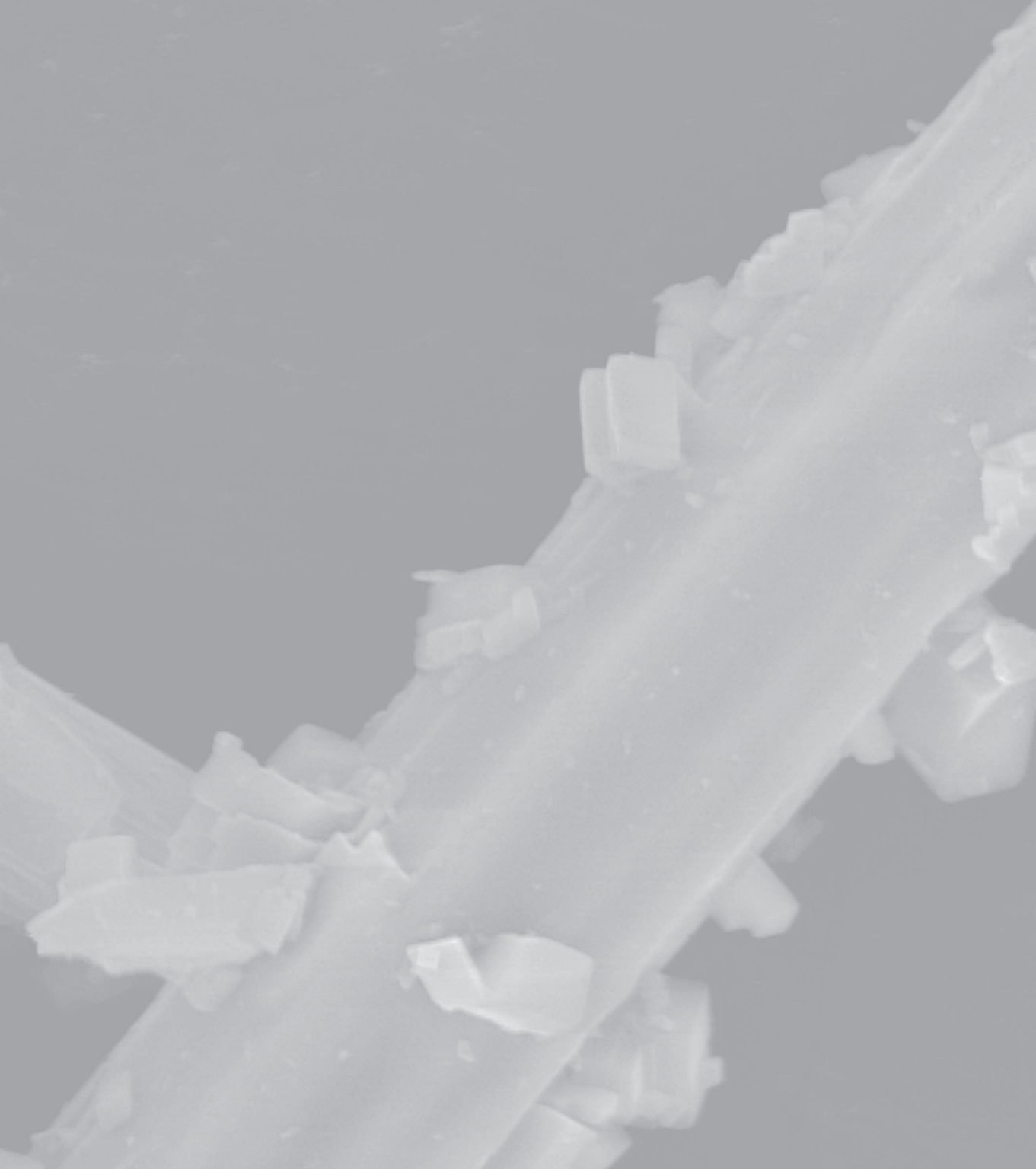
Wouter

Alkmaar, november 2006

CURRICULUM VITAE

CURRICULUM VITAE

Name: Wouter Johannes Joseph Huijgen, MSc

Date of Birth: January 6th 1977 (Haarlem, NL)

1989 - 1995   Secondary school (Gymnasium) (Amersfoort, NL)

1995 - 2001   Chemical Engineering, University of Twente
                               (Enschede, NL). Graduated cum laude.

                               Specializations: Environmental Engineering &
                               Process Technology

2000 - 2001   MSc-student and Researcher, TNO Institute for
                               Environment, Energy, and Process Innovation
                               (TNO-MEP) (Apeldoorn, NL).

2002 - 2006   PhD-student, Energy Research Centre of The
                               Netherlands (ECN), Unit Clean Fossil Fuels
                               (Petten, NL).

2006 - today   Research Scientist, Energy Research Centre of
                               The Netherlands (ECN), Unit Biomass, Coal, and
                               Environmental Research (Petten, NL).

                               Research area: biofuels and biorefinery
                               processes.

PUBLICATIONS

PUBLICATIONS

Reviewed Publications

International Energy Agency Greenhouse Gas (IEA-GHG) (2005) *Carbon dioxide storage by mineral carbonation*, report PH05/11, Cheltenham, United Kingdom, prepared by Huijgen, W.J.J. & Comans, R.N.J., Energy Research Centre of The Netherlands, Petten, The Netherlands.
(also published as: *Carbon dioxide sequestration by mineral carbonation: Literature review update 2003-2004*, ECN-C--05-022).

Huijgen, W.J.J., Witkamp, G.J. & Comans, R.N.J. (2005) *Mineral CO_2 sequestration by steel slag carbonation*, Environmental Science and Technology 39(*24*), 1976-1982 (ECN-RX--05-074).

Huijgen, W.J.J. & Comans, R.N.J. (2006) *Carbonation of steel slag for CO_2 sequestration: Leaching of products and reaction mechanisms*, Environmental Science and Technology 40(*8*), 2790-2796 (ECN-RX--06-057).

Huijgen, W.J.J., Witkamp, G.J. & Comans, R.N.J. (2006) *Mechanisms of aqueous wollastonite carbonation as a possible CO_2 sequestration process*, Chemical Engineering Science 61(*13*), 4242-4251 (ECN-RX--06-056).

Huijgen, W.J.J., Ruijg, G.J., Comans, R.N.J. & Witkamp, G.J. (2006) *Energy consumption and net CO_2 sequestration of aqueous mineral carbonation*, Industrial & Engineering Chemistry Research (in press).

Huijgen, W.J.J., Comans, R.N.J. & Witkamp, G.J. (2006) *Cost evaluation of CO_2 sequestration by aqueous mineral carbonation*, submitted for possible publication in Energy Conversion and Management.

Oral and Poster Presentations at Conferences

Comans, R.N.J. & Huijgen, W.J.J. (2004) *Carbonation of alkaline waste materials and its application to mineral CO_2 sequestration*, 32nd International Geological Congress (IGC-32), Florence, Italy (ECN-RX--05-088).

Huijgen, W.J.J., Witkamp, G.J. & Comans, R.N.J. (2004) *Mineral CO_2 sequestration in alkaline solid wastes*, Proceedings of the 7th International

Conference on Greenhouse Gas Control Technologies (GHGT-7), Vancouver, BC, Canada, Volume 2, Part 2, 2415-2418 (ECN-RX--04-079).

Huijgen, W.J.J., Witkamp, G.J. & Comans, R.N.J. (2004) *CO$_2$ sequestration by mineral carbonation*, 4th Netherlands Process technology Symposium (NPS4), Veldhoven, The Netherlands (ECN-RX--05-089).

Huijgen, W.J.J. & Comans, R.N.J. (2005) *CO$_2$ sequestration by aqueous mineral carbonation*, 2nd CO$_2$-NET meeting, Paris, France (ECN-RX--05-153).

Huijgen, W.J.J., Ruijg, G.J., Witkamp, G.J. & Comans, R.N.J. (2006) *Aqueous mineral carbonation as a possible CO$_2$ sequestration process: energetic efficiency and costs*, 8th International Conference on Greenhouse Gas Control Technologies (GHGT-8), Trondheim, Norway (ECN-RX--06-069).

Others ECN Reports

Huijgen, W.J.J. & Comans, R.N.J. (2003) *Carbon dioxide sequestration by mineral carbonation: Literature review*, ECN-C--03-016, Energy Research Centre of The Netherlands, Petten, The Netherlands.

Huijgen, W.J.J. & Comans, R.N.J. (2005) *Mineral CO$_2$ sequestration by carbonation of industrial residues: Literature review and selection of residue*, ECN-C--05-074, Energy Research Centre of The Netherlands, Petten, The Netherlands.